University of St Andrews

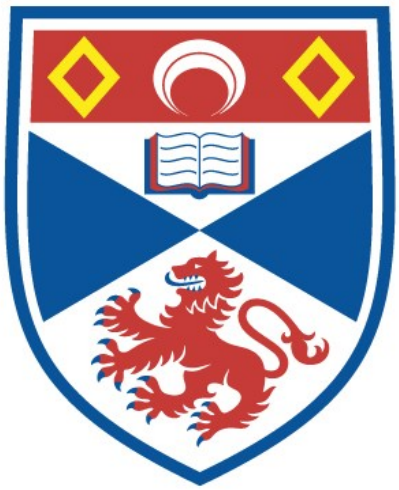

Full metadata for this thesis is available in
St Andrews Research Repository
at:
http://research-repository.st-andrews.ac.uk/

This thesis is protected by original copyright

The Synthesis and Photolysis Studies of Caged TRPV1 Ligands

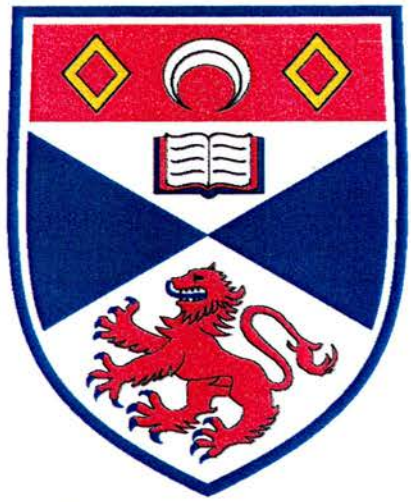

University
of
St Andrews

School of Chemistry and
Centre for Biomolecular Sciences
University of St Andrews
Fife, Scotland

March 2006

Michael Van Ryssen

Dissertation submitted to the University of St Andrews in application for the degree of

Master of Philosophy

Supervisor: Dr Stuart J. Conway

Th F405

Abstract

A number of transient receptor potential vanilloid subtype 1 (TRPV1) ligands were synthesised and protected with photolabile protecting groups in order to furnish "caged" compounds **79**, **120**, **121** and **123**.

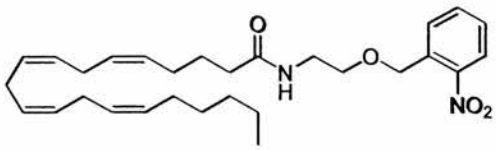

79

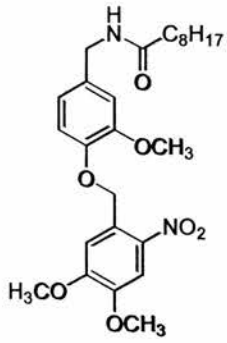

120

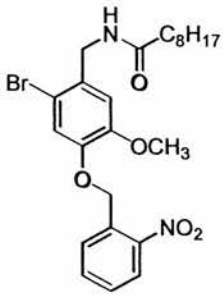

121

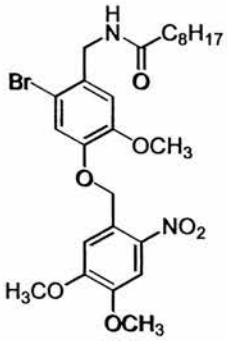

123

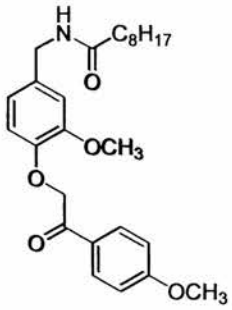

125

Photolysis of compounds **120** and **125** was studied both *in vitro* and using ^{1}H NMR analysis. It was demonstrated that photolysis of compound **120** and **125** was occurring to different extents when photolysed with a 375 nm immersion lamp. In subsequent studies it was shown that compound **125** could be photolysed using a 405 nm laser, while compound **120** was unaffected under these conditions. The UV/Vis spectra of the remaining caged compounds were studied and indicate that it should be possible to photolyse these compounds in a wavelength dependent manner.

Acknowledgements

First of all I am indebted to my supervisor, Dr S. J. Conway, for his endless patience, guidance and support throughout the course of this work.

Secondly, I would like to thank all the members of the Conway group and BMS Lab. 3.08 for their experimental assistance and encouragement, with special thanks to Dr G. Miller, D. Bello, J. Nemeth and R. Murray. I would also like to thank the members of the chemistry department who maintained and ran the nuclear magnetic resonance, mass spectrometry and elemental analysis facilities, as well as the school of chemistry and EPSRC for funding.

Further thanks go to Dr T. Brown, Dr B. Agate, S. Paterson and the Physics department for their collaboration and large involvement in the photolytic studies conducted and also to Dr R. H. Scott, Dr R. A. Ross and Dr K. N. Wease for their *in vitro* photolytic studies conducted at the University of Aberdeen.

Finally, I would like to thank my family for their support, especially my girlfriend Laura for her sacrifices and understanding.

DECLARATION

I, Michael Van Ryssen, hereby certify that this dissertation, which is approximately 29,320 words in length, has been written by me, that it is the record of work carried out by me and that it has not been submitted in any previous application for a higher degree.

Date: 05/09/2006 Signature of candidate

I was admitted as a research student in October, 2004 and as a candidate for the degree of Master of Philosophy in March, 2006; the higher study for which this is a record was carried out in the Biomolecular Sciences (BMS), School of Chemistry and School of Physics departments at the University of St Andrews between 2004 and 2006.

Date: 05/09/2006 Signature of candidat

I hereby certify that the candidate has fulfilled the conditions of the Resolution and Regulations appropriate for the degree of Master of Philosophy in the University of St Andrews and that the candidate is qualified to submit the dissertation in application for that degree.

Date: 05/09/2006 Signature of supervisor:

(Dr S. J. Conway)

COPYRIGHT DECLARATION

Unrestricted access

In submitting this thesis to the University of St Andrews I understand that I am giving permission for it to be made available for use in accordance with the regulations of the University Library for the time being in force, subject to any copyright vested in the work not being affected thereby. I also understand that the title and abstract will be published, and that a copy of the work may be made and supplied to any *bona fide* library or research worker.

Date: 05/09/2006

Table of Contents

Table of Contents 1

List of Figures 3

List of Schemes 7

List of Abbreviations 9

Introduction 11

1.1. The endocannabinoid system 11

1.1.1. The structure of the CB_1 and CB_2 receptors 11
1.1.2. Cannabinoid receptor subtype 1 (CB_1) 12
1.1.2.1. Distribution and Biological properties of CB_1 receptors 13
1.1.3. Cannabinoid receptor subtype 2 (CB_2) 15
1.1.3.1. Distribution and Biological properties of CB_2 receptors 15
1.1.4. Activation of cannabinoid receptors 16
1.1.5. Ligands for the CB_1 and CB_2 receptors 17
1.1.5.1. Endogenous cannabinoids 17
1.1.5.2. Anandamide 19

1.2. Capsaicin and the TRPV1 Receptor 22

1.2.1. The structure and binding sites of the TRPV1 receptor 23
1.2.2. Distribution of the TRPV1 receptor 24
1.2.3. Biological properties of the TRPV1 receptor 25
1.2.4. Activation of the TRPV1 receptor 26
1.2.5. Capsaicin 27

1.3. Caging Groups 31

1.3.1. Introduction 31
1.3.2. Popular caging groups and their mode of action 33
1.3.3. Orthogonal caging 37

1.4. Summary 40

2 Results and Discussion: Synthesis 41

2.1. Synthesis of caged anandamide 41
2.2. Synthesis of caged capsaicin analogues 51
2.3. Summary 53

3 Results and Discussion: Photolysis Studies 55

4 Conclusion 73

5 Future Work 74

6 Experimental Section 76

6.1. General 76

7 Appendix Selected NMR spectra 105

8 References 133

Appendix 1 136

List of Figures

Fig. 1.1 The models of CB_1 (A) and CB_2 (B) receptors shown as ribbon diagrams. The conserved patterns are shown in the ball-and-stick representation. Figure generated with Molscript and Raster3D.[6] 11

Fig. 1.2 Two-dimensional model of CB_1 and CB_2 receptor. The conserved patterns in the GPCR family are shown as colour cycles. The red lines show the different length in these three areas.[6] 12

Fig. 1.3 The molecular structure of Δ^9-THC, a potent agonist of the CB_1 receptor. 13

Fig. 1.4 The molecular structure of AM1241, a CB_2 receptor agonist.[19] 16

Fig. 1.5 Activation of the cannabinoid receptor can result in several cellular events through a signalling cascade. These events include the reduction of neuron transmitter release by a decrease in cellular Ca^{2+}, a decrease in cell firing by a decrease in cellular K^+ and the reduction in cellular cyclic adenosine 3', 5'-monophosphate (cAMP). 17

Fig. 1.6 The molecular structures of the five known endogenous cannabinoids. 18

Fig. 1.7 Illustration of affinity and efficacy of a drug. 18

Fig. 1.8 An example of the linear approach used in the synthesis of AEA analogues, O. Dasse.[25] 19

Fig. 1.9 Inactivation (cellular reuptake and intracellular metabolism) of anandamide and 2-arachidonoylglycerol (2-AG). P denotes a phosphate group, R the head group of the endocannabinoid, R_1 the acyl chain of other fatty acids and X the base in phosphoglycerides. Monoacylglycerol lipase (MAGL). [24] 21

Fig. 1.10 The key regions of structural activity of anandamide. 21

Fig. 1.11 Topological organization of a TRPV1 channel subunit. The model consists of an *N*-terminal domain containing three ankyrin units and a phosphorylation site for protein kinase A. There are six transmembrane domains and a large stretch connecting the S5 and S6 membrane segments, which give rise to the pH sensitive areas of the receptor. The cytosolic *C*-terminus domain carries the calmodulin and phosphatydylinositol-4,5-bisphosphate (PIP_2) binding sites. [34] 23

Fig. 1.12 A plausible structural model of the TRPV1 pore module. Secondary and tertiary structure of the S5-P-S6 motif of a TRPV1 subunit (left); the functional channel would be formed by the assembly of four identical subunits around a central aqueous pore (right). The P-loop configures the narrowest part of the pore conduit at the extracellular side, whereas the S6 segment is the inner α-helix that structures the walls of the pore at the cytosolic side. Taken from Ferrer-Montiel *et al.*[34] 24

Fig. 1.13 An illustration showing the activation of a TRPV1 receptor. The receptor is known to be activated by heat ~42 °C, a pH < 5.5, capsaicin and analogues, resiniferatoxin (RTX) and anandamide. Activation results in a localized effect by substance P release and an acute effect by cell signalling. 26

Fig. 1.14 The molecular structures of capsaicin and resiniferatoxin (RTX), potent agonists of the TRPV1 receptor. 27

Fig. 1.15 Molecular structure of vanillin. 27

Fig. 1.16 Molecular structures of two analogues of capsaicin.[43] 28

Fig. 1.17 Comparison of EC_{50} (nM) values of capsaicin, two analogues of capsaicin and RTX.[43] 28

Fig. 1.18 The molecular structures of capsazepine and SB-366791, potent antagonists of the TRPV1 receptor. 29

Fig. 1.19 The molecular structure of capsaicin sectioned into three regions of SAR importance: Aromatic region A, amide bond region B and the hydrophobic side-chain region C. 30

Fig. 1.20 The molecular structure of a potent capsaicin analogue with a pseudo-cyclic conformation. 30

Fig. 1.21 The molecule structure of 4-hydroxy-3-methoxy-*N*-nonanoylbenzylamine, an extremely potent capsaicin derivative. 31

Fig. 1.22 A cartoon representing the activation of a receptor by a biologically active molecule. 32

Fig. 1.23 A cartoon showing the caging of a biologically active compound and its subsequent inertness to its specific ligand. 32
Fig. 1.24 A cartoon representing uncaging of a biologically active compound within a cell by photolysis and its subsequent activation of its specific ligand. 33
Fig. 1.25 The molecular structures of caged acetylcholine and caged glutamate.[47] 33
Fig. 1.26 The molecular structures of several *ortho*-nitrobenzyl alcohol caging groups. 34
Fig. 1.27 Nitroveratryl (NV) and pivaloyl glycol (PG) linkers and resins for differential photo-release studies.[59] 39

Fig. 2.1 Target molecules for analogues of anandamide including two caged derivatives. 41
Fig. 2.2 Possible mechanism for the synthesis of 2-benzyloxy-4,5-dihydrooxazole. 44
Fig. 2.3 Possible mechanism for the synthesis of 2-(4'-methoxyacetophenone)-4,5-dihydrooxazole. 45
Fig. 2.4 Possible equilibria present after the addition of NaH to *N*-(*tert*-butoxycarbonyl)-2-aminoethanol and *N*-(benzyloxycarbonyl)-2-aminoethanol. 47
Fig. 2.5 Molecular and X-ray structures of Pearson *et al.* compounds showing distortion of Br-C-C-N-O angle in 103 compared to that of Br-C-C-N angle in 104.[64] 47
Fig. 2.6 Aromatic region of the ^{1}H NMR of 2-bromo-5-methoxy-4-(triisopropylsilyloxy)-*N*-nonanoylbenzylamine showing δ_H (300 MHz; $CDCl_3$) 7.20 (Chloroform), 6.95 (1H, s, Ar-H_5), 6.81 (1H, s, Ar-H_2). 52
Fig. 2.7 The molecular structures of a caged analogue of anandamide 77 and three caged analogues of capsaicin (118, 121 and 122). 53

Fig. 3.1 The structure of the three caged capsaicin analogues (118, 121 and 123), the TRPV1 agonist (32), the structure of anandamide (3) and caged anandamide (77). 55
Fig. 3.2 Capsaicin 24 and compound 32 evoked Ca^{2+} transients in the same population of cultured DRG neurons. For fura-2 Ca^{2+} imaging, DRG neurons were incubated for 1 hour in NaCl-based extracellular solution containing in mM: NaCl, 130; KCl, 3.0; $MgCl_2$, 0.6; $CaCl_2$, 2.0; $NaHCO_3$, 1.0; HEPES, 10.0; glucose, 5.0 and 0.01 fura-2AM (1 mM stock in DMF). The pH of this solution was adjusted with NaOH to 7.4 and the osmolarity to 310-320 mOsm with sucrose. The neurons were then washed for 10-20 min with NaCl-based extracellular solution, containing 0.1% DMSO, to remove the extracellular fura-2AM. During the experiment the neurons were constantly perfused (1-2 cm^3/min) with extracellular solution containing DMSO, and the actions of capsaicin 24, compound 32 and extracellular solution containing 30 mM KCl tested. The high KCl concentration produced depolarisation, activation of voltage-gated Ca^{2+} channels and transient increases in intracellular Ca^{2+} in the DRG neurons, but not background cells also present in the culture. Ca^{2+} transient amplitudes (fluorescence ratio values after background subtraction) were measured. A. Bar chart showing mean data (± S.E.M) for responses with similar amplitudes produced by 100 nM capsaicin and 1 μM compound 32. The chart also shows that desensitisation with compound 32 abolished subsequent responses to capsaicin. (n = number of experiments) B. Example record showing Ca^{2+} transients evoked by capsaicin, compound 32 and 30 mM KCl (clearly identifies a DRG neuron). C. Example record showing a response to compound 32 and subsequent desensitisation of the capsaicin response, however, a response to 30 mM KCl could be elicited. Note the difference in time scale between B and C.[46] 56
Fig. 3.3 Intracellular actions of compound 123 photolysis on the excitability of cultured DRG neurons. The same extracellular solution was used for both the electrophysiology and the Ca^{2+} imaging experiments. The patch pipette solution contained (in mM): KCl, 140; EGTA, 5; $CaCl_2$, 0.1; $MgCl_2$, 2.0; HEPES, 10.0; ATP, 2.0; compound 123 0.5–0.1% and 2.5% DMSO. This solution after correction with Tris and sucrose had a pH of 7.2 and osmolarity of 320 $mOsmL^{-1}$. An Axoclamp 2 A switching amplifier (Axon Instruments) operated at a switching frequency of 15 kHz was used. (A) Record showing two depolarising responses to intracellular

photolysis of compound 123 from the same neuron. No action potentials were evoked in this neuron and no further depolarisation was obtained with additional photolysis (3rd flash not shown). (B) Example record showing a single action potential and sustained depolarisation obtained in response to intracellular photolysis of compound 123.[46] 57
Fig. 3.4 Line chart showing the diversity of DRG neuron current responses to capsaicin and intracellular photolysis of compound 123. Only 2 out of 7 DRG neurons responded to capsaicin but both these neurons also responded to intracellular photolysis of compound 123. Five cells failed to respond to both drugs.[46] 58
Fig. 3.5 (A) Example voltage clamp record showing a non-responding neuron that failed to respond to both capsaicin and intracellular photolysis of compound 123. (B) Records showing inward currents activated by capsaicin and intracellular photolysis of compound 123; note the difference in current scale. (C) Action currents evoked by intracellular photolysis of compound 123; showing the burst firing behaviour that gradually declines as the neuron recovers to a resting state. This neuron was voltage clamped at a holding potential of -70 mV; the excitatory action of photoreleased compound 32 appears to have occurred in an unclamped region of the cell and a burst of action potentials has spread into the cell body to be recorded as currents. (D) The same record as (C) but on an expanded time scale to show the high frequency action potential firing and that the first action potential was not initiated by a clear inward current in the cell soma. Arrows mark the points at which 300 V flashes (175 mJ; lasting 1 ms) from a xenon flash lamp, equipped with a 360 nm filter, were applied to the DRG neurons. Under voltage clamp all neurons were held at -70 mV.[46] 58
Fig. 3.6 The dimethoxynitrobenzyl caged analogue of capsaicin employed in photolytic experiments conducted by Katritzky *et al.*[65] 60
Fig. 3.7 Partial 300 MHz ^{1}H NMR spectra of compound 32 irradiated, for the time indicated, with a 125 W mercury arc lamp through a 375 nm filter 60
Fig. 3.8 Partial 300 MHz ^{1}H NMR spectrum of equimolar amounts of compounds 32 and 123. The ^{1}H NMR shows an apparent triplet owing to a doublet derived from coupling of the -CH_2NH- protons on compound 32 and an overlapping doublet derived from coupling of the -CH_2NH- protons of compound 123. 61
Fig. 3.9 Partial 300 MHz ^{1}H NMR spectra of compound 118 irradiated, for the time shown, with a 125 W mercury arc lamp through a 375 nm filter. 35% uncaging (as adjudged by appearance of compound 32 vs total material) was observed after 30 min. The doublet at 4.19 ppm is from compound 118; the doublet at 4.14 ppm is from compound 32. 61
Fig. 3.10 Partial 300 MHz ^{1}H NMR spectrum of equimolar amounts of compounds 32 and 118. The ^{1}H NMR shows a doublet at 4.10 ppm derived from coupling of the -CH_2NH- protons on compound 32 and a doublet at 4.15 ppm derived from coupling of the -CH_2NH- protons of compound 118. 62
Fig. 3.11 UV spectra of caged capsaicin analogue 118 in acetonitrile (A) and the 4,5-dimethoxynitrobenzyl bromide reagent in acetonitrile (B) 62
Fig. 3.12 UV spectrum of caged phenacyl capsaicin analogue 123 in acetonitrile, showing no absorption at 375 nm wavelength 63
Fig. 3.13 Partial 300 MHz ^{1}H NMR spectra of compound 118 irradiated for a range of 1-90 min, with a 405 nm violet diode laser. These spectra show the disappearance of the -CH_2NH- from compound 118 and the appearance of the -CH_2NH- from compound 32, indicating that uncaging has occurred. 64
Fig. 3.14 The uncaging profile of 118 on irradiation at 405 nm. The disappearance of the caging group -C*H*$_2$O-, the disappearance of the -C*H*$_2$NH- of compound 118, and the appearance of the -C*H*$_2$NH- of compound 32 were monitored. The integrals were obtained using 1DWINNMR to perform deconvolution calculations. 65
Fig. 3.15 Partial 300 MHz ^{1}H NMR spectra of compound 118 irradiated for x min with a 405 nm violet diode laser, at the power setting shown. These spectra show the disappearance of the -C*H*$_2$NH- from compound 118 and the appearance of the -C*H*$_2$NH- from compound 32, indicating that uncaging occurs in a power-dependent manner. 67

Fig. 3.16 Partial 300 MHz ^{1}H NMR spectra of compound 123 irradiated, for the time shown. These spectra show the -CH_2NH- from compound 123 does not disappear and that the -CH_2NH- from compound 32 is not observed.[46] 68
Fig. 3.17 Partial 300 MHz ^{1}H NMR spectra of compounds 118 and 123 irradiated, for the time shown. These spectra show the -CH_2OH- of both compounds and that compound 123 does not disappear as the -CH_2OH- from compound 118 decreases by photolysis. 69
Fig. 3.18 The uncaging profiles of 118 and 123 on irradiation at 405 nm. The disappearance of the -CH_2O- of the caging group was monitored by ^{1}H NMR, the integrals were obtained using 1D WINNMR to perform deconvolution calculations. The gray bars show the percentage of compound 123 present after the given time. The clear bars show the percentage of compound 118 present after the given time. 69
Fig. 3.19 UV spectra of caged anandamide analogue 77 in acetonitrile (A) and the 2-nitrobenzyl bromide reagent in acetonitrile (B). 70
Fig. 3.20 UV spectra of caged anandamide analogue 77 in acetonitrile (A) and caged capsaicin analogue 118 in acetonitrile (B). 71
Fig. 3.21 UV spectra of caged anandamide analogue 121 in dichloromethane. 72

Fig. 5.1 The molecule structures of two proposed future work caged capsaicin analogues..... 76

List of Schemes

Scheme 1.1 Proposed biosynthesis of anandamide. R_1 denotes the acyl chain in arachidonic acid, R_2 and R_3 are acyl chains of other fatty acids. X denotes the base in phosphoglycerides.[24] 20
Scheme 1.2 Photolysis of caged ATP, resulting in the release of the biologically active compound ATP and two by-products, 2-nitrobenzyaldehyde and a proton.[47] 33
Scheme 1.3 Proposed photolytic activation of the 2-nitrobenzyl caging group and the resulting formation of the aci-nitro intermediate.[52,50] 35
Scheme 1.4 Current proposed mechanism for the thermal reactions of the primary photochemical aci-transients A, formed from photolysis of 2-nitrobenzyl caging groups in aqueous solution.[50] 35
Scheme 1.5 Latest proposed mechanism for the photolysis of the 4-hydroxyphenacyl caging group.[56] 36
Scheme 1.6 Proposed mechanism for photolysis of the 4-methoxyacetophenone caging group. The arrows on structure 61 correspond to the pathway leading to phenylacetic acid 64.[56,57] 37
Scheme 1.7 This scheme shows an example of intermolecular wavelength orthogonality using the nitroveratrole and the benzoin caging groups on a simple carboxylic acid. This example illustrates how one caging group can be removed in the presents of the other.[58] 38
Scheme 1.8 This scheme shows an example of intramolecular wavelength orthogonality using the nitroveratrole and the benzoin caging groups on a simple diester. This example illustrates how one caging group can be removed in the presents of the other.[58] 39

Scheme 2.1 Retrosynthetic plan for the synthesis of the AEA analogues. 41
Scheme 2.2 Attempted synthesis of 2-(4'-methoxyacetophenone)-*N*-(*tert*-butoxycarbonyl)ethylamine 86. *Reagents and conditions*: i. Di-*tert*-butyldicarbonate, CH_2Cl_2, 97%; ii. a. NaH, DMF, 0 °C; b. 2-Bromo-(4'-methoxyacetophenone), DMF, 0 °C→RT. iii. a. NaH, THF, 0 °C; b. 2-Bromo-(4'-methoxyacetophenone), THF, 0 °C → RT. 42
Scheme 2.3 Attempted synthesis of 2-(4'-methoxyacetophenone)-*N*-(benzyloxycarbonyl)ethylamine. *Reagents and conditions*: i. Benzyl chloroformate, 1,4-dioxane:water (1:1), 4-DMAP, triethylamine, 68%; ii. NaH, THF, 0 °C; or 2-Bromo-(4'-methoxyacetophenone), THF, 0 °C → RT. 43
Scheme 2.4 Attempted synthesis of 2-benzyloxy-*N*-(benzyloxycarbonyl)ethylamine. *Reagents and conditions*: i. a. NaH, THF, 0 °C; b. Benzyl bromide, THF, 0 °C → RT. 43
Scheme 2.5 Synthesis of 2-(4'-methoxyacetophenone)-4,5-dihydrooxazole. *Reagents and conditions*: i. a. NaH, DMF, 0 °C; b. 2-Bromo-(4'-methoxyacetophenone), DMF, 0 °C → RT, 18%. 44
Scheme 2.6 Attempted synthesis of 2-benzyloxy-*N*-(benzyloxycarbonyl)ethylamine. *Reagents and conditions*: i. Benzyl chloride, NaOH, CH_2Cl_2, tetrabutylammonium hydrogensulfate/water, reflux. 45
Scheme 2.7 Synthesis of eicosa-5,8,11,14-tetraenoic acid (2-benzyloxyethyl)amide. *Reagents and conditions*: i. Di-*tert*-butyldicarbonate, CH_2Cl_2, 97%; ii. Benzyl chloride, NaOH, CH_2Cl_2, tetrabutylammonium hydrogensulfate/water, reflux, 63%; iii. a. Trifluoroacetic acid; b. Conc. HCl, 55%; iv. a. Arachidonic acid, oxalyl chloride, cat. dry DMF, CH_2Cl_2; b. Triethylamine, CH_2Cl_2, 58%. 46
Scheme 2.8 Attempted synthesis of *O*-2-nitrobenzyloxy-*N*-(*tert*-butoxycarbonyl)ethylamine and 2-(4'-methoxyacetophenone)-*N*-(*tert*-butoxycarbonyl)ethylamine. *Reagents and conditions*: i. 2-Nitrobenzyl chloride, NaOH, CH_2Cl_2, tetrabutylammonium hydrogensulfate/water, reflux; ii. 2-Bromo-(4'-methoxyacetophenone), NaOH, CH_2Cl_2, tetrabutylammonium hydrogensulfate/water, reflux. 48
Scheme 2.9 Synthesis of eicosa-5,8,11,14-tetraenoic acid (2-nitrobenzyloxy-ethyl)amide. *Reagents and conditions*: i. Phthalic anhydride, reflux, 82%; ii. a. NaH, DMF, 0 °C; b. 2-Nitrobenzyl bromide, DMF, 0 °C, then RT, 7%; iii. Hydrazine

hydrate, EtOH, 45 °C; iv. a. Arachidonic acid, oxalyl chloride, cat. dry DMF, CH_2Cl_2; b. Triethylamine, CH_2Cl_2, 35% (over two steps). 48
Scheme 2.10 Synthesis of 2-benzyloxy-*N*-phthaloylethylamine. *Reagents and conditions*: i. a. NaH, DMF, 0 °C; b. 2-nitrobenzyl bromide, DMF, 0 °C → RT, 19%. 49
Scheme 2.11 Synthesis of 2-bromomethyl-2-(4-methoxyphenyl)-1,3-dioxolane. *Reagents and conditions*: i. a. Ethylene glycol, camphor sulfonic acid, dry toluene, reflux into Dean-Stark apparatus, 84%. 50
Scheme 2.12 Attempted synthesis of *O*-2-methoxy(4'-methoxyphenyl)-1,3-dioxolane-2-phthalimidoethyl. *Reagents and conditions*: i. a. NaH, THF, 0 °C; b. 2-Nitrobenzyl bromide, THF, 0 °C → RT; or ii. a. NaH, DMF, 0 °C; b. 2-Nitrobenzyl bromide, DMF, 0 °C → RT. 50
Scheme 2.13 Attempted synthesis of *O*-2-nitrobenzyl-2-phthalimidoethanol. *Reagents and conditions*: i. a. Phthalic anhydride, reflux; b. PBr_3, RT, then 100 °C, 79%; ii. a. 2-nitrobenzyl alcohol, NaH, THF, 0 °C; b. 2-Phthalimidoethyl-2-bromide, THF, 0 °C → RT. 50
Scheme 2.14 Synthesis of 3-methoxy-4-(4,5-dimethoxy-2-nitrobenzyl)-*N*-nonanoylbenzylamine. *Reagents and conditions*: i. Triisopropylsilyl chloride, imidazole, DMF, 80%; ii. Lithium aluminium hydride, Et_2O, 89%; iii. a. DMAP, CH_2Cl_2, 0 °C; b. Pyridine, nonanoyl chloride, 0 °C → RT 69%; iv. Tetrabutylammonium fluoride, THF, 97%; v. a. Potassium *tert*-butoxide, THF; b. 4,5-Dimethoxy-2-nitrobenzyl bromide, 66%. 51
Scheme 2.15 Synthesis of 2-bromo-5-methoxy-4-(4,5-dimethoxy-2-nitrobenzyl)-*N*-nonanoylbenzylamine. *Reagents and conditions*: i. Bromine, CH_2Cl_2, N_2 at -78 °C, 73%; ii. Tetrabutylammonium fluoride, THF, 86%; iii. a. Potassium *tert*-butoxide, THF; b. 4,5-Dimethoxy-2-nitrobenzyl bromide, 53%. 52
Scheme 2.16 *ortho* and *para* directing effect of the methoxy substiunent of 117. 52
Scheme 2.17 Synthesis of 2-bromo-5-methoxy-4-(2-nitrobenzyl)-*N*-nonanoylbenzylamine. *Reagents and conditions*: i. a. Potassium *tert*-butoxide, THF; b. 4,5-Dimethoxy-2-nitrobenzyl bromide, 22%. 53

Scheme 3.1 Proposed photolytic and subsequent dark reaction mechanism for 4,5-dimethoxynitrobenzyl caged capsaicin analogue 118. 66

List of Abbreviations

% v/v	percentage volume by volume
% w/w	percentage weight by weight
°C	degrees Celsius
2-AG	2-arachidonoylglycerol
2-AGE	2-arachidonyl-glyceryl ether, (noladin)
4-DMAP	4-(dimethylamino)pyridine
Å	angstrom
AA	arachidonic acid
Ac	acetyl
AEA	*N*-arachidonoyl ethanolamide, (anandamide)
AMT	anandamide membrane transporter
ATP	adenosine 5'-trisphosphate
Bn	benzyl
BnOH	benzyl alcohol
BOC	*tert*-butoxycarbonyl
cAMP	cyclic adenosine-3', 5'-monophosphate
cat.	catalytic
CB_1	cannabinoid receptor subtype 1
CB_2	cannabinoid receptor subtype 2
Cbz	benzyloxycarbonyl
cm	centimetres
CNS	central nervous system
conc.	concentration
d^6-DMSO	deuterated dimethyl sulfoxide
dm	decimetres
DMF	*N,N*-dimethyl formamide
DMNB	4,5-dimethoxynitrobenzyl
DNA	deoxyribonucleic acid
DNBOC	di(nitrobenzyl)oxycarbonyl
DRG	dorsal root ganglion
EC_{50}	effective concentration for 50% maximum response
EGTA	ethylene glycol bis(β-aminoethylether)-*N,N'*-tetraacetic acid
equiv.	equivalent
Et	ethyl
FAAH	fatty acid amide hydrolase
FTIR	Fourier transform infrared
g	grams
GPCR	G-protein-coupled receptor
h	hours
HEPES	*N*-2-hydroxyethylpiperazine-*N'*-2-ethanesulfonic acid
HPLC	high pressure liquid chromatography
^{i}Bu	*iso*-butyl
^{i}Pr	*iso*-propyl
kDa	kiloDalton
kHz	kiloHertz
Lit.	literature value
M	molar
m/z (CI)	mass spectrometry, chemical ionisation method
m/z (ES-)	mass spectrometry, negative electrospray method
m/z (ES+)	mass spectrometry, positive electrospray method
MAGL	monoacylglycerol lipase
Me	methyl
mg	milligrams
MHz	megaHertz
min	minutes
mJ	millijoules
mmol	millimoles

mol	moles
mOsm	milliosmoles
mp	melting point
mRNA	messenger ribonucleic acid
ms	milliseconds
mV	millivolts
mW	milliwatts
NADA	*N*-arachidonoyl-dopamine
NB	2-nitrobenzyl group
NBOC	nitrobenzyloxycarbonyl
^{n}Bu	*normal*-butyl
nm	nanometres
nM	nanomolar
NMR	nuclear magnetic resonance
NVOC	6-nitroveratroyloxycarbonyl group
OH	hydroxide group
p	pressure
PIP_2	phosphatidylinositol-4,5-bisphosphate
PKA	protein kinase A
PKC	protein kinase C
PLC	phospholipase C
PMA	phosphomolybdic acid
ppm	parts per million
Pr	propyl
R_f	retention factor
RNA	ribonucleic acid
RT	room temperature
RT-PCR	reverse transcription polymerase chain reaction
RTX	resiniferatoxin
S.E.M.	standard error of the means
SARs	structural activity relationships
S_N2	nucleophilic substitution type 2
T.L.C.	thin layer chromatography
TBAF	tetrabutylammonium fluoride
TBAI	tetrabutylammonium iodide
TFA	trifluoroacetic acid
TG	trigeminal ganglion
THF	tertahydrofuran
TIPS	triisopropylsilyl
TMS	tetramethylsilane
TRP	transient receptor potential
TRPV1	transient receptor potential vanilloid subtype1
UV/Vis	ultra violet/visible region
V	volts
ν_{max}	wavelength of maximum absorption (IR)
Vs	versus
W	watts
Δ^9-THC	Δ^9-tetrahydrocannabinol
δ_c	carbon chemical shift (ppm)
δ_H	hydrogen chemical shift (ppm)
ε	extinction coefficient
λ_{max}	wavelength of maximum absorption (UV)
µL	microlitres
µM	micromolar
µmol	micromoles

Introduction

1.1. The endocannabinoid system

The 'cannabinoid receptor' was identified in 1988 by Devane *et al.*[1] through the use of potent cannabinoid agonists developed two years previously. The discovery of the cannabinoid receptor subtype 1 (CB_1) was followed by its cloning in 1990[2] and the discovery and characterisation of a second receptor, the cannabinoid receptor subtype 2 (CB_2), cloned in 1993.[3] The presence of at least two types of cannabinoid receptor in mammalian tissue is now well established and the characterisation of these receptors has led to the unearthing of the endogenous CB_1 and CB_2 agonists *N*-arachidonoyl ethanolamide (anandamide, AEA),[4] 2-arachidonoylglycerol (2-AG)[5] and 2-arachidonylglyceryl ether (noladin ether), which are named 'endocannabinoids'. It is these receptors and the endocannabinoids that comprise and are referred to as, the "endocannabinoid system".

1.1.1. The structure of the CB_1 and CB_2 receptors

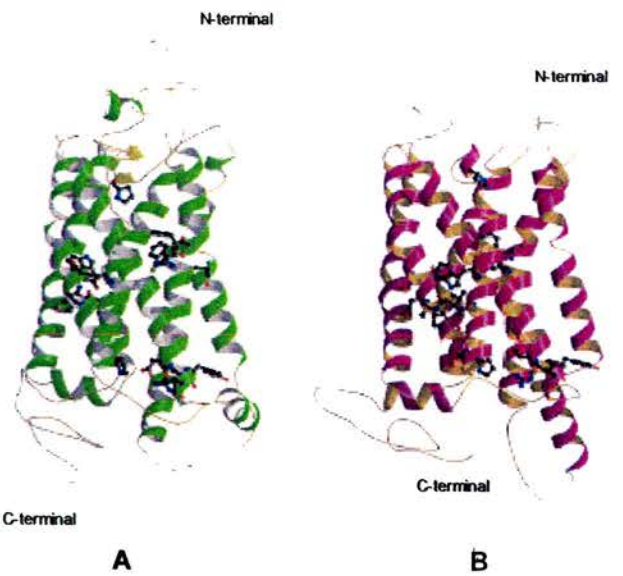

Fig. 1.1 The models of CB_1 (**A**) and CB_2 (**B**) receptors shown as ribbon diagrams. The conserved patterns are shown in the ball-and-stick representation. Figure generated with Molscript and Raster3D.[6]

Figure 1.1 illustrates the structures of the CB_1 (**A**) and CB_2 (**B**) receptors.[6] As members of the G-protein coupled receptor (GPCR) superfamily, most of the key

residues characteristic of these receptor types are conserved in both CB_1 and CB_2. As members of the GPCR family, both CB_1 and CB_2 contain the characteristic seven helical transmembrane domains, which can be envisaged as encircling the membrane bound binding site (Figure 1.2). There is preliminary pharmacological evidence for the existence of additional subtypes of cannabinoid receptor and research on this area is on-going.[7]

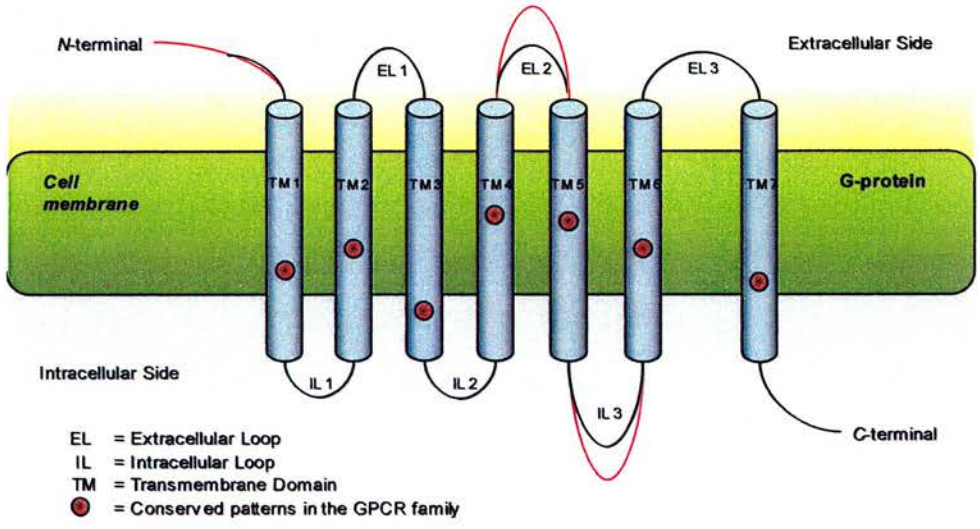

Fig. 1.2 Two-dimensional model of CB_1 and CB_2 receptor. The conserved patterns in the GPCR family are shown as colour cycles. The red lines show the different length in these three areas.[6]

1.1.2. Cannabinoid receptor subtype 1 (CB_1)

The CB_1 receptors are expressed mainly by neurons of the peripheral and central nervous system (CNS) and are found predominantly at the nerve terminals. The role of CB_1 receptors appears to be the modulation or suppression of neuronal release of a range of excitatory and inhibitory transmitters in the brain, generating several prominent physiological properties, such as their ability to impair cognition and memory and to alter the control of motor function.

1.1.2.1. Distribution and Biological properties of CB_1 receptors

Distribution of CB_1 receptors has been characterised in the brains of rat, mouse, bird, primate and human. In all cases the distribution is heterogenous, with the highest densities found in the cerebral cortex, hippocampus (involved in cognition and short-term memory) and substantia nigra (involved in motor function and movement). These findings are in accord with the observed effects of administered cannabinoid agonists such as Δ^9-tetrahydrocannabinol (Δ^9-THC, **1**) (Figure 1.3), which have been shown to effect movement, memory and pain modulation.

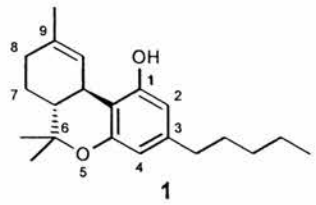

1

Fig. 1.3 The molecular structure of Δ^9-THC, a potent agonist of the CB_1 receptor.

Although CB_1 receptors are expressed mainly in the CNS, they are also found in peripheral tissues in many organs throughout the body. However in all cases, the CB_1 receptor has been shown to function predominantly presynapticly.[8-12]

The density of CB_1 protein is approximately 10-fold higher than that of opioid receptors,[13] and is similar to the density of glutamate receptors. The relevance of this large reserve is that partial agonists such as AEA with low efficacy have the ability to produce a full functional effect. A comparison to this is that of α-adrenergic receptors, where 50% of maximal functional effect occurs at approximately 4% receptor occupancy. Similar results have been reported, where cannabinoid-induced effects were achieved at very low receptor occupancy.[11]

In rodents, cannabinoid drugs are observed to have a "tetrad" of pharmacological effects namely, increased antinociception (hypoalgesia/pain relief), hypothermia (abnormally low body temperature), a decrease in general mobility (sedation), and increased catalepsy (a condition characterised by lack of response to external stimuli and by muscular rigidity seen in physical and psychological disorders such as epilepsy and schizophrenia). Cannabinoids have also been shown to impair

learning and memory in rodents and this indicates the function of endocannabinoids as neuronal modulators.[10,14,15]

It has been found that low doses of both Δ^9-THC and AEA cause hyperlocomotion (increased activity) and high doses cause a decrease in locomotor activity. In mice, both hyperactivity and hypoactivity have been observed, as well as small but significant increases in levels of substance P, dynorphin, enkephalin and glutamic acid decarboxylase. It is suggested that it is the initiation rather than coordination and maintenance of movement processes that are affected by CB_1 deficiency.[11]

The perception of pain comes from the relaying of noxious information to the spinal cord and the brain from primary afferent nociceptors. The nociceptive pathway is complex and pain management can be regulated through interaction at many different levels such as at the peripheral nerves, spinal cord or the brain. It is now clear, as indicated by the use of cannabis for pain relief, that endogenous cannabinoid mechanisms are also involved in the pain pathway and that this system is distinct, but parallel to that involving opiates. The administration of many classes of cannabinoid receptor agonists has demonstrated their antinociceptive and antihyperalgesic effects through behavioural and electrophysiological studies.[10]

Stimulation of presynaptic CB_1 receptors with cannabinoid agonists has been shown to inhibit the release of a number of excitatory or inhibitory neurotransmitters, both in the brain and in the peripheral nervous system. For acetylcholine, noradrenaline, dopamine, 5-hydroxytryptamine, D-aspartate and cholecystokinin this evidence derives from experiments in which release has been directly monitored either *in vivo* or *in vitro*.[16] These findings explain the properties of impaired cognition and memory with regards to administration of agonist cannabinoids.

1.1.3. Cannabinoid receptor subtype 2 (CB_2)

1.1.3.1. Distribution and Biological properties of CB_2 receptors

The distribution of CB_2 receptors is very different to that of CB_1. They are predominantly expressed in peripheral tissues, but have also been found in rodent embryos during the first divisions of the zygote, the later stages of embryogenesis in liver, placental cone and smooth muscle of maternal uterus.[17]

In humans, messenger ribonucleic acid (mRNA) encoding of CB_2 receptor protein has been found in the tonsils, spleen and many types of white blood cells. The tonsils were found to contain the highest concentration of CB_2 mRNA, where occurrence was at levels matching that of CB_1 mRNA in human cerebellum. Other human peripheral tissues where CB_2 mRNA greatly exceeds CB_1 were in the spleen, thymus, pancreas and leukocytes. Of these, B-cells and natural killer cells occurred almost four-fold that of CB_1 and 20-fold in monocytes and spleen. However, smaller amounts of CB_2 mRNA have been found in many other peripheral tissues throughout the body.[12,18]

At present, the characterisation of CB_2 effects is not complete and research in this field is ongoing. However, it is evident that CB_2 receptors do play a large role in the immune system.

To study the effects of CB_2 receptors the gene encoding the protein was knocked out by replacing the entire region with a neomycin resistant cassette, which completely removed the CB_2 gene and its function. Despite this, no differences were observed between wild type and knock out type mice, with regards to immune cell population, though administration of Δ^9-THC did inhibit T-cell activation through macrophages derived from the wild-type, but not in knock out type animals.[11]

Furthermore, peripheral CB_2 receptors have been shown to mediate antinociception in rat models. Injection of a CB_2 receptor agonist AM121 **2** produced antinociception to thermal stimuli but did not produce central cannabinoid effects such as hypothermia, catalepsy or inhibition of locomotor activity (Figure 1.4). This indicates CB_2 receptors as potentially effective analgesic targets, as central cannabinoid CB_1 side effects can be avoided.[19]

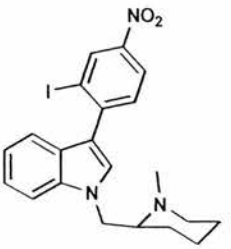

2

Fig. 1.4 The molecular structure of AM1241, a CB_2 receptor agonist.[19]

1.1.4. Activation of cannabinoid receptors

CB_1 and CB_2 receptors are G-protein coupled receptors which exert their effects through a G-protein signalling cascade. Using naturally expressed cannabinoid receptors these cascades have now been mostly characterised. For the mainstream, it has been found that these systems are coupled in the following ways:[12]

(1) Negatively to adenylate cyclase.

(2) Positively to A-type and inwardly rectifying potassium ion channels.

(3) Negatively to N-type and P/Q type calcium ion channels and to D-type potassium channels.

(4) Positively to mitogen-activated protein kinase.

(5) Negatively coupled to postsynaptic M-type potassium channels.

In addition:-

(6) CB_1 receptors may also close $5HT_3$ ion channels.

(7) Modulate nitric oxide production.

(8) Mobilise arachidonic acid (AA) when activated.

(9) Mobilise intracellular calcium stores both in neurons and in smooth muscle cells.

Some of the more important coupling systems are illustrated in (Figure 1.5).

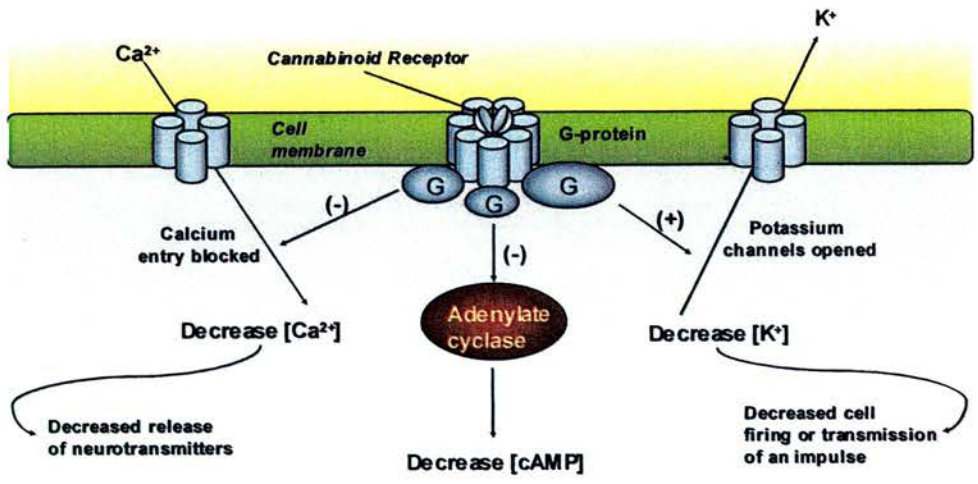

Fig. 1.5 Activation of the cannabinoid receptor can result in several cellular events through a signalling cascade. These events include the reduction of neuron transmitter release by a decrease in cellular Ca^{2+}, a decrease in cell firing by a decrease in cellular K^+ and the reduction in cellular cyclic adenosine 3', 5'-monophosphate (cAMP).

It should be noted that experiments have also revealed other signalling mechanisms within which cannabinoid receptors are implicit. For example, CB_1 receptors have been reported to be positively coupled to phospholipase, activate adenylate cyclase and/or reduce outward potassium K^+ current. Further more, CB_1 receptor signalling does not appear to be the same in all parts of the brain. It has been found that rat hippocampal neurons seem to be negatively coupled to both N- and P/Q-type calcium channels, but in rat striatum they appear to be coupled only to N-type calcium channels or possibly not to calcium channels at all. Similar discrepancies have been observed in other animals.[20]

It is clear that much research is still required in understanding and exploiting the full potential of the CB_1 and CB_2 receptors and for this reason tools to further study this area are greatly needed.

1.1.5. Ligands for the CB_1 and CB_2 receptors

1.1.5.1. Endogenous cannabinoids

After the cloning of the CB_1 receptor in 1990, a search for endogenous ligands became a priority. This soon led to the discovery of anandamide (AEA) by Devane *et al.*[4] in 1992 and this discovery was shortly followed by that of 2-arachidonoylglycerol (2-AG),

a more abundant but less potent cannabinoid. There are now five known endocannabinoids, AEA, 2-AG, 2-arachidonylglyceryl ether (noladin, 2-AGE), *O*-arachidonoylethanolamine (virhodamine) and *N*-arachidonoyldopamine (NADA) (Figure1.6).[5,21-23]

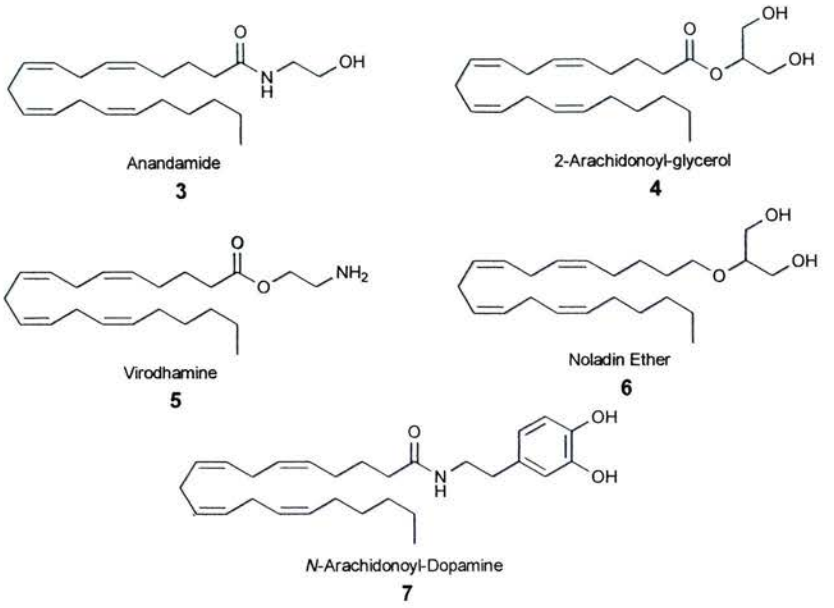

Fig. 1.6 The molecular structures of the five known endogenous cannabinoids.

As agonists, these compounds bind to the receptor to produce a cellular response and possess affinity and efficacy. This is in contrast to antagonists, which are compounds that block the actions of an agonist by binding, but not activating, a given receptor. Antagonists, therefore, possess affinity but lack efficacy (Figure 1.7).

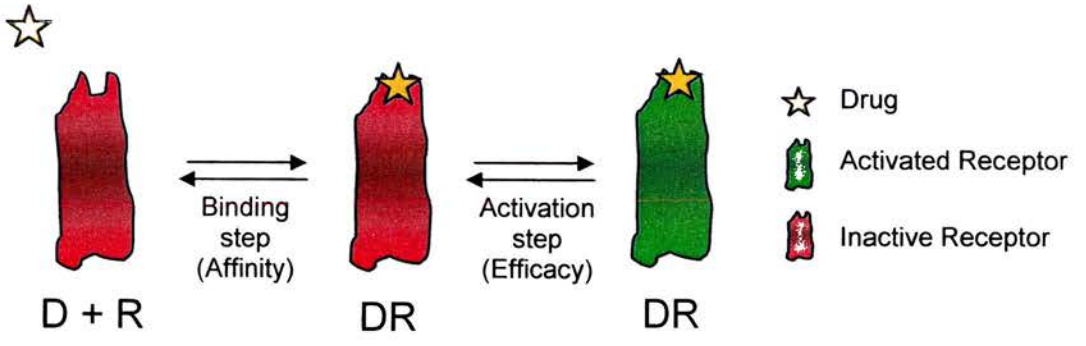

Fig. 1.7 Illustration of affinity and efficacy of a drug.

These endocannabinoids have been compared by De Petrocellis *et al.* and, in summary, it has been found that AEA, 2-AGE and NADA are more selective toward the

CB_1 receptor than CB_2. Likewise, it has been shown that virodhamine is more selective toward CB_2 and 2-AG is equipotent for both receptors.[24]

In the past six years, the biological properties of AEA have been of great interest as it has shown not only to bind to the cannabinoid receptors, but also to the transient receptor potential vanilloid subtype1 (TRPV1) receptor.

1.1.5.2. Anandamide

The first synthesis of anandamide was achieved from arachidonic acid by Devane *et al.*[4] in 1992. However, the need for analogues led to the development of full syntheses from readily available starting materials. In general, synthetic strategies for AEA derivatives have incorporated a linear addition approach, using alkyne units, followed by global reduction of the triple bonds (Figure 1.8).[25-28] These routes are now well established and the use of solid phase methods for the synthesis of libraries of AEA analogues have been employed.[28]

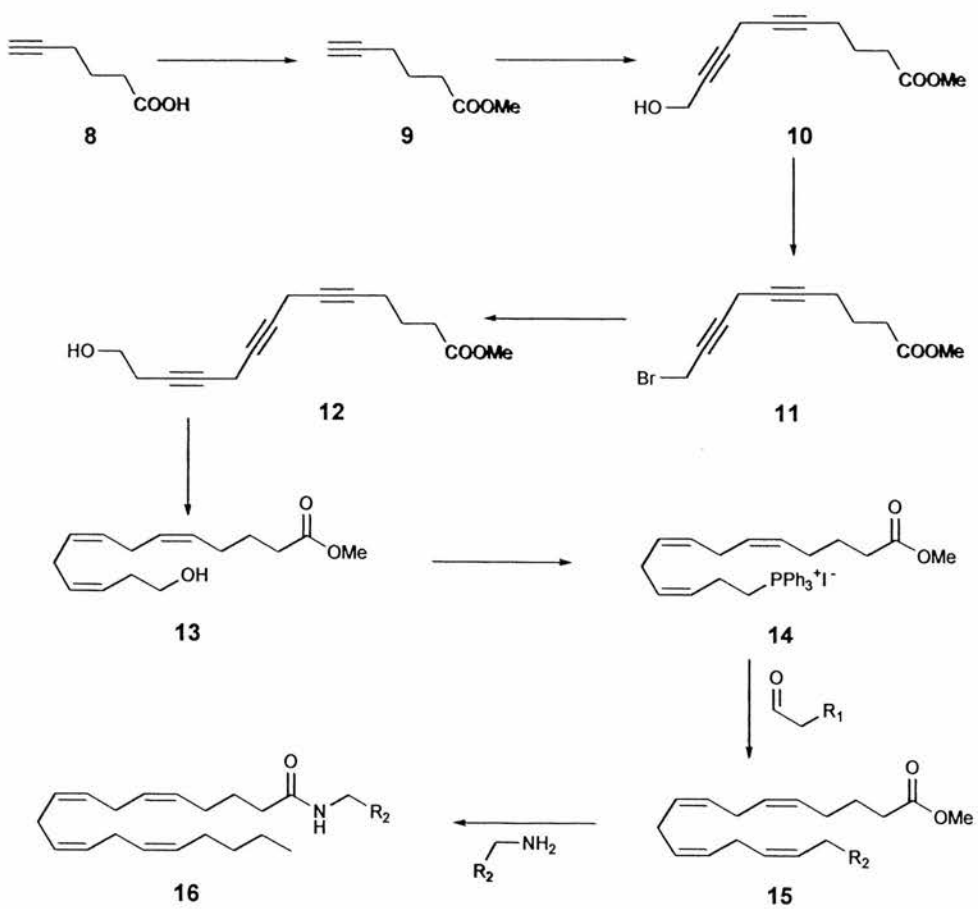

Fig. 1.8 An example of the linear approach used in the synthesis of AEA analogues, O. Dasse.[25]

Anandamide has been shown to bind to CB_1 and CB_2 receptors, through which it exerts its roles as a neurotransmitter and a neuromodulator. It has been proposed that AEA is produced on demand from phospholipid precursors and is released by hydrolysis of *N*-arachidonylphosphatidylethanolamine (Scheme 1.1).[24]

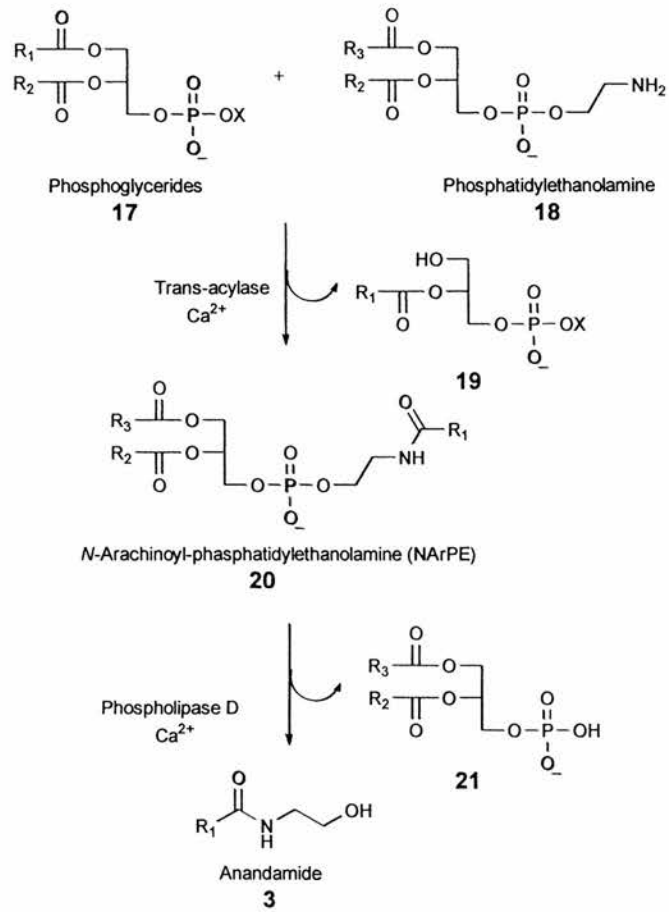

Scheme 1.1 Proposed biosynthesis of anandamide. R_1 denotes the acyl chain in arachidonic acid, R_2 and R_3 are acyl chains of other fatty acids. X denotes the base in phosphoglycerides.[24]

Entry of AEA into neurons is accomplished through both diffusion and more rapidly through transportation by the 'anandamide membrane transporter' (AMT). Here, AEA is subsequently hydrolysed by 'fatty acid amide hydrolase' (FAAH) to AA and ethanolamine. This mechanism of reuptake is shared by all the endocannabinoids (Figure 1.9).

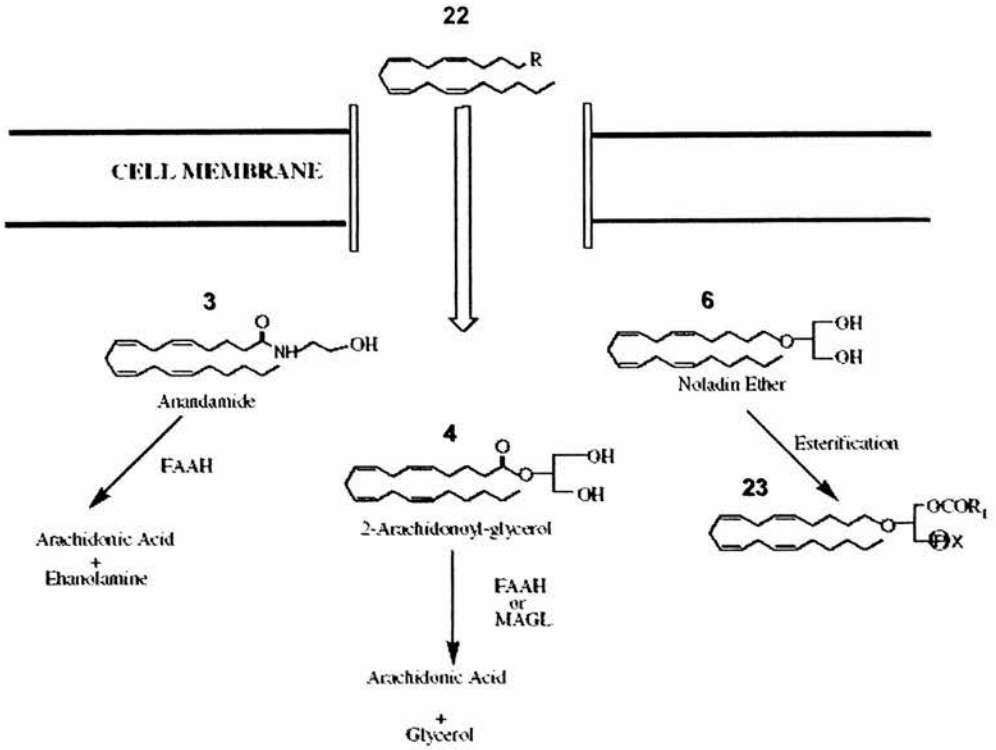

Fig. 1.9 Inactivation (cellular reuptake and intracellular metabolism) of anandamide and 2-arachidonoylglycerol (2-AG). P denotes a phosphate group, R the head group of the endocannabinoid, R_1 the acyl chain of other fatty acids and X the base in phosphoglycerides. Monoacylglycerol lipase (MAGL).[24]

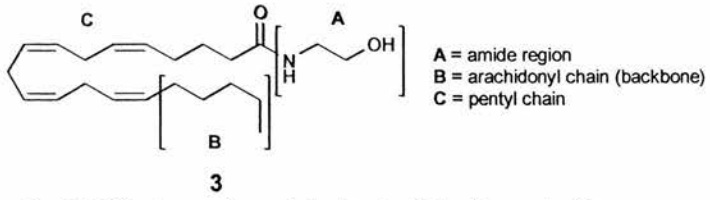

3

Fig. 1.10 The key regions of structural activity of anandamide.

Detailed structure activity relationship studies of the action of the AEA analogues on the cannabinoid receptors have also been carried out.[29,30] The key elements to activity include mono-substitution of the amide, where alkyl, fluoroalkyl or a hydroxyalkyl were found to increase activity. Amongst these derivatives, optimal activity was obtained with two or three carbon chain length extension (Figure 1.10). Substitution of the hydroxyl group with methyl ether, phenyl ether or phosphate groups was found to decrease activity and introduction of amino, carboxylic acid or more bulky moieties destroyed activity all together.

Branching at the α-carbon and in the ethanolamine moiety, with a methyl group being optimal, retains activity and increases resistance to metabolism by FAAH. With regards to the arachidonyl moiety of AEA, the number of double bonds required to retain activity in a twenty carbon chain is three or four. Finally, the number of methylene units

in the C_5H_9 chain is also important for activity. Reducing the chain by two methylenes dramatically reduces or removes activity of AEA analogues, though increasing the number of methylenes by two retains activity.[30]

AEA has also been shown to activate the TRPV1 receptor. Indeed, SARs studies of AEA analogues toward the TRPV1 receptor have also been conducted.[31] These studies showed that lengthening or shortening of the arachidonyl chain by two carbons or the reduction of the number of double bonds in the chain by two had little effect on the affinity of the AEA analogues toward TRPV1.

In studies conducted by De Petrocellis *et al.*,[24] the average potency of AEA was found to be 5-20 fold lower for TRPV1 than its potency toward CB_1 receptors in heterologous expression systems.[24] Another interesting study showed that, given TRPV1 is activated by AEA on the cytosolic side of the receptor, the biosynthesis of the AEA in cells expressing TRPV1 such as sensory and central neurons and epithelial cells, can first activate TRPV1 prior to release from the cell and then exert its biological activity on CB_1 receptors on nearby neurons.[24] Expression of these receptors is found to be equivalent in certain cell types. There is now growing evidence that in some cells these receptors have intrinsic relationships with each other, which have yet to be determined.

Although there are many cannabinoid agonists and antagonists for use in studying CB_1 and CB_2, AEA's ability to active these and the TRPV1 receptors, make it a compound of particular interest and the need for molecular tools to study its biological activity is imperative.

1.2. Capsaicin and the TRPV1 Receptor

The TRPV1, is a member of the TRP channel family and was cloned in 1997.[32] Currently there are six subfamilies of TRP receptors (TRPA, TRPC, TRPM, TRPN, TRPP and TRPV), of which the TRPV subtype has a further six subtypes TRPV1-6. Of these, TRPV1 shares most similarity of amino acid sequence with TRPV2 (46%), TRPV3 (43%) and TRPV4 (43%). Only TRPV1 is activated by capsaicin.

1.2.1. The structure and binding sites of the TRPV1 receptor

The TRPV1 receptor is a ~95-kDa protein consisting of six transmembrane domains, characteristic of the TRP channel family. Studies have shown that the second and third segments and especially the protein loop connecting these segments are involved in the binding of the potent receptor agonist capsaicin. Indeed, when these segments were mutated, affinity for both capsaicin and resiniferatoxin (RTX) (another potent agonist of TRPV1) was completely removed.[33] Furthermore, it is interesting to note that unlike other ligand-gated channels involved in fast synaptic transmission, these binding sites are thought to be intracellular, thus activation by capsaicin and other ligands may only occur when inside the cell (Figure 1.11).[34]

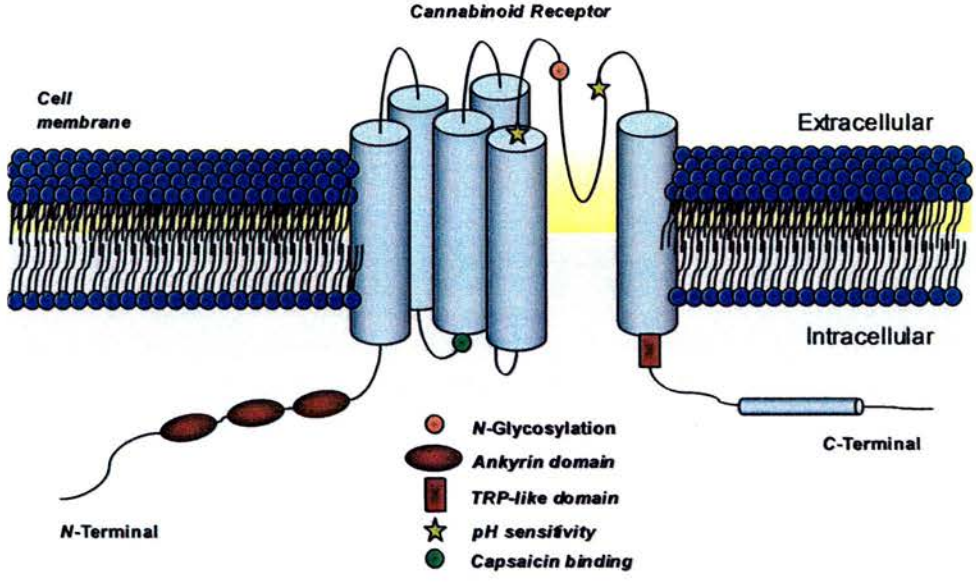

Fig. 1.11 Topological organization of a TRPV1 channel subunit. The model consists of an *N*-terminal domain containing three ankyrin units and a phosphorylation site for protein kinase A. There are six transmembrane domains and a large stretch connecting the S5 and S6 membrane segments, which give rise to the pH sensitive areas of the receptor. The cytosolic *C*-terminus domain carries the calmodulin and phosphatydylinositol-4,5-bisphosphate (PIP_2) binding sites. [34]

The receptor also has a pore region formed by S5-P-S6, were S5 and S6 are the fifth and sixth segments and P represents the loop that connects the two. This pore region is thought to consist of a tetramer of subunits, where the 6th segment forms the inner pore helix and the loops are involved in the selectivity of the channel (Figure 1.12). It is this region that is involved in receptor activation within environments of pH < 5.5 and this is consistent with findings that the P loop contains acidic amino acid residues.

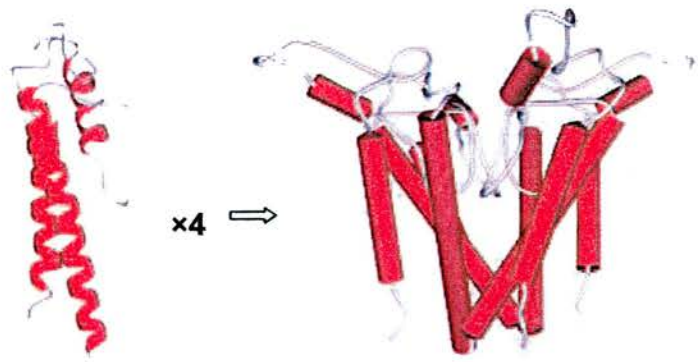

Fig. 1.12 A plausible structural model of the TRPV1 pore module. Secondary and tertiary structure of the S5-P-S6 motif of a TRPV1 subunit (left); the functional channel would be formed by the assembly of four identical subunits around a central aqueous pore (right). The P-loop configures the narrowest part of the pore conduit at the extracellular side, whereas the S6 segment is the inner α-helix that structures the walls of the pore at the cytosolic side. Taken from Ferrer-Montiel *et al.*[34]

1.2.2. Distribution of the TRPV1 receptor

Within cells TRPV1 receptors are found to be localised in at least three areas. These include the cytoplasmic membrane, endoplasmic reticulum and cytoplasmic vesicles. The presence of TRPV1 in the cytoplasmic membrane is expected, as this coincides with the observed TRPV1 effects of inward currents or transmitter release. However, the presence of TRPV1 in the cytoplasmic reticulum has not yet been fully characterised, although they are thought to be involved in Ca^{2+} regulation.

The distribution of TRPV1 receptors in tissues has been well characterised using techniques such as radioactive ligand-binding, reverse transcription polymerase chain reaction (RT-PCR) and various staining techniques such as the Northern blot stain. The majority of TRPV1 expression is in small nociceptive cells expressing substance P, found in the dorsal root and trigeminal ganglion (DRG/TG), where 33-50% of these cells are located. On these cells, TRPV1 receptors are expressed along the entire neuron, from the peripheral terminals, along the axons to the somata and addition the TRPV1 receptors are found in free nerve endings. This is in concurrence with the nociceptive role played by TRPV1 receptors.[35] Second to this localization, TRPV1 receptors are also found in vagal afferents in jugular and nodose ganglion neurons. TRPV1 receptors are thus found in tissues such as the skin *via* free nerve endings of primary sensory neurons, the CNS and the spinal cord.

Although TRPV1 receptors are associated with primary sensor neurons, they have also been observed in a range of other neuronal and non-neuronal cells. TRPV1 receptors have also been identified in cells of the inner ear, gastric and urinary epithelial, bladder smooth muscle, prostate and macrophages. They are also present in superficial fibres along the airway such as the mucosa or deep pulmonary fibres of the alveolar septa and involved in circulation as they are expressed in the sensory fibres of the myocardium and perivascular plexi of coronary arteries.

1.2.3. Biological properties of the TRPV1 receptor

The TRPV1 receptor is involved in numerous pathological conditions, of which only some are adequately characterised. Heat hyperalgesia, is the perception of a burning pain, and is strongly associated with the activation of the TRPV1 receptor and the subsequent inflammatory response. Using TRPV1 knock-out and wild type mice, it has been shown that although inflammation reduced the threshold for heat-evoked pain-related responses in wild type mice, this response was not observed in mice lacking the TRPV1 receptor.[36] There are currently two theories of how TRPV1 receptors are activated in this instance. Firstly, the effect is thought to be a result of inflammatory mediators such bradykinin and adenosine 5'-trisphosphate (ATP) that activate their own receptors, which causes the release of intracellular systems involving protein kinase A (PKA), protein kinase C (PKC) and phospholipase C (PLC). These in turn lower the heat threshold and open the TRPV1 channel. The second idea is the combination of several activators and/or endogenous ligands such as heat >42 °C and acidic conditions cause activation.[37] Recently, TRPV1 has also been associated with a role in diabetic heat hyperalgesia. This coincides with the finding that insulin activates the TRPV1 receptor and in certain neuronal cells co-expression of TRPV1 and the insulin receptor is observed.[37]

The function of TRPV1 in the gastrointestinal tract is one of maintenance. Here the receptor is involved in the thickening of the protective mucus layer present in the stomach and duodenum by a system that detects harmful compounds such as acid and activated enzymes. Interestingly, studies on cells expressing TRPV1 in the gastric

epithelium have shown that activators such as acid (pH 4.0) and ethanol (10%) cause cell damage, yet activators such as vanilloids, capsaicin and resiniferatoxin concentration-dependently prevent these harmful activators. Comparison of these receptors, with TRPV1 from primary sensory neurons has shown 99.8% similarity. These findings suggest that very slight differences in the TRPV1 structure can considerably change its role.[37]

1.2.4. Activation of the TRPV1 receptor

The TRPV1 receptor is a ligand-gated cation selective ion channel that can be activated by several mechanisms and can generate a number of responses depending on the type of cell where it is expressed. In general, activation of the receptor can be achieved by heat above 42 °C, pH < 5.5 and by many endogenous ligands including bradykinin, ATP, AEA and NADA. Phosphorylation of TRPV1 by Ca^{2+}-calmodulin-dependent kinase II is required for ligand binding to TRPV1 and various kinases such as protein kinase A and C modulate the receptors activity. TRPV1 can also be activated by capsaicin, a potent agonist and other noxious compounds such as RTX (Figure 1.13).

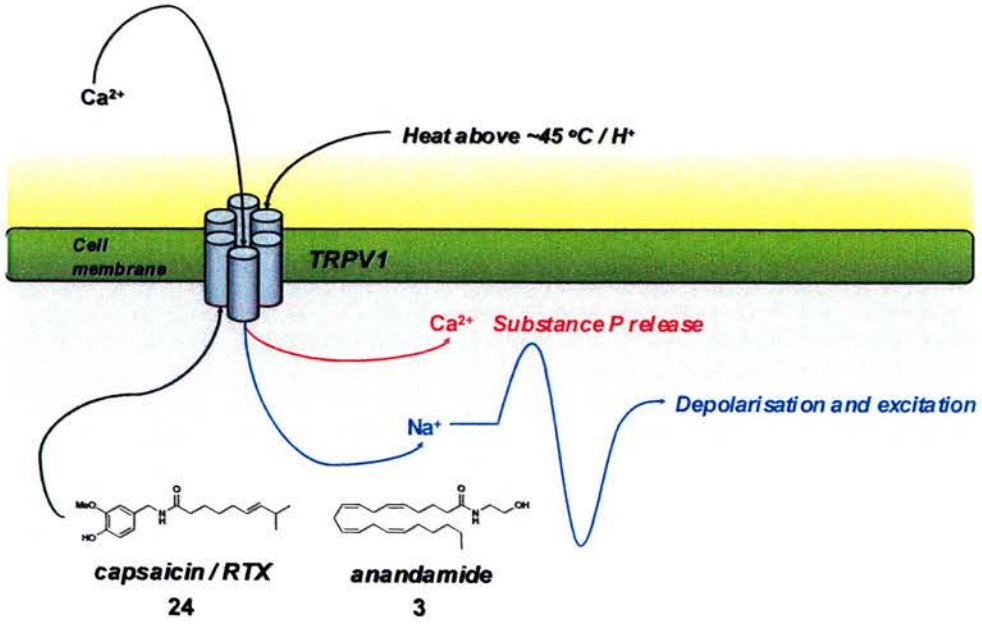

Fig. 1.13 An illustration showing the activation of a TRPV1 receptor. The receptor is known to be activated by heat ~42 °C, a pH < 5.5, capsaicin and analogues, resiniferatoxin (RTX) and anandamide. Activation results in a localized effect by substance P release and an acute effect by cell signalling.

Activation of TRPV1 leads to the opening of the ligand-gated cation channel and an inward current of Ca^{2+} is generated. As a result, two major effects are observed. The first is the deplorisation and excitation of the cell resulting in a neural impulse to the brain, which is thereby interrupted as pain (nociception).The second effect is the release of the inflammatory agent, substance P induced by the increased concentration of intracellular calcium.

1.2.5. Capsaicin

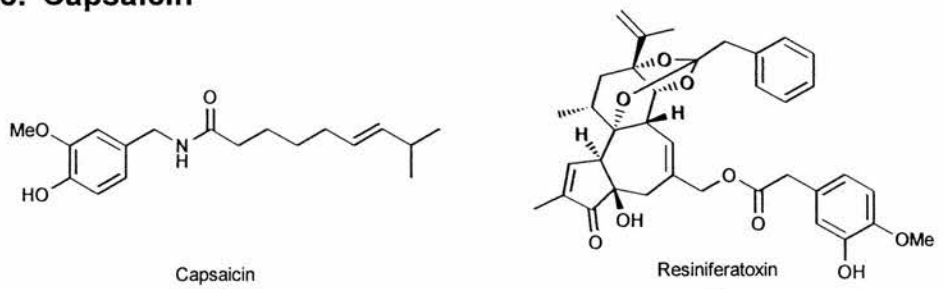

Capsaicin
24

Resiniferatoxin
25

Fig. 1.14 The molecular structures of capsaicin and resiniferatoxin (RTX), potent agonists of the TRPV1 receptor.

Hot chilli peppers have been a spicy ingredient in foods around the world for over 500 years and were cultivated in South America for many years previously. The "spiciness" of the chilli pepper originates from the pungent molecule 'capsaicin' **24**, which is an extremely successful deterrent in chilli pepper plants. Indeed, the burning pain sensation experienced by humans on eating this ingredient is not as profound as that experienced by other mammals.

It is now established that capsaicin **24** (Figure 1.14) exerts its biological effects by acting as an agonist at TRPV1. Activation of TRPV1 by capsaicin opens the cation selective channel to both monovalent and divalent cations such as Na^+, K^+, Cs^+ and Ca^{2+}. Given the distribution of TRPV1, it is not surprising that capsaicin has effects such as skin, mouth and eye irritation/burning, stinging, coughing, sneezing, bronchoconstriction and several forms of inflammatory heat hyperalgesia.

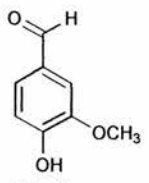

Vanillin
26

Fig. 1.15 Molecular structure of vanillin.

Capsaicin has a low melting point, significant hydrophobicity and is classed as a 'vanilloid', as it is structurally related to vanillin **26** (Figure 1.15). The structure of capsaicin was first identified and reported in 1919 by Nelson and the first total synthesis achieved by Späth and Darling eleven years later.[38,39] Detailed structural activity relationships SARs studies, in particular those conducted by C. S. J. Walpole *et al.*, have led to numerous analogues of capsaicin, some of which possess greater potency than capsaicin itself (Figure 1.16).[40-43]

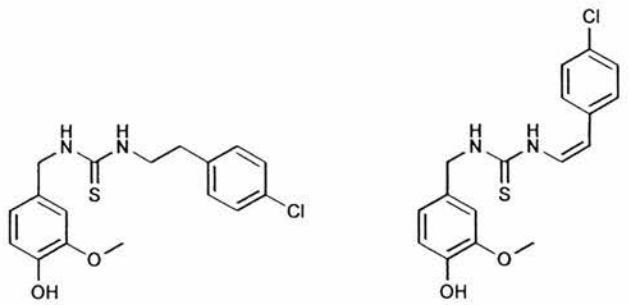

27 **28**

Fig. 1.16 Molecular structures of two analogues of capsaicin.[43]

Comparison of the effective concentration for 50% maximum response (EC_{50}) values as judged by Ca^{2+} uptake shows that these analogues have a 5-8 fold increase in potency compared to capsaicin. However, these analogues are still significantly less active than the ultra potent TRPV1 activator, resiniferatoxin (RTX) **25** (Figure 1.17).

Compound	(EC_{50}, nM)
Capsaicin	300 ± 40
27	56 ± 16
28	41 ± 3
RTX	1.6 ± 0.1

Fig. 1.17 Comparison of EC_{50} (nM) values of capsaicin, two analogues of capsaicin and RTX.[43]

Although RTX **25** has some structural similarities to capsaicin **24**, such as the 3-methoxy-4-hydroxybenzyl moiety, SARs conducted on RTX have actually shown that

the 4-hydroxy position, vital for the biological activity of capsaicin, has little influence on the activity of RTX and that it is the 5-membered ring that is of most importance for the potency observed from RTX.[43] As well as being a potent agonist, capsaicin very quickly desensitises TRPV1 receptors. i.e. loss of activity even though the agonist remains bound to the receptor. These effects have been shown to be both short and long-term, thus giving reason for the use of capsaicin in treating chronic pain conditions such as diabetic neuropathy, osteoarthritis and urinary incontinence. Indeed, several drugs with capsaicin as the topical component are in use, such as Stimurub, Heat, Capsoderma, Axsain and Zostrix used in the treatment of muscle ache.

Desensitisation of the TRPV1 receptor to capsaicin is thought to occur as a result of nerve terminal degradation caused by excessive depolarisation and by the influx and accumulation of intracellular calcium. This has focused research in the past three years to developing antagonists rather than agonists of TRPV1, so that the analgesic properties desired can be obtained without the damaging and irritating side effects. There are now a number of TRPV1 receptor antagonists, such as SB-36679 **30** which is a competitive antagonist at TRPV1 and has potency greater than that of the first competitive vanilloid antagonist capsazepine **29** (Figure 1.18).[44,45]

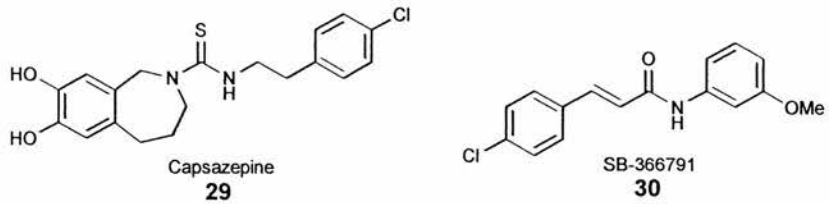

Fig. 1.18 The molecular structures of capsazepine and SB-366791, potent antagonists of the TRPV1 receptor.

In the 1990s, a large study was conducted on SARs of capsaicin toward TRPV1. In these experiments the SARs were described in terms of three regions of importance, these being the aromatic region A, the amide bond region B and the hydrophobic side-chain region C (Figure 1.19).[40-42]

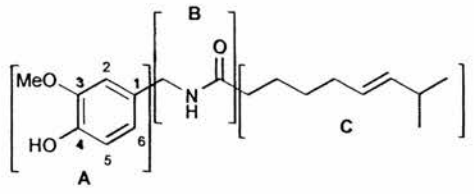

Capsaicin
24

Fig. 1.19 The molecular structure of capsaicin sectioned into three regions of SAR importance: Aromatic region A, amide bond region B and the hydrophobic side-chain region C.

For each region, Walpole *et al.* synthesised a small library of compounds with subtle systematic structural variations to help identify the optimal structure for that region.[40-42]

These studies showed that in the A region, removal or alkylation of the hydroxyl group at the 4-position leads to reduction or loss of activity. Furthermore, substitution at the 2, 5 and 6 positions of the ring yields inactive or poorly active compounds and any variation of the methoxy group at the 3-postion reduces activity. Overall, it is the hydroxyl group at the 4-position which is of most importance as activity is almost entirely dependent upon it. Hence, the most potent analogues contained the 3-methoxy-4-hydroxybenzyl moiety.[40]

Variations such as chain length, *N*-methylation and heteroatom exchange in region B were incorporated in the library of analogues. The results with these analogues indicated that increasing the number of carbons present between the amide moiety and region A, leads to reduced activity. The studies also showed that *N*-methylation reduced or removed activity. Furthermore, the introduction of additional hydrogen-bond donors and/or acceptors tended to partially reduce activity. However, one analogue **31** was found to be more potent than capsaicin and was suggested to incorporate a hydrogen-bonding pseudo-cyclic conformation (Figure 1.20).

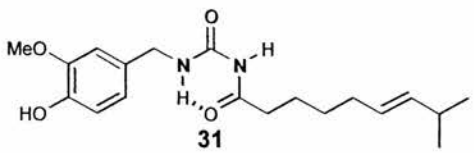

31

Fig. 1.20 The molecular structure of a potent capsaicin analogue with a pseudo-cyclic conformation.

The SAR studies conducted on region C, included varying the chain length, the extent of chain branching and introduction of polar moieties at the end of the chain.

From these studies it was determined that the most important factor on activity was the overall size and/or hydrophobicity of the chain. In general, activity was lost when chain lengths varied from between 5 and 10 carbons in size and when long polar moieties were present.

On the whole, the experiments conducted by the Walpole *et al.* showed that both the phenol and the length of the side chain of capsaicin **24** are essential in activation of TRPV1 receptors.[35,40-42] Thus, an extremely potent capsaicin derivative **32** has been employed in this project (Figure 1.21).[46]

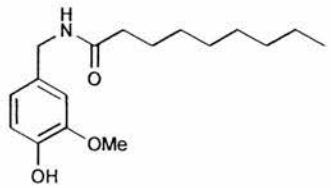

32

Fig. 1.21 The molecule structure of 4-hydroxy-3-methoxy-*N*-nonanoylbenzylamine, an extremely potent capsaicin derivative.

Although there is now an array of agonists and antagonists available to elucidate the actions of TRPV1, other tools to study the role of TRPV1 in cellular signalling are scarce. One method of studying receptors is by using caging groups, which allow the temporal and spatial properties of a biologically active molecule to be controlled. This technique has been incorporated in studying several other receptors but currently there are very few caged compounds available to study the TRPV1 receptor.

1.3. Caging Groups

1.3.1. Introduction

The term 'caging' refers to the use of a photolabile protecting group to mask a functional group of a biologically active compound. On irradiation by light of a specific wavelength the group is photolysed to reveal the molecule of interest. Caged compounds allow temporal and spatial control over the release of the given molecule and hence activation of its biological target. The advantage of such a group has been a driving force in the past two decades in the development of caged compounds for use as tools in studying biological processes.[47] Another advantage of using caging groups is that they don't require any chemical reagents for cleavage. The use of non-photolabile

protecting groups means reagent conditions are very specific as biological compounds often require the use of a variety of protecting groups toward their synthesis and these can now be avoided.

By using caged analogues of active molecules the temporal and spatial control of compound release can be achieved and the biological process studied in 'real time'. In this context, it is also important that the caged analogue is biologically inert to the system being studied and that the uncaging process does not produce fragments that can activate the receptor. This has resulted in the very careful design of caging groups and has led to a number of photolabile protecting groups with specific mechanisms and breakdown pathways.

In biological studies, caging involves the masking of a specific functional group on an active compound. The choice of the functional group protected is important as it should remove the biological activity of the compound (Figure 1.22 and 1.23).

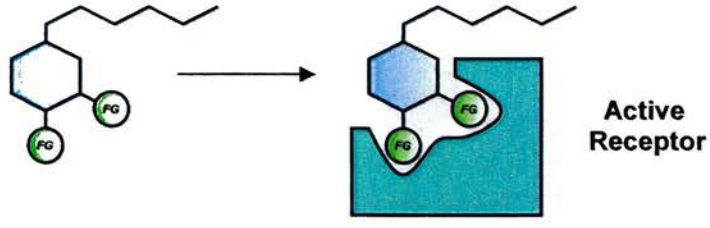

Fig. 1.22 A cartoon representing the activation of a receptor by a biologically active molecule.

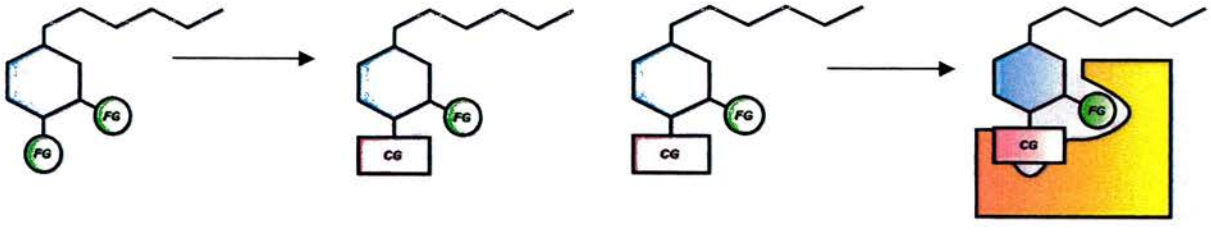

Fig. 1.23 A cartoon showing the caging of a biologically active compound and its subsequent inertness to its specific ligand.

In vitro photolytic cleavage is achieved by the absorption of a photon of light of a specific wavelength and results in the excitation of a functional group, which ultimately leads to the breaking of a chemical bond and the unveiling of the biologically active compound (Figure 1.24).

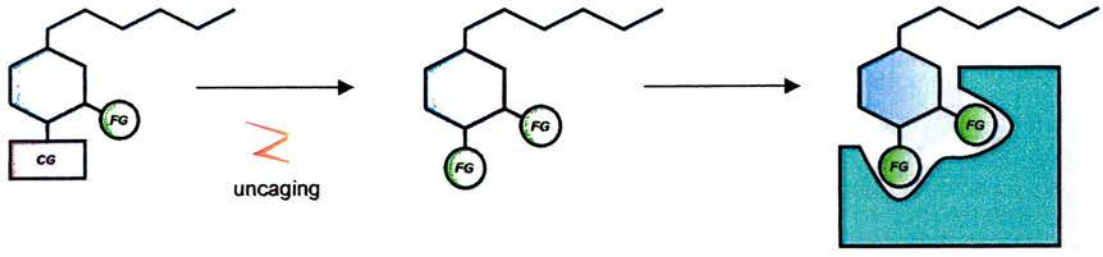

Fig. 1.24 A cartoon representing uncaging of a biologically active compound within a cell by photolysis and its subsequent activation of its specific ligand.

Caged agonists and antagonists have already proven to be very useful in the study of several important molecules such as nucleotides and neurotransmitters as well as receptors. For example the ATP caged analogue P^3-1-(2-nitrophenyl)ethyl ester adenosine 5'-triphosphate **33**, unveils ATP within milliseconds of flash photolysis (Scheme 1.2).[48]

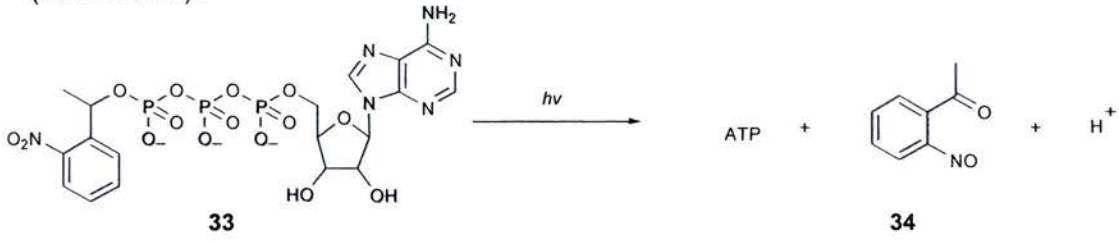

33 **34**

Scheme 1.2 Photolysis of caged ATP, resulting in the release of the biologically active compound ATP and two by-products, 2-nitrobenzyaldehyde and a proton.[47]

Other important molecules that have been successfully caged are acetylcholine (with 4,5-dimethoxy-[2-nitrobenzyl]) and glutamate (with [2-nitrophenyl]ethyl). The latter has been found to be of particular use as it lacks any agonist or antagonist activity and is resistant to hydrolytic release of glutamate. (Figure 1.25)

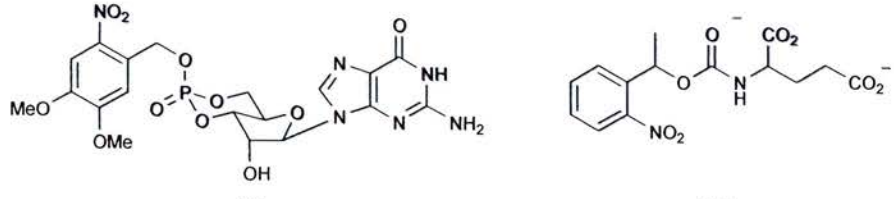

35 **36**

Fig. 1.25 The molecular structures of caged acetylcholine and caged glutamate.[47]

1.3.2. Popular caging groups and their mode of action

There are now a variety of caging molecules available for a number of functional groups. Each caging group has its own specific excitation wavelength and subsequent

'dark reactions'. These are named so, due to the fact that after the initial photon absorption and excitation, no further energy or excitations are required for the release of the caged molecule. In general most caging groups have been developed to be photolabile in the near-UV radiation region between 260 nm and 360 nm. The reason being, that in a biological context, cell damage is caused at wavelengths < 300 nm, due to high absorption in this region by nucleotides and proteins.[47] As a result, caging groups are often found to contain 2-nitrobenzyl and keto-groups as they absorb between 260 nm and 360 nm.

One of the most successful families of caging group is the *ortho*-nitrobenzyl alcohol group. This includes the popular 6-nitroveratroyloxycarbonyl group (NVOC) (used to protect carbamates, carbonates, hydroxy groups, esters and amines),[49] nitrobenzyloxycarbonyl (NBOC) (used for hydroxy groups), di(nitrobenzyl)oxycarbonyl (DNBOC) (used for carboxylic acids), 4,5-dimethoxynitrobenzyl (DMNB) (used to protect phenols) and 2-nitrobenzyl group (NB) (used to protect phosphates, amines and hydroxy groups) (Figure 1.26). Photolysis of these compounds follows a similar mechanism to yield the desired product, *ortho*-nitrosobenzaldehyde and in some cases CO_2.

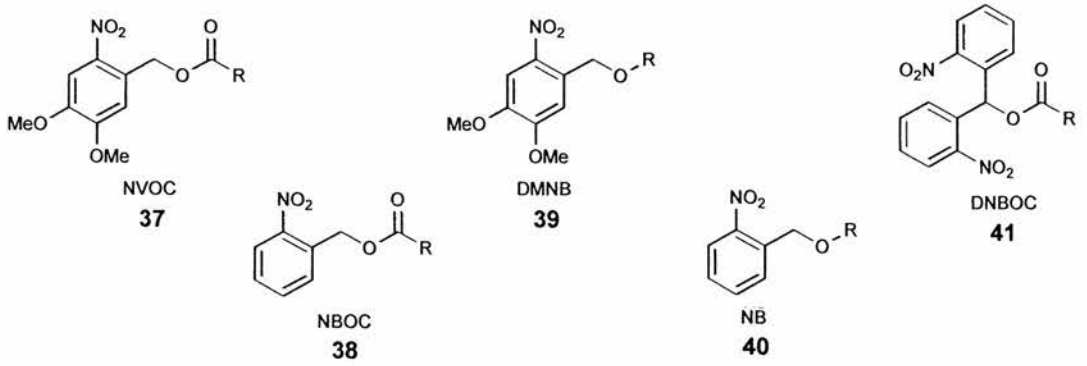

Fig. 1.26 The molecular structures of several *ortho*-nitrobenzyl alcohol caging groups.

Of particular interest is the 2-nitrobenzyl group (NB) **40** which is photolabile at around 260 nm and has been incorporated as a photoremovable protecting group in synthesis, in photolithography (DNA microarrays) and in biochemistry ("Caged compounds").[50,51] The group has been successfully used in caging histidine, several carbohydrates, 5-fluorouracil (an antitumor prodrug) and in the synthesis of several nucleotides.[52,53]

There has been much debate regarding the mechanism by which uncaging of 2-nitrobenzyl compounds occurs, especially with regards to the fate of the aci-nitro intermediate (Scheme 1.3). Upon illumination to light of λ = 260 nm, the nitro group is excited and a diradical state is proposed. This then readily undergoes a 1,5-hydrogen shift to form the aci-nitro intermediate.

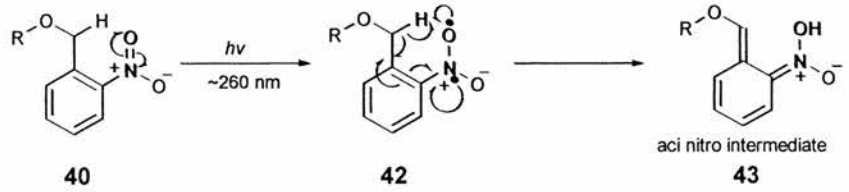

40 **42** **43**

Scheme 1.3 Proposed photolytic activation of the 2-nitrobenzyl caging group and the resulting formation of the aci-nitro intermediate.[52,50]

The most recent and up to date proposal for the subsequent 'dark reactions' is shown in Scheme 1.4, where the aci-nitro resonance forms can cyclise or be attacked by a nucleophile and then breakdown to form a common intermediate (C), which itself then undergoes reduction to form the observed *ortho*-nitrosobenzaldehyde.[50]

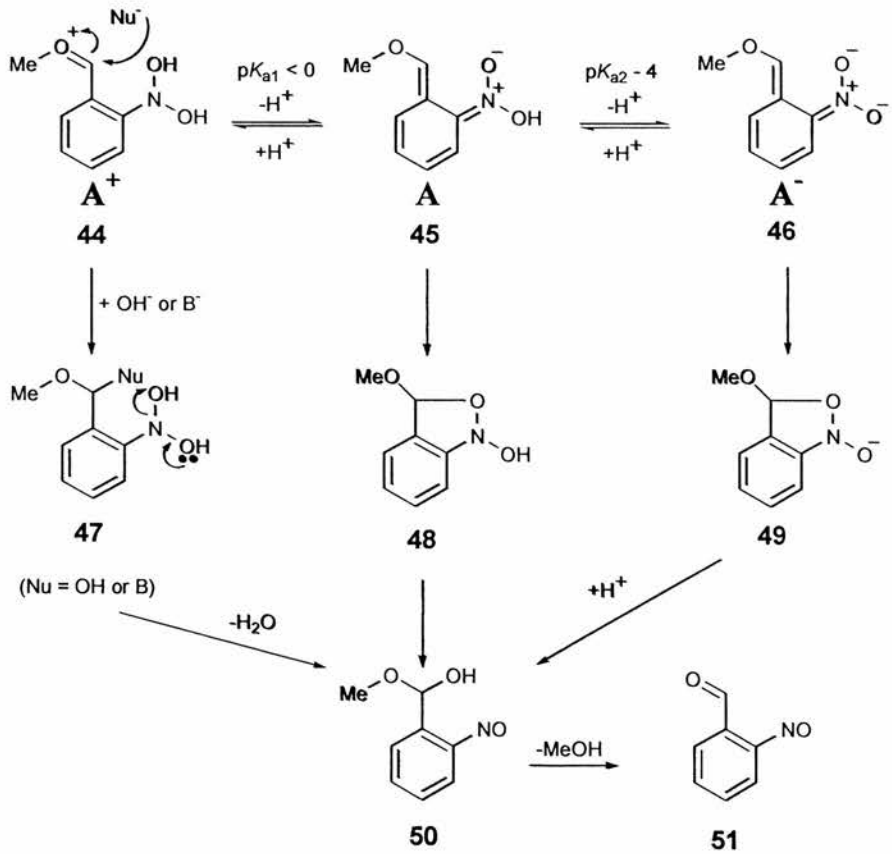

44 **45** **46**

47 **48** **49**

50 **51**

Scheme 1.4 Current proposed mechanism for the thermal reactions of the primary photochemical aci-transients **A**, formed from photolysis of 2-nitrobenzyl caging groups in aqueous solution.[50]

It is thought that the other members of the 2-nitrobenzyl caging family follow similar uncaging mechanisms in their photolysis.

Another caging group is 4-methoxyacetophenone **58**. This compound's use is less common, but it can liberate carboxylic acids or hydroxyl groups upon photolysis. It was previously reported as a protecting group for sodium thiophenoxide, widely used in the caging of phosphates and has the advantage of generally biologically inert side products.[53-55]

The mechanism for photolysis of 4-methoxyacetophenone is also under debate and suggested mechanisms for the analogous 4-hydroxyphenacyl photolysis have been described most recently by Zhang *et al.* shown in Scheme 1.5.[56]

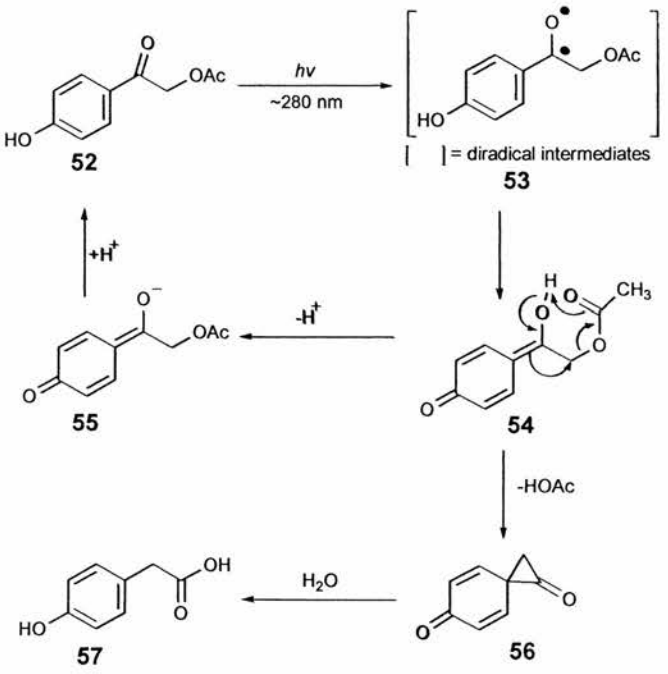

Scheme 1.5 Latest proposed mechanism for the photolysis of the 4-hydroxyphenacyl caging group.[56]

With this mechanism in mind, a proposal for the breakdown of 4-methoxyacetophenone **58** is shown in (Scheme 1.6).

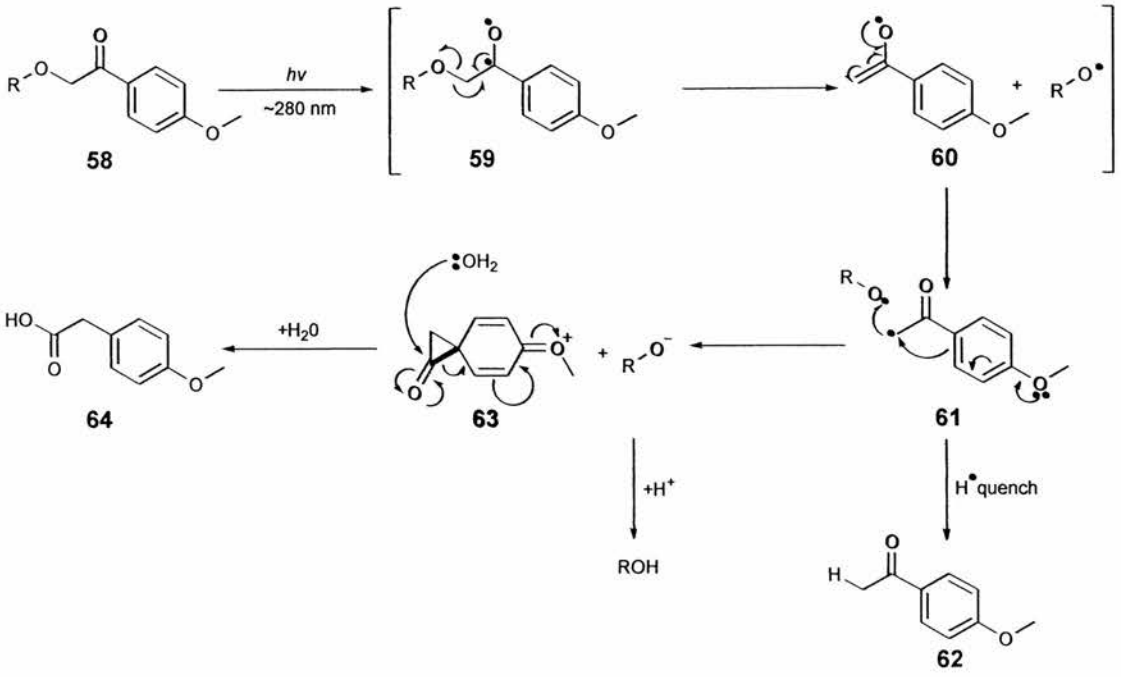

Scheme 1.6 Proposed mechanism for photolysis of the 4-methoxyacetophenone caging group. The arrows on structure **61** correspond to the pathway leading to phenylacetic acid **64**.[56,57]

1.3.3. Orthogonal caging

The term 'orthogonality' refers to the selective cleavage of one protecting group in the presence of another. In photo-chemistry 'wavelength orthogonality' is a growing aspiration and the ability to remove one caging group in the presence of another is highly sought. Currently, there are few examples of wavelength orthogonality, but one early and elegant demonstration of orthogonality, is that by Blanc and Bochet.[58] In these experiments, two caging groups (a nitroveratrole and benzoin ester), were incorporated in two sets of experiments.

The first set of experiments demonstrated intermolecular discrimination in photolysis by subjecting a 1:1 mixture of two differently caged carboxylic acids, dodecanoic acid 4,5-dimethoxy-2-nitrobenzyl ester **65** and dodecanoic acid 1-(3,5-dimethoxyphenyl)-2-oxo-2-phenylethyl ester **66** to irradiation (Scheme 1.7).

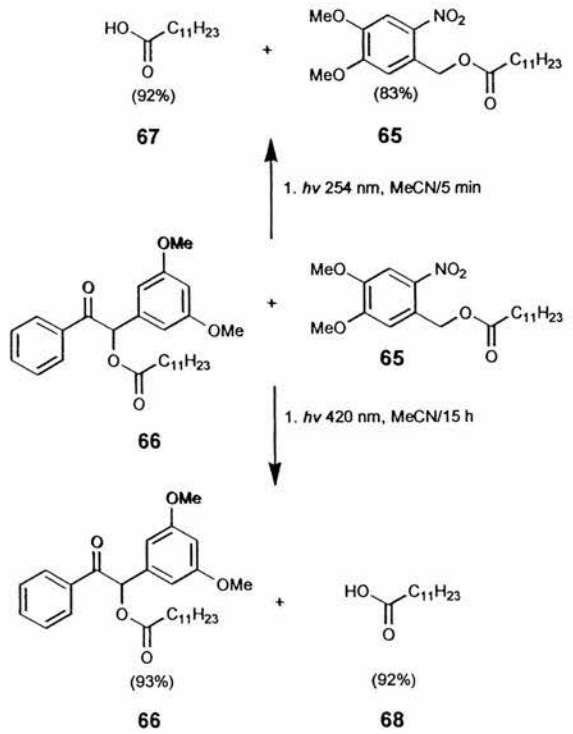

Scheme 1.7 This scheme shows an example of intermolecular wavelength orthogonality using the nitroveratrole and the benzoin caging groups on a simple carboxylic acid. This example illustrates how one caging group can be removed in the presents of the other.[58]

Initially the 1:1 mixture of **65** and **66** in acetonitrile was irradiated at a wavelength of 254 nm for 5 min. Subsequent ^{1}H NMR analysis of the mixture showed that it contained a 92% yield of the carboxylic acid, while 83% of the benzoin ester derivative remained intact. Further evidence showing this system as being orthogonal was obtained when the experiment was repeated at a wavelength of 420 nm for 15 h. However, in this instance ^{1}H NMR analysis of the resulting mixture indicated that it contained a 92% yield of the carboxylic acid, while 93% of the nitroveratrole derivative remained intact.[58]

In a second set of experiments conducted by Blanc and Bochet intramolecular discrimination in photolysis was demonstrated. This was done by using the nitroveratrole and benzoin ester caging groups to protect a simple diester to make **69**. This diester was then irradiated at 254 nm and in a second experiment at 420 nm to yield the nitroveratrole and the benzoin protected derivatives respectively (Scheme 1.8).[58]

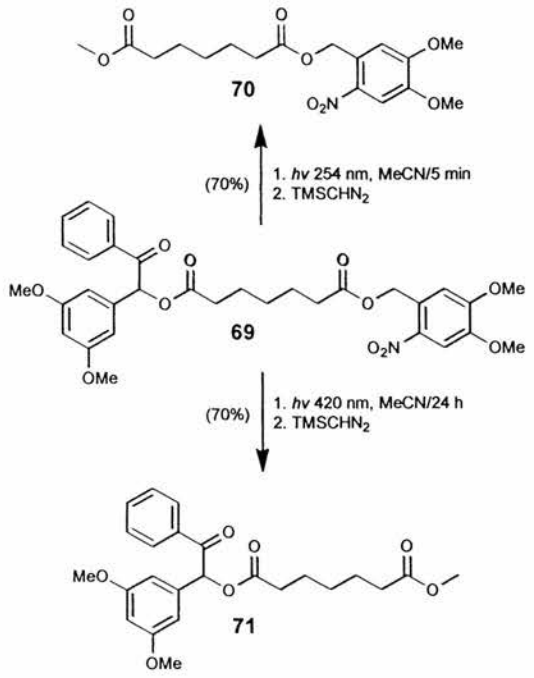

Scheme 1.8 This scheme shows an example of intramolecular wavelength orthogonality using the nitroveratrole and the benzoin caging groups on a simple diester. This example illustrates how one caging group can be removed in the presents of the other.[58]

In these experiments, irradiation of the diester **69** in acetonitrile at 254 nm wavelength for 5 min and subsequent esterification by $TMSCHN_2$ gave the nitroveratrole methyl ester **70** in 70% isolated yield and no indication of the benzoin ester derivative **71**. Again, when the experiment was repeated at 420 nm wavelength irradiation, the benzoin ester derivative **71** was isolated in 70% yield, with no indication of the nitroveratrole methyl ester **70**.[58]

Together these experiments were the first efficient demonstration of 'wavelength orthogonal uncaging' and opened the concept to further research. Since then, additional examples of orthogonality have become apparent including that of Ladlow *et al.*, who utilized this technique in the first photo-controlled differential release of carboxylic acids from solid phase resin.[59]

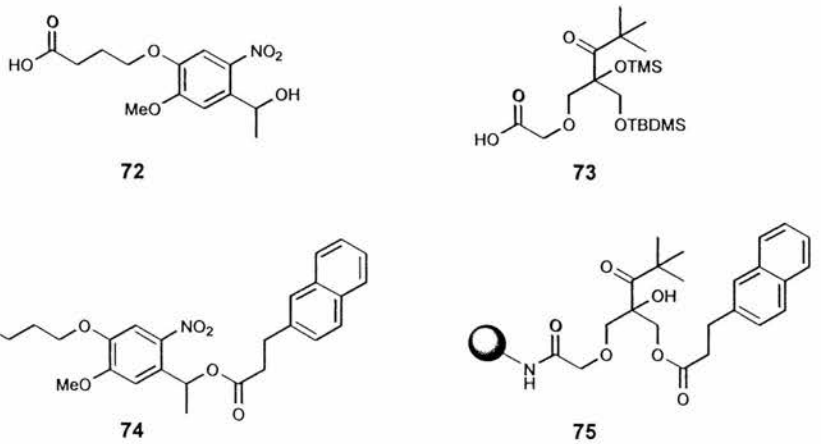

Fig. 1.27 Nitroveratryl (NV) and pivaloyl glycol (PG) linkers and resins for differential photo-release studies.[59]

This research developed an orthogonal system which incorporates the nitroveratryl (NV) **72** and pivaloyl glycol (PG) **73** photolabile linkers. Using these linkers, two resins **74** and **75** were synthesised and orthogonally released at 300 and 355 nm respectively.[59]

1.4. Summary

The cannabinoid and TRPV1 receptors are highly functional systems involved in several prominent physiological areas. Specifically, these receptors modulate function in both the central and peripheral nervous system and play an integral role in higher functions such as memory, motor function and pain perception. Hence, these receptors are key targets for pharmacological intervention and it is thus important to fully characterise the effects of their endogenous/exogenous ligands, in particular anandamide and capsaicin analogues.

The expanding field of caging groups provide a unique way of studying receptors and have already been successfully incorporated in studying the pivotal roles of acetylcholine, glutamate and ATP. Despite these successes, caging group chemistry is still in its infancy and effects such as sensitisation are yet to be explained and goals such as orthogonality fully achieved.

The aim of this project is the synthesis of tools that will facilitate the first wavelength orthogonal photolysis *in vitro*.

2 Results and Discussion: Synthesis

2.1. Synthesis of caged anandamide

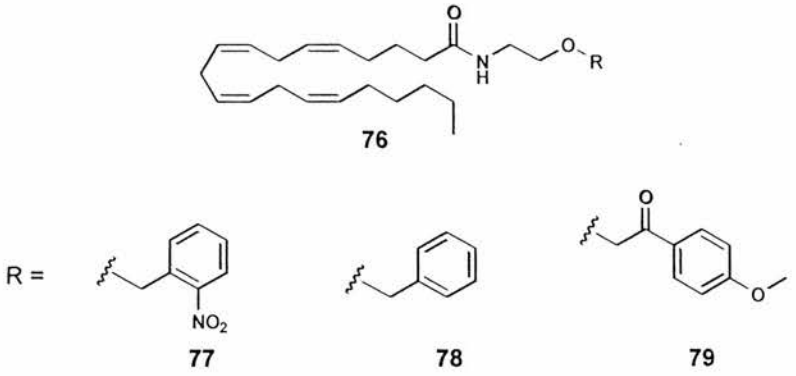

Fig. 2.1 Target molecules for analogues of anandamide including two caged derivatives.

In order to investigate the role played by AEA in the activation of CB_1 and TRPV1 it was desirable to synthesise a caged derivative of this compound (Figure 2.1). Two possible photolabile groups were considered to be of interest, giving rise to the two target molecules **77** and **79**. In addition to these caged compounds, the benzylated derivative of AEA **78** was also considered to be of interest for its use as a control in biological experiments.

The use of **78** as a control compound is two-fold. Firstly, as an indicator of biologically activity of the proposed AEA analogues, which have large moieties attached to the alcohol. This is important as compounds with caging groups attached should be biologically inactive. Secondly, **78** would be used as a comparison in photolysis studies as it is important to determine that the effect was caused by the uncaging of **77** or **79** and not as a result of any other mechanism involving an analogue of AEA or the flash lamp itself.

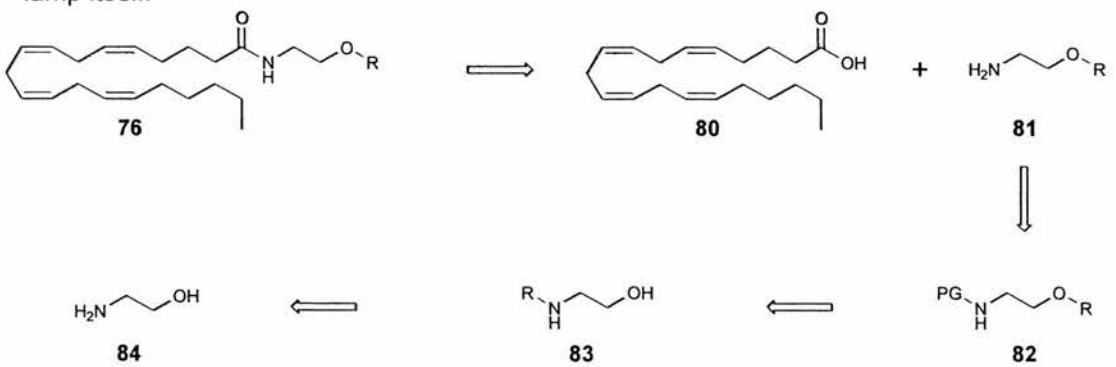

Scheme 2.1 Retrosynthetic plan for the synthesis of the AEA analogues.

The retrosynthetic plan for the formation of the analogues **77-79** provides a four step synthesis including a final step that involves the reaction of the appropriate amine with AA (Scheme 2.1). This final step has been incorporated in many syntheses of AEA analogues and has the benefit of only using the expensive material AA through a single step.[60,25,61,4] Retrosynthetic analysis of analogues of **81** indicated that ethanolamine could be used as a core starting material and that a simple amine protection step followed by addition of the caging or benzyl group to the primary alcohol would be involved. These derivatives would then be deprotected to afford the appropriate amines and subsequently reacted with AA to yield the target molecules **77-79**.

The decision to involve a protection and deprotection step stemmed from the problem of the amine nucleophilicity. Literature research suggested that there was a possibility of the amine attacking the bromide used in acetylation in an S_N2 fashion, which would lead to multiple acetylation and a mixture of products that could be difficult to separate.[62]

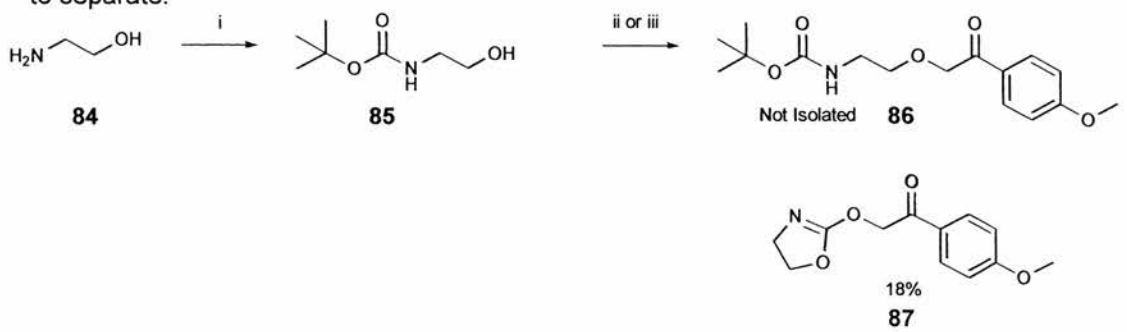

Scheme 2.2 Attempted synthesis of 2-(4'-methoxyacetophenone)-*N*-(*tert*-butoxycarbonyl)ethylamine **86**. *Reagents and conditions*: i. Di-*tert*-butyldicarbonate, CH_2Cl_2, 97%; ii. a. NaH, DMF, 0 °C; b. 2-Bromo-(4'-methoxyacetophenone), DMF, 0 °C→RT. iii. a. NaH, THF, 0 °C; b. 2-Bromo-(4'-methoxyacetophenone), THF, 0 °C → RT.

The first protecting group used was *tert*-butoxycarbonyl (BOC) which was successful in giving **85** in 97% yield. Compound **85** was then reacted with 2-bromo-(4'-methoxyacetophenone) using sodium hydride (NaH) as the base (Scheme 2.2). Analysis of the reaction by T.L.C. indicated numerous products and on purification by silica gel column chromatography most of the combined fractions analysed by ^1H NMR spectroscopy contained more than one product. The only isolated compound was a cyclic derivative 2-(4'-methoxyacetophenone)-4,5-dihydrooxazole **87** in 18% yield. The presence of **87**, and the mixture of products indicated by T.L.C., suggested that multiple

side reactions were occurring. The solvent was changed to THF, but this alteration also yielded multiple products which could not be isolated by silica gel column chromatography.

At the same time as the experiments using the BOC protecting group, a second nitrogen protecting group, benzyloxycarbonyl (Cbz) was also investigated and protection of ethanolamine gave *N*-(benzyloxycarbonyl)-2-aminoethanol **88** in 68% yield. (Scheme 2.3). Compound **88** was reacted with 2-bromo-(4'-methoxy)acetophenone in an attempt to afford the fully protected ethanolamine **89**. However, as with the BOC protecting group (Scheme 2.2) a mixture of products was obtained and silica gel column chromatography did not afford the desired compounds.

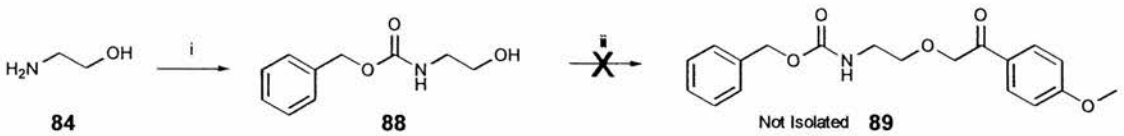

84 **88** **89**

Scheme 2.3 Attempted synthesis of 2-(4'-methoxyacetophenone)-*N*-(benzyloxycarbonyl)ethylamine. *Reagents and conditions*: i. Benzyl chloroformate, 1,4-dioxane:water (1:1), 4-DMAP, triethylamine, 68%; ii. NaH, THF, 0 °C; or 2-Bromo-(4'-methoxyacetophenone), THF, 0 °C → RT.

Possible reasons for the numerous products observed, include the attack of the alkoxide on the electrophilic carbonyl of the phenacyl reagent, instead of attack at the α-carbon. Another possibility is the deprotonation of the α-carbon on 2-bromo-(4'-methoxyacetophenone) by NaH.

Given the difficulties with the phenacyl caging group, attempts to synthesis the control compound were carried out so as to determine the involvement of the phenacyl reagent in the production of so many side products. Deprotonation of **88** was carried out using NaH and analysis of the reaction by T.L.C. before any further reagents were added indicated that both starting material and many by-products were present at this stage. The other reagents were added regardless and again after 24 h T.L.C. showed a mixture, from which **91** was isolated in 10% yield (Scheme 2.4).

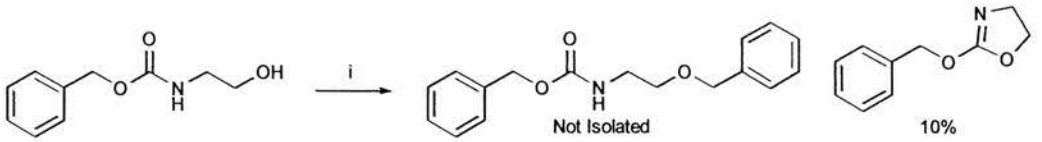

88 **90** **91**

Scheme 2.4 Attempted synthesis of 2-benzyloxy-*N*-(benzyloxycarbonyl)ethylamine. *Reagents and conditions*: i. a. NaH, THF, 0 °C; b. Benzyl bromide, THF, 0 °C → RT.

Since both by-products isolated are cyclic and given the observations on the addition of NaH, this suggests that on formation of the alkoxide the negative charge on the oxygen attacks the carbonyl on the carbamate group, forming a five-membered ring, as favoured by Baldwin's rules. It is postulated that the new alkoxide formed can then react in an S_N2 manner with the alkyl bromide (Figure 2.2). Elimination of benzyl bromide would then give the novel heterocycle **91** observed.

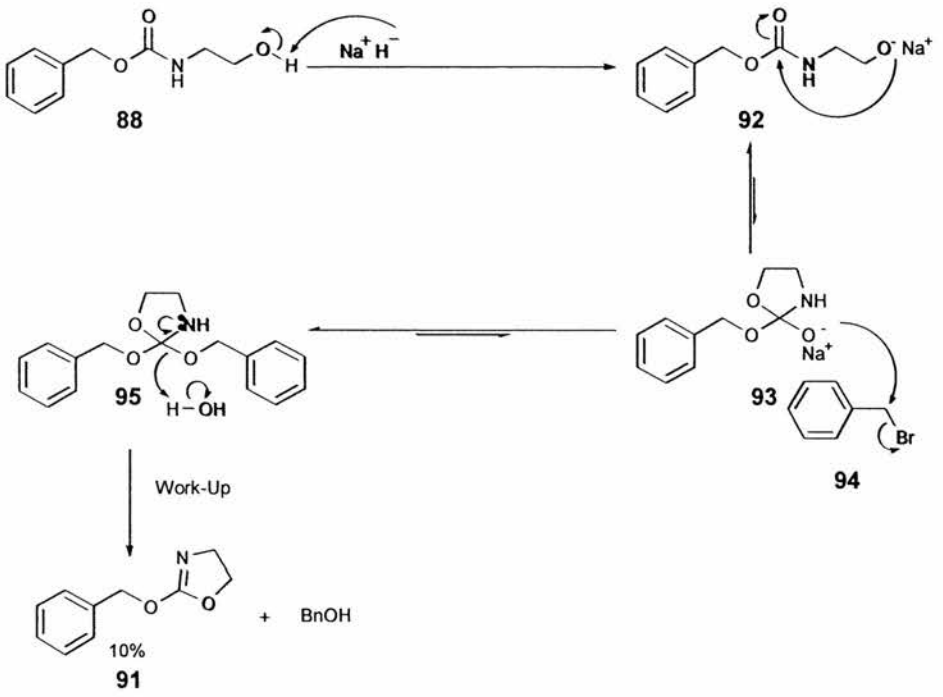

Fig. 2.2 Possible mechanism for the synthesis of 2-benzyloxy-4,5-dihydrooxazole.

In a similar fashion, the reaction of 2-bromo-(4'-methoxyacetophenone) with *N*-(*tert*-butoxycarbonyl)ethanolamine and the subsequent elimination of *tert*-butanol yielded the novel 2-(4'-methoxyacetophenone)-4,5-dihydrooxazole **87** (Scheme 2.5).

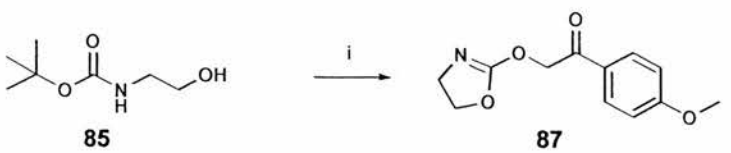

Scheme 2.5 Synthesis of 2-(4'-methoxyacetophenone)-4,5-dihydrooxazole. *Reagents and conditions*: i. a. NaH, DMF, 0 °C; b. 2-Bromo-(4'-methoxyacetophenone), DMF, 0 °C → RT, 18%.

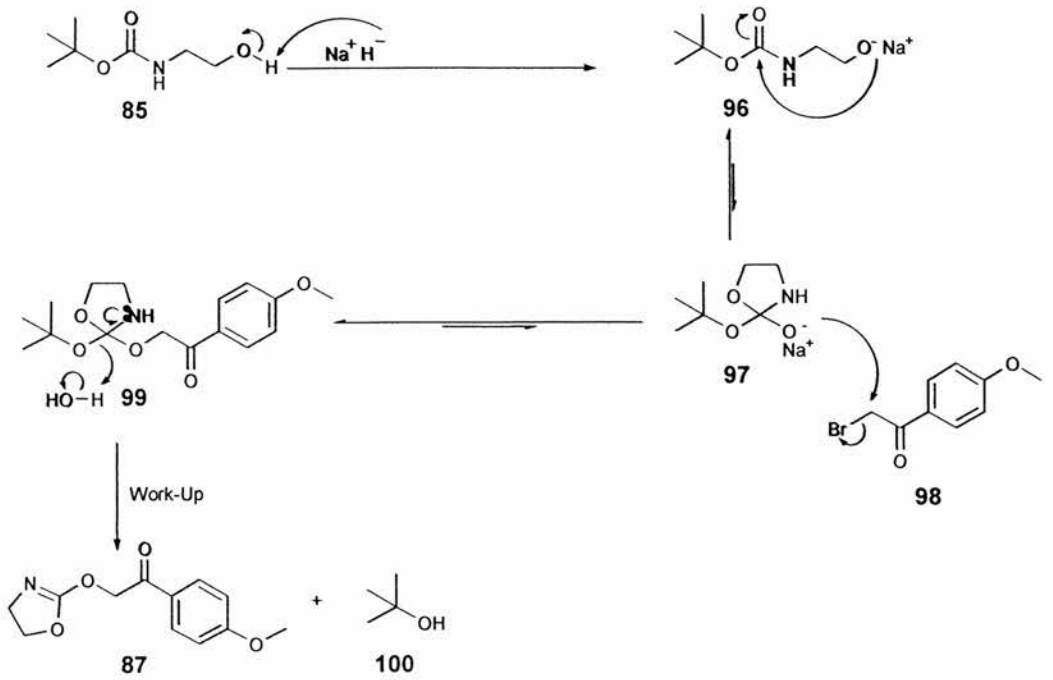

Fig. 2.3 Possible mechanism for the synthesis of 2-(4'-methoxyacetophenone)-4,5-dihydrooxazole.

However, as T.L.C. analysis, yields and crude NMR spectra suggested, the proposed mechanisms (Figures 2.2 and 2.3) are clearly not the only reactions that are occurring.

As the above route did not afford the desired compounds, it was decided that different reagents would be used. Following a procedure reported by Faroux-Corley *et al.*[63], phase transfer conditions were applied in the benzylation of *N*-(benzyloxycarbonyl)-2-aminoethanol **88**. However, these conditions did not yield the desired compound **90**, but again afforded the cyclic compound **91,** this time in 45% yield (Scheme 2.6).

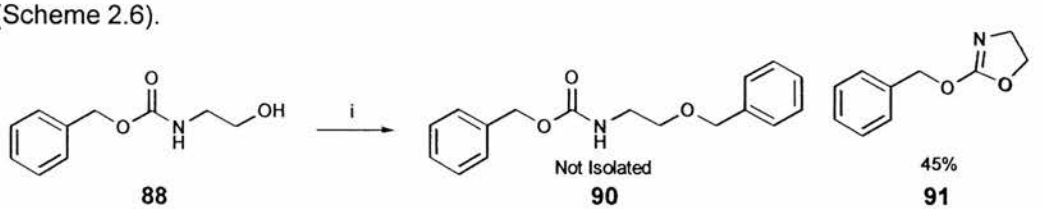

Scheme 2.6 Attempted synthesis of 2-benzyloxy-*N*-(benzyloxycarbonyl)ethylamine. *Reagents and conditions*: i. Benzyl chloride, NaOH, CH_2Cl_2, tetrabutylammonium hydrogensulfate/water, reflux.

Despite this result, the Faroux-Corley *et al.*[63] procedure was attempted using benzyl chloride and sodium hydroxide under phase transfer conditions of dichloromethane and tetrabutylammonium hydrogensulfate/water. This afforded *O*-benzyloxy-*N*-(*tert*-butoxycarbonyl)ethylamine **101** in 63% yield (Scheme 2.7). The

resulting compound **101** was then BOC deprotected using TFA and the amine **102** isolated as its hydrochloride salt. The salt was then reacted with AA to yield the desired eicosa-5,8,11,14-tetraenoic acid (2-benzyloxyethyl)amide **77** in 58% yield (Scheme 2.7).

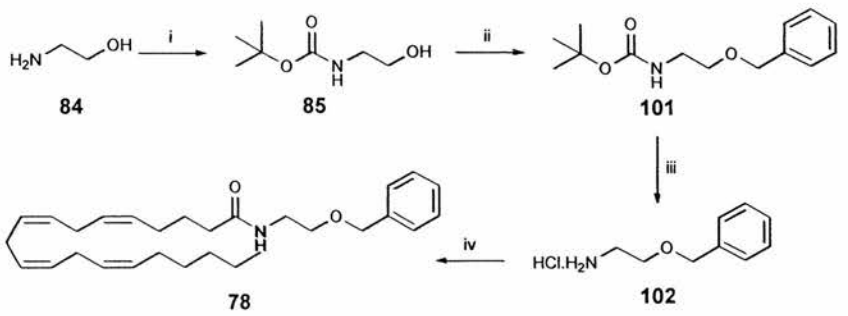

Scheme 2.7 Synthesis of eicosa-5,8,11,14-tetraenoic acid (2-benzyloxyethyl)amide. *Reagents and conditions*: i. Di-*tert*-butyldicarbonate, CH_2Cl_2, 97%; ii. Benzyl chloride, NaOH, CH_2Cl_2, tetrabutylammonium hydrogensulfate/water, reflux, 63%; iii. a. Trifluoroacetic acid; b. Conc. HCl, 55%; iv. a. Arachidonic acid, oxalyl chloride, cat. dry DMF, CH_2Cl_2; b. Triethylamine, CH_2Cl_2, 58%.

The difference in reactivity of the two protecting groups BOC and Cbz under phase transfer conditions is an indicator of difficulties faced with the ethanolamine core. It would seem that cyclisation occurs readily for the Cbz protected ethanolamine but no indication of cyclisation was observed in the BOC protected ethanolamine. A possible explanation could be that upon addition of NaH, an equilibrium is set up between the starting material alkoxide and the heterocyclic alkoxide. This equilibrium could explain the reactivity as the formation of BOC protected heterocycle intermediate **97** would be favoured more than the formation of Cbz protected heterocycle intermediate **99**, due to greater steric hindrance in the formation of a chiral centre next to a *tert*-butyl group (Figure 2.4).

A further explanation of the observed products is 'the inductive effect'. In the case of the *tert*-butoxide group of compound **96**, the methyl groups are pushing electron density toward the alkyl carbon attached to the oxygen. This in turn causes more electron density to be pushed towards the carbonyl carbon, thus nucleophilic attack is further impeded. Conversely, the benzyl group of the Cbz protected compound **98** is electron withdrawing and electron density is pulled away from the alkyl carbon and subsequently the oxygen. This results in the carbonyl carbon being more susceptible to nucleophilic attack (Figure 2.4).

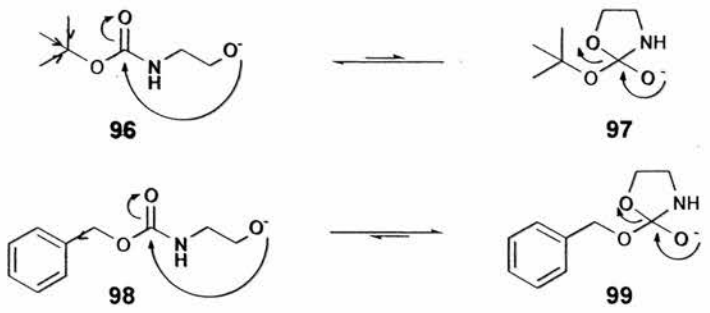

Fig. 2.4 Possible equilibria present after the addition of NaH to *N*-(*tert*-butoxycarbonyl)-2-aminoethanol and *N*-(benzyloxycarbonyl)-2-aminoethanol.

Given the relative success of the phase transfer conditions on the BOC protected ethanolamine, the same conditions were tried using 2-bromo-(4'-methoxyacetophenone (Scheme 2.8). However, analysis by T.L.C. showed the reaction gave many by-products and when column chromatography was attempted no fractions yielded any pure products. Given the problems with the phenacyl caging group it was decided that compound **105** containing a 2-nitrobenzyl caging group would be synthesised. Again, the phase transfer conditions were used, but analysis by T.L.C. showed the reaction had given a large number of by-products. One possible reason for the disparity in reactivity of the benzyl and 2-nitrobenzyl reagents in phase transfer conditions may be the observed and documented problem of developing a negative charge next to an *N*-oxide species.[64] Pearson *et al.*, conducted a number of experiments and electrostatic potential surface map studies demonstrating that build up of a negative charge on the bromine atom in a late transition state of an S_N2-like reaction results in electrostatic repulsion between the *N*-oxide oxygen atom and the bromine (Figure 2.5). Consequently, S_N2 type reactions such as the one in Scheme 2.8 are disfavoured.[64]

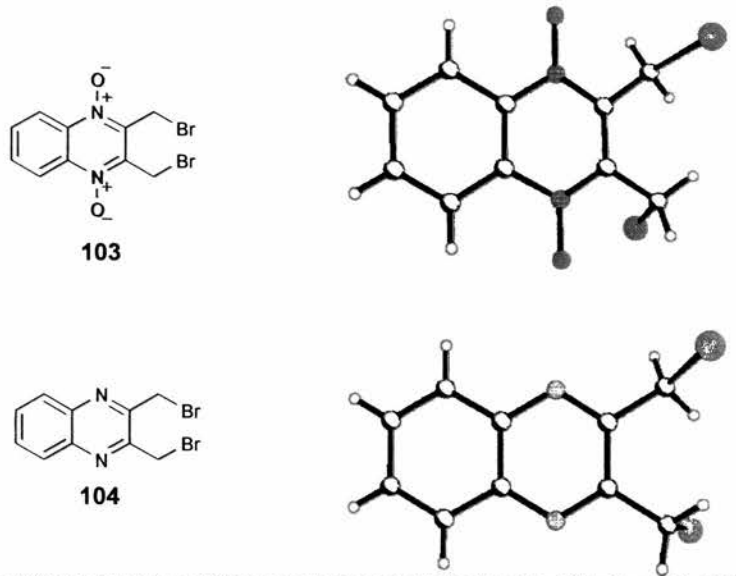

Fig. 2.5 Molecular and X-ray structures of Pearson *et al.* compounds showing distortion of Br-C-C-N-O angle in **103** compared to that of Br-C-C-N angle in **104**.[64]

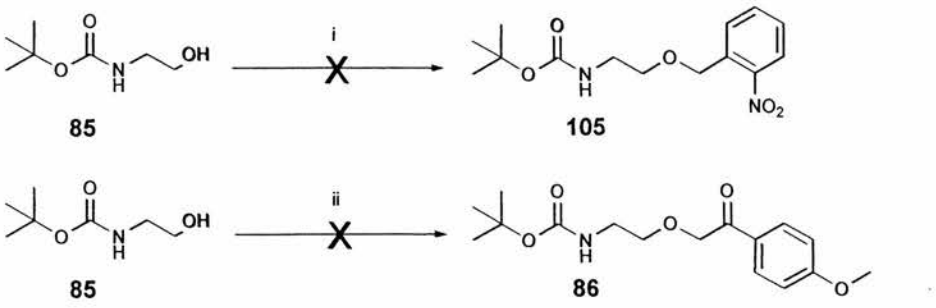

Scheme 2.8 Attempted synthesis of *O*-2-nitrobenzyloxy-*N*-(*tert*-butoxycarbonyl)ethylamine and 2-(4'-methoxyacetophenone)-*N*-(*tert*-butoxycarbonyl)ethylamine. *Reagents and conditions*: i. 2-Nitrobenzyl chloride, NaOH, CH_2Cl_2, tetrabutylammonium hydrogensulfate/water, reflux; ii. 2-Bromo-(4'-methoxyacetophenone), NaOH, CH_2Cl_2, tetrabutylammonium hydrogensulfate/water, reflux.

On consideration of the difficulties encountered with the carbamate protecting groups, it was clear that the formation of 5-membered rings was overriding the resistance of the carbonyl to nucleophilic attack and thus encouraging the formation of the isolated heterocycles **87** and **91**. With this in mind, it was decided that protection of ethanolamine nitrogen should involve a more bulky protecting group. Thus the popular phthalimide group was considered, where the nitrogen lone pair is conjugated with two carbonyl π-systems rendering it less susceptible to carbonyl substitution. Ethanolamine was therefore protected using phthalic anhydride in 82% yield **106**. Using NaH to deprotonate the primary alcohol of **106**, the synthesis of *O*-2-nitrobenzyl-2-phthalimidoethanol **107** was achieved in 7% yield (Scheme 2.9).

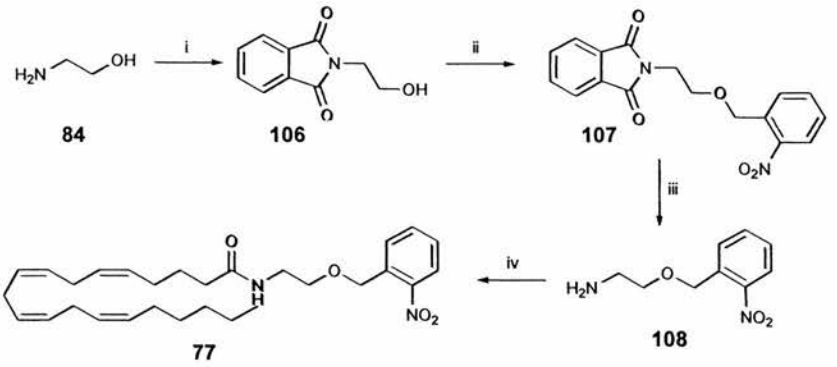

Scheme 2.9 Synthesis of eicosa-5,8,11,14-tetraenoic acid (2-nitrobenzyloxy-ethyl)amide. *Reagents and conditions*: i. Phthalic anhydride, reflux, 82%; ii. a. NaH, DMF, 0 °C; b. 2-Nitrobenzyl bromide, DMF, 0 °C, then RT, 7%; iii. Hydrazine hydrate, EtOH, 45 °C; iv. a. Arachidonic acid, oxalyl chloride, cat. dry DMF, CH_2Cl_2; b. Triethylamine, CH_2Cl_2, 35% (over two steps).

Although the yield is low, 2-phthalimidoethanol starting material was recovered from the reaction, which implies a yield of 20%, based on converted starting material. Also, analysis of the reaction by T.L.C. showed the presence of only 2 new products. When the reaction was repeated, the second compound was isolated and identified as

2-nitrobenzyl alcohol. This indicates that the 2-nitrobenzyl bromide was being hydrolysed to the alcohol and leaving the 2-phthalamidoethanol **106** unreacted. This could be due to wet starting material, were water reacts with NaH and forms sodium hydroxide, which can subsequently react with the 2-nitrobenzyl starting material to give the observed 2-nitrobenzyl alcohol.

Despite the low yield, **107** was deprotected at the nitrogen using hydrazine hydrate yielding the crude amine **108**. This was then reacted without further purification with AA to give the desired eicosa-5,8,11,14-tetraenoic acid (2-nitrobenzyloxyethyl)amide **77** in 33% yield (Scheme 2.9). Although the yield is again low, a possible way for increasing this step is by purification of the amine **108** before reaction. This may be achieved by ion exchange chromatography using an anion resin to trap the amine or by forming the hydrochloride salt of the amine.

The synthesis of 2-benzyloxy-*N*-phthaloylethylamine **109** was also attempted and isolated in 19% yield (Scheme 2.10). Analysis by T.L.C. showed starting material and only two new products. After silica gel column chromatography the mixed fractions containing the two products were analysed using ^{1}H NMR spectroscopy. This indicated that the second product was benzyl alcohol and suggested a similar result as in the 2-nitrobenzyl reaction. However, by recrystallisation from ethanol, **109** was isolated from the impurity.

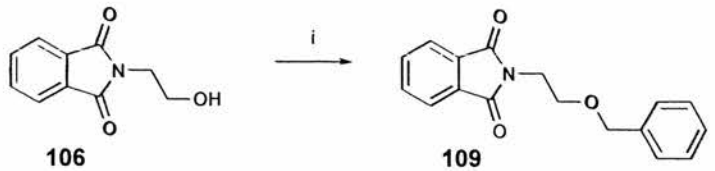

Scheme 2.10 Synthesis of 2-benzyloxy-*N*-phthaloylethylamine. *Reagents and conditions*: i. a. NaH, DMF, 0 °C; b. 2-nitrobenzyl bromide, DMF, 0 °C → RT, 19%.

Given the success in synthesising 2-nitrobenzyl anandamide **79**, attempts to make the phenacyl anandamide were again undertaken. This time, due to the possibility of the carbonyl of the phenacyl caging group being attacked by the alkoxide, it was decided that it would be protected as an acetal. This was achieved using ethylene glycol and gave **111** in 84% yield (Scheme 2.11).

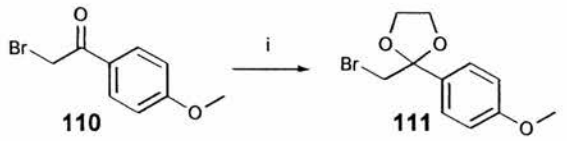

Scheme 2.11 Synthesis of 2-bromomethyl-2-(4-methoxyphenyl)-1,3-dioxolane. *Reagents and conditions*: i. a. Ethylene glycol, camphor sulfonic acid, dry toluene, reflux into Dean-Stark apparatus, 84%.

2-Bromomethyl-2-(4-methoxyphenyl)-1,3-dioxolane **111** was reacted with 2-phthalimidoethanol in either THF or DMF (Scheme 2.12). In both instances, analysis by T.L.C. and crude ^{1}H NMR spectra showed that no reaction had taken place, and that only starting material was present. The main reason for this may be steric hindrance from both the protected carbonyl and the 4-methoxy phenyl group. Given this situation, attempts to make the target molecule via this route were abandoned.

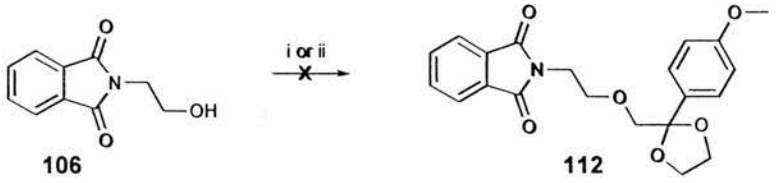

Scheme 2.12 Attempted synthesis of *O*-2-methoxy(4'-methoxyphenyl)-1,3-dioxolane-2-phthalimidoethyl. *Reagents and conditions*: i. a. NaH, THF, 0 °C; b. 2-Nitrobenzyl bromide, THF, 0 °C → RT; or ii. a. NaH, DMF, 0 °C; b. 2-Nitrobenzyl bromide, DMF, 0 °C → RT.

In order to improve the overall yield of the 2-nitrobenzyl anandamide synthesis, an alternative route was devised. In a one pot reaction 2-phthalimidoethyl-2-bromide **113** was synthesised from ethanolamine and phosphorous tribromide. Compound **113** was then reacted with 2-nitrobenzyl alcohol, but analysis by T.L.C. indicated that the reaction did not yield the desired product (Scheme 2.13).

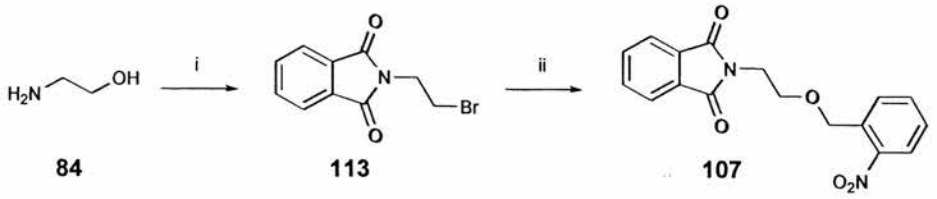

Scheme 2.13 Attempted synthesis of *O*-2-nitrobenzyl-2-phthalimidoethanol. *Reagents and conditions*: i. a. Phthalic anhydride, reflux; b. PBr_3, RT, then 100 °C, 79%; ii. a. 2-nitrobenzyl alcohol, NaH, THF, 0 °C; b. 2-Phthalimidoethyl-2-bromide, THF, 0 °C → RT.

Having made two AEA analogues **77** and **78** it was decided that complementary TRPV1 agonists and antagonists would be synthesised.

2.2. Synthesis of caged capsaicin analogues

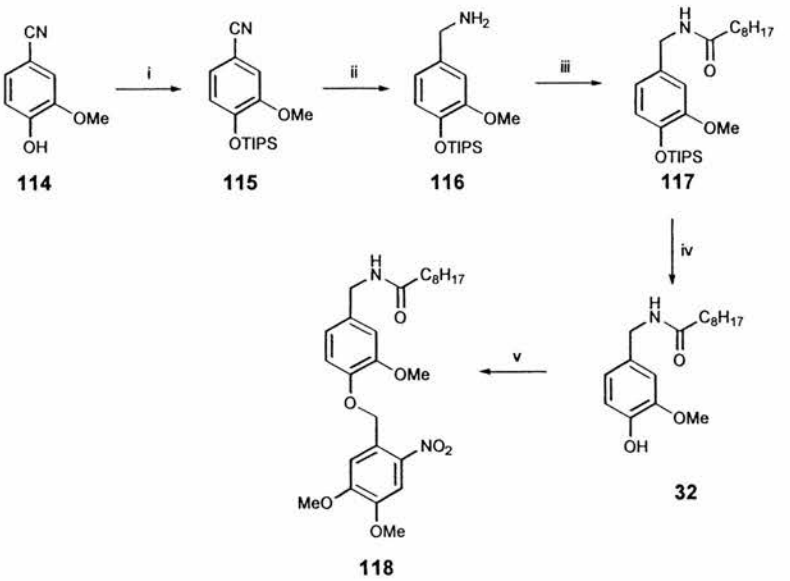

Scheme 2.14 Synthesis of 3-methoxy-4-(4,5-dimethoxy-2-nitrobenzyl)-*N*-nonanoylbenzylamine. *Reagents and conditions*: i. Triisopropylsilyl chloride, imidazole, DMF, 80%; ii. Lithium aluminium hydride, Et_2O, 89%; iii. a. DMAP, CH_2Cl_2, 0 °C; b. Pyridine, nonanoyl chloride, 0 °C → RT 69%; iv. Tetrabutylammonium fluoride, THF, 97%; v. a. Potassium *tert*-butoxide, THF; b. 4,5-Dimethoxy-2-nitrobenzyl bromide, 66%.

The synthesis of the caged capsaicin analogue 3-methoxy-4-(4',5'-dimethoxy-2-nitrobenzyl)-*N*-nonanoylbenzylamine **118** was achieved as shown (Scheme 2.14). This commenced with TIPS alcohol protection of 4-hydroxy-3-methoxybenzonitrile followed by reduction of the nitrile to the crude amine **116** using lithium aluminium hydride. Purification of the amine was not possible due to its high polarity, however, the ^{1}H NMR spectrum indicated a satisfactory level of purity. The amine was acetylated with nonanoyl chloride to give the protected TRPV1 agonist. Compound **117** was then deprotected with TBAF to provide the free phenol **32**, which was subsequently deprotonated with potassium *tert*-butoxide and caged with 4,5-dimethoxy-2-nitrobenzyl bromide.[65]

Previously, Appendino *et al.* had shown that bromination at the 6-position on the aromatic ring leads to significant removal of biological activity of this analogue and **120** thus acts as an antagonist at the TRPV1 receptor.[66] Bromination of the key intermediate **117** provided the TIPS protected antagonist **119**, which was subsequently deprotected with TBAF and caged in the same way as the capsaicin analogue **118** to provide 2-bromo-5-methoxy-4-(4,5-dimethoxy-2-nitrobenzyl)-*N*-nonanoylbenzylamine **121** (Scheme 2.15).

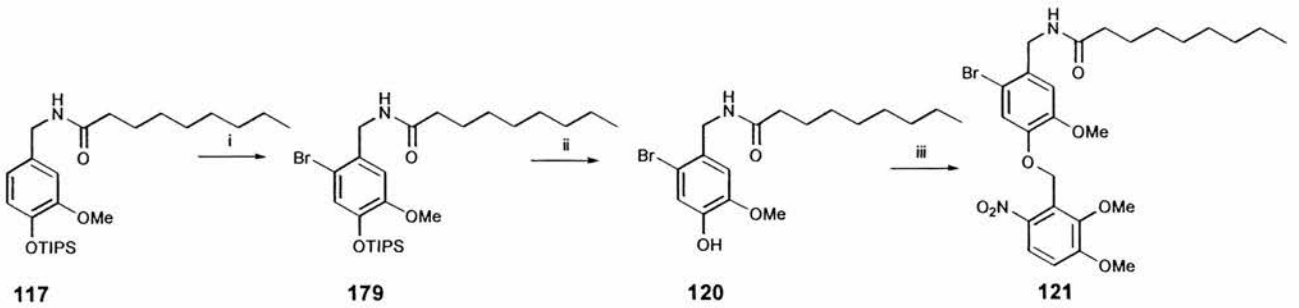

117 179 120 121

Scheme 2.15 Synthesis of 2-bromo-5-methoxy-4-(4,5-dimethoxy-2-nitrobenzyl)-*N*-nonanoylbenzylamine. *Reagents and conditions*: i. Bromine, CH_2Cl_2, N_2 at -78 °C, 73%; ii. Tetrabutylammonium fluoride, THF, 86%; iii. a. Potassium *tert*-butoxide, THF; b. 4,5-Dimethoxy-2-nitrobenzyl bromide, 53%.

It is evident that compound **117** could be brominated at three positions. Analysis of the ring substituents in **117** indicates that the methoxy group is *ortho/para* directing, favouring bromination at positions 2 and 6 (Scheme 2.16). Likewise, the oxygen of the TIPS group is *ortho/para* directing and favours bromination at the 5 position. Lastly, the alkyl group is also weakly *ortho/para* directing and thus favours bromination at the 2 and 6 positions.

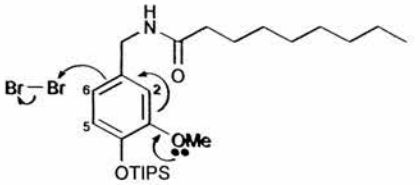

117

Scheme 2.16 *ortho* and *para* directing effect of the methoxy substiunent of **117**.

Overall, this indicates that bromination is most likely to occur at the 2 and 6 positions. However, steric hindrance of the 2 position by the nonanoyl chain and the methoxy group means that bromination at the 6 position is most favoured. Thus, in order to gain the correct selectivity in the brominating reaction and avoid over bromination, low temperatures and dilute conditions were used (Scheme 2.15).

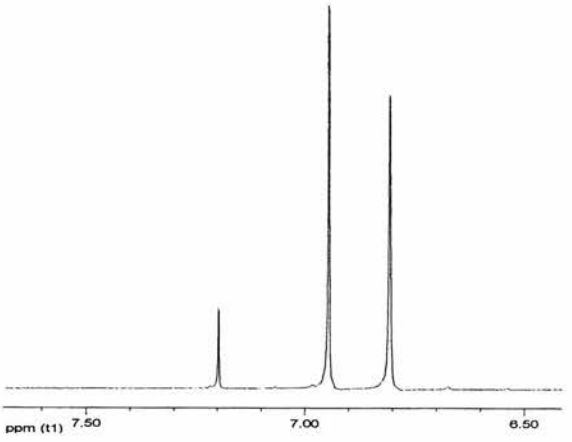

Fig. 2.6 Aromatic region of the ^{1}H NMR of 2-bromo-5-methoxy-4-(triisopropylsilyloxy)-*N*-nonanoylbenzylamine showing δ_H (300 MHz; $CDCl_3$) 7.20 (Chloroform), 6.95 (1H, s, Ar-H_5), 6.81 (1H, s, Ar-H_2).

As shown in Figure 2.6 only two proton singlet peaks derived from the aromatic protons at positions 2 and 5 of the phenyl ring were observed. Bromination of compound **117** at positions 2 and 5 would have shown coupling and therefore peaks involving doublets. Thus it can be concluded that bromination, as expected, was directed to position 6 of the phenyl ring and that no over bromination had occurred.

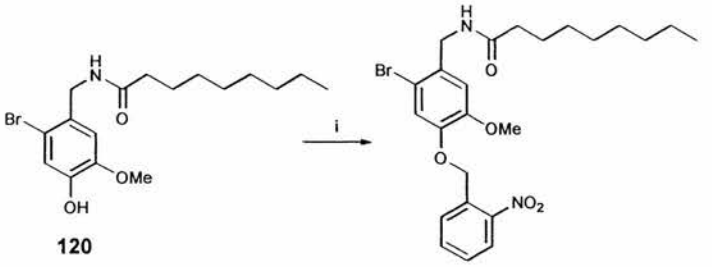

120 **122**

Scheme 2.17 Synthesis of 2-bromo-5-methoxy-4-(2-nitrobenzyl)-*N*-nonanoylbenzylamine. *Reagents and conditions*: i. a. Potassium *tert*-butoxide, THF; b. 4,5-Dimethoxy-2-nitrobenzyl bromide, 22%.

Using the same conditions as the 4,5-dimethoxynitrobenzyl caging group, the caging of the capsaicin antagonist with the 2-nitrobenzyl caging group was achieved (Scheme 2.17).

2.3. Summary

The synthesis of several caged analogues of anandamide and capsaicin for subsequent photolytic studies has been achieved by the incorporation of the 2-nitrobenzyl and 4,5-dimethoxynitrobenzyl caging groups (**77**, **118**, **121** and **122**) (Figure 2.7).

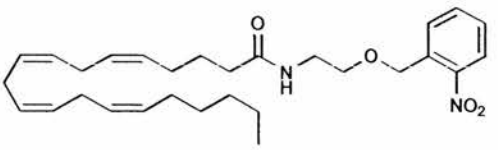

77

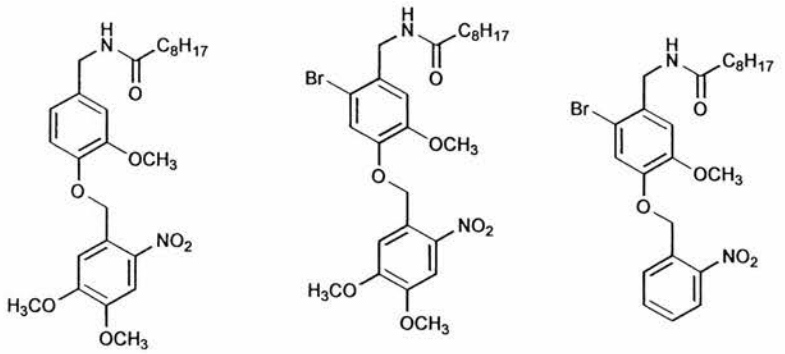

118 **121** **122**

Fig. 2.7 The molecular structures of a caged analogue of anandamide **77** and three caged analogues of capsaicin (**118**, **121** and **122**).

Several strategies were attempted before a route was found for the synthesis of the AEA analogues **77** and **78**. The most prominent synthetic difficulties encountered were the formation of five-membered ring by-products **87** and **91** (Figure 2.2 and 2.3) and the non-reactivity of **111**. This latter aspect meant the synthesis of the key target **79** was not achieved. Other difficulties included the low yields obtained for the intermediates **107** and **109**. However, definitive structural characterisation of the key caged anandamide analogue **77** has been achieved and biological testing is now required.

The synthetic strategy previously employed in the Conway group for the synthesis of the key intermediate **117** had no complications.[46] Intermediate **117** was successfully converted into three novel caged capsaicin analogues (**118**, **121** and **122**). These structures were definitively characterised and compound **118** was subsequently used in photolytic studies described herein.

3 Results and Discussion: Photolysis Studies

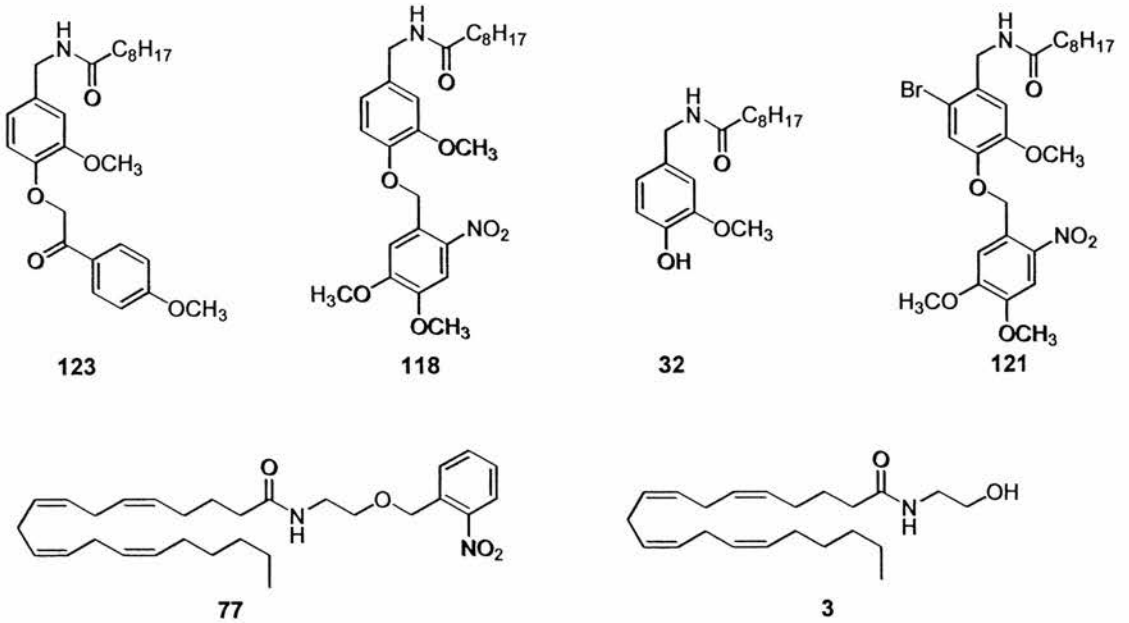

Fig. 3.1 The structure of the three caged capsaicin analogues (**118**, **121** and **123**), the TRPV1 agonist (**32**), the structure of anandamide (**3**) and caged anandamide (**77**).

The key goal of this research was to assess the uncaging properties of several anandamide and capsaicin analogues. Four such caged analogues have been successfully synthesised (**118**,**121**,**123** and **77**) (Figure 3.1), though characterisation of their biological properties *in vitro* and *in vivo* is yet to be fully achieved. Despite this, their chemical uncaging properties have been investigated and are described herein.

Previously, the Conway and Scott groups synthesised and caged the capsaicin analogue **123** and determined its biological properties in a series of *in vitro* tests on a population of cultured dorsal root ganglion (DRG) neurons.[46] Initially, experiments were conducted on the uncaged compound **32**, to identify its biological activity on TRPV1 receptors compared to that of capsaicin **24**. Using fluorescent Fura-2 Ca^{2+} imaging, aliquots of capsaicin (100 nM) and analogue **32** (1 μM) were shown to evoke increases in intracellular Ca^{2+}, which reversed on washing with NaCl-based extracellular solution. The responses of the two compounds were similar in amplitude, suggesting that the capsaicin analogue **32** has a lower potency than capsaicin **24** (Figure 3.2 **B**). TRPV1 desensitisation experiments were conducted by applying compound **32** followed by capsaicin, nearing the end of the DRG recovery period ~ 30 min (Figure 3.2). The DRG

neurons used in these experiments were from a heterogenous population of neurons, meaning not all the neurons would be expected to be populated by TRPV1 receptors. Those neurons that failed to respond to capsaicin also failed to respond to the capsaicin analogue **32** and likewise those that responded to capsaicin **24** responded to the analogue **32**, indicating that **32** is acting selectively on TRPV1.

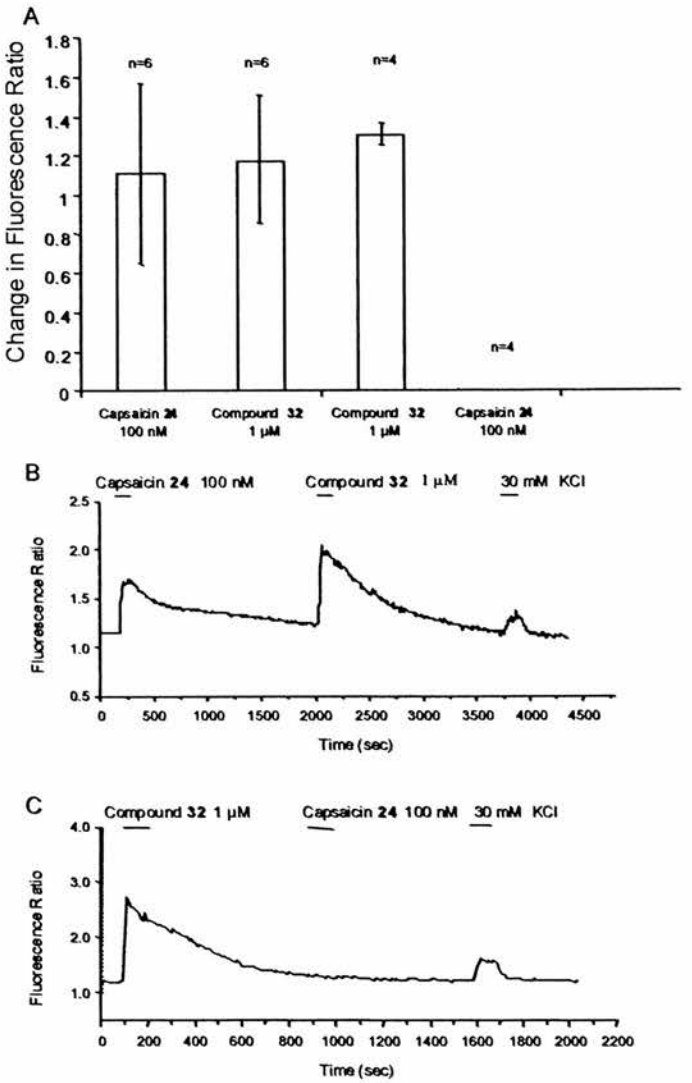

Fig. 3.2 Capsaicin 24 and compound 32 evoked Ca^{2+} transients in the same population of cultured DRG neurons. For fura-2 Ca^{2+} imaging, DRG neurons were incubated for 1 hour in NaCl-based extracellular solution containing in mM: NaCl, 130; KCl, 3.0; $MgCl_2$, 0.6; $CaCl_2$, 2.0; $NaHCO_3$, 1.0; HEPES, 10.0; glucose, 5.0 and 0.01 fura-2AM (1 mM stock in DMF). The pH of this solution was adjusted with NaOH to 7.4 and the osmolarity to 310-320 mOsm with sucrose. The neurons were then washed for 10-20 min with NaCl-based extracellular solution, containing 0.1% DMSO, to remove the extracellular fura-2AM. During the experiment the neurons were constantly perfused (1-2 cm^3/min) with extracellular solution containing DMSO, and the actions of capsaicin **24**, compound **32** and extracellular solution containing 30 mM KCl tested. The high KCl concentration produced depolarisation, activation of voltage-gated Ca^{2+} channels and transient increases in intracellular Ca^{2+} in the DRG neurons, but not background cells also present in the culture. Ca^{2+} transient amplitudes (fluorescence ratio values after background subtraction) were measured. A. Bar chart showing mean data (± S.E.M) for responses with similar amplitudes produced by 100 nM capsaicin and 1 µM compound **32**. The chart also shows that desensitisation with compound **32** abolished subsequent responses to capsaicin. (n = number of experiments) B. Example record showing Ca^{2+} transients evoked by capsaicin, compound **32** and 30 mM KCl (clearly identifies a DRG neuron). C. Example record showing a response to compound **32** and subsequent desensitisation of the capsaicin response, however, a response to 30 mM KCl could be elicited. Note the difference in time scale between B and C.[46]

Given that the capsaicin analogue **32** was shown to evoke a cellular response, photolytic studies were conducted on the caged capsaicin analogue **123**. Using the whole cell patch clamp/pipette technique, where compounds of interest are injected directly into the cell,[67] caged compound **123** (50 μM in a patch pipette solution containing 2.5% DMSO) was placed into several DRG neurons. Photolysis of the caged compound **123** using a 300 V flash from a xenon flash lamp equipped with a 360 nm filter, resulted in the depolarisation of four out of five DRG neurons. This was indicated by a sustained membrane potential of 15 ± 2 mV (Figure 3.3 **A**). In addition to a sustained membrane potential, two of these four neurons also evoked an action potential (Figure 3.3 **B**).

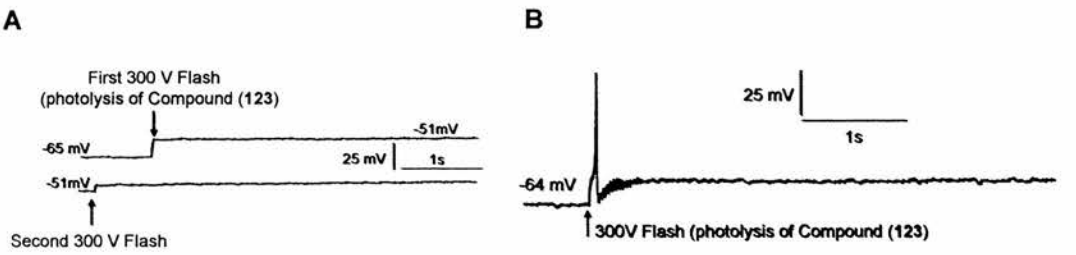

Fig. 3.3 Intracellular actions of compound **123** photolysis on the excitability of cultured DRG neurons. The same extracellular solution was used for both the electrophysiology and the Ca^{2+} imaging experiments. The patch pipette solution contained (in mM): KCl, 140; EGTA, 5; $CaCl_2$, 0.1; $MgCl_2$, 2.0; HEPES, 10.0; ATP, 2.0; compound **123** 0.5–0.1% and 2.5% DMSO. This solution after correction with Tris and sucrose had a pH of 7.2 and osmolarity of 320 $mOsmL^{-1}$. An Axoclamp 2 A switching amplifier (Axon Instruments) operated at a switching frequency of 15 kHz was used. (A) Record showing two depolarising responses to intracellular photolysis of compound **123** from the same neuron. No action potentials were evoked in this neuron and no further depolarisation was obtained with additional photolysis (3rd flash not shown). (B) Example record showing a single action potential and sustained depolarisation obtained in response to intracellular photolysis of compound **123**.[46]

As with the fluorescent imaging data, neurons that failed to evoke a response to capsaicin (1 μM), subsequently failed to evoke a response to intracellular photolysis of caged capsaicin analogue **123** (Figures 3.4 & 3.5 **A**).

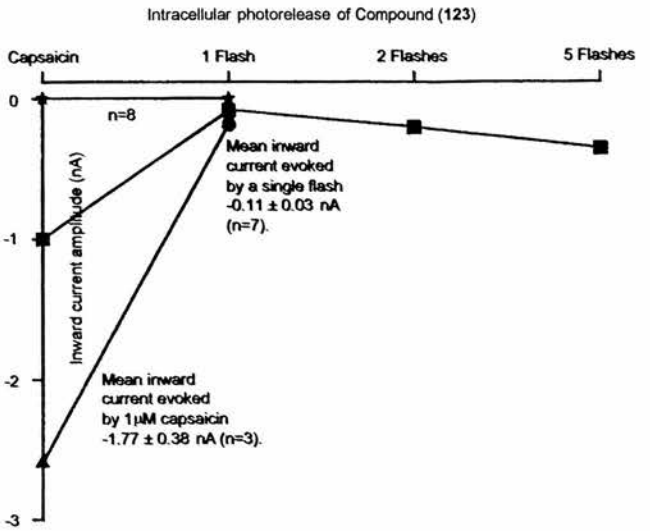

Fig. 3.4 Line chart showing the diversity of DRG neuron current responses to capsaicin and intracellular photolysis of compound **123**. Only 2 out of 7 DRG neurons responded to capsaicin but both these neurons also responded to intracellular photolysis of compound **123**. Five cells failed to respond to both drugs.[46]

For neurons that were found to respond to capsaicin **24**, a response to intracellular flash photolysis of the capsaicin analogue **123** was also observed. For these experiments a rapid inward current was shown, followed by a period of recovery (Figure 3.5 **B**). Furthermore, one photolytic experiment resulted in a burst of action potentials, attributed to the spread of excitation in the voltage clamped cell body (Figure 3.5 **C** & **D**).

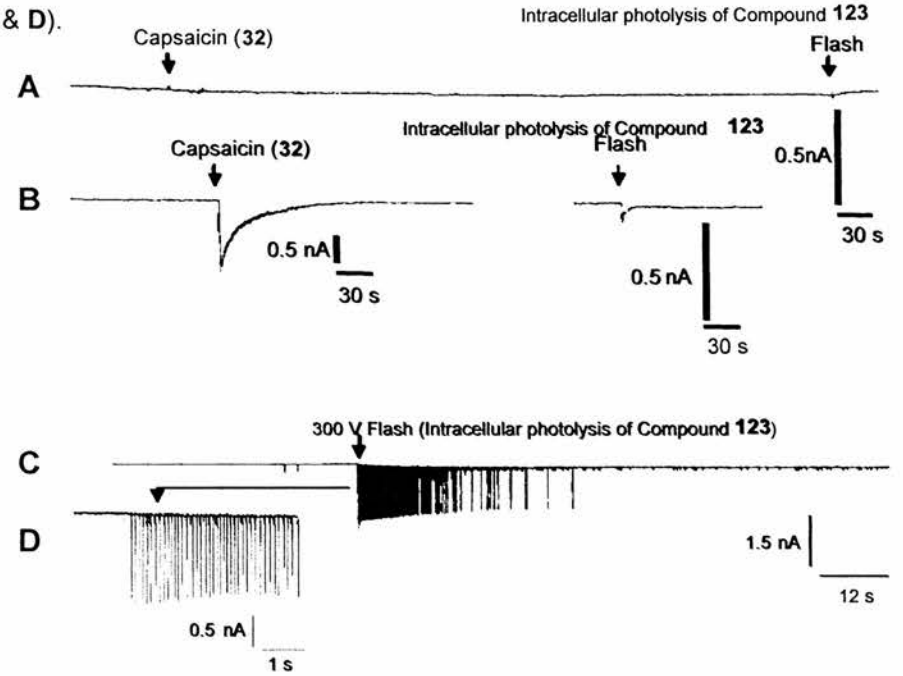

Fig. 3.5 (**A**) Example voltage clamp record showing a non-responding neuron that failed to respond to both capsaicin and intracellular photolysis of compound **123**. (**B**) Records showing inward currents activated by capsaicin and intracellular photolysis of compound **123**; note the difference in current scale. (**C**) Action currents evoked by intracellular photolysis of compound **123**; showing the burst firing behaviour that gradually declines as the neuron recovers to a resting state. This neuron was voltage clamped at a holding potential of -70 mV; the excitatory action of photoreleased compound **32** appears to have occurred in an unclamped region of the cell and a burst of action potentials has spread into the cell body to be recorded as currents. (**D**) The same record as (**C**) but on an expanded time scale to show the high frequency action potential firing and that the first action potential was not initiated by a clear inward current in the cell soma. Arrows mark the points at which 300 V flashes (175 mJ; lasting 1 ms) from a xenon flash lamp, equipped with a 360 nm filter, were applied to the DRG neurons. Under voltage clamp all neurons were held at -70 mV.[46]

In order to explore the extent of photolysis involved in the *in vitro* photolytic studies described, it was decided that the photolytic properties of the capsaicin analogue **123 and the newly synthesised capsaicin analogue 118 would be investigated outside of** the cell, in solution.

The first challenge in investigating these properties was the choice of analytical technique. Initially, it was intended to characterise uncaging at concentrations and conditions similar to those used in the *in vitro* patch clamp/pipette experiments of Carr *et al.* and Zemelman *et al.*[46,68] In particular, the study of compound **123** used solutions of around 50 μM (0.05 μmol/cm^3), of which approximately 10 μl was injected in cells and photolysed.[46] As ^{1}H NMR analysis would be inadequate to follow uncaging at this concentration, mass spectrometry was considered, but disregarded as it would have been impractical. High pressure liquid chromatography (HPLC) was also investigated, but again experiments on uncaged biologically active compound **32** at 4, 0.8 and 0.16 μmol/cm^3 were barely detected, thus giving a clear indication that detection of uncaging of a 0.05 μmol/cm^3 starting solution would not be possible.

Given the difficulty of studying caged compounds (**118** and **123**) at 50 μM, studies at higher concentrations were attempted on compound **123**, using 300 V flashes from a xenon flash lamp equipped with a 360 nm filter. Initial experiments were carried out at 1 μmol/cm^3 concentration and the caged material detected by ^{1}H NMR analysis, but there was no evidence of photolysis. It was expected that if photolysis had occurred the ^{1}H NMR spectrum would show a number of new peaks derived from the uncaged material, in particular, the singlet and doublet derived from the -C*H*$_2$O- and -C*H*$_2$NH- protons respectively. Even with repeated flash photolysis ^{1}H NMR analysis did not provide evidence of uncaging. One of the possible reasons for this was that the amount of irradiation at the correct wavelength applied in each flash was not causing enough photolysis to be observed, and that although these amounts are adequate in a biological context to cause a cellular event, they were not enough to demonstrate chemical uncaging.

It was decided that the photochemical properties of caged capsaicin analogues (**118** and **123**) would be studied using similar conditions to that used by Katritzky *et al.*,

where the dimethoxynitrobenzyl caged capsaicin analogue **124** (Figure 3.6) was photolysed.[65]

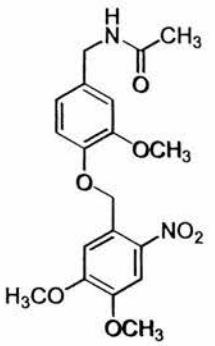

124

Fig. 3.6 The dimethoxynitrobenzyl caged analogue of capsaicin employed in photolytic experiments conducted by Katritzky *et al.*[65]

The photolysis experiments described by Katritzky *et al.* were conducted using a UV 450 W immersion lamp with a 363 nm filter, as the light source. In order to follow these experiments as closely as possible, a 125 W immersion lamp with a 375 nm filter was used. Initially, photolysis was conducted on (1 cm^3) aliquots of a 7.3 mM solution of the caged capsaicin compound **123**, irradiating for 1, 15 and 30 min. ^1H NMR analysis of these aliquots revealed no detectable uncaging. However, irradiation for 60 min indicated a small peak at 4.14 ppm that could possibly be attributed to the appearance of the -CH_2NH- doublet of the uncaged material **32** (Figure 3.7).

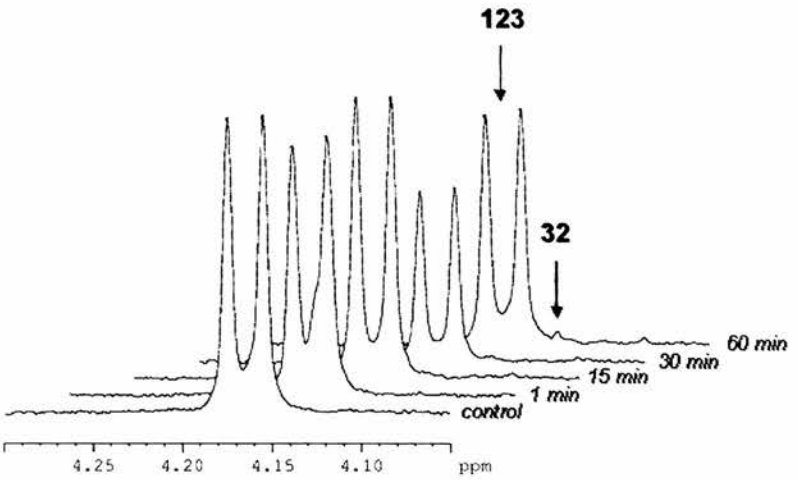

Fig. 3.7 Partial 300 MHz ^1H NMR spectra of compound **32** irradiated, for the time indicated, with a 125 W mercury arc lamp through a 375 nm filter.

Indeed, when equimolar amounts of **32** and **123** were placed in solution ^{1}H NMR analysis confirmed that an apparent triplet would be present in this region of the spectrum as a result of overlapping doublets derived from the coupling of the -CH_2NH- protons in each compound (Figure 3.8).

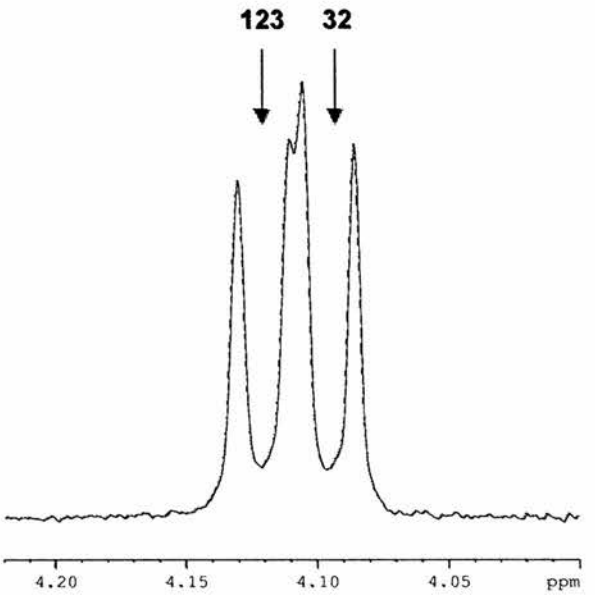

Fig. 3.8 Partial 300 MHz ^{1}H NMR spectrum of equimolar amounts of compounds 32 and 123. The ^{1}H NMR shows an apparent triplet owing to a doublet derived from coupling of the -CH_2NH- protons on compound 32 and an overlapping doublet derived from coupling of the -CH_2NH- protons of compound 123.

In order to validate our photolysis conditions, photolysis experiments were conducted on the dimethoxynitrobenzyl caged capsaicin analogue **118**. Aliquots (1 cm^3) of a 7.3 mM solution were irradiated for 1, 15 and 30 min. It was observed that 35% uncaging had occurred after 30 min, clearly shown by the ^{1}H NMR doublet at 4.14 ppm derived from the -CH_2NH- protons (Figure 3.9).

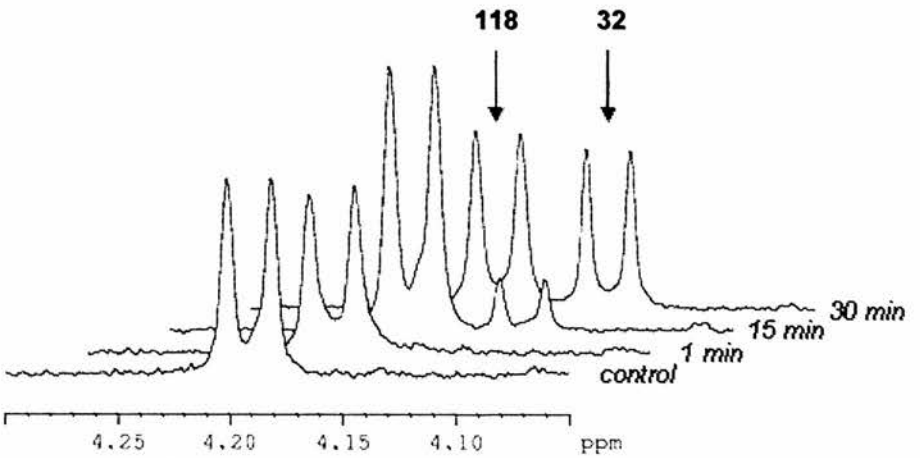

Fig. 3.9 Partial 300 MHz ^{1}H NMR spectra of compound 118 irradiated, for the time shown, with a 125 W mercury arc lamp through a 375 nm filter. 35% uncaging (as adjudged by appearance of compound 32 vs total material) was observed after 30 min. The doublet at 4.19 ppm is from compound 118; the doublet at 4.14 ppm is from compound **32.**

These findings were confirmed when ^{1}H NMR analysis of a solution containing equimolar amounts of **32** and **118** showed the same patterns and shifts of peaks observed in the photolysis studies (Figure 3.10).

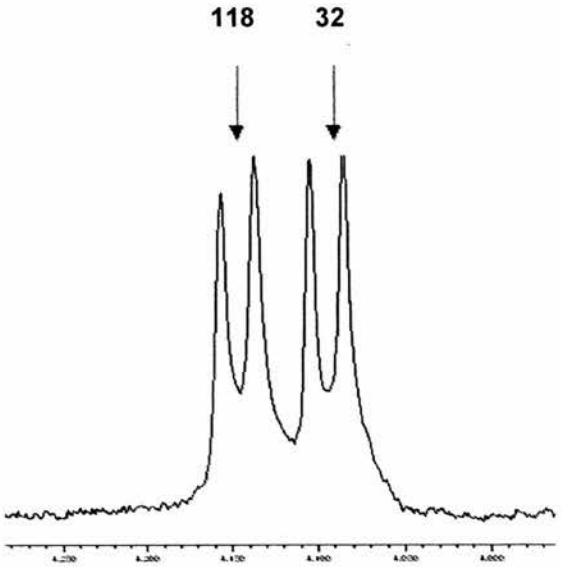

Fig. 3.10 Partial 300 MHz ^{1}H NMR spectrum of equimolar amounts of compounds **32** and **118**. The ^{1}H NMR shows a doublet at 4.10 ppm derived from coupling of the -CH_2NH- protons on compound **32** and a doublet at 4.15 ppm derived from coupling of the -CH_2NH- protons of compound **118**.

The differences observed between caged compounds **118** and **123** are accountable to the fact that photolysis of the phenacyl caging group is thought to be optimal at 278 nm wavelength, where as optimal uncaging of the dimethoxynitrobenzyl group is achieved at 345 nm wavelength, much closer to the wavelength of irradiation.

Indeed, UV analysis of the caged compound **118** revealed that the optimal wavelength at which to remove the caging group is at the absorbance maximum 345 nm (Figure 3.11 **A**). This is consistent with the UV analysis of the 4,5-dimethoxynitrobenzyl bromide reagent which has a maximum absorbance/excitation wavelength of 347 nm (Figure 3.11 **B**).

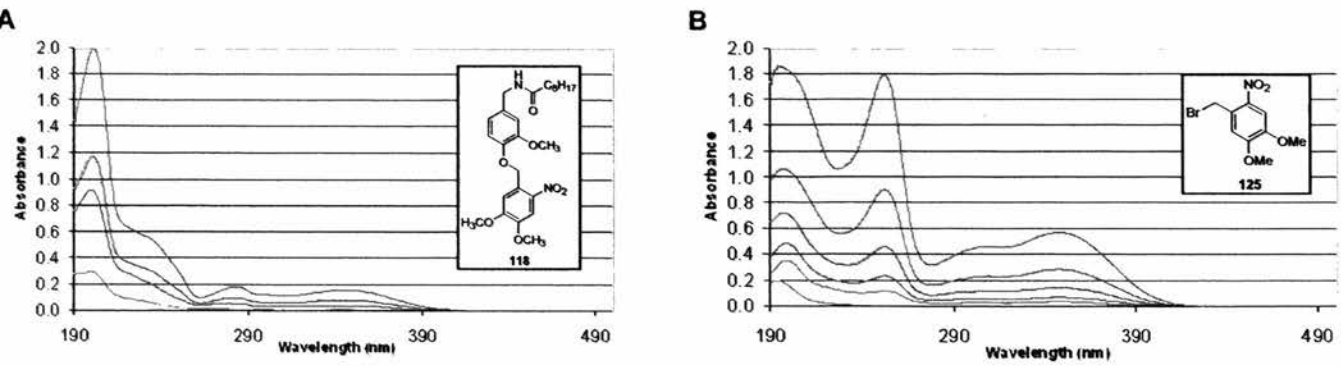

Fig. 3.11 UV spectra of caged capsaicin analogue **118** in acetonitrile (**A**) and the 4,5-dimethoxynitrobenzyl bromide reagent in acetonitrile (**B**).

In contrast, the observed unreactive nature of caged compound **123** is consistent with the UV analysis of the compound, as no significant absorption/excitation at 375 nm is observed, even at the highest of concentrations run (Figure 3.12).

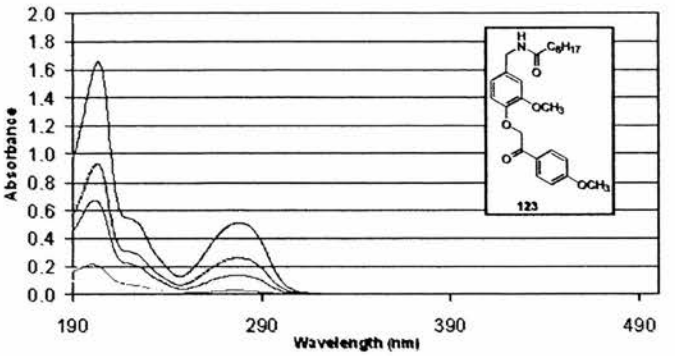

Fig. 3.12 UV spectrum of caged phenacyl capsaicin analogue 123 in acetonitrile, showing no absorption at 375 nm wavelength.

The differences observed in the photolysis properties of **118** and **123** gives rise to the possibility of selectively photolysing these compounds in a wavelength-dependent manner. The use of a 405 nm violet diode laser was considered optimal as this source could provide the focussed irradiation required to remove the DMNB group, but the wavelength was considered sufficiently high and the emission spectrum narrow enough for the phenacyl compound to remain unaffected.

Photolysis studies were attempted on the caged capsaicin analogue **118**, using a 405 nm violet diode laser as the photon source. Initial experiments were conducted on 1 cm^3 aliquots of 6.63 mM solutions in D_6-acetone and runs were of 1, 15, 30 and 45 min duration. Analysis of the resulting D_6-acetone solutions by ^1H NMR spectroscopy indicated photolysis had taken place, as indicated by the many additional peaks attributed to the presence of the uncaged biologically active compound. The most prominent indications being that of the developing doublet for the -CH_2NH- at 4.14 ppm of the uncaged compound and the disappearance of the -CH_2NH- at 4.19 ppm of the caged compound.

Given the successful identification of both the caged and uncaged compounds by ^1H NMR analysis in the initial laser photolysis studies, a time-course of the uncaging process was completed (Figure 3.13).

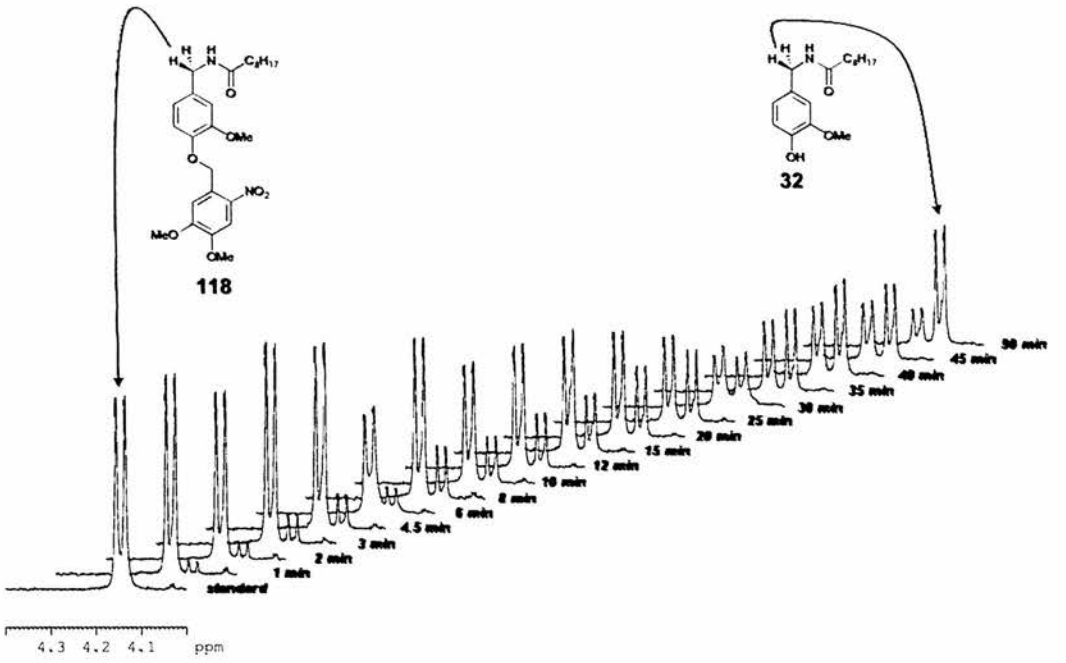

Fig. 3.13 Partial 300 MHz ^{1}H NMR spectra of compound **118** irradiated for a range of 1-90 min, with a 405 nm violet diode laser. These spectra show the disappearance of the -CH_2NH- from compound **118** and the appearance of the -CH_2NH- from compound **32**, indicating that uncaging has occurred.

Experiments were performed on 1 cm^3 aliquots of a 6.63 mM in D_6-acetone stock solution at a range of times from 1-90 min. ^{1}H NMR analysis of the resulting solutions showed the decrease of the doublet corresponding to the caged material, increase of the uncaged doublet (Figure 3.13) and also the disappearance of the singlet derived from **118**.

In order to gain a more detailed understanding of the photolytic properties of caged capsaicin analogue **118**, further analysis and experiments were conducted. It should be noted that although the doublet at 4.19 ppm and the singlet at 5.29 ppm should give integrals that decrease at the same rate, comparison of these throughout the time course (Figure 3.13) consistently showed that the decrease of the singlet was greater than that of the doublet. This suggests that although uncaging is taking place, conversion to the biologically active analogue **32** may not be 100% efficient. This was investigated by comparing the sum of the integrals of both doublets to an external standard. The external standard chosen was the amount of non-deuterated acetone in the ^{1}H NMR spectra. Thus for each aliquot the ratio of these proton integrals was compared to the integral of non-deuterated acetone and these results compared to the

integral of non-deuterated acetone in a control solution, i.e. an aliquot originating from the stock solution that had not undergone any photolysis. This study showed a trend of decreasing overall material with increasing irradiation time. At 180 min, this ratio indicated that 10% of the total material was no longer the caged or uncaged compounds **32** and **118**.

Given that photolysis is not 100% efficient in this system, it is important that the term "uncaging" be defined, as uncaging can be described as either the removal of the caged group or as the production of the uncaged material **32**. As the uncaged material is the compound of biological importance, "uncaging" in this discussion is defined as the appearance of the uncaged product **32**. Thus the appearance of the doublet at 4.14 ppm derived from -C*H*$_2$NH- of **32** in the ^{1}H NMR spectrum represents uncaging. From comparison of the caged and uncaged doublets, the percentage uncaging throughout the time-course was elucidated (Figure 3.14). This showed that in the first 1 min > 5% of uncaging was observed and by 180 mins, over 80% of uncaging had been achieved.

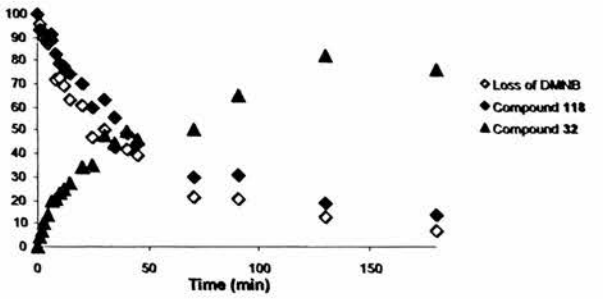

Fig. 3.14 The uncaging profile of **118** on irradiation at 405 nm. The disappearance of the caging group -C*H*$_2$O-, the disappearance of the -C*H*$_2$NH- of compound **118**, and the appearance of the -C*H*$_2$NH- of compound **32** were monitored. The integrals were obtained using 1DWINNMR to perform deconvolution calculations.

In order to explain the loss of material, laser photolysis using the same conditions as for the time course was carried out on the biologically active compound **32**. Experiments of 1, 15 and 30 min duration were completed and in all cases showed no detectable breakdown products. This finding strongly suggests that the observed loss of material in the time course was not due to subsequent breakdown of the uncaged phenol **32** and that side products are a result of the mechanistic nature of the photolysis of compound **118**.

The proposed mechanism for photolysis of compound **118** is shown (Scheme 3.1). This mechanism is derived from the mechanism proposed by K. Zhang.[56]

Possible side reactions that would be consistent with the mechanism proposed and that could explain the loss of material observed include the propagation of radicals in the initial excitation species **127** and/or the nucleophilic attack by a species other then (OH) toward species **129**, yielding a compound that is unable to eliminate *ortho*-nitrosobenzaldehyde and the desired phenol (Scheme 3.1).

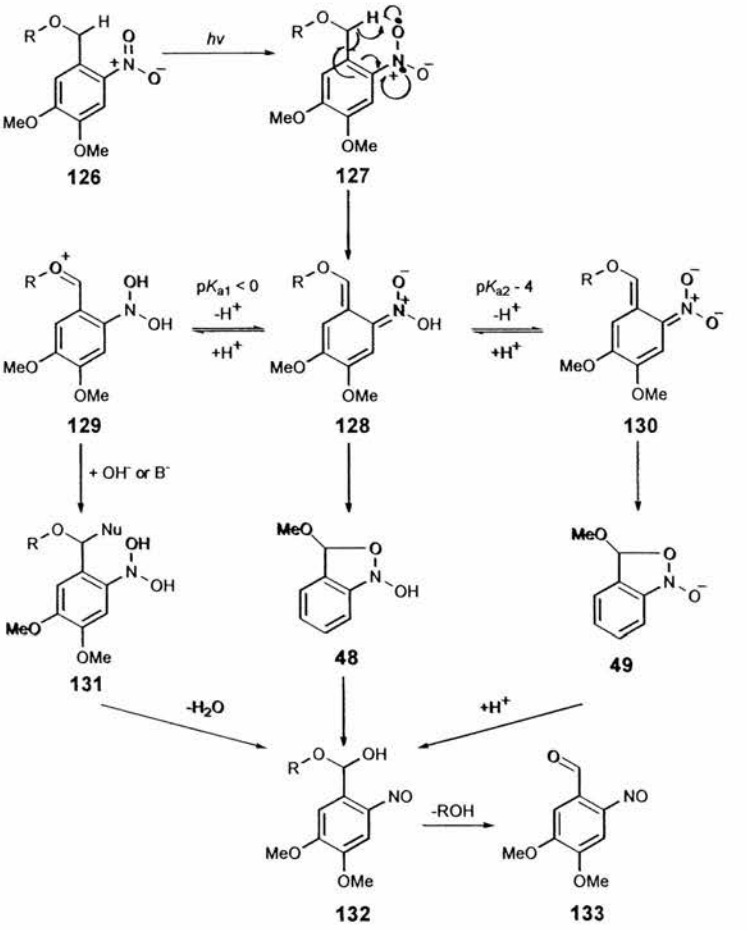

Scheme 3.2 Proposed photolytic and subsequent dark reaction mechanism for 4,5-dimethoxynitrobenzyl caged capsaicin analogue **118**.

A possible way to test these suggestions, would be to lower the concentration of the starting solution, thereby reducing any intermolecular interactions and reduce the occurrence of side reactions. However, problems with this are that by decreasing the concentration, the noise in the ^{1}H NMR analysis would increase, making comparisons more difficult and less reliable. Further investigation of this was not conducted.

These findings are thus a testament to the ability of using a specific wavelength laser as a photon source, rather than mercury and Xenon lamps with a filter in place, as

focused and quantitively controlled energy can be applied. Indeed, additional evidence was acquired when members of the Conway group conducted energy input changes, that show as power input is increased, so does the extent of uncaging (Figure 3.15).

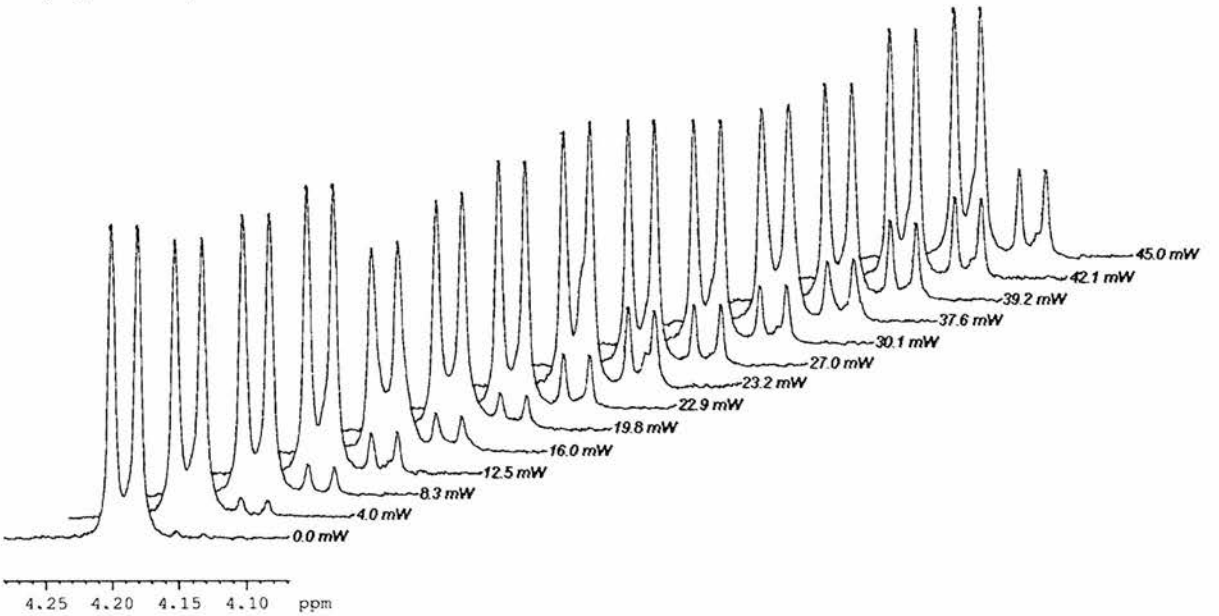

Fig. 3.15 Partial 300 MHz ^{1}H NMR spectra of compound **118** irradiated for x min with a 405 nm violet diode laser, at the power setting shown. These spectra show the disappearance of the -C*H*$_2$NH- from compound **118** and the appearance of the -C*H*$_2$NH- from compound **32**, indicating that uncaging occurs in a power-dependent manner.

In the original time-course photolysis of **118**, the laser power was arbitrarily set to 45 mW, as this was the maximum power setting. To investigate the power input against percentage uncaging, irradiation of **118** was carried out for 10 mins over a range of different powers (Figure 3.15). These experiments showed that uncaging is dependent on power and that as irradiation power is increased, the rate of uncaging decreases.

Given the successful uncaging of **118** using a 405 nm violet diode laser as the photon source, photolysis was attempted on the phenacyl caged capsaicin derivative **123**. Experiments were conducted with conditions identical to those for compound **118**, (1, 15 and 30 min duration). However, in contrast to compound **118**, analysis by ^{1}H NMR showed no indication of photolysis in any of the experiments and spectra were identical to that of the control. Additionally, these observations were checked by spiking the 30 min ^{1}H NMR with an equimolar amount of the uncaged compound **32**. Analysis of this spectrum showed a triplet at 4.28 ppm which derives from the combination of the -

~~CH_2NH-doublets~~ of compounds **32** and **123** (Figure 3.16). Thus it was concluded that if ~~photo~~lysis had taken place, an apparent triplet would be observed as well as overlapping of several other peaks within the spectrum.

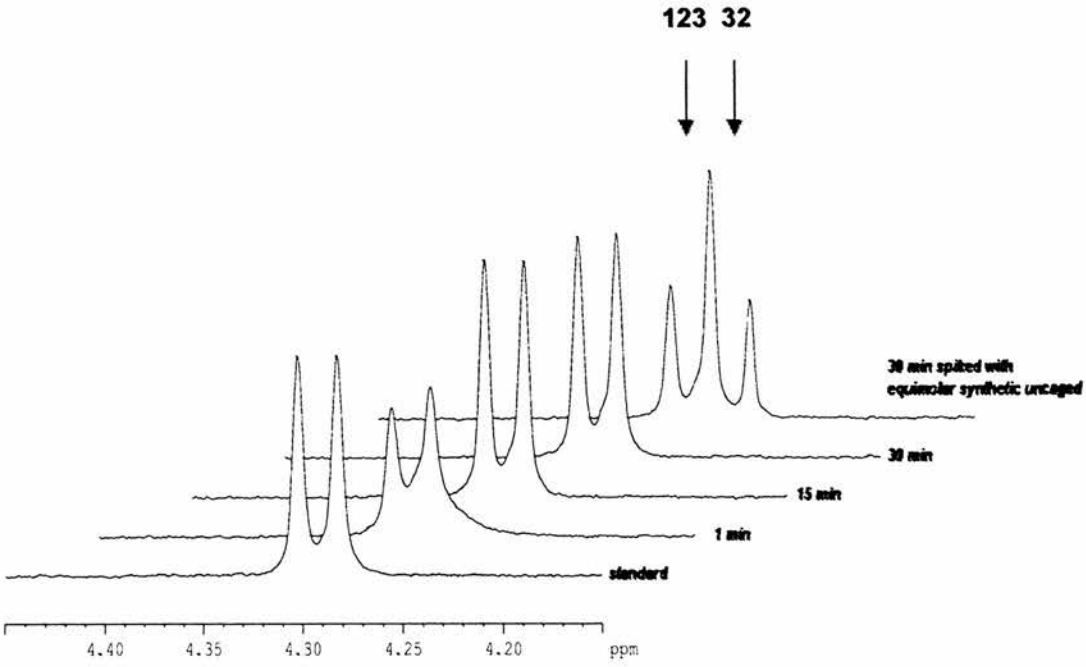

Fig. 3.16 Partial 300 MHz ^{1}H NMR spectra of compound **123** irradiated, for the time shown. These spectra show the -CH_2NH- from compound **123** does not disappear and that the -CH_2NH- from compound **32** is not observed.[46]

An equimolar solution of **32** and **123** was irradiated for 1, 15 and 30 min by the 405 nm laser, the resulting ^{1}H NMR analysis showed that after 30 min the nitroveratrole caged compound **118** had uncaged by 67%, while the phenacyl analogue **123** was found to be unaffected (Figure 3.17 and 3.18). However, in this instance, uncaging was adjudged by comparison of the singlets derived from the -CH_2O- protons of each caged compound with the nitroveratrole analogue **118** shift at 5.29 ppm and the phenacyl analogue **123** shift at 5.20 ppm. This was necessary as overlapping of all three -CH_2NH- doublets made detection of percentage uncaging in this region impossible.

It should also be noted that given all the conditions were the same as the time-course experiments, there was a greater extent of uncaging occurring, as the percentage in these studies showed 67% compared to around 40% expected from the time graph. This greater efficiency, may be an effect of "sensitisation", although as these experiments have only been conducted once this deviation may not be significant. This phenomenon has been reported in similar studies. Blanc and Bochet found that although

they were able to photolyse a nitroveratrole derived carbamate at 419 nm but not at 254 nm, and likewise photolyse a 3,5-dimethoxybenzyl derivative of the same carbamate at 254 nm but not to any degree at 350 nm, the combination of the two compounds in equimolar amounts and subsequent photolysis at 254 nm did not show any selectivity for the nitroveratrole derivative.[69] This occurrence is accredited to one photolabile compound acting as a 'sensitiser' for the other and leads to the loss of any selectivity and more efficient photo uncaging in the mixture. Blanc and Bochet later achieved wavelength controlled orthogonal photolysis using 2-nitroveratryl and 3'-5'-dimethoxybenzoin moieties for the two different caging groups.[58] Despite the occurrence of 'sensitisation' in the Blanc and Bochet model,[69] the photolysis studies conducted here showed wavelength-dependent selectivity of photolysis (Figure 3.17).

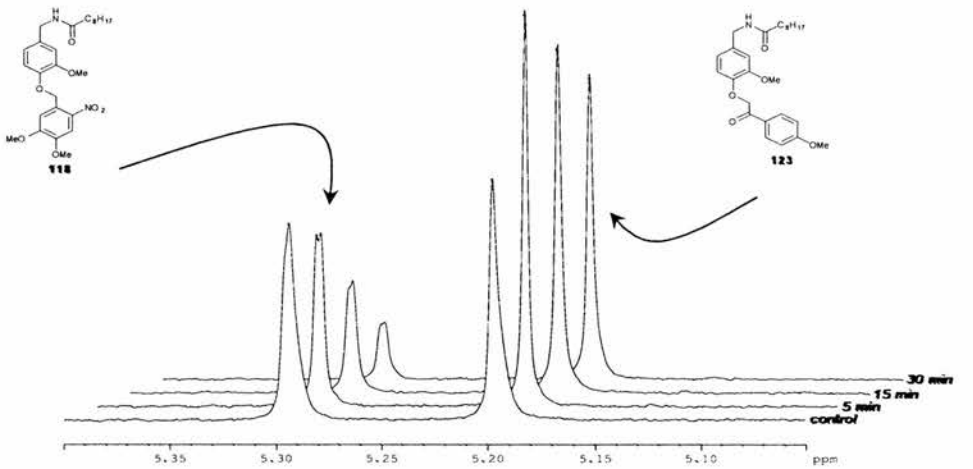

Fig. 3.17 Partial 300 MHz ^{1}H NMR spectra of compounds **118** and **123** irradiated, for the time shown. These spectra show the -C*H*$_2$OH- of both compounds and that compound **123** does not disappear as the -C*H*$_2$OH- from compound **118** decreases by photolysis.

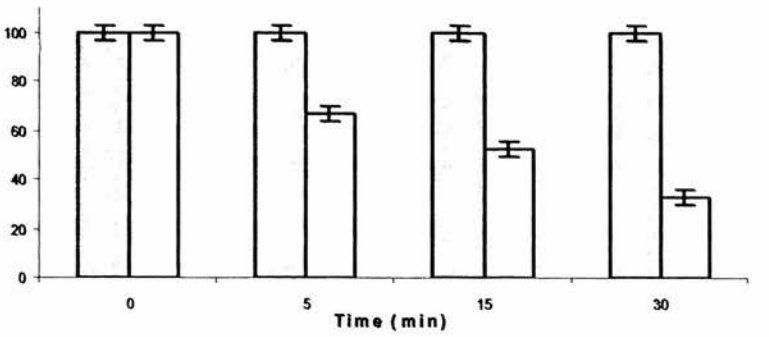

Fig. 3.18 The uncaging profiles of **118** and **123** on irradiation at 405 nm. The disappearance of the -C*H*$_2$O- of the caging group was monitored by ^{1}H NMR, the integrals were obtained using 1D WINNMR to perform deconvolution calculations. The gray bars show the percentage of compound **123** present after the given time. The clear bars show the percentage of compound **118** present after the given time.

These findings are highly significant as the so called wavelength orthogonality of caging groups is a highly desired and sought after technique and these data strongly support this system as orthogonal (Figure 3.17 and 3.18). Indeed, initial experiments conducted by the Conway group where an equimolar solution of **118** and **123** was irradiated at 278 nm wavelength have shown selective photolysis toward compound **123**. The ability to selectively uncage a compound in the presence of another caging group is a powerful tool in both the analysis of caged compounds in biological *in vitro* tests and in synthetic protecting group applications. For instance, the ability in the synthesis of complex molecules to remove one caging group by photolysis, then proceed with a step and subsequently remove a second caging group on the same molecule would be highly favoured, especially with the difficulties often faced in protecting/deprotecting strategies. Furthermore, it can be envisaged that two biologically active compounds that can activate the same receptor could be placed in the exact same cell and subsequently uncaged at different times so as to elucidate their individual properties towards that receptor.

With the success of the wavelength orthogonal system described above, the UV spectrum of the caged anandamide derivative **77** was analysed to examine this compound as a potential candidate for a second orthogonal system. As expected, the UV spectrum showed a maximum at 261 nm derived from absorbance/excitation of the NO_2 group, the same wavelength as observed in the caging group reagent at 260 nm (Figure 3.19).

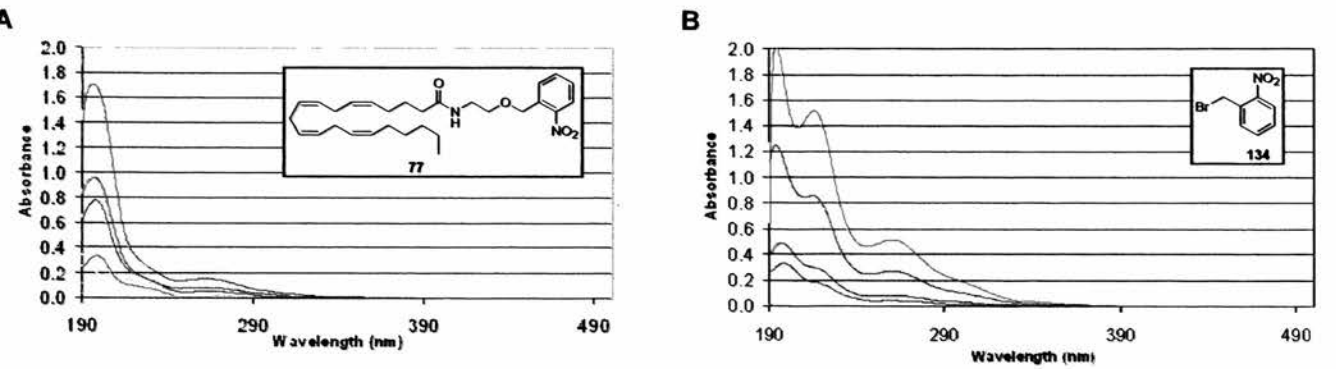

Fig. 3.19 UV spectra of caged anandamide analogue **77** in acetonitrile **(A)** and the 2-nitrobenzyl bromide reagent in acetonitrile **(B)**.

Given the observed UV spectra it is postulated that if the AEA analogue **77** and capsaicin analogue **118** were to be placed together in solution and subsequently irradiated using a laser at 405 nm wavelength, the capsaicin analogue **118** would be orthogonally uncaged, as no absorption/excitation is observed in the AEA analogue UV spectra at 405 nm wavelength (Figure 3.20 **A**). Furthermore it is thought in a biological *in vitro* test, the AEA analogue could then be irradiated and uncaged at a lower wavelength, as this is in the tail region on the UV spectrum of **77** (Figure 3.20 **A**). Although conduction of these experiments is highly desirable, lack of the AEA analogue material **77**and time prevented such tests from being performed.

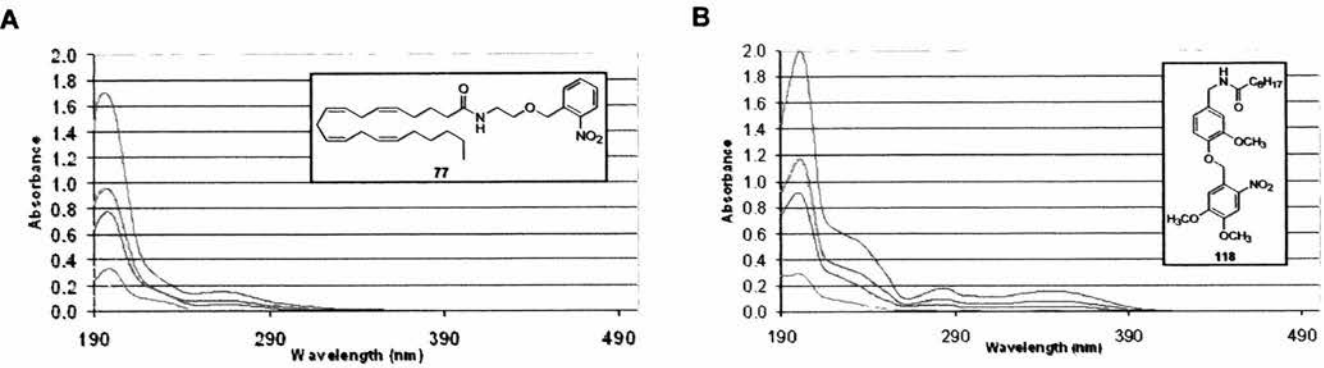

Fig. 3.20 UV spectra of caged anandamide analogue **77** in acetonitrile **(A)** and caged capsaicin analogue **118** in acetonitrile **(B)**.

One advantage of using these particular caging compounds **77** and **118** as the tools for studying TRPV1 receptors is that they give very similar by-products. i.e. Even though one group has two methoxy groups substituted on the caging group ring, the mechanism of photolysis is the same as proposed previously (Scheme 3.1). This means that the inert by-products will be *ortho*-nitrobenzaldehyde and 4,5-dimethoxy-*ortho*-nitrobenzaldehyde.

Another experiment would be to investigate possible orthogonality between caged anandamide analogue **77** and caged capsaicin antagonist **121**. UV analysis of compound **121** shows an absorbance maximum at 347 nm wavelength (Figure 3.21). This was expected as this is in accordance with the caged capsaicin agonist **118** which has an absorbance at 345 nm wavelength. UV analysis therefore suggests antagonist **121** can be removed in a similar manner to compound **118** using a laser at 405 nm wavelength.

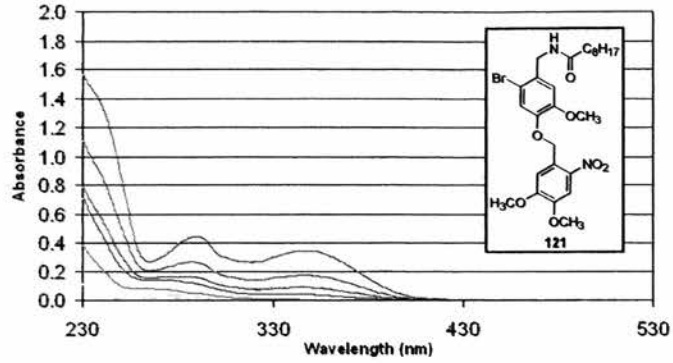

Fig. 3.21 UV spectra of caged anandamide analogue 121 in dichloromethane.

If a wavelength orthogonal system is found between the caged anandamide analogue **77** and caged capsaicin antagonist **121**, this system would be a useful tool in analysing the differences between anandamide and capsaicin toward the TRPV1 receptor. These experiments could also lead to the exciting prospect of switching a cell's activity on and off using anandamide and the capsaicin antagonist **120**.

4 Conclusion

The opportunity for therapeutic drug intervention at the cannabinoid and TRPV1 receptors for management of physiological aspects such as memory, motor function and in particular, pain perception, is becoming a more realistic possibility as the complexity of these systems is slowly being deciphered. However, the need for biological tools to study the endogenous/exogenous ligands, in particular anandamide and capsaicin analogues, has thus far impeded many of these developments. The research conducted in this project has culminated in the synthesis of several potentially useful compounds (**77**, **78**, **118**, **121** and **122**) which will allow the temporal and spatial properties of anandamide and a capsaicin analogue to be controlled *in vitro*. This has been achieved through the use of caging groups.

In addition, several of these compounds have been used in photolysis studies and have given further in-sight into the field of "caged compounds". The illusive goal of 'orthogonality' has been clearly demonstrated in the selective photolysis of a 4,5-dimethoxynitrobenzyl analogue of capsaicin in the presence of phenacyl capsaicin analogue. Furthermore, it has been shown that a 405 nm wavelength laser can be successfully employed to achieve photolysis. The implications of this are that a greater degree of spatial and temporal *in vitro* control during photolytic release can now be achieved, using a non-destructive laser source instead of a flash lamp.

5 Future Work

The success of this project in synthesising and characterising several caged capsaicin and anandamide analogues and the subsequent photolytic results obtained for some of these analogues has provided this field of research with numerous possible angles for future work, both in terms of synthesis and further characterisation of the novel compounds already made.

Immediate suggestions include the biological *in vitro* testing of compounds **77**, **78**, **118**, **121** and **122**, to firstly investigate their biological inertness as caged compounds and secondly, their biological properties with regards to *in vitro* flash photolysis and receptor activation. In addition, given the success of the laser uncaging studies, experiments involving the *in vitro* laser uncaging of these compounds should be conducted. These experiments would be the first example of *in vitro* orthogonal caging.

For the chemist, further exploration of the orthogonal properties demonstrated by the two caging groups attached to caged capsaicin analogues **118** and **123** are of greatest interest. In particular, further laser photolysis studies to help us better understand the phenomenon of sensitisation could be conducted. With regards to the orthogonal properties of the phenacyl and 4,5-dimethoxynitrobenzyl caging groups, these caging groups could be applied to other biologically interesting compounds, so as to provide useful tools in studying their respective receptors, but also to establish if orthogonality is maintained when these caging groups are applied to other compounds.

Furthermore, given the UV spectra of the AEA analogue **77** and capsaicin analogue **118** (Figure 3.20) suggesting that uncaging will not occur for the 2-nitrobenzyl derivative at 405 nm, laser photolysis experiments to establish any orthogonality between the 2-nitrobenzyl and 4,5-dimethoxynitrobenzyl caging groups would be interesting to pursue. Indeed, orthogonal protection of these TRPV1 ligands would allow direct comparison of each of their properties within the same cell. In addition, if these caging groups did not demonstrate orthogonality, then synthesis of the phenacyl caged anandamide analogue **79** would be strongly recommend as orthogonality between the phenacyl and 4,5-dimethoxynitrobenzyl caging groups has already been illustrated in the photolysis studies discussed previously. Another suggestion for future work is to conduct

an investigation into the fine tuning of caging groups, the basis of which could be tuning of the phenacyl and 4,5-dimethoxynitrobenzyl groups. Derivatives of both caging groups could yield compounds that have very narrow photolytic wavelength bands, that is to say, are cleaved in a very specific wavelength range.

Future work directly relevant to this project includes the photolytic study of the synthesised antagonist compound **121**. It would be interesting to see the effect the presence of a bromine atom on laser photolysis, as it is suspected that radicals are likely to be formed, propagation of which would result in decomposition. Synthetically, there is need to improve the yields of the synthetic steps employed and also to synthesise other final compounds such as 3-methoxy-4-(2-nitrobenzyl)-*N*-nonanoylbenzylamine **135** and the phenyl caged anandamide **79** mentioned previously (Figure 5.1).

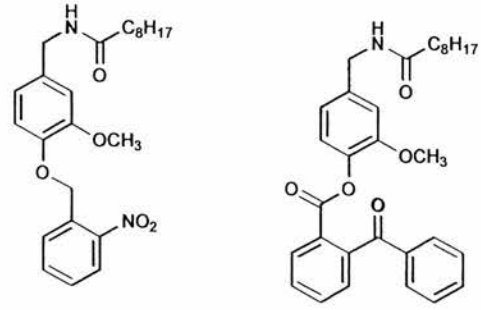

135 **136**

Fig. 5.1 The molecule structures of two proposed future work caged capsaicin analogues.

It would also be of interest to synthesise a capsaicin analogue using the diphenyl caging group **136**, so as to directly compare its properties to the phenacyl and 4,5-dimethoxynitrobenzyl groups in this system.

6 Experimental Section

6.1. General

^1H NMR spectra were recorded on a Bruker Avance 300 (300.1 MHz) instrument, using deuterochloroform (or other indicated solvent) as reference or internal deuterium lock. The chemical shift data for each signal are given as δ in units of parts per million (ppm) relative to tetramethylsilane (TMS) where δ (TMS) = 0.00 ppm. The multiplicity of each signal is indicated by: s (singlet); br s (broad singlet); d (doublet); t (triplet); q (quartet); dd (doublet of doublets) or m (multiplet). The number of protons (n) for a given resonance is indicated by nH. Coupling constants (*J*) are quoted in Hz and are recorded to the nearest 0.1 Hz.

^{13}C NMR spectra were recorded on a Bruker Avance 300 (75.5 MHz) instrument using the PENDANT sequence and internal deuterium lock. The chemical shift data for each signal are given as δ in units of ppm relative to TMS where δ (TMS) = 0.00 ppm. Where appropriate, coupling constants (*J*) are quoted in Hz and are recorded to the nearest 0.1 Hz.

IR spectra were recorded on a Perkin-Elmer Paragon series 1000 FTIR spectrometer as a nujol mull paste. Absorption maxima are reported as ν_{max} wavenumbers (cm^{-1}). Intensities of the maxima are quoted as strong (s), medium (m) or weak (w). Stretches are quoted, were applicable, as asymmetric (asym), symmetric (sym) or adjacent (adj).

UV/Vis spectra were recorded on a Perkin-Elmer Lambda 35 UV/VIS spectrometer using 10 mm Far UV quartz cuvettes. Absorbance is reported as λ_{max} wavelength (nm), intensities as (ε/dm^3 mol^{-1} cm^{-1}) and the shape of the curve is a maximum unless specified as an inflection (infl) or a shoulder (sh).

Melting points were determined using a Gallenkamp MF-370 and are uncorrected.

Analytical thin layer chromatography (TLC) was carried out on pre-coated 0.25 mm ICN Biomedicals GmbH 60 F_{254} silica gel plates. Visualisation was by absorption of UV light, or thermal development after dipping in either an ethanolic solution of phosphomolybdic acid (PMA) or an aqueous solution of potassium permanganate, potassium carbonate and sodium hydroxide.

Column chromatography was carried out on silica gel (Apollo Scientific Ltd 40-63 micron) under a positive pressure of compressed air.

Dry dichloromethane was distilled from calcium hydride in a recycling still. Diethyl ether was distilled from sodium in a recycling still using benzophenone ketyl as an indicator. Anhydrous DMF was purchased from Aldrich UK and dried by distillation from 4 Å molecular sieves onto 4 Å molecular sieves under a nitrogen atmosphere. Chemicals were purchased from Acros UK, Aldrich UK, Avocardo UK, Fischer UK or Fluka UK. All solvents and reagents were purified and dried, where necessary, by standard techniques.[70] Where appropriate and if not stated otherwise, all non-aqueous reactions were performed under inert atmosphere of nitrogen, using a vacuum manifold with nitrogen passed through 4 Å molecular sieves and self-indicating silica gel. Sodium hydride was used as a 60% suspension in mineral oil.

In vacuo or under reduced pressure refers to the use of a rotary evaporator attached to a diaphragm pump. Brine refers to a saturated aqueous solution of sodium chloride. Hexane refers to *n*-hexane and petroleum ether to the fraction boiling between 40-60 °C.

Photolysis was conducted using a 405 nm violet diode laser from T-Optica Photonics with a maximum output power of 50 mW.

6.1.1. *N*-(*tert*-Butoxycarbonyl)-2-aminoethanol

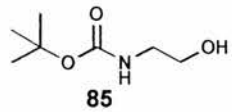

85

To a solution of ethanolamine (2.00 g, 1.98 cm^3, 3.27 mmol, 1.0 equiv) in acetonitrile (1.5 cm^3) under an atmosphere of nitrogen at RT was added 4-DMAP (0.41 g, 3.36 mmol, 1.0 equiv). Di-*tert*-butyldicarbonate (0.71 g, 3.27 mmol, 1.0 equiv) was dissolved in acetonitrile (3 cm^3) and added to the ethanolamine solution, *via* cannula, over a period of 35 min and further washed in with acetonitrile (2 cm^3). After stirring overnight (16 h), analysis by T.L.C. showed that starting material was still present and a second equivalent of di-*tert*-butyldicarbonate (0.71 g, 3.27 mmol, 1.0 equiv) was added. After 6 h stirring, analysis by T.L.C. showed that the starting material had been consumed and therefore water (0.1 cm^3) was added. The solvent was evaporated and the resulting oil extracted with dichloromethane (3 × 50 cm^3) and the organic phase washed with water (50 cm^3). The organic layers were combined, dried ($MgSO_4$), filtered and the solvent removed under reduced pressure. Purification by silica gel column chromatography eluting with petroleum ether/ethyl acetate (50:50) afforded *N*-(*tert*-butoxycarbonyl)-2-aminoethanol (0.64 g, 100%) as a colourless liquid. R_f 0.18 (petroleum ether/ethyl acetate 60:40); δ_H (300 MHz; $CDCl_3$) 5.30 (1H, br s, N*H*), 3.70 (1H, br s, O*H*), 3.59 (2H, t, *J* 5.1, $HOCH_2CH_2NH$), 3.19 (2H, t, *J* 5.1, $HOCH_2CH_2NH$), 1.37 [9H, s, $OC(CH_3)_3$]; *m/z* (ES+) 236 (4%), 184 ($[M+Na]^+$, 100%), 128 (33%). These data are in accord with literature values.[71]

6.1.2 *N*-(*tert*-Butoxycarbonyl)-2-aminoethanol

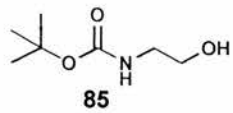

85

To ethanolamine (4.23 g, 4.18 cm^3, 67.4 mmol, 1.0 equiv) in dichloromethane (20 cm^3) was added di-*tert*-butyldicarbonate (15.1 g, 67.4 mmol, 1.0 equiv) in dichloromethane (40 cm^3) dropwise over 20 min and further washed in with dichloromethane (10 cm^3). The resulting solution was stirred overnight (16 h). Analysis by T.L.C. showed no starting

material remained and therefore water (25 cm^3) was added followed by removal of dichloromethane under reduced pressure. Water (50 cm^3) was added and the aqueous phase extracted with ethyl acetate (4 × 75 cm^3). The combined organics were consecutively washed with saturated aqueous $NaHCO_3$ (50 cm^3), brine (50 cm^3), dried ($MgSO_4$) and filtered. Purification by silica gel column chromatography eluting with petroleum ether/ethyl acetate (60:40) afforded *N*-(*tert*-butoxycarbonyl)-2-aminoethanol (10.8 g, 97%) as a colourless oil. R_f 0.19 (petroleum ether/ethyl acetate 60:40); δ_H (300 MHz; $CDCl_3$) 5.30 (1H, br s, N*H*), 3.70 (1H, br s, O*H*), 3.59 (2H, t, *J* 5.1, HOCH_2CH_2NH), 3.19 (2H, t, *J* 5.1, HOCH_2CH_2NH), 1.37 [9H, s, OC(CH_3)$_3$]; δ_c (75.5 MHz; $CDCl_3$) 157.3 (*C*=O), 80.2 (*C*CH_3), 63.0 (*C*H_2OH), 43.7 (*C*H_2NH), 28.8 (*C*H_3). These data are in accord with literature values.[71]

6.1.3 Attempted synthesis of 2-(4'-methoxyacetophenone)-*N*-(*tert*-butoxycarbonyl)ethylamine

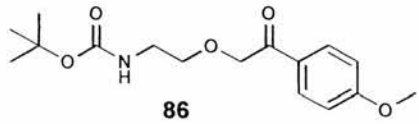

86

A solution of *N*-(*tert*-butoxycarbonyl)-2-aminoethanol (0.11 g, 0.67 mmol, 1.0 equiv) in THF (5 cm^3) under nitrogen was cooled to 0 °C and sodium hydride (27.4 mg, 0.67 mmol, 1.0 equiv) added in four portions over a period of 15 min. The reaction was then warmed to RT and stirred for 1.5 h. The mixture was cooled to 0 °C and a solution of 2-bromo-(4'-methoxyacetophenone) (0.16 g, 0.67 mmol, 1.0 equiv) in THF (3 cm^3) was added *via* cannula in three portions over a period of 15 min and further washed in with THF (1 cm^3). The mixture was stirred at 0 °C for 50 min, warmed to RT and stirred overnight (16 h). Analysis by T.L.C. showed that the starting material had been consumed and therefore water (10 cm^3) was added. The solvent was removed under reduced pressure and the resulting oil suspended in water (50 cm^3) and extracted with ethyl acetate (3 × 50 cm^3). The organic fractions were combined, dried ($MgSO_4$), filtered and the product concentrated *in vacuo*. Analysis by 2D T.L.C. showed many products and purification by silica gel column chromatography did not yield any pure products as adjudged by ^{1}H NMR spectroscopy.

6.1.4 Attempted synthesis of 2-(4'-methoxyacetophenone)-*N*-(*tert*-butoxycarbonyl)ethylamine

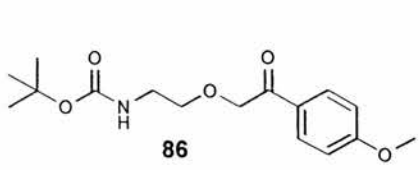

86

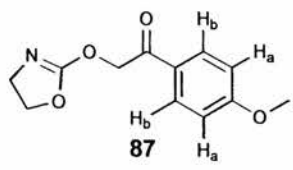

87

To *N*-(*tert*-butoxycarbonyl)-2-aminoethanol (0.31 g, 1.92 mmol, 1.0 equiv) in DMF (10 cm^3) under nitrogen was added a suspension of sodium hydride (0.13 g, 1.92 mmol, 1.0 equiv) in DMF (10 cm^3) at 0 °C over a period of 35 min. The reaction was warmed to RT and stirred for 2 h. The resulting slurry was cooled to 0 °C and a solution of 2-bromo-(4'-methoxyacetophenone) (0.44 g, 1.93 mmol, 1.0 equiv) in DMF (3 cm^3) was added in three portions *via* cannula, over a period of 30 min. The reaction was stirred at 0 °C for 2 h, warmed to RT and stirred overnight (16 h). Analysis by T.L.C showed that the starting material had been consumed. The solvent was removed under reduced pressure and the resulting oil taken up in diethyl ether (50 cm^3) and washed with water (50 cm^3). The aqueous layer was extracted with ethyl acetate (3 × 50 cm^3) and the organic fractions combined, dried ($MgSO_4$), filtered and the solvent removed under reduced pressure. Purification by silica gel column chromatography eluting with petroleum ether/ethyl acetate (50:50) did not isolate the desired 2-(4'-methoxyacetophenone)-*N*-(*tert*-butoxycarbonyl)ethylamine, but elution with pure ethyl acetate afforded *2-(4'-methoxyacetophenone)-4,5-dihydrooxazole* (0.08 g, 18%) as a yellow solid. R_f 0.24 (petroleum ether/ethyl acetate 30:70); mp 126-127 °C; (Found: C, 61.29; H, 5.48; N, 5.87. $C_{12}H_{13}NO_4$ requires C, 61.27; H, 5.48; N, 5.87); ν_{max}/cm^{-1} 2922.9 (s)(CH), 2854.1 (s)(CH), 1731.5 (s)(C=N), 1682.5 (s)(C=O), 1604.0 (m), 1462.8 (s), 1377.4 (m), 1289.2 (w), 1267.8 (w), 1238.1 (m), 1198.7 (m), 1175.9 (m), 1091.6 (m)(C-O), 1023.2 (m), 836.1 (m)(2 × two adj. Ar-H), 812.0 (w), 759.6 (w); δ_H (300 MHz; $CDCl_3$) 7.87 (2H, dd, *J* 8.7, 2.5, Ar-H_a), 6.89 (2H, dd, *J* 8.7, 2.5, Ar-H_b), 4.60 (2H, s, CH_2COPh), 4.41-4.33 (2H, m, OCH_2CH_2N), 3.82 (3H, s, OCH_3), 3.71-3.63 (2H, m, OCH_2CH_2N); δ_c (75.5 MHz; $CDCl_3$) 192.2 (*C*=O), 164.5 ($COCH_3$), 159.4 (OCNO), 130.6 (CH_a), 128.0 (*C*C=O), 114.5 (CH_b), 62.7 ($COCH_2O$), 56.0 (OCH_3), 50.3 (OCH_2CH_2N),

45.6 (OCH_2CH_2N); *m/z* (ES+) [Found: $(M+Na)^+$ 258.0736. $C_{12}H_{13}NO_4Na$ requires M^+, 258.0742]; *m/z* (ES+) 258 ($[M+Na]^+$, 100%).

6.1.5 *N*-(Benzyloxycarbonyl)-2-aminoethanol

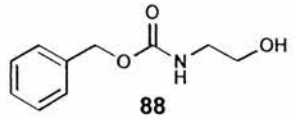

88

To a solution of ethanolamine (6.07 g, 6.0 cm^3, 100 mmol, 1.0 equiv) in 1,4-dioxane:water (1:1, 200 cm^3) was added 4-DMAP (55 mg, 4.0 mmol, 0.04 equiv), benzyl chloroformate (19.1 g, 16.0 cm^3, 110 mmol, 1.1 equiv) and triethylamine (10.1 g, 13.9 cm^3, 110 mmol, 1.1 equiv) and the resulting solution was stirred overnight (16 h) at RT. Analysis by T.L.C. showed that the starting material had been consumed. The solvents were removed under reduced pressure, the mixture reconstituted with dichloromethane (150 cm^3) and washed with water (50 cm^3). The aqueous layer was re-extracted with dichloromethane (3 × 50 cm^3), the organic fractions combined, successively washed with an aqueous solution of HCl (100 cm^3, 0.1 M), water (100 cm^3), brine (100 cm^3), dried ($MgSO_4$) and filtered. The solvent was removed under reduced pressure and the resulting solid dissolved in the minimum amount of ethyl acetate and crystallised from petroleum ether. Recrystallisation yielded pure (*N*-benzyloxycarbonyl)-2-aminoethanol (13.3 g, 68%) as a colourless crystalline solid. R_f 0.18 (petroleum ether/ethyl acetate 50:50); mp 63-65 °C (Lit.,[72] 61-62 °C); δ_H (300 MHz; $CDCl_3$) 7.31-7.24 (5H, m, Ar-*H*), 5.09 (1H, br s, N*H*), 5.04 (2H, s, OCH_2Ph), 3.66 (2H, t, *J* 5.2, NCH_2CH_2OH), 3.30 (2H, apparent q, *J* 5.2, NCH_2CH_2OH), 2.07 (1H, br s, O*H*); *m/z* (ES+) 218 ($[M+Na]^+$, 100%). These data are in accord with literature values.[72]

6.1.6 Attempted synthesis of 2-(4'-methoxyacetophenone)-*N*-(benzyloxycarbonyl)ethylamine

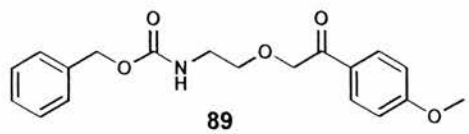

89

A solution of (*N*-benzyloxycarbonyl)-2-aminoethanol (0.5 g, 2.56 mmol, 1.0 equiv) in THF (30 cm^3) under nitrogen was cooled to 0 °C and sodium hydride (0.102 g, 2.56 mmol, 1.0 equiv) added in three portions, over a period of 10 min. The mixture was maintained at 0 °C for 45 min, before warming to RT and stirring for 1.5 h. The mixture was then re-cooled to 0 °C and a solution of 2-bromo-(4'-methoxyacetophenone) (0.59 g, 2.56 mmol, 1.0 equiv) in THF (15 cm^3) was added *via* cannula over a period of 15 min and washed in with further THF (5 cm^3). The reaction was warmed to RT and then stirred overnight (16 h). Analysis by T.L.C. showed that the starting material had been consumed and therefore water (10 cm^3) was added. The solvent was removed under reduced pressure and the resulting oil was suspended in water (50 cm^3) and extracted with ethyl acetate (3 × 50 cm^3). The organic fractions were combined, dried ($MgSO_4$), filtered and the product concentrated *in vacuo*. Silica gel column chromatography did not yield any product.

6.1.7 Attempted synthesis of 2-benzyloxy-*N*-(benzyloxycarbonyl)ethylamine

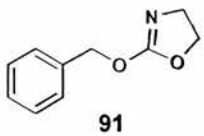

91

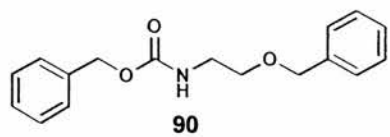

90

A solution of (*N*-benzyloxycarbonyl)-2-aminoethanol (0.5 g, 2.56 mmol, 1.0 equiv) in THF (30 cm^3) under nitrogen was cooled to 0 °C and sodium hydride (0.10 g, 2.56 mmol, 1.0 equiv) was added in three portions over a period of 10 min. The reaction was warmed to RT, stirred for 50 min, re-cooled to 0 °C and benzyl bromide (0.44 g, 305 µl, 2.56 mmol, 1.0 equiv) added dropwise over a period of 10 min. The mixture was stirred at 0 °C for 30 min, before warming to RT and stirred overnight (16 h). Analysis by

T.L.C. showed that all the benzyl bromide had been consumed and therefore water (30 cm^3) was added and the mixture stirred for 30 min. The organic solvent was removed under reduced pressure and the remaining aqueous suspension washed with ethyl acetate (3 × 50 cm^3). The combined organic layers were washed with brine (50 cm^3), dried ($MgSO_4$) and filtered. Purification by silica gel column chromatography eluting with petroleum ether/ethyl acetate (80:20) did not isolate the desired 2-benzyloxy-(*N*-benzyloxycarbonyl)ethylamine, but afforded *2-benzyloxy-4,5-dihydrooxazole* (50 mg, 10%) as an off-white solid. R_f 0.25 (petroleum ether/ethyl acetate 50:50); mp 76-78 °C; (Found: C, 67.74; H, 6.03; N, 7.83. $C_{10}H_{11}NO_2$ requires C, 67.78; H, 6.26; N, 7.90); ν_{max}/cm^{-1} 2924.8 (s)(CH), 2854.6 (s)(CH), 1733.1 (s)(C=N), 1481.7 (m), 1458.4 (m), 1441.3 (m), 1431.7 (m), 1374.5 (m), 1349.4 (w), 1251.6 (m), 1206.9 (w), 1177.3 (w), 1089.2 (m), 1065.6 (m), 1034.2 (m), 977.5 (w), 927.9 (w), 823.2 (w), 760.6 (m)(five adj. Ar-H), 708.5 (m)(five adj. Ar-H), 659.9 (m); δ_H (300 MHz; $CDCl_3$) 7.32-7.19 (5H, m, Ar-C*H*), 4.36 (2H, s, OCH_2Ph), 4.23 (2H, m, NCH_2CH_2O), 3.35 (2H, m, NCH_2CH_2O); δ_c (75.5 MHz; $CDCl_3$) 159.0 (-C=N), 136.2 (*C*, Ph), 129.2 and 128.6 (2 x 2*C*H, *ortho* and *meta* Ph), 128.4 (*C*H, *para* Ph), 62.2 (OCH_2Ph), 48.8 (NCH_2CH_2O) and 44.4 (NCH_2CH_2O); *m/z* (ES+) [Found: $(M+Na)^+$ 200.0687. $C_{10}H_{11}NO_2Na$ requires M^+, 200.0687]; *m/z* (ES+) 200 ($[M+Na]^+$, 100%).

6.1.8 Attempted synthesis of 2-benzyloxy-*N*-(benzyloxycarbonyl)ethylamine

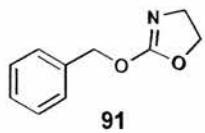

91

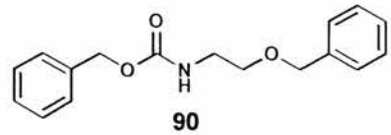

90

A solution of (*N*-benzyloxycarbonyl)-2-aminoethanol (5.0 g, 2.56 mmol, 1.0 equiv) and benzyl chloride (4.86 g, 4.42 cm^3, 2.79 mmol, 1.1 equiv) in dichloromethane (11 cm^3) was added to a solution of sodium hydroxide (0.10 g, 2.56 mmol, 1.0 equiv) and tetrabutylammonium hydrogensulfate (0.61 g, 1.79 mmol, 0.07 equiv) in water (16 cm^3) *via* cannula. The mixture was heated under reflux with vigorous stirring for 24 h. Analysis by T.L.C. showed no starting material remained and therefore the solution was diluted

with water (75 cm^3). This was then extracted with dichloromethane (3 × 50 cm^3), washed with brine (100 cm^3) and dried ($MgSO_4$). Filtration and removal of the solvent under reduced pressure yielded a crude oil. Purification by silica gel column chromatography eluting with hexane, followed by hexane/diethyl ether (90:10) afforded *2-benzyloxy-4,5-dihydrooxazole* (2.04 g, 45%) as an off white solid. R_f 0.25 (ethyl acetate/petroleum ether 50:50); mp 77-80 °C; δ_H (300 MHz; $CDCl_3$) 7.33-7.20 (5H, m, Ar-C*H*), 4.37 (2H, s, OCH_2Ph), 4.24 (2H, m, NCH_2CH_2O), 3.35 (2H, m, NCH_2CH_2O); *m/z* (ES+) 200 ($[M+Na]^+$, 100%). **These data are in accord with previous characterisation.**

6.1.9 *O*-Benzyloxy-*N*-(*tert*-butoxycarbonyl)ethylamine

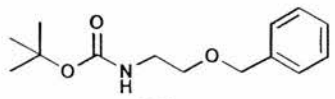

101

A solution of *N*-(*tert*-butoxycarbonyl)-2-aminoethanol (2.92 g, 18.61 mmol, 1.0 equiv) and benzyl chloride (3.53 g, 3.21 cm^3, 27.9 mmol, 1.5 equiv) in dichloromethane (8.0 cm^3) was added to a solution of sodium hydroxide (7.44 g, 186 mmol) and tetrabutylammonium hydrogensulfate (0.44 g, 1.30 mmol) in water (12 cm^3) *via* cannula. The mixture was heated under reflux with vigorous stirring for 24 h. Analysis by T.L.C. showed no starting material remained and therefore water (50 cm^3) and dichloromethane (50 cm^3) were added. The organic phase was removed and the aqueous phase extracted with dichloromethane (3 × 50 cm^3), washed with brine (100 cm^3) and dried ($MgSO_4$). Filtration and removal of the solvent under reduced pressure yielded a crude oil. Purification by silica gel column chromatography eluting with hexane, followed by hexane/diethyl ether (90:10), afforded *O*-benzyloxy-*N*-(*tert*-butoxycarbonyl)ethylamine (2.85 g, 63%) as a colourless oil. R_f 0.35 (hexane/diethyl ether 70:30); δ_H (300 MHz; $CDCl_3$) 7.32-7.20 (5H, m Ar-C*H*), 4.84 (1H, br s, N*H*), 4.45 (2H, s, OCH_2Ph), 3.48 (2H, t, *J* 5.2, OCH_2CH_2NH), 3.28 (2H, apparent q, *J* 5.2, OCH_2CH_2NH), 1.37 [9H, s, $OC(CH_3)_3$]; *m/z* (ES+) 274 ($[M+Na]^+$, 100%), (218, 35%). These data are in accord with literature values.[63]

6.1.10 Attempted synthesis of 2-(4'-methoxyacetophenone)-*N*-(*tert*-butoxycarbonyl)ethylamine

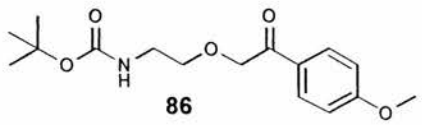

86

A solution of *N*-(*tert*-butoxycarbonyl)-2-aminoethanol (3.02 g, 18.7 mmol, 1.0 equiv) and 2-bromo-(4'-methoxyacetophenone) (4.27 g, 18.6 mmol, 1.0 equiv) in dichloromethane (8 cm^3) was added to a solution of sodium hydroxide (7.42 g, 186 mmol, 10.0 equiv) and tetrabutylammonium hydrogensulfate (0.44 g, 1.30 mmol) in water (12 cm^3) *via* cannula. The mixture was heated under reflux with vigorous stirring for 21 h. Analysis by T.L.C. showed that the starting material had been consumed and therefore water (150 cm^3) was added. The aqueous phase was then extracted with dichloromethane (5 × 50 cm^3). The organic fractions were combined, washed with brine (100 cm^3) and dried ($MgSO_4$). Filtration and removal of the solvent under reduced pressure yielded a crude oil. Purification by silica gel column chromatography eluting with hexane, followed by hexane/diethyl ether (90:10) did not yield the desired product.

6.1.11 Attempted synthesis of *O*-(2-nitrobenzyloxy)-*N*-(*tert*-butoxycarbonyl)ethylamine

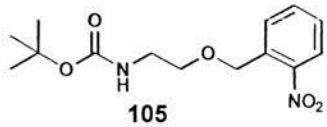

105

A solution of *N*-(*tert*-butoxycarbonyl)-2-aminoethanol (3.01 g, 18.6 mmol, 1.0 equiv) and 2-nitrobenzyl chloride (4.79 g, 27.9 mmol, 1.5 equiv) in dichloromethane (8 cm^3) was added to a solution of sodium hydroxide (7.49 g, 186 mmol, 10.0 equiv) and tetrabutylammonium hydrogensulfate (0.44 g, 1.30 mmol) in water (12 cm^3). The mixture was heated under reflux with vigorous stirring for 72 h. Analysis by T.L.C. showed no starting material remained and therefore water (50 cm^3) and dichloromethane (50 cm^3) were added. The aqueous phase was extracted with dichloromethane (3 × 50 cm^3), washed with brine (100 cm^3) and dried ($MgSO_4$). Filtration and removal of solvent under

reduced pressure yielded a crude oil. Analysis by T.L.C. showed a complex mixture of products.

6.1.12 2-*O*-Benzylethylamine

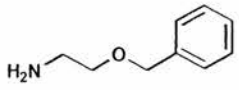

102

A solution of *O*-benzyloxy-*N*-(*tert*-butoxycarbonyl)ethylamine (0.50 g, 1.99 mmol, 1.0 equiv) was stirred with trifluoroacetic acid (0.64 g, 442 µl, 5.65 mmol, 2.84 equiv) at RT under nitrogen overnight (16 h). Analysis by T.L.C. showed no starting material remained. The solution was evaporated under reduced pressure and the resulting residue dissolved in dichloromethane (15 cm^3) and washed with water (20 cm^3). The aqueous phase was extracted with dichloromethane (3 × 10 cm^3), the organic fractions combined, dried ($MgSO_4$), filtered and concentrated *in vacuo*. The crude *O*–benzylethylamine was dissolved in diethyl ether (5 cm^3) and precipitated as the hydrochloride salt by adding concentrated hydrochloric acid dropwise. The resulting solid was filtered to afford *O*–benzylethylamine hydrochloride (0.21 g, 55%) as a colourless solid. δ_H (300 MHz; CD_3OD) 7.32-7.16 (5H, m, Ar-C*H*), 4.50 (2H, s, OCH_2Ph), 3.57 (2H, t, *J* 5.1, $OCH_2CH_2NH_2$), 3.03 (2H, t, *J* 5.1, $OCH_2CH_2NH_2$); *m/z* (ES+) [Found: $(M+H)^+$ 152.1071. $C_9H_{14}NO$ requires M^+, 152.1075]; *m/z* (ES+) 152 ($[M+H]^+$, 100%).[73]

6.1.13 Eicosa-5,8,11,14-tetraenoic acid (2-benzyloxy-ethyl)amide

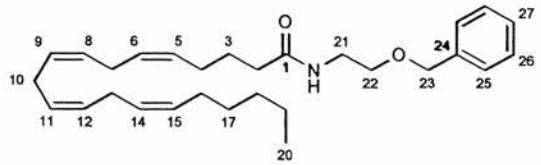

78

To arachidonic acid (162 mg, 176 µl, 0.53 mmol, 1.0 equiv) in dichloromethane (0.5 cm^3) under nitrogen at RT was added oxalyl chloride (81 mg, 56 µl, 0.64 mmol, 1.2 equiv) and dry DMF (2.83 mg, 3.0 µl, 39 µmol, 0.07 equiv). After 1 h the mixture was added

dropwise *via* cannula to a solution of *O*–benzylethylamine hydrochloride (0.1 g, 0.53 mmol, 1.0 equiv) and triethylamine (0.16 g, 178 µl, 1.28 mmol, 2.4 equiv) in dichloromethane (1.2 cm^3) and further washed in with dichloromethane (1 cm^3). The reaction was stirred for 40 h after which time analysis by T.L.C. indicated that no starting material remained. The solvents were removed under reduced pressure and the crude material purified by silica gel column chromatography eluting with petroleum ether/ethyl acetate (80:20) affording *eicosa-5,8,11,14-tetraenoic acid (2-benzyloxy-ethyl)amide* (0.11 g, 58%) as a light brown oil. R_f 0.53 (ethyl acetate/petroleum ether 70:30); ν_{max}/cm^{-1} 3304.0 (s)(NH), 3011.8 (m)(Ar-H), 2927.7 (m)(CH), 2857.8 (m)(CH), 1647.8 (s)(C=O), 1545.8 (m)(NH), 1454.3 (m), 1355.7 (w), 1264.0 (w), 1101.7 (m)(C-O), 1028.4 (w), 911.5 (w), 733.8 (m)(five adj. Ar-H), 697.7 (m)(five adj. Ar-H); δ_H (300 MHz; $CDCl_3$) 7.33-7.20 (5H, m, Ar-C*H*), 5.76 (1H, br s, N*H*), 5.39-5.20 (8H, m, C*H*), 4.44 (2H, s, CH_2Ph), 3.52-3.44 (2H, m, OCH_2CH_2NH), 3.44-3.36 (2H, m, OCH_2CH_2NH), 2.81-2.69 (6H, m, 3 × CH_2 [C-7,C-10,C-13]), 2.14-1.93 (6H, m, [3 × CH_2]), 1.71-1.57 (2H, m, CH_2), 1.35-1.15 (6H, m, [3 × CH_2]), 0.82 (3H, t, *J* 6.9, CH_3); δ_c (75.5 MHz; $CDCl_3$) 172.8 (*C*=O), 137.9 (Ar-*C*), 130.5, 129.2, 128.7, 128.6, 128.5, 128.2, 128.2, 127.9, 127.8, 127.5 [(*C*H)-5, 6, 8, 9, 11, 12, 14, 15, 25, 26, 27], 73.2 (OCH_2CH_2NH), 69.0 (OCH_2CH_2NH), 39.2, 36.1, 31.5, 29.3, 27.2, 26.7, 25.6, 25.5, 22.6 [(CH_2)-2, 3, 4, 7, 10, 13, 16, 17, 18, 19], 14.1 (CH_3); *m/z* (ES+) [Found: $(M+H)^+$ 438.3374. $C_{29}H_{44}NO_2$ requires M^+, 438.3372]; *m/z* (ES+) 460 ($[M+Na]^+$, 100%); *m/z* (ES-) 436 ($[M-H]^-$, 100%).

6.1.14 2-Phthalimidoethanol

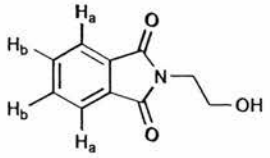

106

A mixture of phthalic anhydride (14.8 g, 0.1 mol, 1.0 equiv) and ethanolamine (6.11 g, 6.04 cm^3, 0.1 mol, 1.0 equiv) was heated under reflux for 5 h and the resulting yellow solid was crystallised twice from ethanol to afford 2-phthalimidoethanol as colourless plate-like crystals (15.7 g, 82%). R_f 0.33 (ethyl acetate/petroleum ether 50:50);

mp 129-131 °C (Lit.,[74] 127-128 °C); δ_H (300 MHz; $CDCl_3$) 7.78 (2H, ddd, *J* 5.5, 5.5, 2.9, Ar-H_a), 7.66 (2H, ddd, *J* 5.5, 5.5, 2.9, Ar-H_b), 3.84-3.80 (4H, m, NCH_2CH_2OH), 2.31 (1H, br s, *OH*); (δ_c (300 MHz; $CDCl_3$) 169.3 (2 × *C*O), 134.5 (Ar-*C*H), 132.4 (*C*), 123.8 (Ar-*C*H), 61.5 (OCH_2CH_2N), 41.3 (OCH_2CH_2N). These data are in accord with literature values.[74]

6.1.15 2-(Nitrobenzyloxy)-2-phthalimidoethane

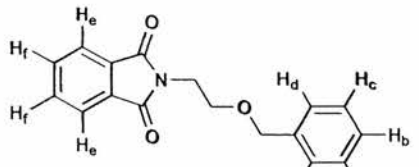

107

A solution of 2-phthalimidoethanol (2.0 g, 10.5 mmol, 1.0 equiv) in dry DMF (16 cm^3) under nitrogen was cooled to 0 °C and sodium hydride (0.419 g, 10.5 mmol, 1.0 equiv) was added in small portions, over a period of 15 min. The mixture was stirred for a further 30 min at 0 °C and 2-nitrobenzyl bromide (2.72 g, 12.6 mmol, 1.2 equiv) in dry DMF (4 cm^3) was added *via* cannula and washed in with further dry DMF (1 cm^3). The reaction was stirred for 2 h at 0 °C and then overnight (16 h) at RT. Analysis by T.L.C. showed that starting material was still present and therefore a catalytic amount of TBAI was added and the mixture stirred for 4 h. Further analysis by T.L.C. showed no change, therefore water (4 cm^3) was added and the mixture stirred for 10 min. The reaction mixture was partitioned between water (50 cm^3) and ethyl acetate (50 cm^3). The aqueous phase was then extracted with ethyl acetate (3 × 50 cm^3) and the organic fractions combined, dried ($MgSO_4$), filtered and concentrated *in vacuo*. Purification by silica gel column chromatography eluting with petroleum ether/ethyl acetate (90:10) afforded a mixture of two products, one of which crystallised from ethanol as *2-(nitrobenzyloxy)-2-phthalimidoethane* (0.24 g, 7%) as a colourless solid. R_f 0.62 (ethyl acetate/petroleum ether 50:50); mp 129-130 °C; ν_{max}/cm^{-1} 2924.9 (s)(CH), 2855.3 (s)(CH), 1771.7 (w), 1716.0 (s)(C=O), 1704.6 (s), 1520.7 (s)(asym. NO_2), 1465.8 (s), 1432.0 (m), 1395.9 (s), 1375.3 (m), 1354.4 (m), 1332.5 (s)(sym. NO_2), 1124.1 (m)(C-O), 1060.9 (w), 1045.1 (w), 1030.2 (m), 802.2 (m), 735.5 (m)(Ar-H), 720.0 (s)(Ar-H);

δ_H (300 MHz; $CDCl_3$) 7.97 (1H, dd, *J* 7.8, 1.2, Ar-H_a), 7.80 (2H, ddd, *J* 5.4, 5.4, 2.8, Ar-H_e), 7.69-7.64 (3H, m, Ar-H_f and Ar-H_d), 7.52 (1H, dt, *J* 7.8, 1.2, Ar-H_b), 7.33 (1H, dt, *J* 7.8, 1.2, Ar-H_c), 4.84 (2H, s, OCH_2Ph), 3.95 (2H, t, *J* 5.5, NCH_2CH_2O), 3.78 (2H, t, *J* 5.5, NCH_2CH_2O); δ_c (75.5 MHz; $CDCl_3$) 168.6 (*C*=O), 147.3 (CNO_2), 135.2 ($CCNO_2$), 134.4 (Ar-CH_e), 134.2 (Ar-CH_a), 132.5 (*C*CO), 128.9 (Ar-CH_b), 128.3 (Ar-CH_c), 125.0 (Ar-CH_d), 123.7 (Ar-CH_f), 69.8 (NCH_2CH_2O), 68.5 (NCH_2CH_2O), 38.0 (CH_2Ph); *m/z* (ES+) [Found: $(M+Na)^+$ 349.0802. $C_{17}H_{14}N_2O_5Na$ requires M^+, 349.0800]; *m/z* (ES+) 349 ($[M+Na]^+$, 100%).

6.1.16 2-Benzyloxy-*N*-phthaloylethylamine

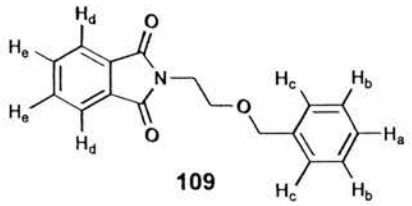

109

A solution of 2-phthalimidoethanol (2.0 g, 10.5 mmol, 1.0 equiv) in dry DMF (16 cm^3) under nitrogen was cooled to 0 °C and sodium hydride (419 mg, 10.5 mmol, 1.0 equiv) was added in small portions, over a period of 15 min. The mixture was stirred for a further 30 min and benzyl bromide (1.79 g, 1.24 cm^3, 12.6 mmol, 1.2 equiv) was then added. The reaction was stirred for 2 h at 0 °C and overnight (16 h) at RT. Analysis by T.L.C. showed the presence of a new product, therefore water (4 cm^3) was added and the mixture stirred for 10 min. The reaction was partitioned between water (50 cm^3) and ethyl acetate (50 cm^3). The aqueous phase was extracted with ethyl acetate (3 × 50 cm^3), the organic fractions combined, dried ($MgSO_4$), filtered and concentrated *in vacuo*. Purification by silica gel column chromatography eluting with petroleum ether/ethyl acetate (90:10) afforded a mixture of two products, one of which crystallised from ethanol to yield 2-benzyloxy-*N*-phthaloylethylamine (0.57 g, 19%) as a white solid. R_f 0.66 (ethyl acetate/petroleum ether 60:40); mp 70-73 °C (Lit.,[73] 69 °C); (Found: C, 72.58; H, 5.55; N 4.96. $C_{17}H_{15}NO_3$ requires C, 72.58; H, 5.37; N, 4.98); ν_{max}/cm^{-1} 2924.2 (s)(CH), 2854.3 (s)(CH), 1772.1 (w), 1704.7 (s)(C=O), 1497.5 (w), 1465.1 (s), 1426.3 (s), 1394.4 (S), 1376.3 (m), 1357.3 (m), 1319.5 (m), 1096.4 (s)(C-O), 1048.8 (s), 1020.3 (m), 1001.6 (m), 968.5 (w), 891.0 (m), 877.3 (w), 845.3 (w),

799.2 (w), 739.0 (m)(Ar-H), 721.4 (s)(Ar-H), 695.7 (m); δ_H (300 MHz; $CDCl_3$) 7.89-7.82 (2H, m, Ar-H_d), 7.76-7.69 (2H, m, Ar-H_e), 7.31-7.19 (5H, m, Ar-H_{abc}), 4.55 (2H, s, CH_2Ph), 3.95 (2H, t, *J* 5.7, NCH_2CH_2O), 3.74 (2H, t, *J* 5.7, NCH_2CH_2O); ***m/z*** **(CI+)** [Found: $(M+H)^+$ 282.1133. $C_{17}H_{16}NO_3$ requires M^+, 282.1130]; *m/z* (CI+) 282 ($[M+H]^+$, 33%), 204 ($[M-Ph]^+$, 9%), 190 ($[M-CH_2Ph]^+$, 23%), 175 ($[MH-OCH_2Ph]^+$, 100%), **160 ($[M-CH_2OCH_2Ph]^+$, 50%), 91 ($[CH_2Ph]^+$, 38%). These data are in accord with literature values.**[73]

6.1.17 2-(Nitrobenzyloxy)ethylamine

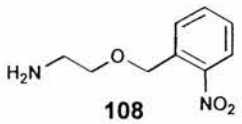

108

To a solution of *2-(nitrobenzyloxy)-2-phthalimidoethane* (0.17 g, 0.53 mmol, 1.0 equiv) in ethanol (10 cm^3) was added hydrazine hydrate (0.17 g, 166 µl, 10 equiv) and the solution heated to 45 °C for 2 h. On cooling, the precipitate which had formed was filtered and the remaining solution evaporated under reduced pressure. The resulting solid was dissolved in dichloromethane and the precipitate was filtered. The solvent was removed under reduced pressure to yield crude *2-(nitrobenzyloxy)ethylamine* (0.12 g, crude) as a brown oil. δ_H (300 MHz; DMSO) (assignable peaks) 4.83 (2H, s, OCH_2Ph), 3.50 (2H, t, *J* 5.7, NCH_2CH_2O), 2.77 (2H, t, *J* 5.7, NCH_2CH_2O); *m/z* (ES+) 197 ($[M+Na]^+$, 100%) and 136 ($[M+Na]^+$, 3%).

6.1.18 Eicosa-5,8,11,14-tetraenoic acid (2-nitrobenzyloxy-ethyl)amide

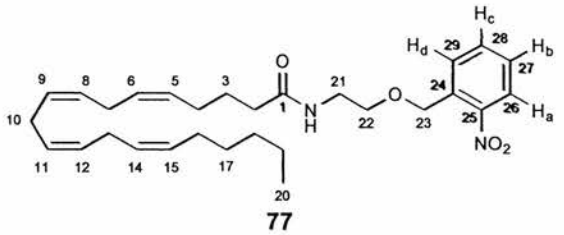

77

To arachidonic acid (0.17 g, 187 µl, 0.57 mmol, 1.0 equiv) in dichloromethane (0.5 cm^3) under nitrogen at RT was added oxalyl chloride (86 mg, 60 µl, 0.68 mmol, 1.2 equiv) and

dry DMF (2.8 mg, 3 µl, 0.04 mmol, 0.07 equiv). After 30 min the mixture was added dropwise *via* cannula to a solution of *2-(nitrobenzyloxy)ethylamine* (0.11 g, 0.57 mmol, 1.0 equiv) and triethylamine (0.17 g, 237 µl, 1.70 mmol, 3.0 equiv) in dichloromethane (1.5 cm^3) and washed in with further dichloromethane (0.7 cm^3). The reaction was stirred for 18 h at RT, after which time analysis by T.L.C. indicated no starting material remained. The solvents were removed under reduced pressure and the resulting mixture purified by silica gel column chromatography eluting with petroleum ether/ethyl acetate (70:30) to afford *eicosa-5,8,11,14-tetraenoic acid (2-nitrobenzyloxyethyl)amide* (91 mg, 33%) as an orange oil. R_f 0.51 (ethyl acetate/petroleum ether 70:30); (Found: C, 71.80; H, 8.88; N, 6.04. $C_{29}H_{42}N_2O_4$ requires C, 72.17; H, 8.77; N, 5.80); λ_{max} (CH_3CN)/nm 261 (ε/dm^3 mol^{-1} cm^{-1} 5619), 236infl (3642) and 197 (63484); ν_{max}/cm^{-1} 3301.2 (m)(NH), 3012.9 (m)(Ar-H), 2928.3 (s)(CH), 2858.4 (m)(CH), 1648.5 (s)(C=O), 1527.5 (s)(asym. NO_2), 1459.1 (m), 1342.0 (s)(sym. NO_2), 1112.9 (s)(C-O), 859.0 (w), 790.9 (w), 728.9 (m)(cis C=C); δ_H (500 MHz; $CDCl_3$) 8.01 (1H, dd, *J* 8.4, 1.0, Ar-C*H*$_a$), 7.67-7.62 (2H, m, Ar-C*H*$_b$, Ar-C*H*$_c$), 7.50-7.45 (1H, m, Ar-C*H*$_d$), 5.86-5.81 (1H, br s, N*H*), 5.44-5.30 (8H, m, C*H*), 4.87 (2H, s, CH_2Ph), 3.64 (2H, t, *J* 5.1, OCH_2CH_2NH), 3.52 (2H, dt, *J* 5.1, 5.2, OCH_2CH_2NH), 2.87-2.78 (6H, m, 3 × CH_2 [C-7,C-10,C-13]), 2.23 (2H, t, *J* 7.6, CH_2), 2.13 (2H, dt, *J* 5.6, 7.2, CH_2), 2.06 (2H, dt, *J* 7.1, 7.1, CH_2), 1.74 (2H, apparent qn, *J* 7.6, CH_2CH_3), 1.40-1.24 (6H, m, [3 × CH_2]), 0.89 (3H, t, *J* 7.0, CH_3); δ_c (125.7 MHz; $CDCl_3$) 173.0 (*C*=O), 153.2 (*C*NO_2), 133.8 (Ar-*C*), 133.3, 130.5, 129.2, 129.1, 128.7, 128.6, 128.5, 128.2, 128.2, 127.9, 127.5, 124.6 [(*C*H)-5, 6, 8, 9, 11, 12, 14, 15, 26, 27, 28, 29], 70.1 (OCH_2CH_2NH), 69.9 (OCH_2CH_2NH), 39.1, 36.1, 31.5, 29.3, 27.2, 26.7, 25.6, 25.5, 22.6 [(CH_2)-2, 3, 4, 7, 10, 13, 16, 17, 18, 19)], 14.1 (CH_3); *m/z* (ES+) [Found: $(M+Na)^+$ 505.3039. $C_{29}H_{42}N_2O_4Na$ requires M^+, 505.3042]; *m/z* (ES+) 505 ($[M+Na]^+$, 100%).

6.1.19 2-Bromomethyl-2-(4-methoxyphenyl)-1,3-dioxolane

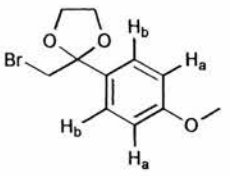

111

To a solution of 2-bromo-4'-methoxy acetophenone (5.0 g, 21.8 mmol, 1.0 equiv) in dry toluene (100 cm^3) was added ethylene glycol (8.13 g, 7.30 cm^3, 131 mmol, 5.0 equiv) and camphor sulfonic acid (76 mg, 0.33 mmol, 0.02 equiv). The resulting solution was heated under reflux with a Dean-Stark apparatus attached for 60 h under nitrogen. Analysis by T.L.C. showed that the starting material had been consumed and therefore triethylamine (1 cm^3) was added. The solvents were removed *in vacuo* to yield 2-bromomethyl-2-(4-methoxyphenyl)-1,3-dioxolane (5.03 g, 84%) as a cream coloured solid. R_f 0.42 (ethyl acetate/petroleum ether 20:80); mp 77-78 °C (Lit.,[75] 78-79 °C); δ_H (300 MHz; $CDCl_3$) 7.36 (2H, dt, *J* 8.9, 2.5, Ar-CH_a), 6.81 (2H, dt, *J* 8.9, 2.5, Ar-CH_b), 4.13-4.07 (2H, m, OCH_2CH_2O), 3.85-3.79 (2H, m, OCH_2CH_2O), 3.74 (3H, s, OCH_3), 3.58 (2H, s, CH_2Br); ***m/z*** **(ES+) 297 ([^{81}M+Na]$^+$, 89%), 295 ([^{79}M+Na]$^+$, 97%), 275 ([^{81}M]$^+$,** 16%), 273 ([^{79}M]$^+$, 18%), 193 ([M-Br]$^+$, 100%). These data are in accord with literature values.[75]

6.1.20 Attempted synthesis of 2-*O*-methoxy(4'-methoxyphenyl)-1,3-dioxolane-2-phthalimidoethane

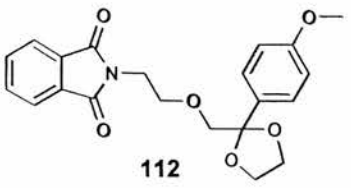

112

To a solution of 2-phthalimidoethanol (1.00 g, 5.23 mmol, 1.0 equiv) in dry THF (8 cm^3) and dry DMF (0.5 cm^3) at 0 °C under nitrogen was added sodium hydride (0.31 g, 7.85 mmol, 1.5 equiv) over a period of 15 min. The mixture was stirred for 30 min at 0 °C and then at RT for 30 min. The reaction was cooled to 0 °C and a solution of 2-bromomethyl-2-(4-methoxyphenyl)-1,3-dioxolane (2.14 g, 7.85 mmol, 1.5 equiv) in dry THF (3 cm^3) added dropwise. A catalytic amount of tetra-*N*-butylammonium iodide was added and

the reaction then left at 0 °C for 1.5 h before warming to RT and stirring overnight (16 h). Analysis by T.L.C. indicated that starting material was still present and therefore the reaction was stirred for another 24 h. Further analysis by T.L.C and a ^{1}H NMR spectrum of the crude product showed the presence of both starting materials and that no reaction had taken place.

6.1.21 Attempted synthesis of *O*-2-methoxy(4'-methoxyphenyl)-1,3-dioxolane-2-phthalimidoethane

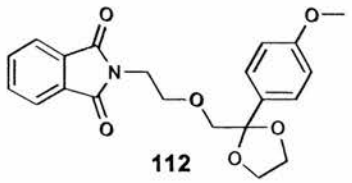

112

To a solution of 2-phthalimidoethanol (1.00 g, 5.23 mmol, 1.0 equiv) in dry DMF (8 cm^3) at 0 °C under nitrogen was added sodium hydride (0.31 g, 7.85 mmol, 1.5 equiv) over a period of 15 min. The mixture was stirred for 30 min at 0°C and then at RT for 30 min. The reaction was re-cooled to 0 °C and a solution of 2-bromomethyl-2-(4-methoxyphenyl)-[1,3]dioxolane (2.14 g, 7.85 mmol, 1.5 equiv) in dry THF (3 cm^3) was added dropwise. A catalytic amount of tetra-*N*-butylammonium iodide was then added and the reaction left at 0 °C for 2 h, before warming to RT and stirring for 3 days. Analysis by T.L.C. showed little presence of 2-phthalimidoethanol and therefore water (2 cm^3) was added and the solvent removed *in vacuo*. ^{1}H NMR analysis of the crude product showed the presence of both starting materials and that no reaction had taken place.

6.1.22 *N*-(2-Bromoethyl)phthalimide

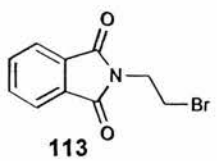

113

A mixture of phthalic anhydride (14.8 g, 0.10 mol, 1.0 equiv) and ethanolamine (6.11 g, 6.04 cm^3, 0.1 mol, 1.0 equiv) was heated under reflux for 2 h. The solution was cooled to RT and to the resulting solid was added phosphorous tribromide (18.4 g, 6.57 cm^3, 68.0

mmol, 0.68 equiv). The reaction was heated to 100 °C over 20 min and then maintained at 100 °C with occasional shaking. After the consumption of the solid present in the reaction, the resulting solution was poured onto ice (150 g). When the ice had melted the mixture was filtered and the resulting solid washed with cold water (100 cm^3). Crystallisation from ethanol/water afforded *N*-(2-bromoethyl)phthalimide (20.2 g, 79%) as a white solid. R_f 0.60 (ethyl acetate/petroleum ether 50:50); mp 83-85 °C (from ethanol) (Lit.,[76] 83 °C); δ_H (300 MHz; $CDCl_3$) 7.85-7.78 (2H, m, Ar-H), 7.72-7.65 (2H, m, Ar-H), 4.05 (2H, t, *J* 6.7, NCH_2CH_2), 3.55 (2H, t, *J* 6.7, NCH_2CH_2). These data are in accord with literature values.[76]

6.1.23 3-Methoxy-4-(triisopropylsilyloxy)benzonitrile

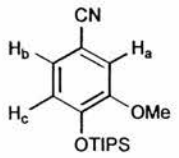

115

To a solution of 4-hydroxy-3-methoxybenzonitrile (10.0 g, 67.1 mmol, 1.0 equiv) and imidazole (14.2 g, 208 mmol, 3.1 equiv) in dry DMF (100 cm^3) at RT was added triisopropylsilyl chloride (16.8 g, 87.2 mmol, 1.3 equiv) and the resulting solution stirred overnight (16 h). Analysis by T.L.C. showed that the starting material had been consumed and therefore the solvents were removed *in vacuo*. Purification by silica gel column chromatography eluting with ethyl acetate/petroleum ether (5:95) afforded *3-methoxy-4-(triisopropylsilyloxy)benzonitrile* (16.3 g, 80%) as a colourless solid. R_f 0.38 (ethyl acetate/petroleum ether 10:90); mp 47-49 °C; (Found: C, 66.89; H, 9.19; N 4.54. $C_{17}H_{27}NO_2Si$ requires C, 66.89; H, 8.91; N, 4.59); ν_{max}/cm^{-1} 2926.8 (s)(CH), 2868.2 (s)(CH), 2224.4 (m)(CN), 1595.7 (m), 1572.3 (w), 1513.6 (s), 1463.7 (s), 1413.2 (m), 1386.5 (w), 1321.9 (s), 1285.2 (s), 1248.8 (s)(C-O), 1157.9 (m), 1133.2 (m), 1064.1 (w), 1036.4 (m), 990.4 (w), 937.6 (m), 886.9 (s), 821.3 (m), 714.4 (m), 685.7 (s), 666.5 (m), 647.6 (m), 620.9 (w); δ_H (300 MHz; $CDCl_3$) 7.09 (1H, dd, *J* 8.2, 2.0, Ar-H_b), 7.00 (1H, d, *J* 2.0, Ar-H_a), 6.82 (1H, d, *J* 8.2, Ar-H_c), 3.76 (3H, s, OCH_3), 1.27-1.11 (3H, m, $OSi[CH(CH_3)_2]_3$), 1.02 (10H, s, $OSi[CH(CH_3)_2]_3$), 1.01 (8H, s, $OSi[CH(CH_3)_2]_3$);

δ_c (75.5 MHz; $CDCl_3$) 151.6 (*C*OCH_3), 150.5 (*C*$OSi[CH(CH_3)_2]_3$), 126.5 (*C*-H_a), 121.2 (*C*-H_c), 119.8 (*C*N), 115.3 (*C*-H_b), 104.7 (*C*CN), 56.0 (OCH_3), 18.2 ($OSi[CH(CH_3)_2]_3$), 13.3 ($OSi[CH(CH_3)_2]_3$); *m/z* (ES+) [Found: $(M+Na)^+$ 328.1715. $C_{17}H_{27}NO_2NaSi$ requires M^+, 328.1709]; *m/z* (ES+) 360.20 ($[M+NaMeOH]^+$, 15%); 328 ($[M+Na]^+$, 100%).

6.1.24 3-Methoxy-4-(triisopropylsilyloxy)benzylamine

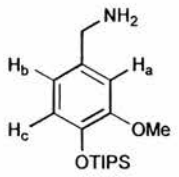

116

A solution of 3-methoxy-4-(triisopropylsilyloxy)benzonitrile (15.0 g, 49.1 mmol, 1.0 equiv) in dry diethyl ether (150 cm^3) was added to a stirred suspension of lithium aluminium hydride (2.80 g, 73.7 mmol, 1.5 equiv) in dry diethyl ether (450 cm^3) under nitrogen and stirred at RT for 2 h. Analysis by T.L.C. showed that starting material was present and therefore further lithium aluminium hydride (1.40 g, 19.0 mmol, 0.5 equiv) was added and the mixture stirred for 1 h. Further analysis by T.L.C showed that no starting material remained and therefore wet diethyl ether (200 cm^3) followed by water (20 cm^3) was added. When the reaction colour had turned from grey to clear, the mixture was filtered and the solvents removed *in vacuo* to afford crude *3-methoxy-4-(triisopropylsilyloxy)benzylamine* (13.6 g, 89%) as a brown oil which was used without further purification. R_f 0.12 (ethyl acetate/petroleum ether 30:70); δ_H (300 MHz; $CDCl_3$) 6.70 (1H, d, *J* 8.8, Ar-H_c), 6.69 (1H, apparent s, Ar-H_a), 6.58 (1H, dd, *J* 8.8, 2.0, Ar-H_b), 3.66 (3H, s, OCH_3), 3.62 (2H, s, CH_2NH_2), 1.74 (2H, br s, CH_2NH_2), 1.23-1.06 (3H, m, $OSi[CH(CH_3)_2]_3$), 1.00 (10H, s, $OSi[CH(CH_3)_2]_3$), 0.97 (8H, s, $OSi[CH(CH_3)_2]_3$).

6.1.25 3-Methoxy-4-(triisopropylsilyloxy)-*N*-nonanoylbenzylamine

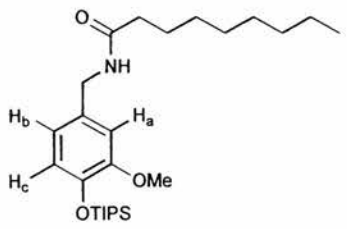

117

To a solution of 3-methoxy-4-(triisopropylsilyloxy)benzylamine (13.0 g, 42.0 mmol, 1.0 equiv) in dry dichloromethane (250 cm^3) was added DMAP (0.26 g, 2.10 mmol, 0.05 equiv). The resulting solution was cooled to 0 °C and dry pyridine (4.98 g, 5.1 cm^3, 63.0 mmol, 1.5 equiv) was added dropwise. After 45 min stirring, nonanoyl chloride (8.16 g, 8.33 cm^3, 46.1 mmol, 1.1 equiv) was added dropwise and the reaction stirred at 0 °C for 5 mins and then at RT for 3 days. Analysis by T.L.C. showed that the starting material had been consumed and therefore water (200 cm^3) was added. The resulting layers were separated and the aqueous layer extracted with diethyl ether (2 × 200 cm^3). The ether fractions were combined and washed with HCl (2 M, 200 cm^3). The aqueous fraction was then re-extracted with diethyl ether (200 cm^3), the organic fractions combined, dried ($MgSO_4$), filtered and concentrated *in vacuo*. Purification by silica gel column chromatography eluting with ethyl acetate/petroleum ether (10:90) afforded *3-methoxy-4-(triisopropylsilyloxy)-N-nonanoylbenzylamine* (13.1 g, 69%) as a colourless oil. R_f 0.32 (ethyl acetate/petroleum ether 30:70); ν_{max}/cm^{-1} 3284.5 (m)(NH), 3071.1 (w)(Ar-H), 2927.6 (s)(CH), 2866.9 (s)(CH), 1644.3 (s)(C=O), 1549.7 (m)(NH), 1515.4 (s), 1464.9 (s), 1418.8 (m), 1284.7 (s), 1234.1 (s)(C-O), 1159.3 (m), 1127.9 (m), 1040.8 (m), 884.1 (m), 814.6 (w), 681.8 (m); δ_H (300 MHz; $CDCl_3$) 6.81 (1H, d, *J* 8.0, Ar-H_c), 6.76 (1H, d, *J* 2.1, Ar-H_a), 6.69 (1H, dd, *J* 8.0, 2.1, Ar-H_b), 5.69 (1H, br s, N*H*), 4.35 (2H, d, *J* 5.6, CH_2NH), 3.78 (3H, s, OCH_3), 2.20 (2H, t, *J* 7.6, $COCH_2$), 1.76-1.58 (3H, m, $OSi[CH(CH_3)_2]_3$), 1.39-1.16 (12H, m, $CH_2(CH_2)_6CH_3$), 1.10 (10H, s, $OSi[CH(CH_3)_2]_3$), 1.07 (8H, s, $OSi[CH(CH_3)_2]_3$), 0.88 (3H, t, *J* 6.8, CH_2CH_3); δ_c (75.5 MHz; $CDCl_3$) 173.3 (C=O), 151.4 ($COCH_3$), 145.3 ($COSi[CH(CH_3)_2]_3$), 131.8 (CCH_2NH), 120.7 (C-H_a), 120.4 (C-H_c), 112.3 (C-H_b), 55.9 (OCH_3), 43.9 (CH_2NH), 37.3 (CH_2), 32.2 (CH_2), 29.7 (CH_2), 29.6 (CH_2), 26.2 (CH_2), 23.1 (CH_2),

18.3 (OSi[CH(CH_3)$_2$]$_3$), 14.5 (OSi[CH(CH$_3$)$_2$]$_3$), 13.2 (CH_2CH_3); *m/z* (ES+) [Found: (M+Na)$^+$ 472.3217. $C_{26}H_{47}NO_3NaSi$ requires M^+, 472.3223]; *m/z* (ES+) 472 ([M+Na]$^+$, 100%); *m/z* (ES-) 448 ([M-H]$^-$, 100%).

6.1.26 2-Bromo-5-methoxy-4-(triisopropylsilyloxy)-*N*-nonanoylbenzylamine

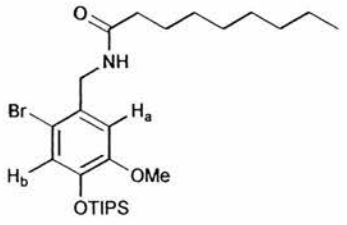

119

To 3-methoxy-4-(triisopropylsilyloxy)-*N*-nonanoylbenzylamine (3.00 g, 6.67 mmol, 1.0 equiv) in dry dichloromethane (500 cm^3) was added dropwise a solution of bromine (2.24 g, 720 µl, 14.01 mmol, 2.1 equiv) in dry dichloromethane (200 cm^3), over 1.5 h under an atmosphere of nitrogen at -78 °C. The solution was stirred for a further 2 h and analysis by T.L.C. showed the starting material had been consumed and therefore an aqueous solution of $NaSO_4$ (100 cm^3, 10% w/v) was added. The mixture was filtered through Celite and the solvent removed under reduced pressure. Purification by silica gel column chromatography eluting with ethyl acetate/petroleum ether (10:90) yielded *2-bromo-5-methoxy-4-(triisopropylsilyloxy)-N-nonanoylbenzylamine* (2.58 g, 73%) as a colourless solid. R_f 0.42 (ethyl acetate/petroleum ether 30:70); mp 53-54 °C; (Found: C, 59.42; H, 9.02; N 2.59. $C_{26}H_{46}BrNO_3Si$ requires C, 59.07; H, 8.77; N, 2.65); ν_{max}/cm^{-1} 3288.7 (s)(NH), 3064.8 (w)(Ar-H), 2924.0 (s)(CH), 2854.2 (s)(CH), 1644.8 (s)(C=O), 1542.4 (s)(NH), 1504.9 (s), 1465.1 (s), 1422.9 (m), 1380.3 (s), 1353.6 (w), 1309.0 (m), 1267.7 (s), 1236.8 (w), 1204.1 (s), 1186.7 (w), 1158.3 (m), 1041.5 (m), 995.8 (w), 972.0 (m), 908.2 (m), 883.9 (s), 858.1 (m), 727.4 (m), 670.6 (m); δ_H (300 MHz; $CDCl_3$) 6.95 (1H, s, Ar-H_b), 6.81 (1H, s, Ar-H_a), 5.84 (1H, t, *J* 5.7, N*H*), 4.35 (2H, d, *J* 5.7, CH_2NH), 3.70 (3H, s, OCH_3), 2.12 (2H, t, *J* 7.6, COCH_2), 1.62-1.48 (3H, m, OSi[CH(CH$_3$)$_2$]$_3$), 1.29-1.08 (12H, m, $CH_2(CH_2)_6CH_3$), 1.02 (10H, s, OSi[CH(CH_3)$_2$]$_3$), 0.99 (8H, s, OSi[CH(CH_3)$_2$]$_3$), 0.80 (3H, t, *J* 6.7, CH_2CH_3); δ_c (75.5 MHz; $CDCl_3$) 173.3

(*C*=O), 150.8 (*C*OCH$_3$), 146.1 (*C*OSi[CH(CH$_3$)$_2$]$_3$), 130.5 (*C*CH$_2$NH), 124.4 (*C*-H), 114.4 (*C*-H), 113.7 (*C*Br), 56.0 (O*C*H$_3$), 43.9 (*C*H$_2$NH), 37.2 (*C*H$_2$), 32.2 (*C*H$_2$), 29.7 (*C*H$_2$), 29.7 (*C*H$_2$), 29.6 (*C*H$_2$), 26.2 (*C*H$_2$), 23.0 (*C*H$_2$), 18.3 (OSi[CH(*C*H$_3$)$_2$]$_3$), 14.5 (OSi[*C*H(CH$_3$)$_2$]$_3$), 13.2 (CH$_2$*C*H$_3$); *m/z* (CI+) [Found: {(^{81}M+H)$^+$ 530.2485. $C_{26}H_{47}NO_3Si^{81}Br$ requires *M*$^+$, 530.2488}, {(^{79}M+H)$^+$ 528.2517. $C_{26}H_{47}NO_3Si^{79}Br$ requires *M*$^+$, 528.2509}]; *m/z* (CI+) 530 ([^{81}M+H]$^+$, 40%), 528 ([^{79}M+H]$^+$, 52%), 486 {[^{81}M-CH(CH$_3$)$_2$]$^+$, 100%}, 484 {[^{79}M-CH(CH$_3$)$_2$]$^+$, 98%}, 448 ([M-Br]$^+$, 67%), 373 {[^{81}MH-Si(CH(CH$_3$)$_2$)$_3$]$^+$, 80%}, 373 {[^{79}MH-Si(CH(CH$_3$)$_2$)$_3$]$^+$, 79%}.

6.1.27 2-Bromo-4-hydroxy-5-methoxy-*N*-nonanoylbenzylamine

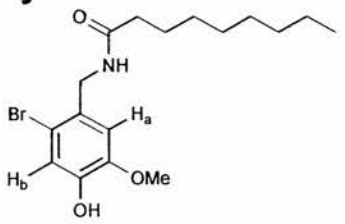

120

To a solution of 2-bromo-5-methoxy-4-(triisopropylsilyloxy)-*N*-nonanoylbenzylamine (2.0 g, 3.78 mmol, 1.0 equiv) in dry THF (50 cm^3) was added tetra-*N*-butylammonium fluoride in THF (1 M, 1.48 g, 5.30 cm^3, 5.3 mmol, 1.4 equiv) at RT and the solution stirred for 3 h. Analysis by T.L.C. showed that the starting material had been consumed and therefore the solution was partitioned between diethyl ether (100 cm^3) and aqueous HCl (1 M, 100 cm^3). The aqueous phase was extracted with diethyl ether (3 × 75 cm^3) and the organic fractions combined, washed with brine, dried ($MgSO_4$), filtered and concentrated *in vacuo*. Purification by silica gel column chromatography eluting with ethyl acetate/petroleum ether (30:70) afforded *2-bromo-4-hydroxy-5-methoxy-N-nonanoylbenzylamine* (1.22 g, 86%) as a colourless solid. R_f 0.51 (ethyl acetate/petroleum ether 70:30); mp 96-97°C; (Found: C, 54.94; H, 7.22; N 3.74. $C_{17}H_{26}BrNO_3$ requires C, 54.84; H, 7.04; N, 3.76); ν_{max}/cm^{-1} 3383.6 (m)(NH), 3136.0 (m)(OH), 2923.2 (s)(CH), 2854.1 (s)(CH), 1652.5 (s)(C=O), 1604.2 (w), 1529.5 (m), 1502.0 (s), 1464.6 (s), 1421.7 (s), 1377.9 (m), 1364.5 (m), 1269.9 (s), 1226.9 (w), 1201.1 (m), 1183.0 (w), 1154.0 (m)(C-O), 1122.8 (w), 1082.0 (w), 1040.4 (w), 963.2 (w),

870.6 (m), 828.9 (w), 723.0 (m), 633.7 (m); δ_H (300 MHz; $CDCl_3$) 7.02 (1H, s, Ar-H_b), 6.84 (1H, s, Ar-H_a), 6.12 (1H, s, O*H*), 5.97 (1H, t, *J* 5.6, N*H*), 4.34 (2H, d, *J* 5.6, CH_2NH), 3.77 (3H, s, OCH_3), 2.12 (2H, t, *J* 7.6, $COCH_2$), 1.63-1.46 (2H, m, $CH_2(CH_2)_6CH_3$), 1.30-1.07 (10H, m, $CH_2(CH_2)_6CH_3$), 0.80 (3H, t, *J* 6.7, CH_2CH_3); δ_c (75.5 MHz; $CDCl_3$) 173.5 (*C*=O), 146.5 ($COCH_3$), 146.3 (*C*OH), 129.4 (CCH_2NH), 118.8 (*C*-H_a), 114.8 (*C*Br), 113.5 (*C*-H_b), 56.5 (OCH_3), 44.0 (CH_2NH), 37.2 (CH_2), 32.2 (CH_2), 29.7 (CH_2), 29.7 (CH_2), 29.6 (CH_2), 26.1 (CH_2), 23.0 (CH_2), 14.5 (CH_2CH_3); *m/z* (ES+) [Found: {(^{79}M+Na)$^+$ 394.0995. $C_{17}H_{26}NO_3Na^{79}Br$ requires M^+, 394.0994}, {(^{81}M+Na)$^+$ 396.0975. $C_{17}H_{26}NO_3Na^{81}Br$ requires M^+, 396.0973}]; *m/z* (ES+) 396 ([^{79}M+Na]$^+$, 90%), 394 ([^{81}M+Na]$^+$, 100%); *m/z* (ES-) 372.10 ([^{81}M-H]$^-$, 92%), 370.10 ([^{79}M-H]$^-$, 100%); *m/z* (EI+) 292.19 ([M-Br]$^+$, 100%).

6.1.28 2-Bromo-5-methoxy-4-(4,5-dimethoxy-2-nitrobenzyl)-*N*-nonanoylbenzylamine

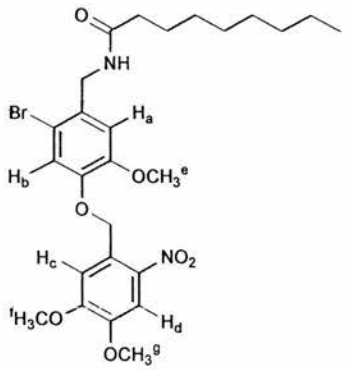

121

To a solution of 2-bromo-4-hydroxy-5-methoxy-*N*-nonanoylbenzylamine (0.40 g, 1.07 mmol, 1.0 equiv) in dry THF (20 cm^3) was added potassium *tert*-butoxide (0.12 g, 1.07 cm^3, 1 M in THF, 1.07 mmol, 1.0 equiv) and the solution stirred for 20 min at RT. To this was added 4,5-dimethoxy-2-nitrobenzyl bromide (0.30 g, 1.07 mmol, 1.0 equiv) and the resulting mixture stirred overnight (16 h). Analysis by T.L.C showed that the starting material had been consumed and therefore the solvent was removed *in vacuo*. The resulting solid was purified by silica gel column chromatography eluting with petroleum ether/ethyl acetate (50:50) followed by ethyl acetate (100), furnishing *2-bromo-5-methoxy-4-(4,5-dimethoxy-2-nitrobenzyl)-N-nonanoylbenzylamine* (0.32 g, 53%) as an

off yellow solid. R_f 0.58 (methanol/dichloromethane 5:95); mp 185-186°C; (Found: C, 55.30; H, 6.55; N 4.82. $C_{26}H_{35}BrN_2O_7$ requires C, 55.03; H, 6.22; N, 4.94); λ_{max} (CH_2Cl_2)/nm 347 (ε/dm^3 mol^{-1} cm^{-1} 6985), 317infl (5300), 289 (8814), 265infl (5287); ν_{max}/cm^{-1} 3274.3 (m)(NH), 2924.7 (s)(CH), 2854.4 (s)(CH), 1644.9 (s)(C=O), 1546.8 (w)(NH), 1524.2 (s)(asym. NO_2), 1509.5 (m), 1459.9 (S), 1410.9 (w), 1378.4 (m)(sym. NO_2), 1322.1 (m), 1280.2 (s), 1231.4 (m)(C-O), 1194.1 (w), 1171.4 (w), 1074.1 (m), 1042.5 (w), 990.4 (w), 956.0 (w), 872.8 (m), 852.6 (w), 796.5 (w), 756.3 (w), 722.7 (w); δ_H (300 MHz; $CDCl_3$) 7.70 (1H, s, Ar-H_c), 7.38 (1H, s, Ar-H_d), 7.01 (1H, s, Ar-H_a), 6.94 (1H, s, Ar-H_b), 5.88 (1H, br s, NH), 5.44 (2H, s, CH_2O), 4.37 (2H, d, J 6.1, CH_2NH), 3.91 (3H, s, OCH_3[f]), 3.90 (3H, s, OCH_3[g]), 3.81 (3H, s, OCH_3[e]), 2.13 (2H, t, J 7.6, COCH_2), 1.69-1.48 [2H, m, CH_2(CH_2)$_6$$CH_3$], 1.31-1.10 [10H, m, CH_2(CH_2)$_6$$CH_3$], 0.80 (3H, t, J 6.8, CH_2CH_3); δ_c (75.5 MHz; $CDCl_3$) 173.1 (*C*=O), 154.1 (*C*), 149.3 (*C*), 147.9 (*C*), 147.6 (*C*), 138.9 (*C*), 131.2 (*C*), 129.1 (*C*), 118.4 (Ar-*C*H), 114.2 (Ar-*C*H), 113.8 (*C*Br), 109.4 (Ar-*C*H), 108.0 (Ar-*C*H) 68.6 (OCH_2), 56.4 (2 × OCH_3), 56.2 (OCH_3), 43.6 (*C*H_2NH), 36.8 (*C*H_2), 31.8 (*C*H_2), 29.3 (*C*H_2), 29.2 (*C*H_2), 25.7 (*C*H_2), 22.6 (*C*H_2), 14.1 (CH_2*C*H_3); *m/z* (ES+) [Found: {(^{79}M+Na)$^+$ 589.1529. $C_{26}H_{35}N_2O_7Na^{79}Br$ requires M^+, 589.1525}, {(^{81}M+Na)$^+$ 591.1512. $C_{26}H_{35}N_2O_7Na^{81}Br$ requires M^+, 591.1505}]; *m/z* (ES+) 591 ([^{81}M+Na]$^+$, 83%), 589 ([^{79}M+Na]$^+$, 100%).

6.1.29 2-Bromo-5-methoxy-4-(2-nitrobenzyl)-*N*-nonanoylbenzylamine

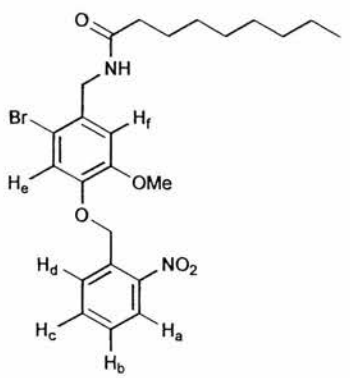

122

To a solution of 2-bromo-4-hydroxy-5-methoxy-*N*-nonanoylbenzylamine (0.3 g, 0.81 mmol, 1.0 equiv) in dry THF (15 cm^3) was added potassium *tert*-butoxide in THF

(1 M, 0.09 g, 806 µl, 0.81 mmol, 1.0 equiv). After stirring the mixture for 20 min at RT, 2-nitrobenzyl bromide (0.17 g, 0.81 mmol, 1.0 equiv) was added and the reaction stirred overnight (16 h). Analysis by T.L.C. showed the starting material had been consumed and therefore water (10 cm^3) was added and the solvent removed *in vacuo*. The resulting solid was partitioned between dichloromethane (50 cm^3) and water (50 cm^3) and then the aqueous phase extracted with dichloromethane (3 × 50 cm^3). The organic fractions were combined, dried ($MgSO_4$), filtered and concentrated *in vacuo*. To the resulting crude solid (0.39 g, 95%) was added ethyl acetate (20 cm^3). The suspension was then filtered and the colourless solid washed with excess cold ethyl acetate. Recrystallisation from ethyl acetate yielding 2-bromo-5-methoxy-4-(2-nitrobenzyl)-*N*-nonanoylbenzylamine (0.09 g, 22%) as a colourless solid. R_f 0.52 (ethyl acetate/petroleum ether 60:40); mp 146-147 °C; (Found: C, 56.93; H, 6.31; N 5.49. $C_{24}H_{31}BrN_2O_5$ requires C, 56.81; H, 6.16; N, 5.52); ν_{max}/cm^{-1} 3297.5 (m)(NH), 2924.5 (s)(CH), 2854.0 (s)(CH), 1645.8 (m)(C=O), 1545.4 (m)(NH), 1526.3 (m)(asym. NO_2), 1509.1 (m), 1463.9 (s), 1377.7 (m)(sym. NO_2), 1332.9 (m), 1306.6 (w), 1264.7 (m), 1233.6 (w), 1211.8 (m), 1191.2 (m), 1162.5 (m), 861.1 (w), 797.2 (w), 731.1 (m)(four adj. Ar-H); δ_H (300 MHz; $CDCl_3$) 8.13 (1H, dd, *J* 8.2, 1.6, Ar-H_a), 7.85 (1H, dd, *J* 7.7, 1.0, Ar-H_d), 7.64 (1H, apparent dt, *J* 7.7, 7.7, 1.3, Ar-H_c), 7.48-7.40 (1H, m, Ar-H_b), 6.98 (1H, s, Ar-H_f), 6.94 (1H, s, Ar-H_e), 5.83 (1H, br s, N*H*), 5.44 (2H, s, CH_2O), 4.38 (2H, d, *J* 6.0, CH_2NH), 3.82 (3H, s, OCH_3), 2.13 (2H, t, *J* 7.6, $COCH_2$), 1.63-1.53 (2H, m, $CH_2(CH_2)_6CH_3$), 1.31-1.11 (10H, m, $CH_2(CH_2)_6CH_3$) and 0.80 (3H, t, *J* 6.8, CH_2CH_3); δ_c (75.5 MHz; $CDCl_3$) 173.1 (*C*=O), 149.2 (*C*), 147.6 (*C*), 146.7 (*C*), 134.2 (Ar-*C*H), 133.4 (*C*), 131.1 (*C*), 128.5 (Ar-*C*H), 125.1 (Ar-*C*H), 118.1 (Ar-*C*H), 114.2 (Ar-*C*H), 113.6 (*C*Br), 68.3 (OCH_2), 56.2 (OCH_3), 43.6 (CH_2NH), 36.8 (CH_2), 31.8 (CH_2), 29.3 (CH_2), 29.2 (CH_2), 25.7 (CH_2), 22.7 (CH_2), 14.1 (CH_2CH_3); *m/z* (ES+) [Found: {($^{81}M+Na)^+$ 531.1285. $C_{24}H_{31}N_2O_5Na^{81}Br$ requires M^+, 531.1294}, {($^{79}M+Na)^+$, 529.1298. $C_{24}H_{31}N_2O_5Na^{79}Br$ requires M^+, 529.1314}]; *m/z* (ES+) 531 ($[^{81}M+Na]^+$, 88%), 529 ($[^{79}M+Na]^+$, 100%).

6.1.30 4-Hydroxy-3-methoxy-*N*-nonanoylbenzylamine

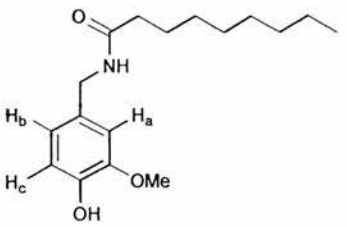

32

To a solution of 3-methoxy-4-(triisopropylsilyloxy)-*N*-nonanoylbenzylamine (2.0 g, 4.45 mmol, 1.0 equiv) in dry THF (50 cm^3) was added tetra-*N*-butylammonium fluoride in THF (1 M, 1.74 g, 6.67 cm^3, 6.67 mmol, 1.5 equiv) and the solution stirred at RT for 3 h. Analysis by T.L.C. showed that the starting material had been consumed and therefore the solution was partitioned between diethyl ether (100 cm^3) and HCl (100 cm^3, 1 M). The aqueous phase was extracted with diethyl ether (3 × 75 cm^3) and the organic fractions combined, washed with brine, dried ($MgSO_4$), filtered and concentrated *in vacuo*. Purification by silica gel column chromatography eluting with ethyl acetate/petroleum ether (40:60) afforded *4-hydroxy-3-methoxy-N-nonanoylbenzylamine* (1.26 g, 97%) as a colourless solid. R_f 0.23 (ethyl acetate/petroleum ether 50:50); mp 60-63 °C; (Found: C, 69.61; H, 9.64; N 4.64. $C_{26}H_{36}N_2O_7$ requires C, 69.59; H, 9.28; N, 4.77); λ_{max} (CH_3CN)/nm 281 (ε/dm^3 mol^{-1} cm^{-1} 3233), 252infl (277), 230sh and 202sh; ν_{max}/cm^{-1} 3505.9 (w), 3449.2 (w), 3290.7 (s)(NH), 2924.4 (s)(CH), 2854.2 (s)(CH), 1642.9 (s)(C=O), 1543.4 (m)(NH), 1519.3 (s), 1460.4 (s), 1377.7 (m), 1276.8 (m), 1253.7 (w), 1234.8 (w), 1199.8 (w), 1156.6 (w), 1122.0 (w)(C-O), 1032.8 (m), 999.6 (w), 851.0 (w), 820.1 (w), 703.8 (w); δ_H (300 MHz; $CDCl_3$) 6.87 (1H, d, *J* 8.0, Ar-H_c), 6.81 (1H, d, *J* 1.9, Ar-H_a), 6.76 (1H, dd, *J* 8.0, 1.9, Ar-H_b), 5.77-5.60 (2H, m, (O*H*) and (N*H*)), 4.35 (2H, d, *J* 5.7, CH_2NH), 3.88 (3H, s, OCH_3), 2.20 (2H, t, *J* 7.6, $COCH_2$), 1.74-1.56 (2H, m, $CH_2(CH_2)_6CH_3$), 1.39-1.16 (10H, m, $CH_2(CH_2)_6CH_3$) and 0.87 (3H, t, *J* 6.8, CH_2CH_3); δ_c (75.5 MHz; $CDCl_3$) 173.4 (*C*=O), 147.1 ($COCH_3$), 145.5 (*C*OH), 130.8 (CCH_2NH), 121.2 (*C*H), 114.7 (*C*H), 111.1 (*C*H), 56.3 (OCH_3), 43.9 (CH_2NH), 37.3 (CH_2), 32.2 (CH_2), 29.7 (CH_2), 29.6 (CH_2), 26.2 (CH_2), 23.0 (CH_2), 14.5 (CH_2CH_3); *m/z*

(ES+) [Found: $(M+Na)^+$ 316.1892. $C_{17}H_{27}NO_3Na$ requires M^+, 316.1889]; *m/z* (ES+) 316 ($[M+Na]^+$, 100%); *m/z* (ES-) 292 ($[M-H]^-$, 100%), 156 {$[NH_2CO(CH_2)_7CH_3\text{-}H]^-$, 5%}.

6.1.31 3-Methoxy-4-(4,5-dimethoxy-2-nitrobenzyl)-*N*-nonanoylbenzylamine

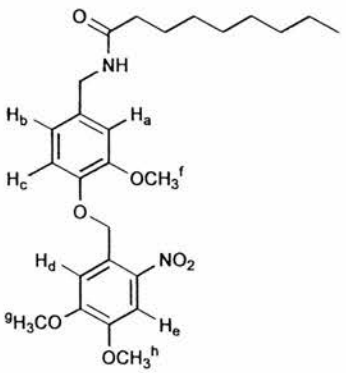

118

To a solution of 4-hydroxy-3-methoxy-*N*-nonanoylbenzylamine (0.40 g, 1.36 mmol, 1.0 equiv) in dry THF (25 cm^3) was added potassium *tert*-butoxide (0.15 g, 1.36 cm^3, 1 M in THF, 1.36 mmol, 1.0 equiv) and the mixture was stirred for 25 min under nitrogen at RT. To this was added 4,5-dimethoxy-2-nitrobenzyl bromide (0.38 g, 1.36 mmol, 1.0 equiv) and the resulting mixture stirred overnight (16 h). Analysis by T.L.C showed that the starting material had been consumed and therefore the solvent was removed *in vacuo*. The resulting solid was partitioned between water (100 cm^3) and ethyl acetate (150 cm^3) and the aqueous phase extracted with ethyl acetate (2 × 150 cm^3). The organic fractions were combined, dried ($MgSO_4$) and concentrated *in vacuo*. The resulting solid was recrystallised from dichloromethane and diethyl ether. This gave *3-methoxy-4-(4,5-dimethoxy-2-nitrobenzyl)-N-nonanoylbenzylamine* (0.44 g, 66%) as a yellow solid. R_f 0.20 (ethyl acetate/petroleum ether 50:50); mp 137-138°C; (Found: C, 63.98; H, 7.30; N 5.60. $C_{26}H_{36}N_2O_7$ requires C, 63.92; H, 7.43; N, 5.73); λ_{max} (CH_3CN)/nm 345 (ε/dm^3 mol^{-1} cm^{-1} 6416), 281 (6980), 262infl (3727), 235sh and 200 (86977); ν_{max}/cm^{-1} 3268.0 (m)(NH), 2925.1 (s)(CH), 2854.5 (s)(CH), 1635.0 (s)(C=O), 1582.8 (w), 1543.1 (m)(NH), 1523.5 (s)(asym. NO_2), 1509.0 (m), 1466.3 (s), 1387.3 (m)(sym. NO_2), 1320.0 (s), 1279.7 (s), 1233.0 (s)(C-O), 1198.3 (w), 1168.1 (w), 1139.5 (m), 1075.5 (m), 1035.2 (m), 991.9 (w), 871.5 (m), 851.1 (w), 819.9 (w), 796.6 (m), 756.2

(w), 721.8 (w); δ_H (300 MHz; $CDCl_3$) 7.69 (1H, s, Ar-H_d), 7.42 (1H, s, Ar-H_e), 6.81 (1H, s, Ar-H_a), 6.80 (1H, d, *J* 8.2, Ar-H_c), 6.71 (1H, dd, *J* 8.2, 2.0, Ar-H_b), 5.61 (1H, br s, N*H*), 5.48 (2H, s, CH_2O), 4.32 (2H, d, *J* 2.9, CH_2NH), 3.90 (6H, s, OCH_3[g,h]), 3.83 (3H, s, OCH_3[f]), 2.14 (2H, t, *J* 7.6, $COCH_2$), 1.64-1.55 (2H, m, $CH_2(CH_2)_6CH_3$), 1.30-1.13 (10H, m, $CH_2(CH_2)_6CH_3$) and 0.80 (3H, t, *J* 6.8, CH_2CH_3); δ_c (75.5 MHz; $CDCl_3$) 173.0 (*C*=O), 154.0 (*C*), 149.9 (*C*), 147.8 (*C*), 147.0 (*C*), 132.6 (*C*), 129.9 (*C*), 120.2 (Ar-*C*H), 114.5 (Ar-*C*H), 111.8 (Ar-*C*H), 109.5 (Ar-*C*H), 107.9 (Ar-*C*H) 68.5 (OCH_2), 56.4 (2 × OCH_3), 56.0 (OCH_3), 43.3 (CH_2NH), 36.9 (CH_2), 31.8 (CH_2), 29.3 (CH_2), 29.2 (CH_2), 25.8 (CH_2), 22.6 (CH_2), 14.1 (CH_2CH_3); *m/z* (ES+) [Found: $(M+Na)^+$ 511.2402. $C_{26}H_{36}N_2O_7Na$ requires M^+, 511.2420]; *m/z* (ES+) 511 ($[M+Na]^+$, 100%); *m/z* (ES-) 487 ($[M-H]^-$, 100%), 212 {$[C_6H_2NO_2(OCH_3)_2CH_2OH-H]^-$, 49%}.

6.1.32 Typical Photolysis Experiment

From a stock solution of *3-methoxy-4-(4,5-dimethoxy-2-nitrobenzyl)-N-nonanoylbenzylamine* (0.0875 g, 0.179 mmol) in D_6-acetone (27 cm^3) were taken aliquots (3.24 mg, 1 cm^3, 6.63 nmol) and placed in a 10 mm optical silica cuvette. An aliquot was left out in the background light for 30 min as a control sample. Aliquots were taken from the remaining stock solution and placed in the beam of a 405 nm, 45 mW (or other power as indicated) violet diode laser and irradiated for periods of between 1-180 min as specified. The resulting solutions were transferred to sample vials and then to NMR sample tubes for ^1H NMR analysis. ^1H NMR integrals were obtained using 1DWINNMR to perform deconvolution calculations.

7 Appendix Selected NMR spectra

2-(4'-Methoxyacetophenone)-4,5-dihydrooxazole

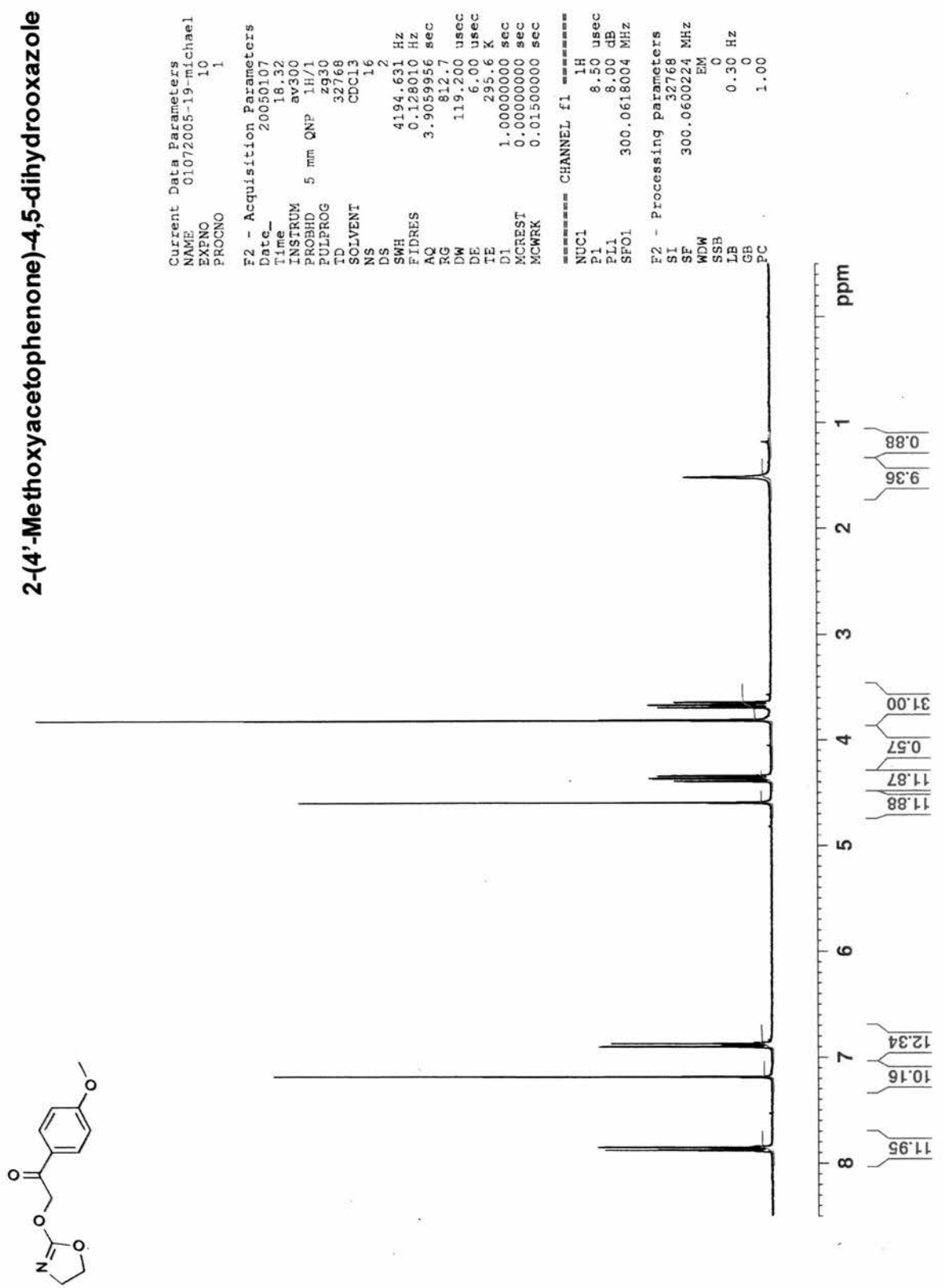

2-(4'-Methoxyacetophenone)-4,5-dihydrooxazole

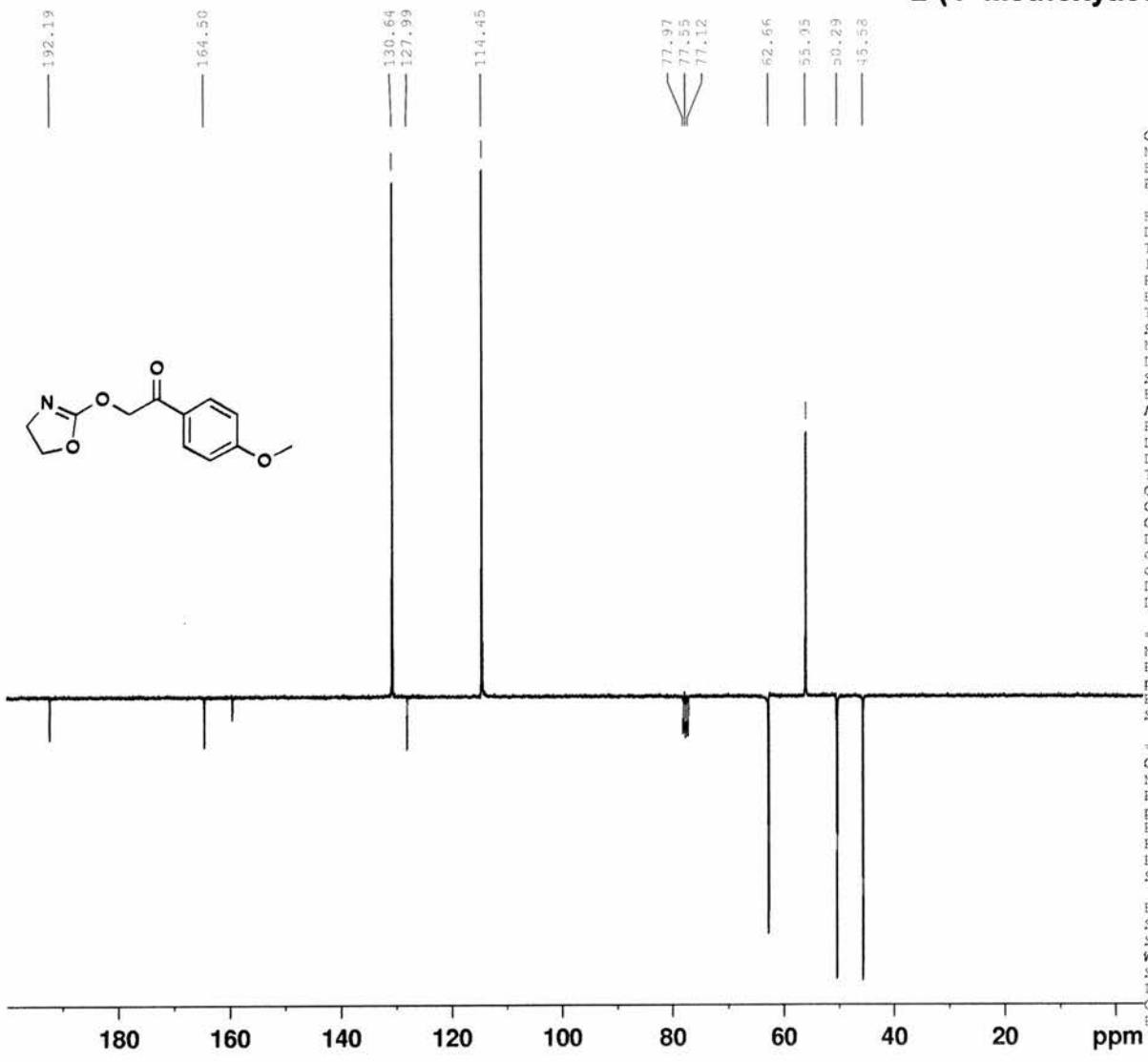


```
Current Data Parameters
NAME      01082005-28-michael
EXPNO                      10
PROCNO                      1

F2 - Acquisition Parameters
Date_              20050108
Time                  17.39
INSTRUM               av300
PROBHD    5 mm QNP  1H/1
PULPROG         pendantnew
TD                     65536
SOLVENT                CDCl3
NS                       800
DS                         8
SWH               18115.941 Hz
FIDRES             0.276427 Hz
AQ                 1.8088436 sec
RG                   18390.4
DW                    27.600 usec
DE                     6.00 usec
TE                    295.7 K
CNST2             145.0000000
CNST3               1.0000000
CNST4               5.0000000
D1                  1.50000000 sec
d2                  0.00172414 sec
d3                  0.00431034 sec
D12                 0.00002000 sec
D13                 0.00000400 sec

======== CHANNEL f1 ========
NUC1                      13C
P1                       7.50 usec
p2                      15.00 usec
PL1                      5.00 dB
SFO1               75.4587938 MHz

======== CHANNEL f2 ========
CPDPRG2                waltz16
NUC2                       1H
P3                       8.50 usec
p4                      17.00 usec
PCPD2                   80.00 usec
PL2                      8.00 dB
PL12                    27.47 dB
SFO2              300.0615003 MHz

F2 - Processing parameters
SI                       32768
SF                 75.4501170 MHz
WDW                         EM
SSB                          0
LB                        2.00 Hz
GB                           0
PC                        1.40
```

2-Benzyloxy-4,5-dihydrooxazole

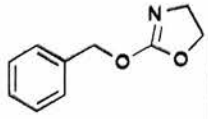

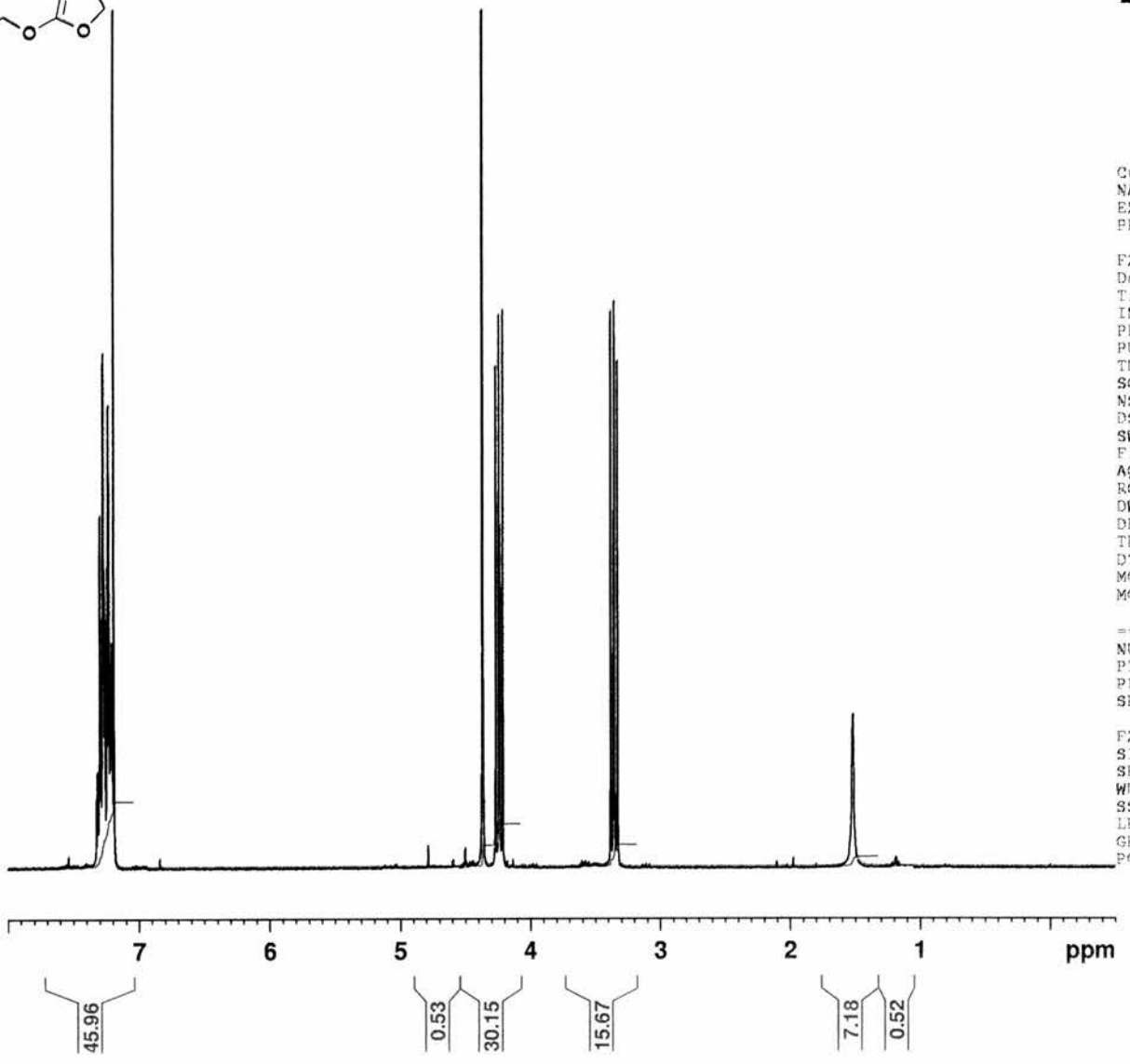


```
Current Data Parameters
NAME      02032005-4-projects
EXPNO                      10
PROCNO                      1

F2 - Acquisition Parameters
Date_               20050203
Time                   10.00
INSTRUM                av300
PROBHD   5 mm BBO BB-1H
PULPROG                zg30
TD                    32768
SOLVENT               CDCl3
NS                       16
DS                        2
SWH                4194.631 Hz
FIDRES            0.128010 Hz
AQ                3.9059956 sec
RG                    812.7
DW                  119.200 usec
DE                     6.00 usec
TE                   296.1 K
D1                1.00000000 sec
MCREST            0.00000000 sec
MCWRK             0.01500000 sec

======== CHANNEL f1 ========
NUC1                       1H
P1                       7.10 usec
PL1                      0.00 dB
SFO1             300.1318008 MHz

F2 - Processing parameters
SI                        32768
SF               300.1300265 MHz
WDW                          EM
SSB                           0
LB                         0.30 Hz
GB                            0
PC                         1.00
```

2-Benzyloxy-4,5-dihydrooxazole

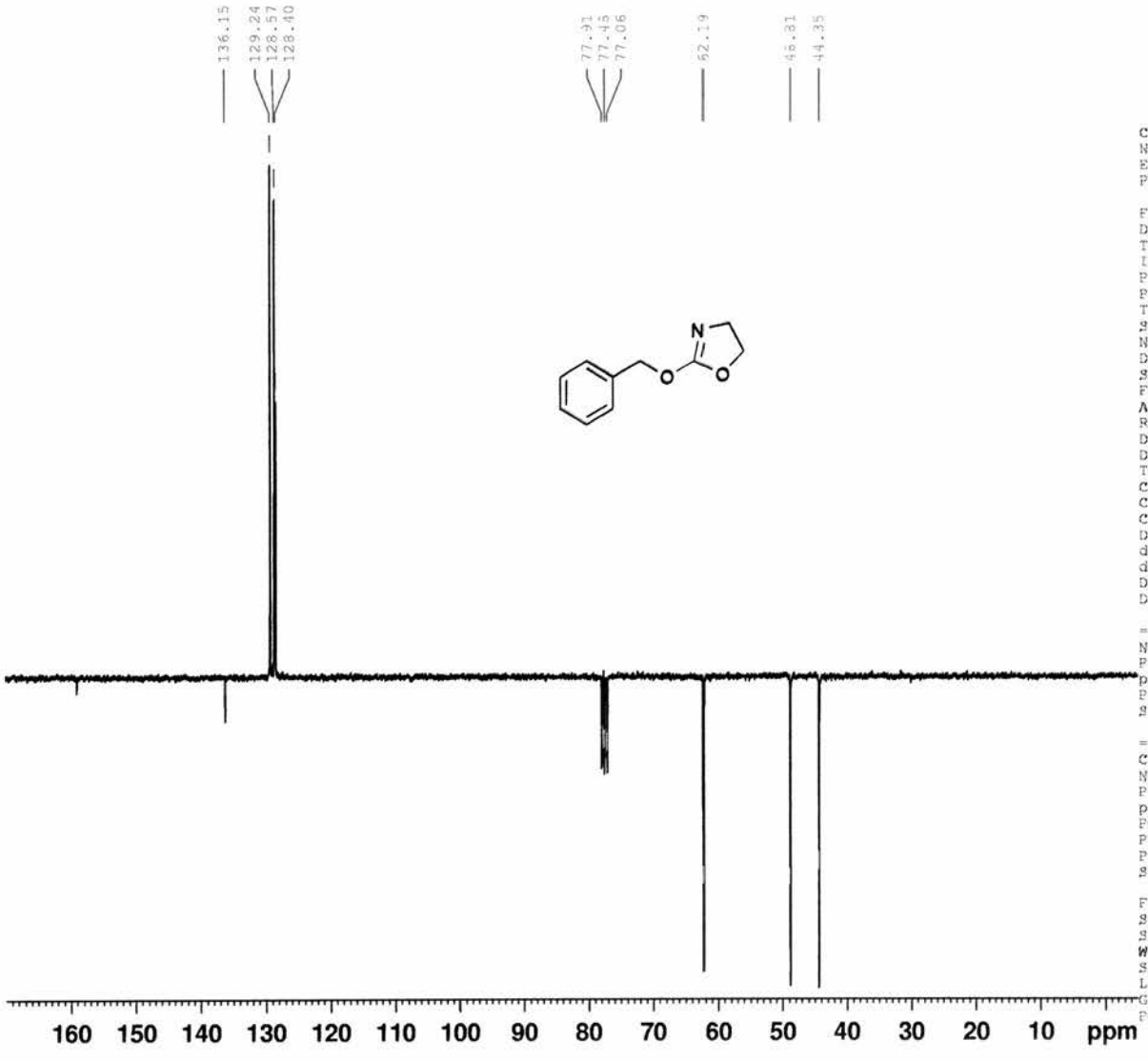


```
Current Data Parameters
NAME      01242005-5-michael
EXPNO                     11
PROCNO                     1

F2 - Acquisition Parameters
Date_              20050124
Time                  23.00
INSTRUM               av300
PROBHD   5 mm QNP  1H/1
PULPROG        pendantnew
TD                    65536
SOLVENT               CDCl3
NS                      800
DS                        8
SWH               18115.941 Hz
FIDRES            0.276427 Hz
AQ                1.8088436 sec
RG                   18390.4
DW                   27.600 usec
DE                    6.00 usec
TE                  295.9 K
CNST2           145.0000000
CNST3             1.0000000
CNST4             5.0000000
D1                1.50000000 sec
d2                0.00172414 sec
d3                0.00431034 sec
D12               0.00002000 sec
D13               0.00000400 sec

======== CHANNEL f1 ========
NUC1                     13C
P1                    7.50 usec
p2                   15.00 usec
PL1                   5.00 dB
SFO1           75.4587938 MHz

======== CHANNEL f2 ========
CPDPRG2              waltz16
NUC2                     1H
P3                    8.50 usec
p4                   17.00 usec
PCPD2                80.00 usec
PL2                   8.00 dB
PL12                 27.47 dB
SFO2          300.0615003 MHz

F2 - Processing parameters
SI                    32768
SF             75.4501170 MHz
WDW                      EM
SSB                       0
LB                    2.00 Hz
GB                        0
PC                    1.40
```

Eicosa-5,8,11,14-tetraenoic acid (2-benzyloxyethyl)amide

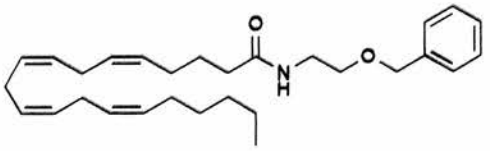

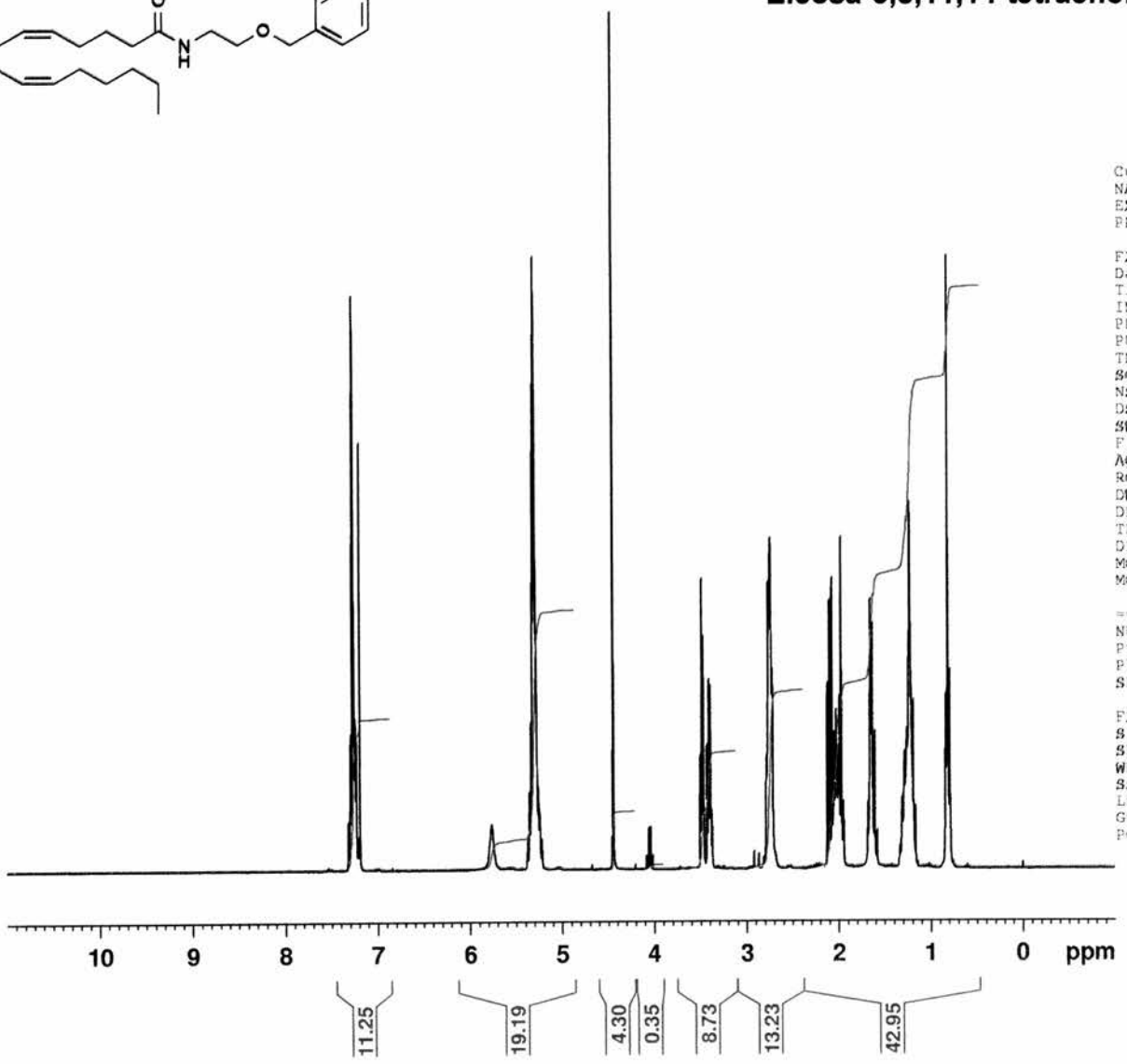


```
Current Data Parameters
NAME      02282005-17-projects
EXPNO                       10
PROCNO                       1

F2 - Acquisition Parameters
Date_               20050228
Time                   16.49
INSTRUM                av300
PROBHD   5 mm BBO BB-1H
PULPROG                zg30
TD                    32768
SOLVENT               CDCl3
NS                       16
DS                        2
SWH                4194.631 Hz
FIDRES             0.128010 Hz
AQ                 3.9059956 sec
RG                     203.2
DW                   119.200 usec
DE                     6.00 usec
TE                    296.1 K
D1                 1.00000000 sec
MCREST             0.00000000 sec
MCWRK              0.01500000 sec

======== CHANNEL f1 ========
NUC1                       1H
P1                       7.10 usec
PL1                      0.00 dB
SFO1           300.1318008 MHz

F2 - Processing parameters
SI                        32768
SF             300.1300265 MHz
WDW                          EM
SSB                           0
LB                         0.30 Hz
GB                            0
PC                         1.00
```

Eicosa-5,8,11,14-tetraenoic acid (2-benzyloxyethyl)amide

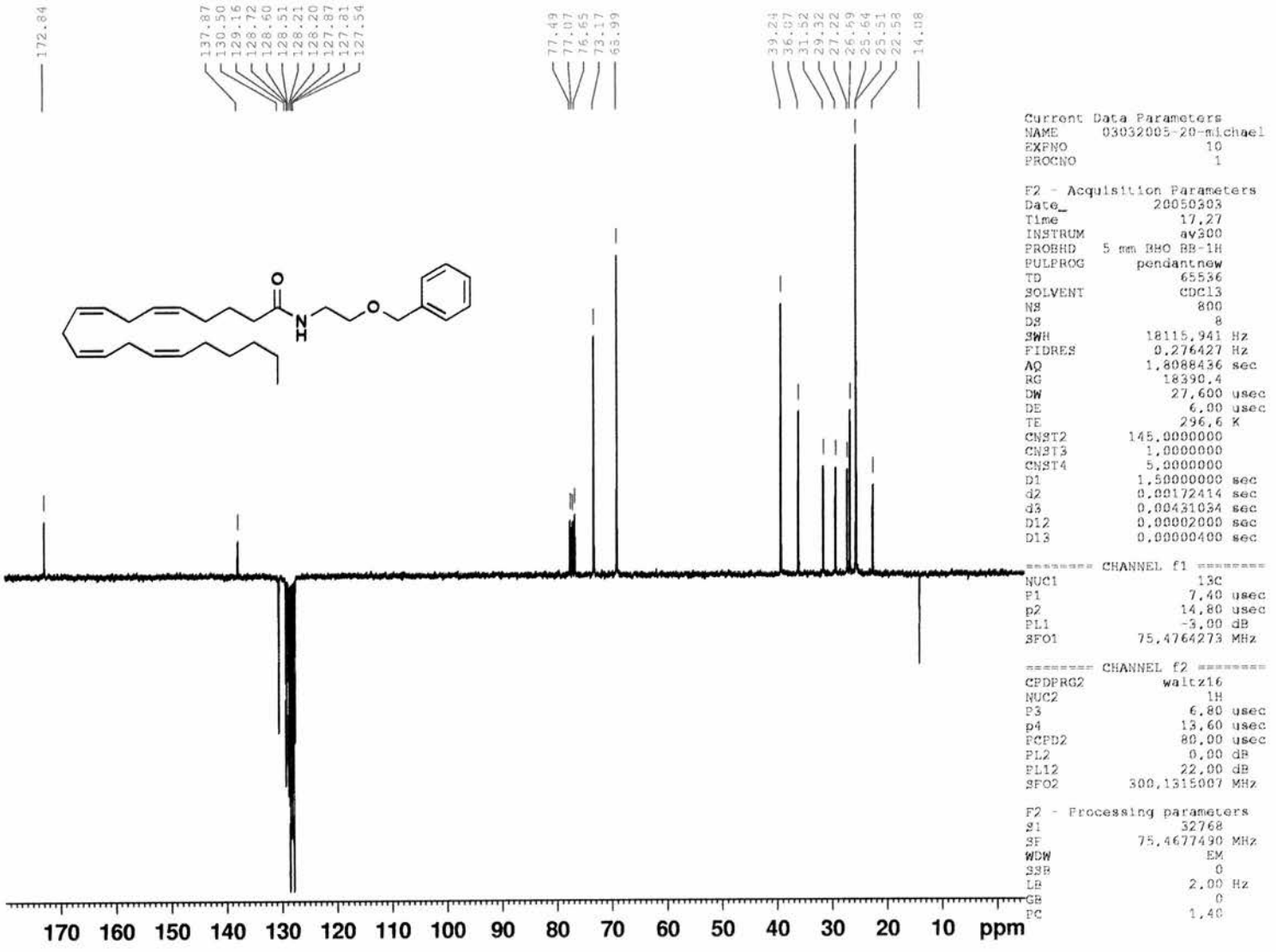


```
Current Data Parameters
NAME      03032005-20-michael
EXPNO                      10
PROCNO                      1

F2 - Acquisition Parameters
Date_               20050303
Time                   17.27
INSTRUM                av300
PROBHD   5 mm BBO BB-1H
PULPROG          pendantnew
TD                     65536
SOLVENT                CDCl3
NS                       800
DS                         8
SWH                18115,941 Hz
FIDRES             0,276427 Hz
AQ                 1,8088436 sec
RG                    18390,4
DW                    27,600 usec
DE                     6,00 usec
TE                    296,6 K
CNST2             145,0000000
CNST3               1,0000000
CNST4               5,0000000
D1                  1,50000000 sec
d2                  0,00172414 sec
d3                  0,00431034 sec
D12                 0,00002000 sec
D13                 0,00000400 sec

======== CHANNEL f1 ========
NUC1                      13C
P1                      7,40 usec
p2                     14,80 usec
PL1                    -3,00 dB
SFO1              75,4764273 MHz

======== CHANNEL f2 ========
CPDPRG2                waltz16
NUC2                       1H
P3                      6,80 usec
p4                     13,60 usec
PCPD2                  80,00 usec
PL2                     0,00 dB
PL12                   22,00 dB
SFO2             300,1315007 MHz

F2 - Processing parameters
SI                       32768
SF                75,4677490 MHz
WDW                         EM
SSB                          0
LB                      2,00 Hz
GB                           0
PC                      1,40
```

2-(Nitrobenzyloxy)-2-phthalimidoethane

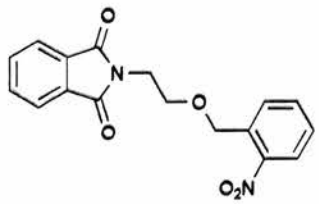

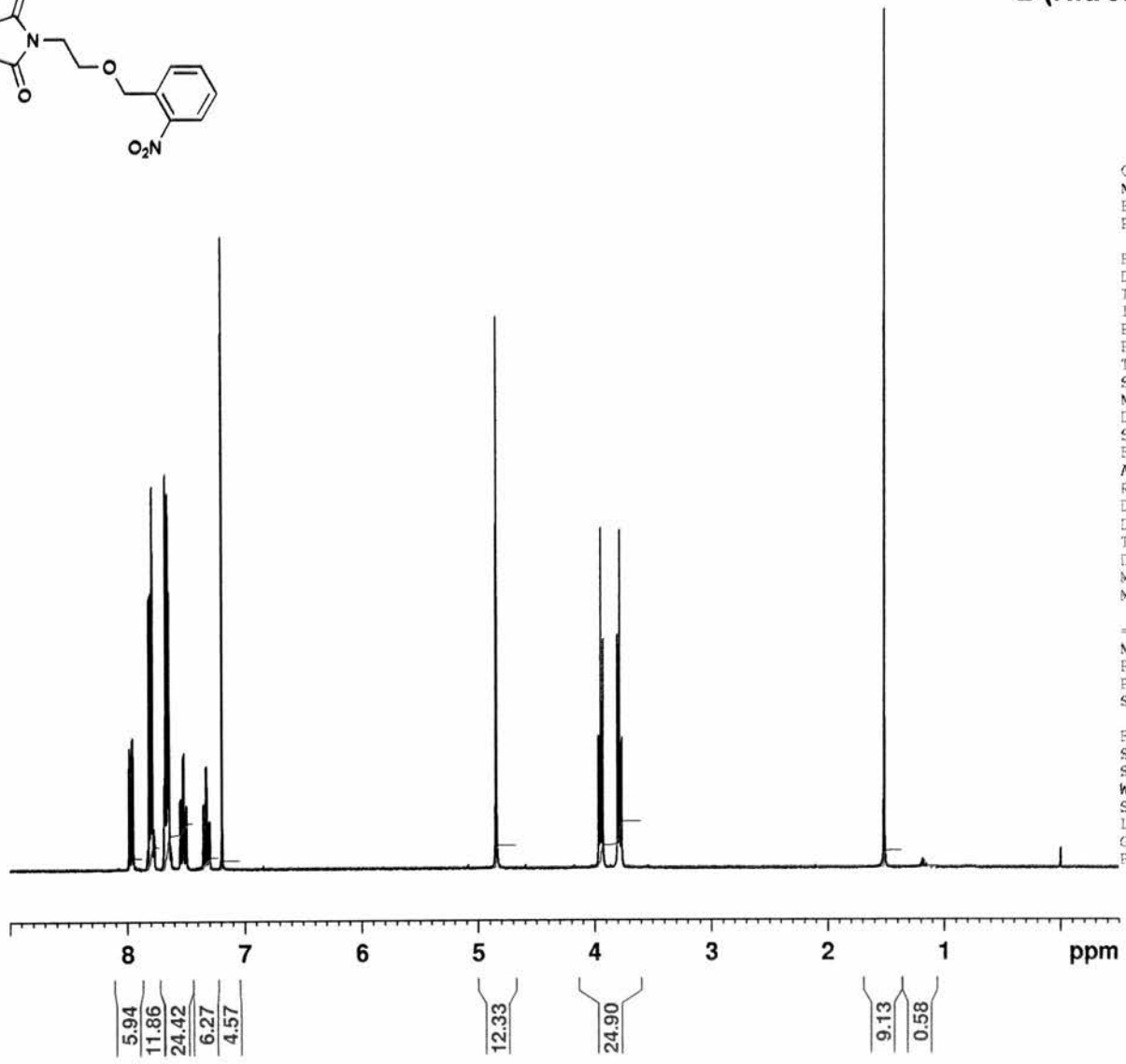


```
Current Data Parameters
NAME      03242005-8-michael
EXPNO                     10
PROCNO                     1

F2 - Acquisition Parameters
Date_               20050324
Time                   10.38
INSTRUM                av300
PROBHD   5 mm QNP  1H/1
PULPROG                 zg30
TD                     32768
SOLVENT                CDCl3
NS                        16
DS                         2
SWH                 4194.631 Hz
FIDRES              0.128010 Hz
AQ                  3.9059956 sec
RG                     912.3
DW                   119.200 usec
DE                     6.00 usec
TE                    295.7 K
D1                  1.00000000 sec
MCREST              0.00000000 sec
MCWRK               0.01500000 sec

======== CHANNEL f1 ========
NUC1                       1H
P1                      8.50 usec
PL1                     8.00 dB
SFO1              300.0618004 MHz

F2 - Processing parameters
SI                         32768
SF                300.0600225 MHz
WDW                           EM
SSB                            0
LB                          0.30 Hz
GB                             0
PC                          1.00
```

2-(Nitrobenzyloxy)-2-phthalimidoethane

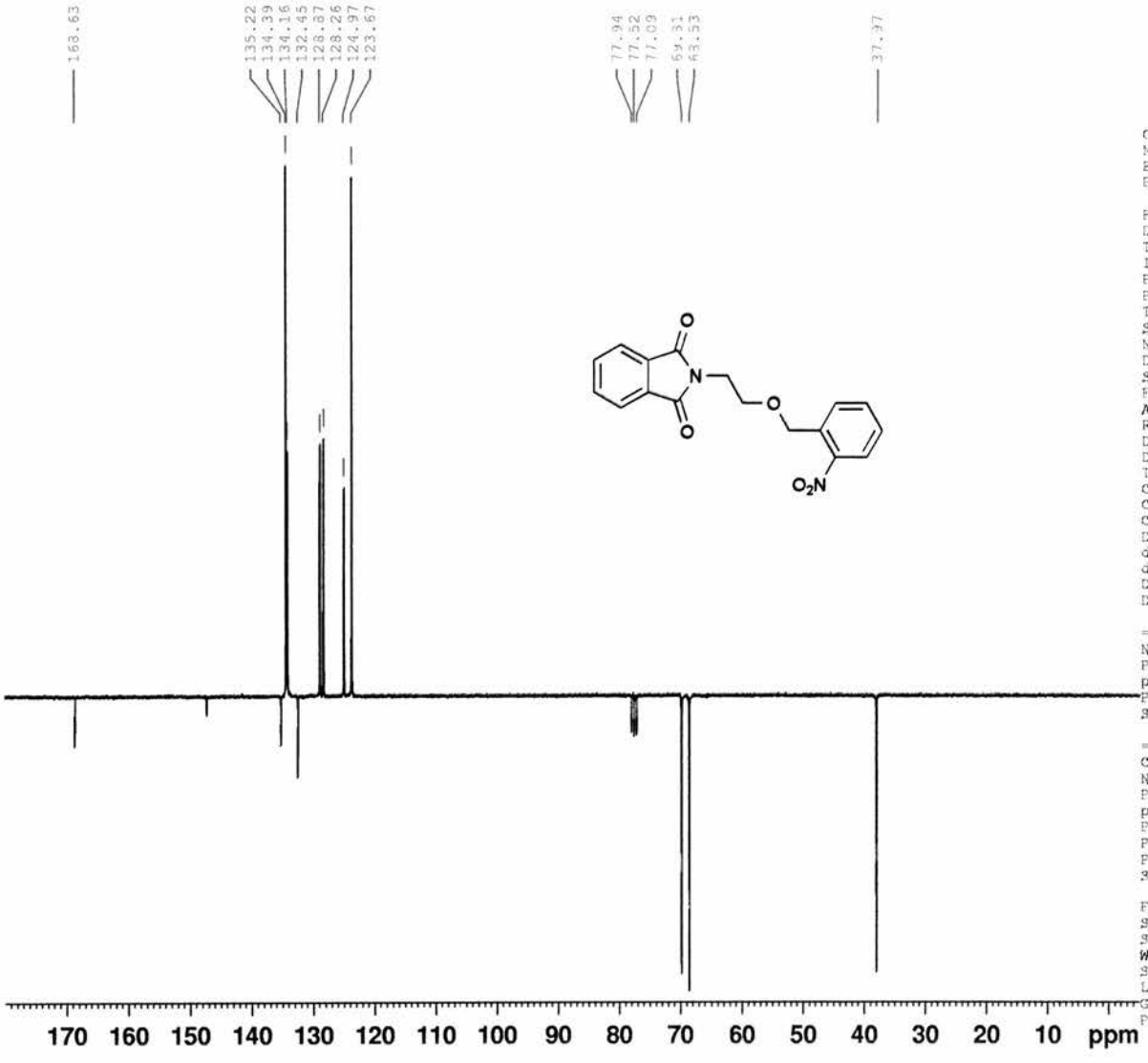


```
Current Data Parameters
NAME      03282005-45-michael
EXPNO                      10
PROCNO                      1

F2 - Acquisition Parameters
Date_               20050328
Time                   20.16
INSTRUM                av300
PROBHD    5 mm QNP  1H/1
PULPROG          pendantnew
TD                      65536
SOLVENT                 CDCl3
NS                        800
DS                          8
SWH                 18115.941 Hz
FIDRES              0.276427 Hz
AQ                  1.8088436 sec
RG                     18390.4
DW                    27.600 usec
DE                     6.00 usec
TE                    296.1 K
CNST2              145.0000000
CNST3                1.0000000
CNST4                5.0000000
D1                   1.50000000 sec
d2                   0.00172414 sec
d3                   0.00431034 sec
D12                  0.00002000 sec
D13                  0.00000400 sec

======== CHANNEL f1 ========
NUC1                       13C
P1                       7.50 usec
p2                      15.00 usec
PL1                      5.00 dB
SFO1                75.4587938 MHz

======== CHANNEL f2 ========
CPDPRG2                waltz16
NUC2                       1H
P3                       8.50 usec
p4                      17.00 usec
PCPD2                   80.00 usec
PL2                      8.00 dB
PL12                    27.47 dB
SFO2               300.0615003 MHz

F2 - Processing parameters
SI                        32768
SF                  75.4501170 MHz
WDW                        EM
SSB                         0
LB                       2.00 Hz
GB                          0
PC                       1.40
```

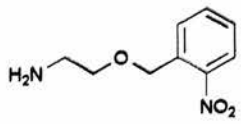

2-(Nitrobenzyloxy)ethylamine (Crude)

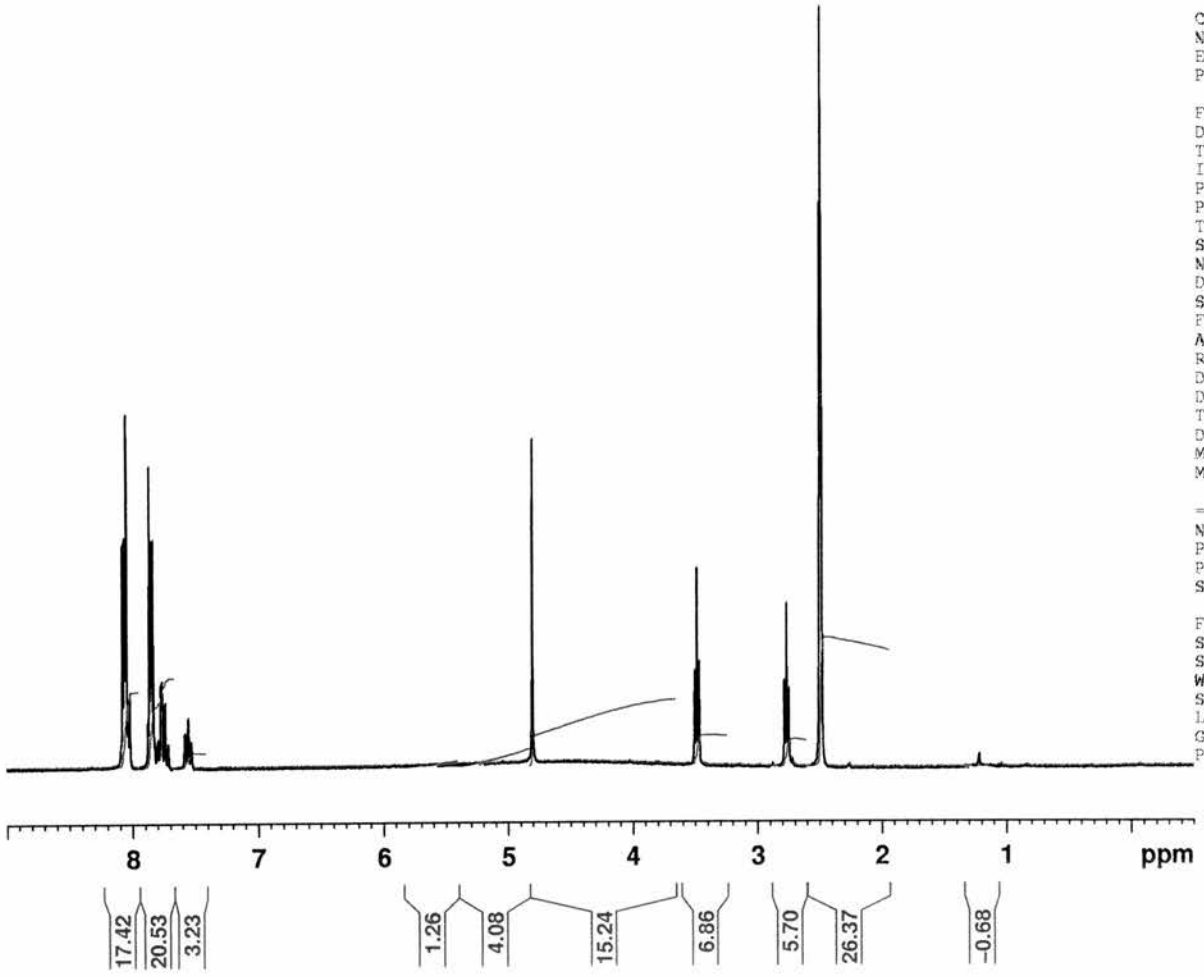


```
Current Data Parameters
NAME      03282005-30-michael
EXPNO                      10
PROCNO                      1

F2 - Acquisition Parameters
Date_               20050328
Time                   16.14
INSTRUM                av300
PROBHD   5 mm QNP  1H/1
PULPROG                zg30
TD                    32768
SOLVENT                DMSO
NS                        16
DS                         2
SWH                4194.631 Hz
FIDRES            0.128010 Hz
AQ                3.9059956 sec
RG                     812.7
DW                   119.200 usec
DE                     6.00 usec
TE                    295.7 K
D1              1.00000000 sec
MCREST          0.00000000 sec
MCWRK           0.01500000 sec

======== CHANNEL f1 ========
NUC1                       1H
P1                       8.50 usec
PL1                      8.00 dB
SFO1            300.0618004 MHz

F2 - Processing parameters
SI                        32768
SF              300.0600000 MHz
WDW                        EM
SSB                         0
LB                       0.30 Hz
GB                          0
PC                       1.00
```

Eicosa-5,8,11,14-tetraenoic acid (2-nitrobenzyloxyethyl)amide

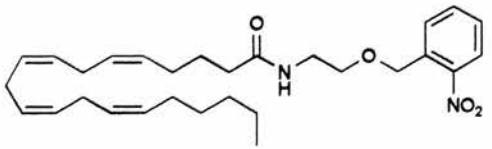

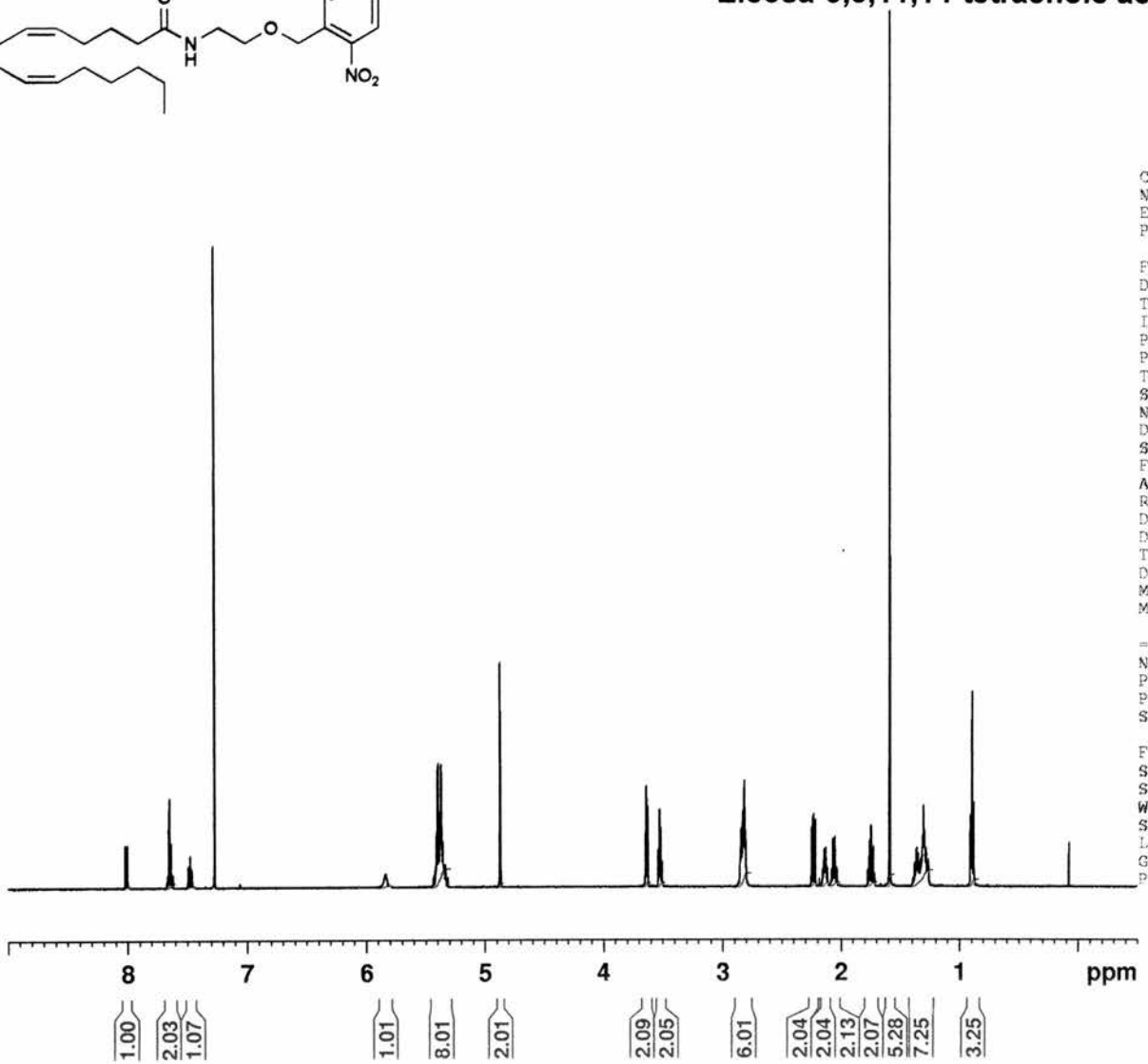


```
Current Data Parameters
NAME          MPVR_A36(a)
EXPNO                   1
PROCNO                  1

F2 - Acquisition Parameters
Date_            20050607
Time                11.25
INSTRUM             spect
PROBHD   5 mm QNP 1H/13
PULPROG              zg30
TD                  65536
SOLVENT             CDCl3
NS                     16
DS                      2
SWH              7002.801 Hz
FIDRES           0.106854 Hz
AQ              4.6793203 sec
RG                  574.7
DW                 71.400 usec
DE                   6.00 usec
TE                  294.4 K
D1             1.00000000 sec
MCREST         0.00000000 sec
MCWRK          0.01500000 sec

======== CHANNEL f1 ========
NUC1                   1H
P1                  10.60 usec
PL1                 -3.00 dB
SFO1          499.9029994 MHz

F2 - Processing parameters
SI                  65536
SF            499.9000047 MHz
WDW                    EM
SSB                     0
LB                   0.30 Hz
GB                      0
PC                   1.00
```

Eicosa-5,8,11,14-tetraenoic acid (2-nitrobenzyloxyethyl)amide

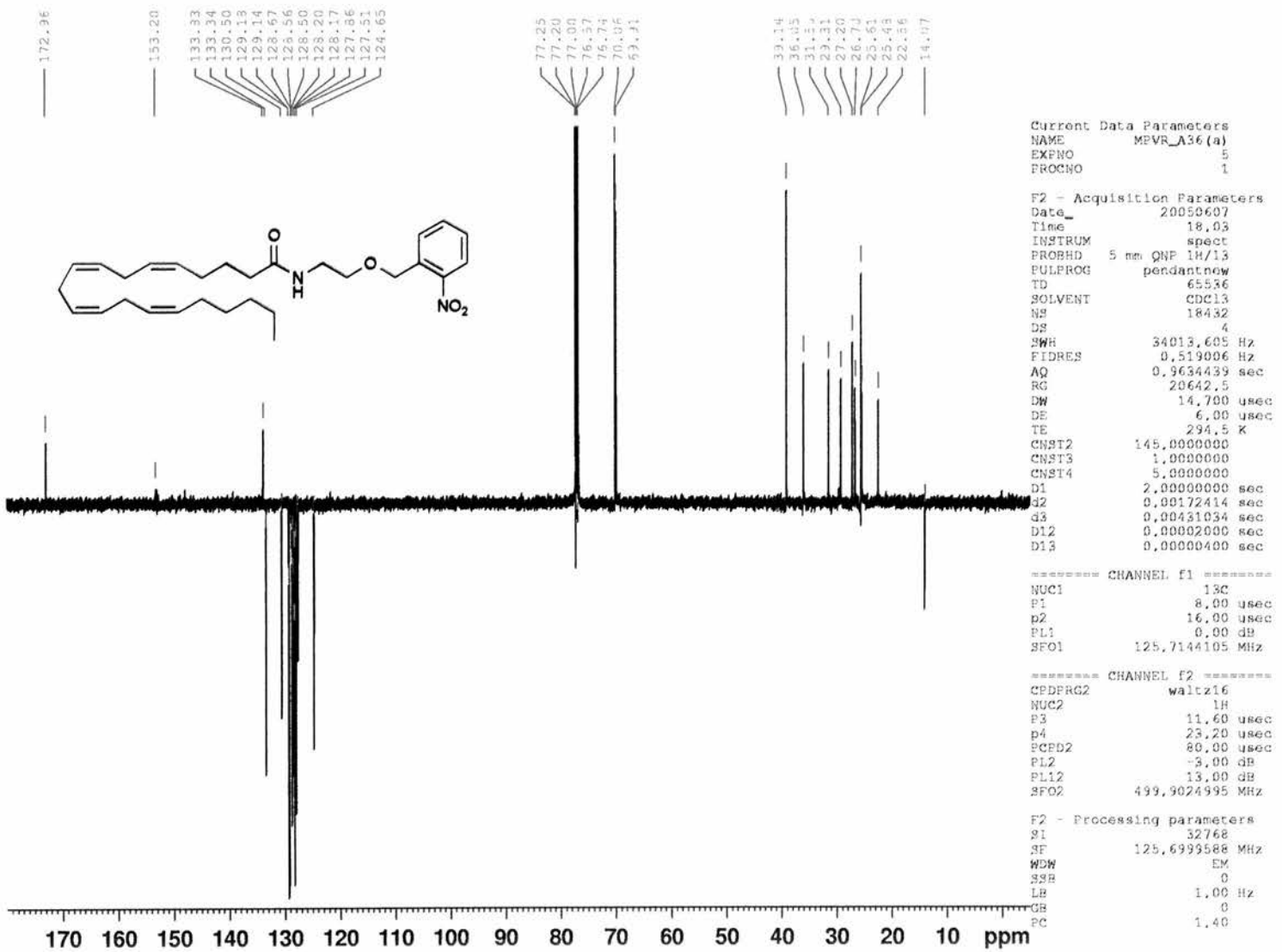


```
Current Data Parameters
NAME          MPVR_A36(a)
EXPNO                   5
PROCNO                  1

F2 - Acquisition Parameters
Date_            20050607
Time                18.03
INSTRUM             spect
PROBHD   5 mm QNP 1H/13
PULPROG       pendantnew
TD                  65536
SOLVENT             CDCl3
NS                  18432
DS                      4
SWH           34013.605 Hz
FIDRES         0.519006 Hz
AQ             0.9634439 sec
RG               20642.5
DW                14.700 usec
DE                 6.00 usec
TE                294.5 K
CNST2        145.0000000
CNST3          1.0000000
CNST4          5.0000000
D1             2.00000000 sec
d2             0.00172414 sec
d3             0.00431034 sec
D12            0.00002000 sec
D13            0.00000400 sec

======== CHANNEL f1 ========
NUC1                  13C
P1                   8.00 usec
p2                  16.00 usec
PL1                  0.00 dB
SFO1         125.7144105 MHz

======== CHANNEL f2 ========
CPDPRG2           waltz16
NUC2                  1H
P3                  11.60 usec
p4                  23.20 usec
PCPD2               80.00 usec
PL2                 -3.00 dB
PL12                13.00 dB
SFO2         499.9024995 MHz

F2 - Processing parameters
SI                  32768
SF           125.6999588 MHz
WDW                    EM
SSB                     0
LB                   1.00 Hz
GB                      0
PC                   1.40
```

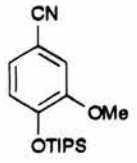

3-Methoxy-4-(triisopropylsilyloxy)benzonitrile

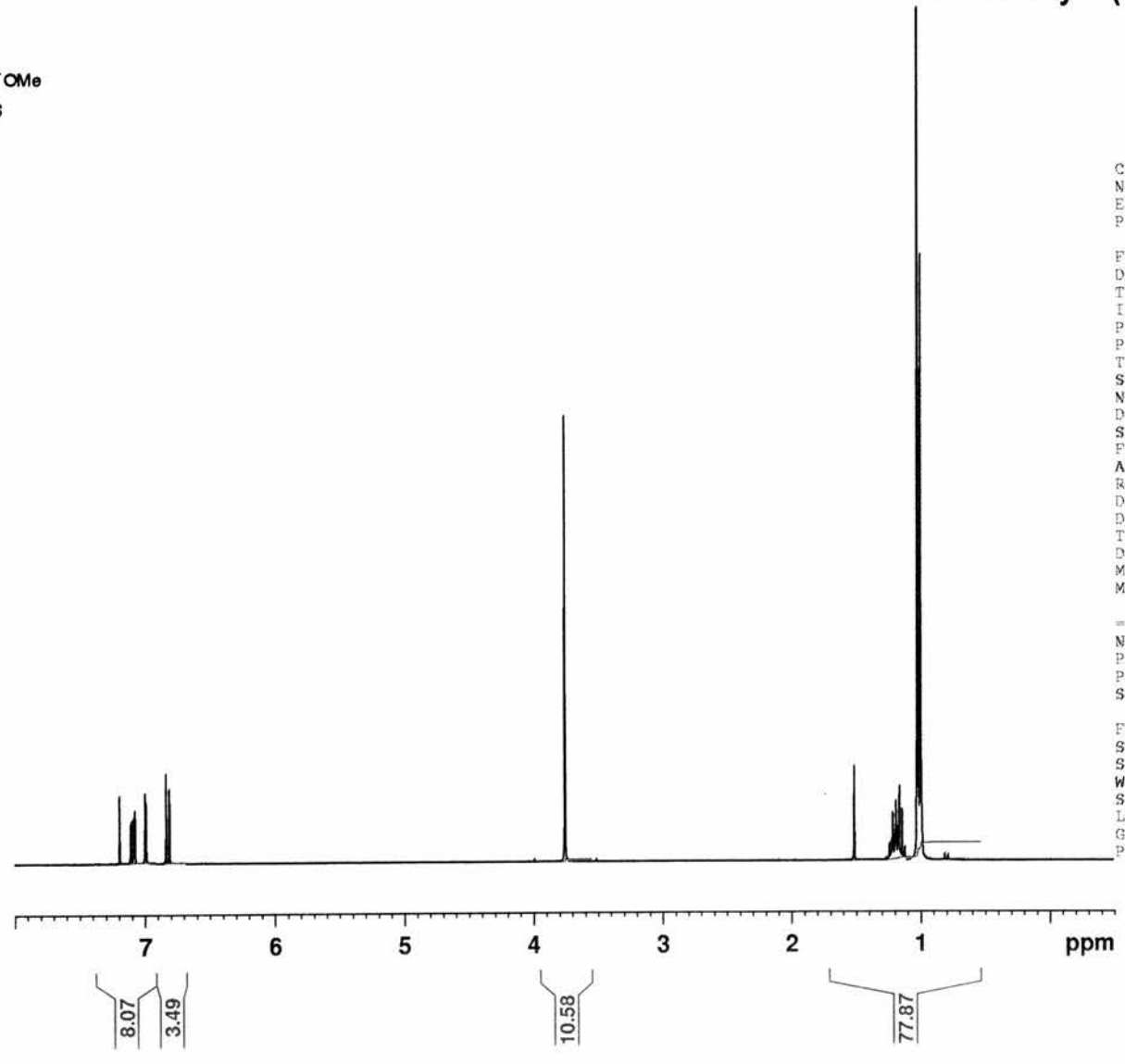


```
Current Data Parameters
NAME      05232005-1-michael
EXPNO                     10
PROCNO                     1

F2 - Acquisition Parameters
Date_              20050523
Time                   9.45
INSTRUM               av300
PROBHD   5 mm QNP  1H/1
PULPROG                zg30
TD                    32768
SOLVENT               CDCl3
NS                       16
DS                        2
SWH                4194.631 Hz
FIDRES             0.128010 Hz
AQ                 3.9059956 sec
RG                      362
DW                  119.200 usec
DE                    6.00 usec
TE                   293.7 K
D1                1.00000000 sec
MCREST            0.00000000 sec
MCWRK             0.01500000 sec

======== CHANNEL f1 ========
NUC1                      1H
P1                     8.50 usec
PL1                    8.00 dB
SFO1           300.0618004 MHz

F2 - Processing parameters
SI                    32768
SF             300.0600223 MHz
WDW                      EM
SSB                       0
LB                     0.30 Hz
GB                        0
PC                     1.00
```

3-Methoxy-4-(triisopropylsilyloxy)benzonitrile

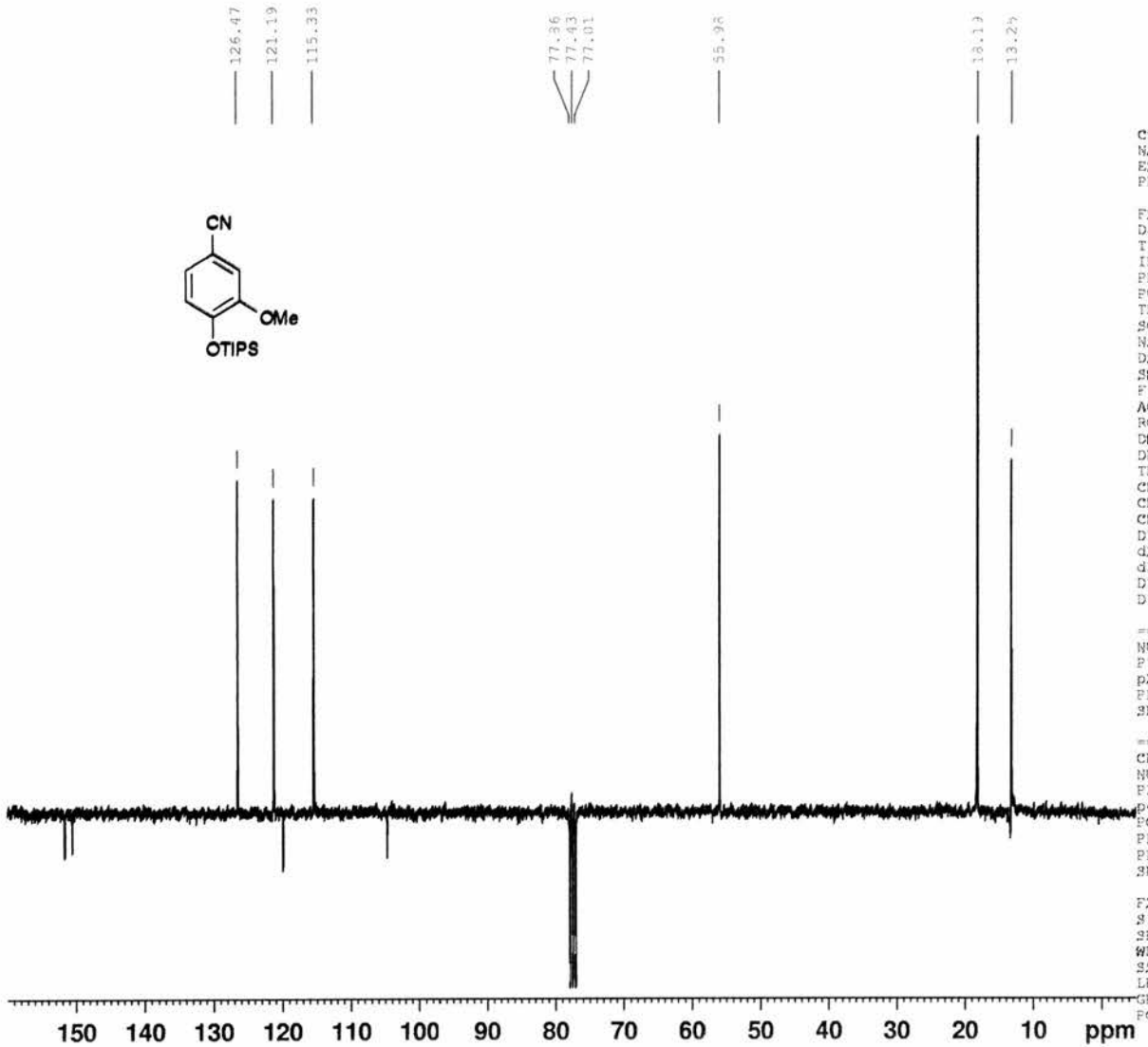


```
Current Data Parameters
NAME      08012005-17-michael
EXPNO                      10
PROCNO                      1

F2 - Acquisition Parameters
Date_              20050801
Time                  23.19
INSTRUM               av300
PROBHD   5 mm QNP  1H/1
PULPROG         pendantnew
TD                   65536
SOLVENT              CDCl3
NS                     800
DS                       8
SWH               18115.941 Hz
FIDRES            0.276427 Hz
AQ                1.8088436 sec
RG                  18390.4
DW                   27.600 usec
DE                    6.00 usec
TE                   293.9 K
CNST2           145.0000000
CNST3             1.0000000
CNST4             5.0000000
D1                1.50000000 sec
d2                0.00172414 sec
d3                0.00431034 sec
D12               0.00002000 sec
D13               0.00000400 sec

======== CHANNEL f1 ========
NUC1                    13C
P1                     7.50 usec
p2                    15.00 usec
PL1                    5.00 dB
SFO1           75.4587938 MHz

======== CHANNEL f2 ========
CPDPRG2             waltz16
NUC2                    1H
P3                     8.50 usec
p4                    17.00 usec
PCPD2                 80.00 usec
PL2                    8.00 dB
PL12                  27.47 dB
SFO2          300.0615003 MHz

F2 - Processing parameters
SI                     32768
SF              75.4501170 MHz
WDW                       EM
SSB                        0
LB                      2.00 Hz
GB                         0
PC                      1.40
```

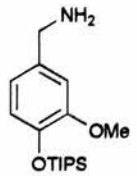

3-Methoxy-4-(triisopropylsilyloxy)benzylamine (Crude)

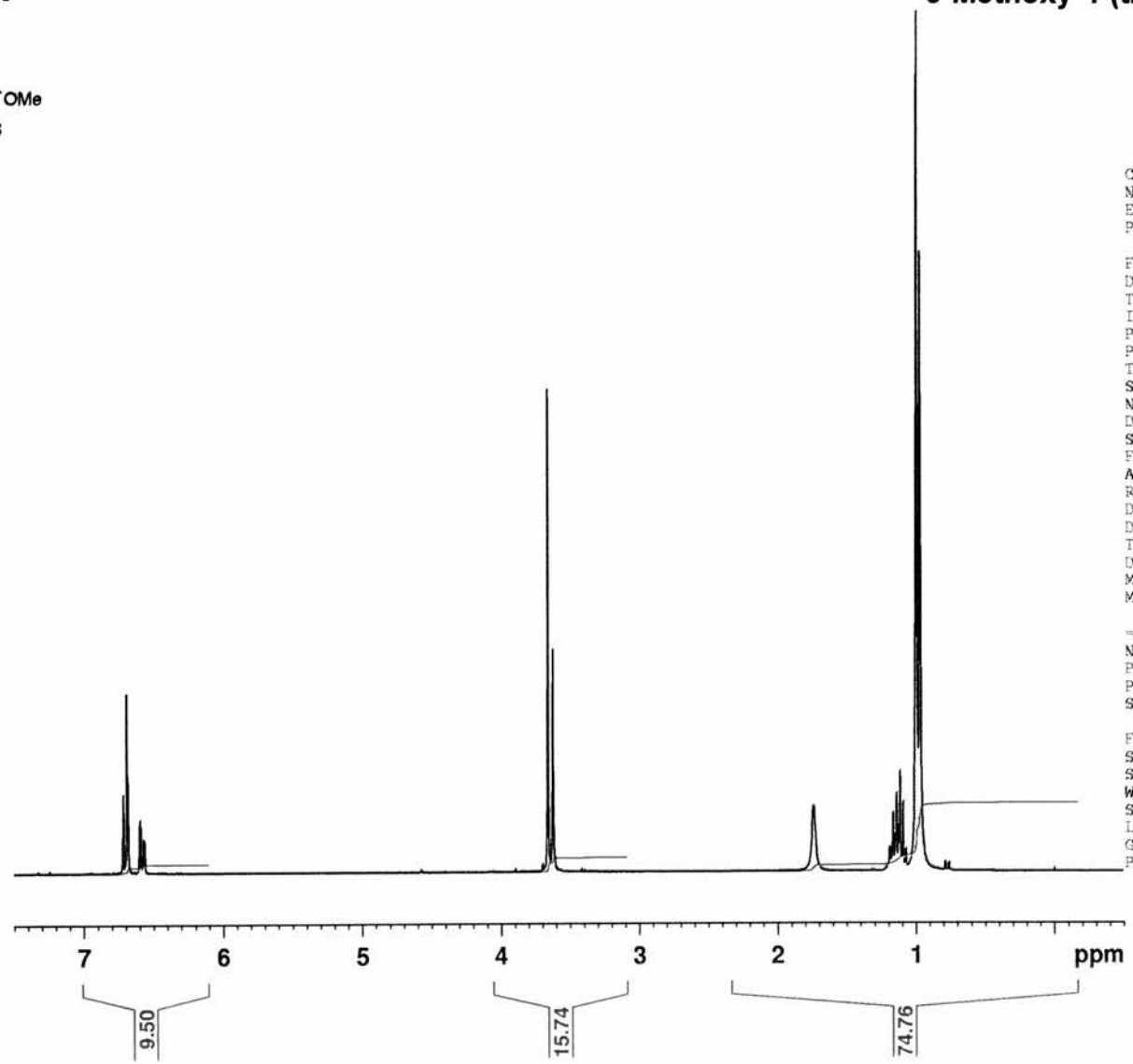


```
Current Data Parameters
NAME      05262005-11-michael
EXPNO                      10
PROCNO                      1

F2 - Acquisition Parameters
Date_              20050526
Time                  16.18
INSTRUM                av300
PROBHD   5 mm QNP  1H/1
PULPROG                zg30
TD                    32768
SOLVENT               CDCl3
NS                       16
DS                        2
SWH                4194.631 Hz
FIDRES             0.128010 Hz
AQ                 3.9059956 sec
RG                      14.3
DW                   119.200 usec
DE                     6.00 usec
TE                    293.7 K
D1                 1.00000000 sec
MCREST             0.00000000 sec
MCWRK              0.01500000 sec

======== CHANNEL f1 ========
NUC1                       1H
P1                      8.50 usec
PL1                     8.00 dB
SFO1            300.0618004 MHz

F2 - Processing parameters
SI                        32768
SF              300.0600071 MHz
WDW                          EM
SSB                           0
LB                         0.30 Hz
GB                            0
PC                         1.00
```

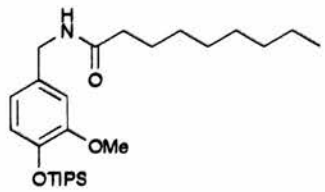

3-Methoxy-4-(triisopropylsilyloxy)-*N*-nonanoylbenzylamine

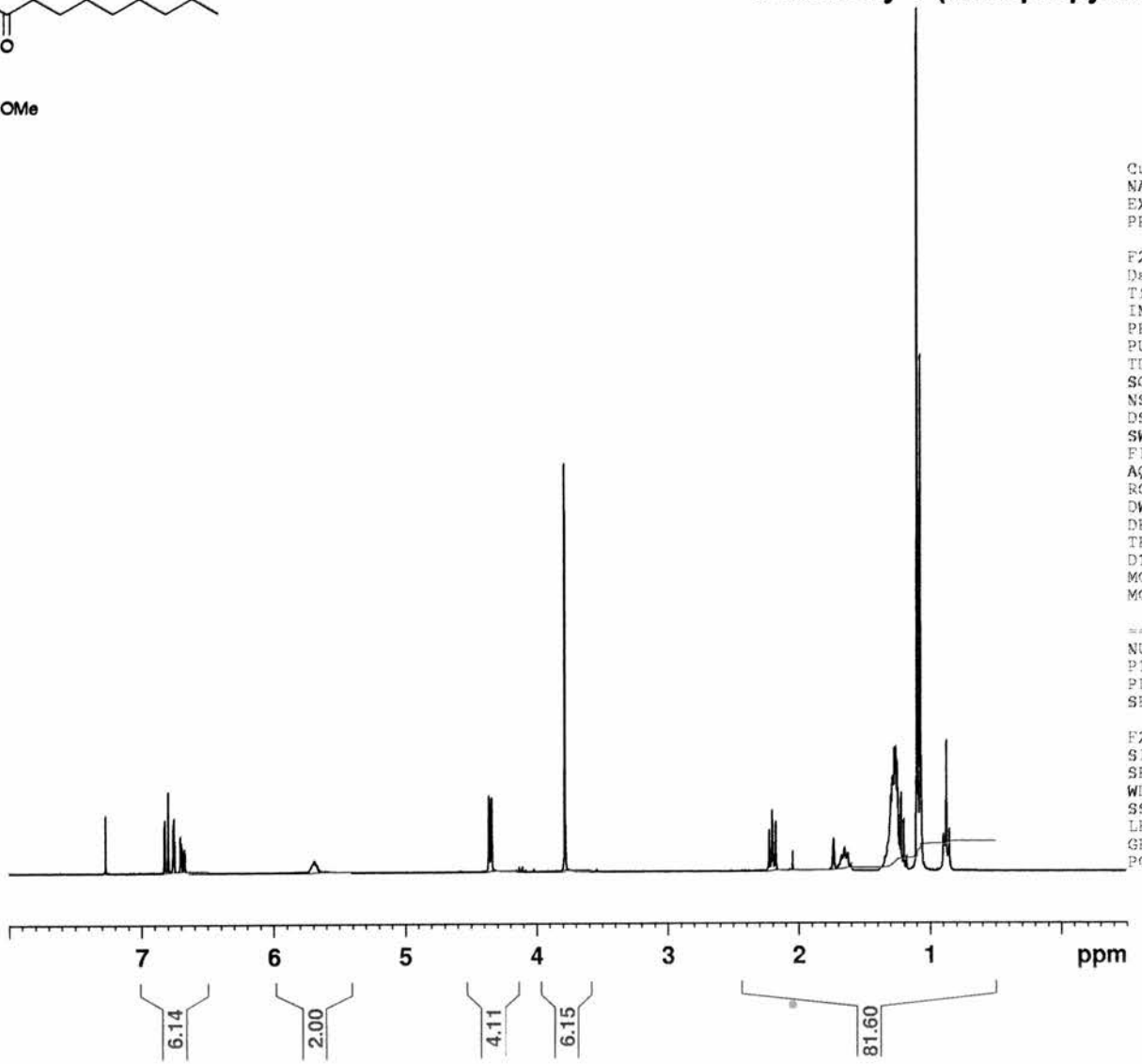


```
Current Data Parameters
NAME      06162005-26-michael
EXPNO                      10
PROCNO                      1

F2 - Acquisition Parameters
Date_              20050616
Time                  12.59
INSTRUM               av300
PROBHD   5 mm QNP  1H/1
PULPROG                zg30
TD                    32768
SOLVENT               CDCl3
NS                       16
DS                        2
SWH                4194.631 Hz
FIDRES             0.128010 Hz
AQ                 3.9059956 sec
RG                      181
DW                 119.200 usec
DE                   6.00 usec
TE                   293.7 K
D1                 1.00000000 sec
MCREST             0.00000000 sec
MCWRK              0.01500000 sec

======== CHANNEL f1 ========
NUC1                      1H
P1                     8.50 usec
PL1                    8.00 dB
SFO1           300.0618004 MHz

F2 - Processing parameters
SI                    32768
SF             300.0600000 MHz
WDW                      EM
SSB                       0
LB                     0.30 Hz
GB                        0
PC                     1.00
```

3-Methoxy-4-(triisopropylsilyloxy)-*N*-nonanoylbenzylamine

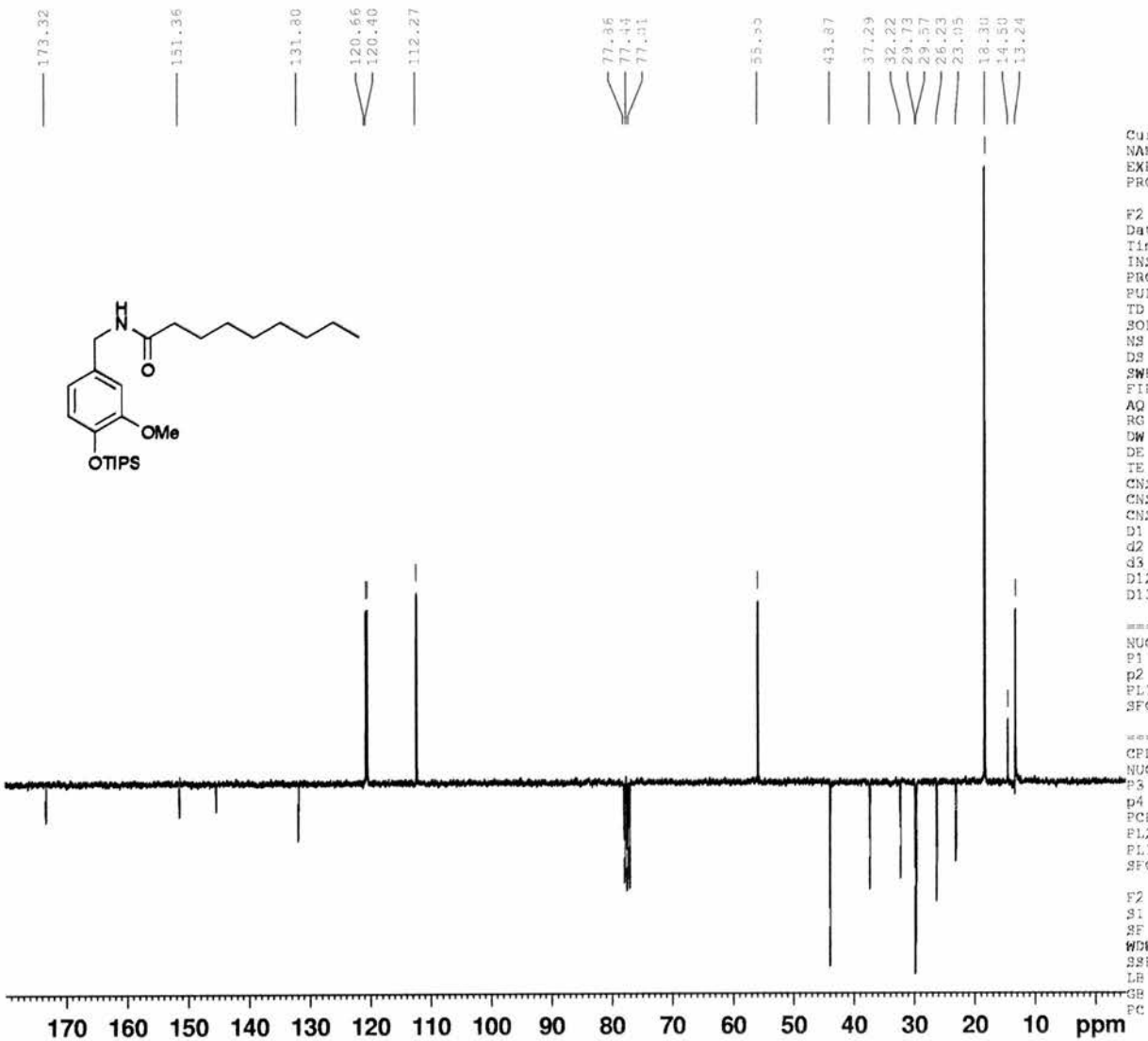


```
Current Data Parameters
NAME      06022005-28-michael
EXPNO                      11
PROCNO                      1

F2 - Acquisition Parameters
Date_              20050602
Time                  19.38
INSTRUM               av300
PROBHD    5 mm QNP  1H/1
PULPROG         pendantnew
TD                     65536
SOLVENT                CDCl3
NS                       800
DS                         8
SWH                18115.941 Hz
FIDRES             0.276427 Hz
AQ                 1.8088436 sec
RG                   18390.4
DW                    27.600 usec
DE                     6.00 usec
TE                    293.9 K
CNST2             145.0000000
CNST3               1.0000000
CNST4               5.0000000
D1                  1.50000000 sec
d2                  0.00172414 sec
d3                  0.00431034 sec
D12                 0.00002000 sec
D13                 0.00000400 sec

======== CHANNEL f1 ========
NUC1                      13C
P1                       7.50 usec
p2                      15.00 usec
PL1                      5.00 dB
SFO1               75.4587938 MHz

======== CHANNEL f2 ========
CPDPRG2                waltz16
NUC2                       1H
P3                       8.50 usec
p4                      17.00 usec
PCPD2                   80.00 usec
PL2                      8.00 dB
PL12                    27.47 dB
SFO2              300.0615003 MHz

F2 - Processing parameters
SI                       32768
SF                 75.4501170 MHz
WDW                         EM
SSB                          0
LB                        2.00 Hz
GB                           0
PC                        1.40
```

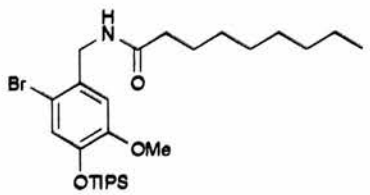

2-Bromo-5-methoxy-4-(triisopropylsilyloxy)-*N*-nonanoylbenzylamine

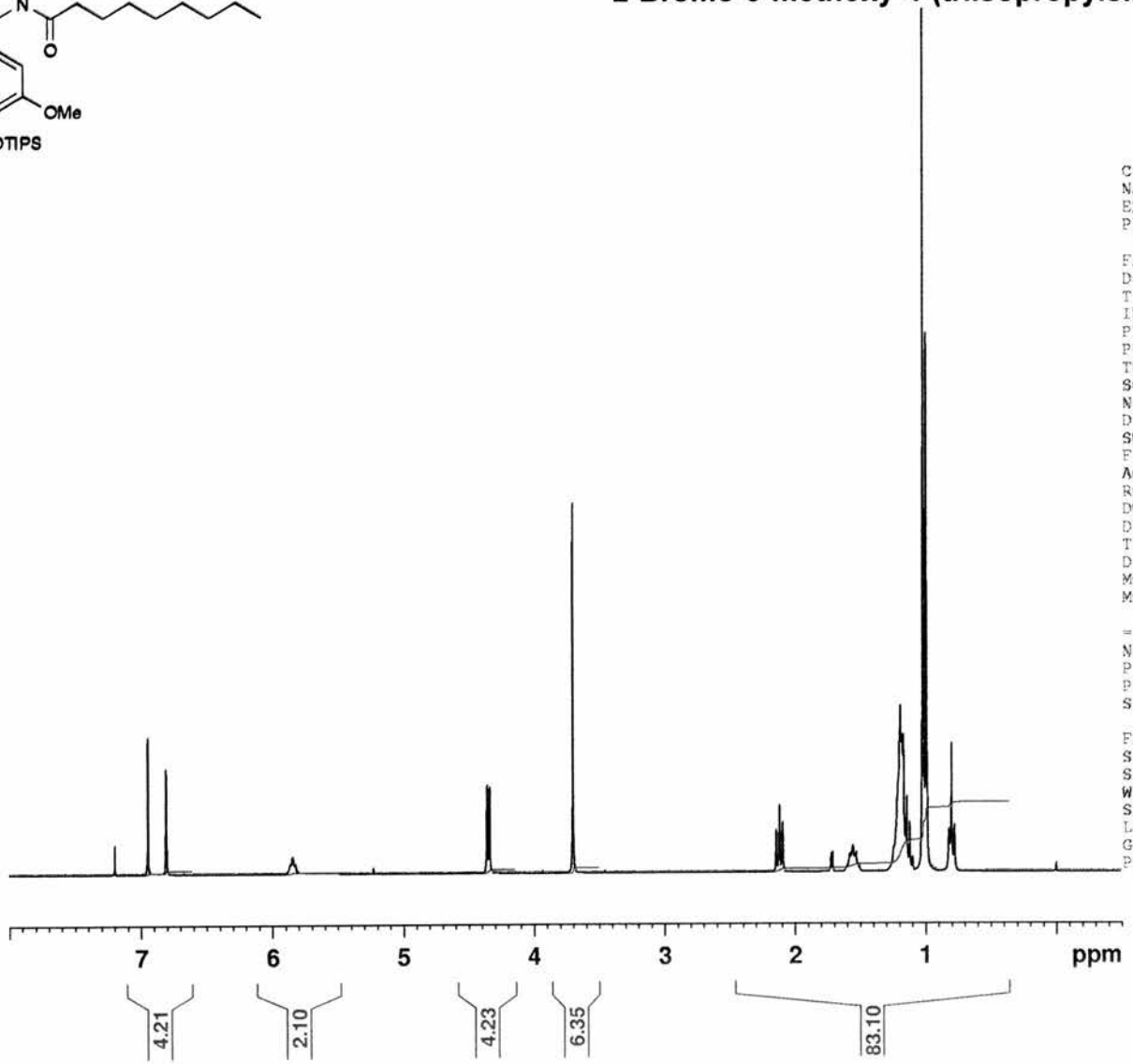


```
Current Data Parameters
NAME      06092005-24-michael
EXPNO                  10
PROCNO                  1

F2 - Acquisition Parameters
Date_            20050610
Time                 1.28
INSTRUM             av300
PROBHD   5 mm QNP  1H/1
PULPROG              zg30
TD                  32768
SOLVENT             CDCl3
NS                     16
DS                      2
SWH              4194.631 Hz
FIDRES           0.128010 Hz
AQ              3.9059956 sec
RG                    128
DW                119.200 usec
DE                   6.00 usec
TE                  293.8 K
D1             1.00000000 sec
MCREST         0.00000000 sec
MCWRK          0.01500000 sec

======== CHANNEL f1 ========
NUC1                   1H
P1                   8.50 usec
PL1                  8.00 dB
SFO1          300.0618004 MHz

F2 - Processing parameters
SI                  32768
SF            300.0600210 MHz
WDW                    EM
SSB                     0
LB                   0.30 Hz
GB                      0
PC                   1.00
```

2-Bromo-5-methoxy-4-(triisopropylsilyloxy)-*N*-nonanoylbenzylamine

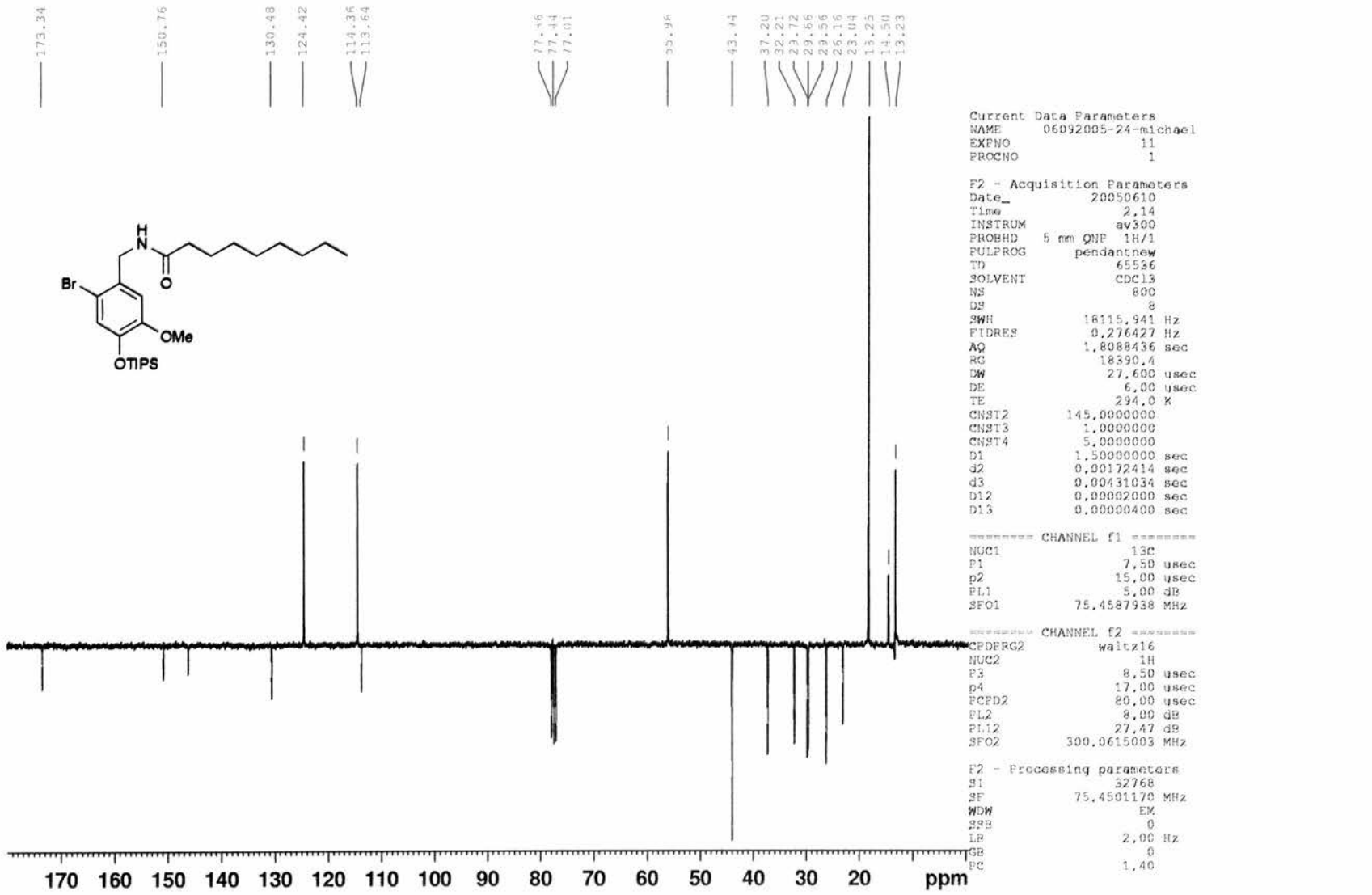

2-Bromo-5-methoxy-4-(triisopropylsilyloxy)-*N*-nonanoylbenzylamine

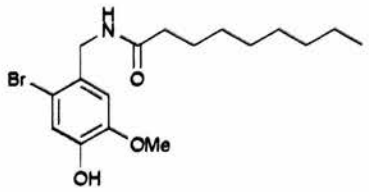

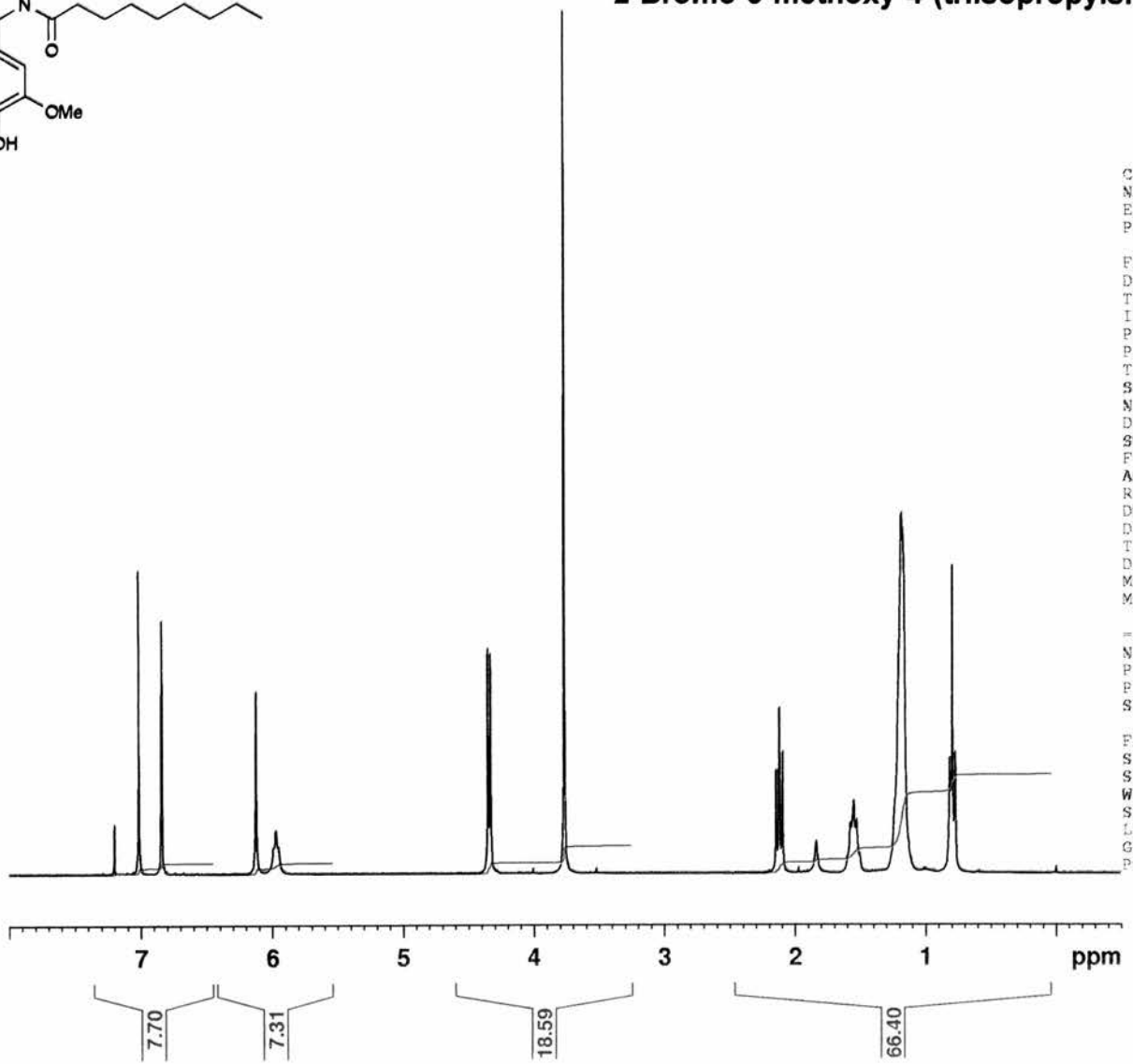


```
Current Data Parameters
NAME      06102005-27-michael
EXPNO                      10
PROCNO                      1

F2 - Acquisition Parameters
Date_              20050610
Time                  14.02
INSTRUM               av300
PROBHD    5 mm QNP  1H/1
PULPROG                zg30
TD                    32768
SOLVENT               CDCl3
NS                       16
DS                        2
SWH                4194.631 Hz
FIDRES             0.128010 Hz
AQ                 3.9059956 sec
RG                     161.3
DW                   119.200 usec
DE                     6.00 usec
TE                    293.7 K
D1                 1.00000000 sec
MCREST             0.00000000 sec
MCWRK              0.01500000 sec

======== CHANNEL f1 ========
NUC1                      1H
P1                      8.50 usec
PL1                     8.00 dB
SFO1           300.0618004 MHz

F2 - Processing parameters
SI                    32768
SF             300.0600200 MHz
WDW                      EM
SSB                       0
LB                     0.30 Hz
GB                        0
PC                     1.00
```

2-Bromo-4-hydroxy-5-methoxy-*N*-nonanoylbenzylamine

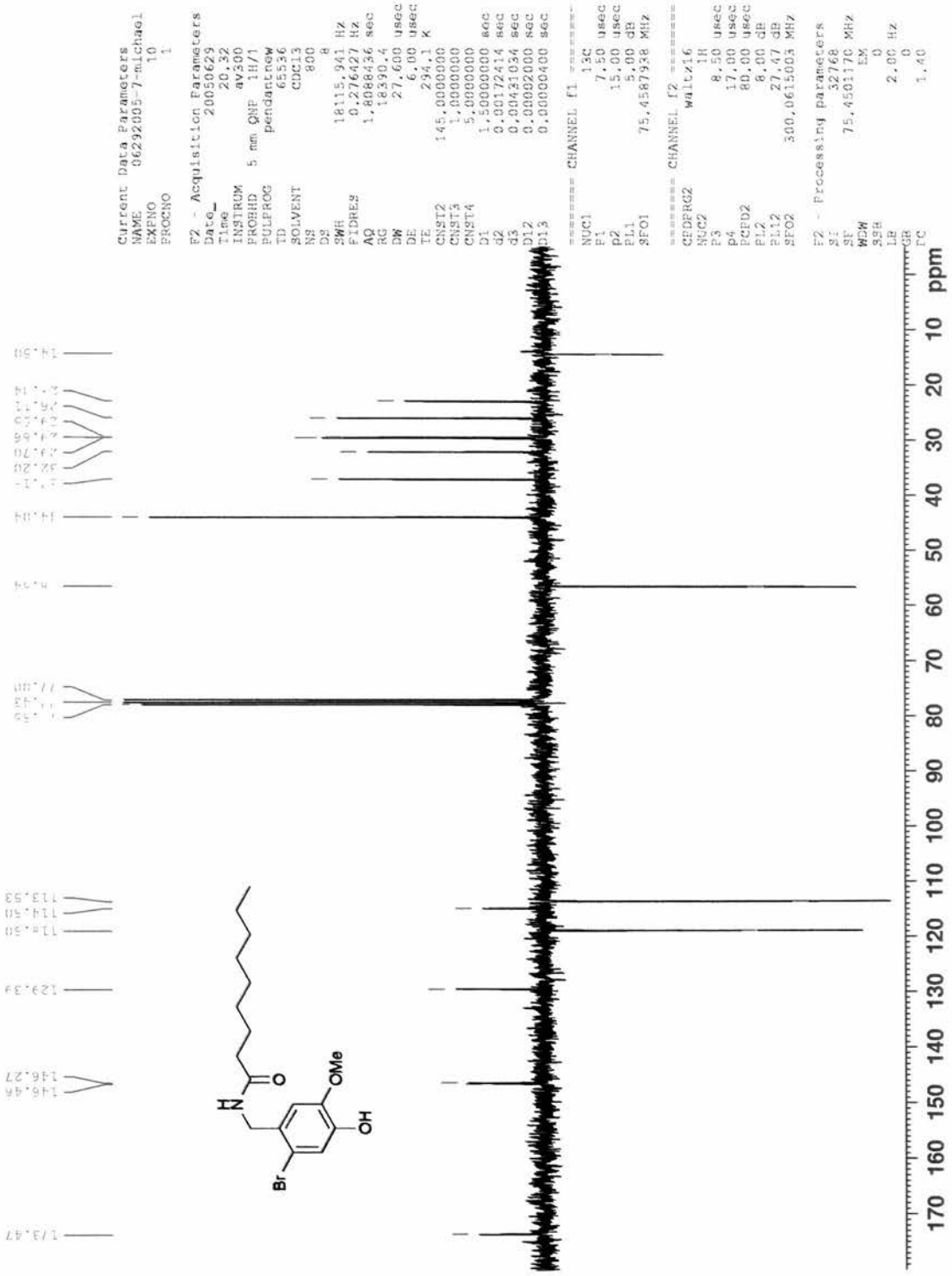

2-Bromo-5-methoxy-4-(4,5-dimethoxy-2-nitrobenzyl)-*N*-nonanoylbenzylamine

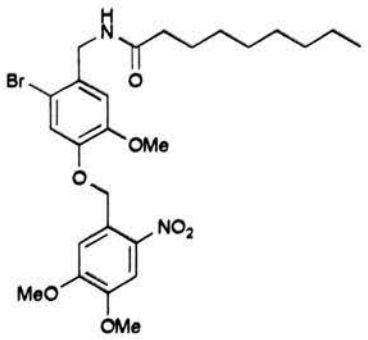

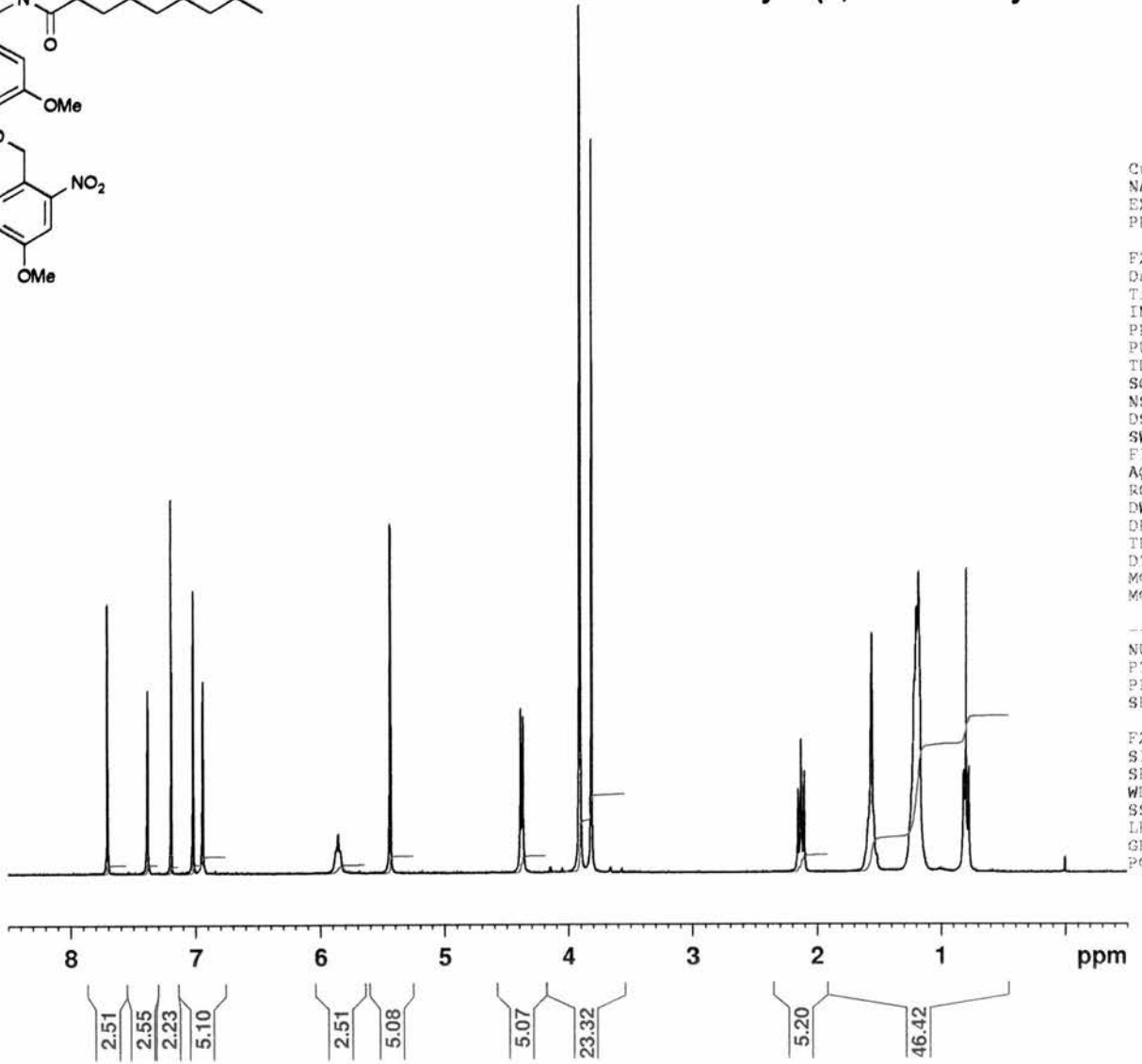


```
Current Data Parameters
NAME      01152006-27-michael
EXPNO                      10
PROCNO                      1

F2 - Acquisition Parameters
Date_               20060115
Time                   15.13
INSTRUM                av300
PROBHD   5 mm BBO BB-1H
PULPROG                 zg30
TD                     32768
SOLVENT                CDCl3
NS                        16
DS                         2
SWH                4194.631 Hz
FIDRES            0.128010 Hz
AQ                3.9059956 sec
RG                       362
DW                 119.200 usec
DE                   6.00 usec
TE                   295.4 K
D1              1.00000000 sec
MCREST          0.00000000 sec
MCWRK           0.01500000 sec

-------- CHANNEL f1 --------
NUC1                       1H
P1                   7.10 usec
PL1                   0.00 dB
SFO1          300.1318008 MHz

F2 - Processing parameters
SI                      32768
SF            300.1300257 MHz
WDW                        EM
SSB                         0
LB                   0.30 Hz
GB                          0
PC                       1.00
```

2-Bromo-5-methoxy-4-(4,5-dimethoxy-2-nitrobenzyl)-*N*-nonanoylbenzylamine

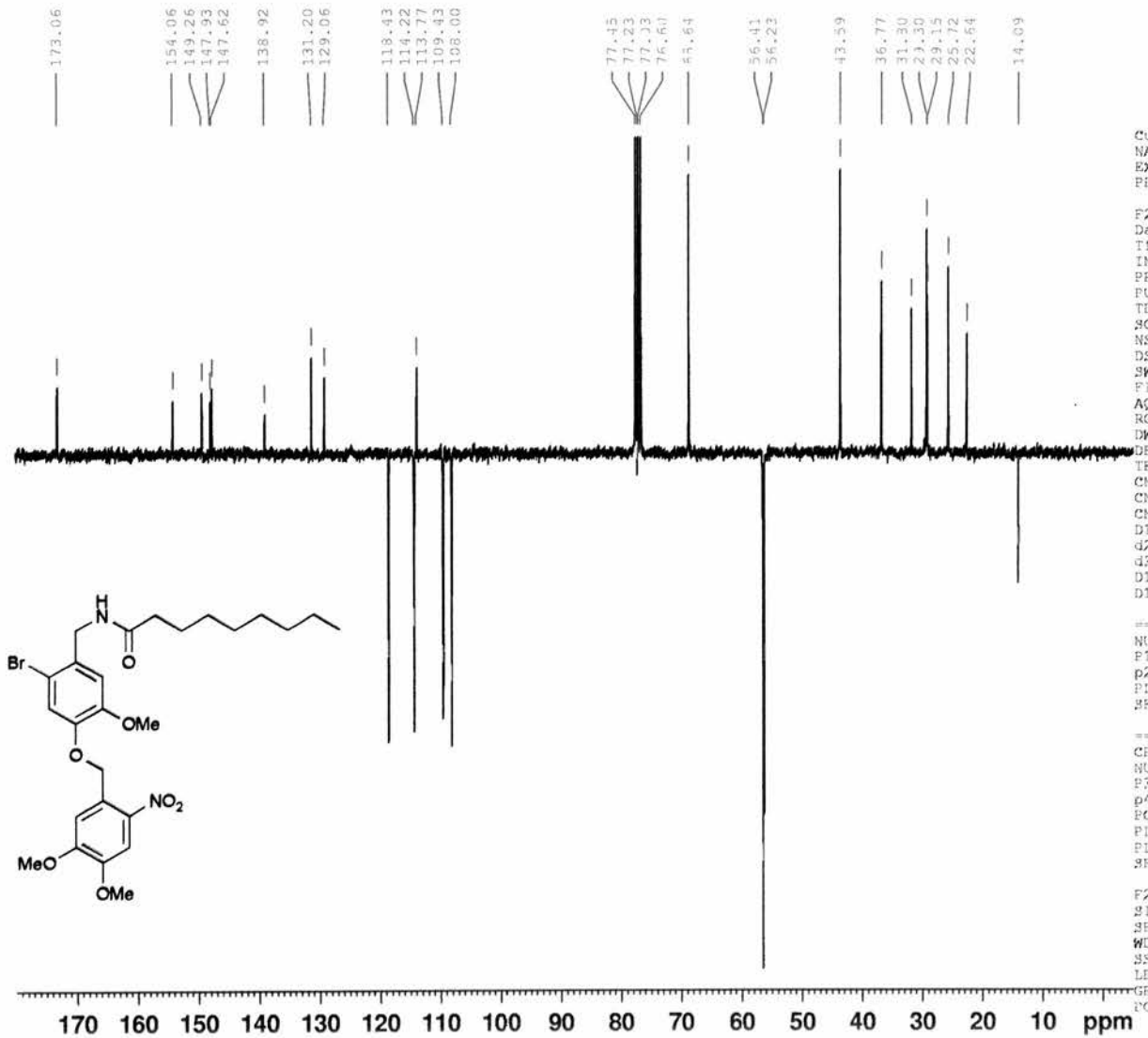


```
Current Data Parameters
NAME      01152006-27-michael
EXPNO                      11
PROCNO                      1

F2 - Acquisition Parameters
Date_               20060115
Time                   20.47
INSTRUM                av300
PROBHD   5 mm BBO BB-1H
PULPROG          pendantnew
TD                      65536
SOLVENT                 CDCl3
NS                       6000
DS                          8
SWH                18115.941 Hz
FIDRES              0.276427 Hz
AQ                  1.8088436 sec
RG                    18390.4
DW                   27.600 usec
DE                    6.00 usec
TE                   296.1 K
CNST2              145.0000000
CNST3                1.0000000
CNST4                5.0000000
D1                   1.50000000 sec
d2                   0.00172414 sec
d3                   0.00431034 sec
D12                  0.00002000 sec
D13                  0.00000400 sec

======== CHANNEL f1 ========
NUC1                      13C
P1                       7.40 usec
p2                      14.80 usec
PL1                     -3.00 dB
SFO1                75.4764273 MHz

======== CHANNEL f2 ========
CPDPRG2                waltz16
NUC2                       1H
P3                       6.80 usec
p4                      13.60 usec
PCPD2                   80.00 usec
PL2                      0.00 dB
PL12                    22.00 dB
SFO2               300.1315007 MHz

F2 - Processing parameters
SI                        32768
SF                 75.4677490 MHz
WDW                          EM
SSB                           0
LB                       2.00 Hz
GB                            0
PC                         1.40
```

2-Bromo-5-methoxy-4-(2-nitrobenzyl)-*N*-nonanoylbenzylamine

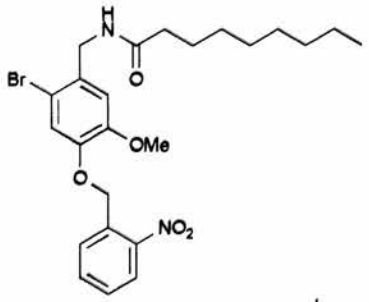

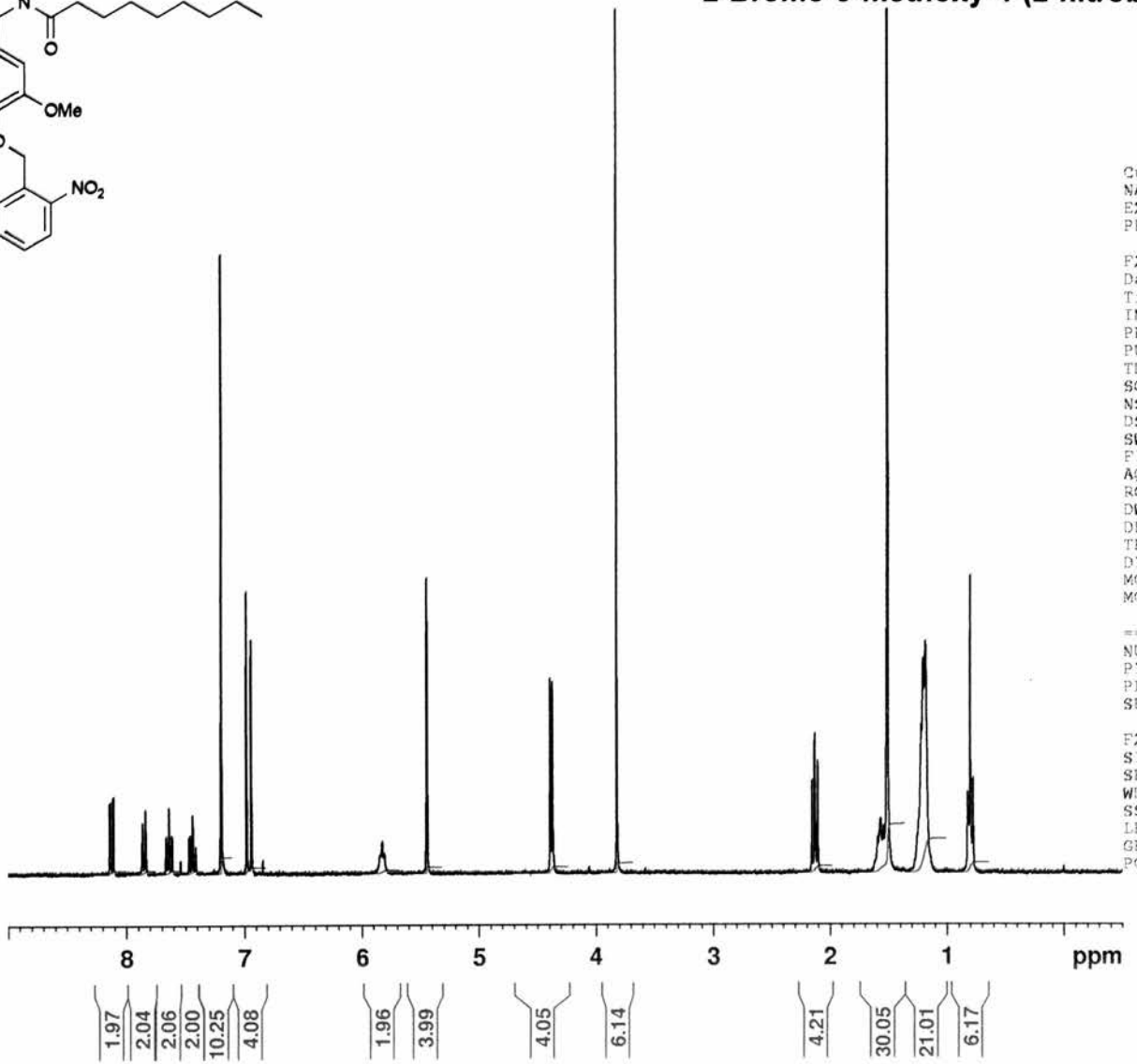


```
Current Data Parameters
NAME      01122006-4-michael
EXPNO                      10
PROCNO                      1

F2 - Acquisition Parameters
Date_              20060112
Time                  17.39
INSTRUM               av300
PROBHD   5 mm QNP  1H/1
PULPROG                zg30
TD                    32768
SOLVENT               CDCl3
NS                       16
DS                        2
SWH                4194.631 Hz
FIDRES            0.128010 Hz
AQ                3.9059956 sec
RG                     1024
DW                  119.200 usec
DE                    6.00 usec
TE                   294.4 K
D1                1.00000000 sec
MCREST            0.00000000 sec
MCWRK             0.01500000 sec

======== CHANNEL f1 ========
NUC1                      1H
P1                      8.50 usec
PL1                     8.00 dB
SFO1           300.0618004 MHz

F2 - Processing parameters
SI                     32768
SF             300.0600223 MHz
WDW                       EM
SSB                        0
LB                      0.30 Hz
GB                         0
PC                      1.00
```

2-Bromo-5-methoxy-4-(2-nitrobenzyl)-*N*-nonanoylbenzylamine

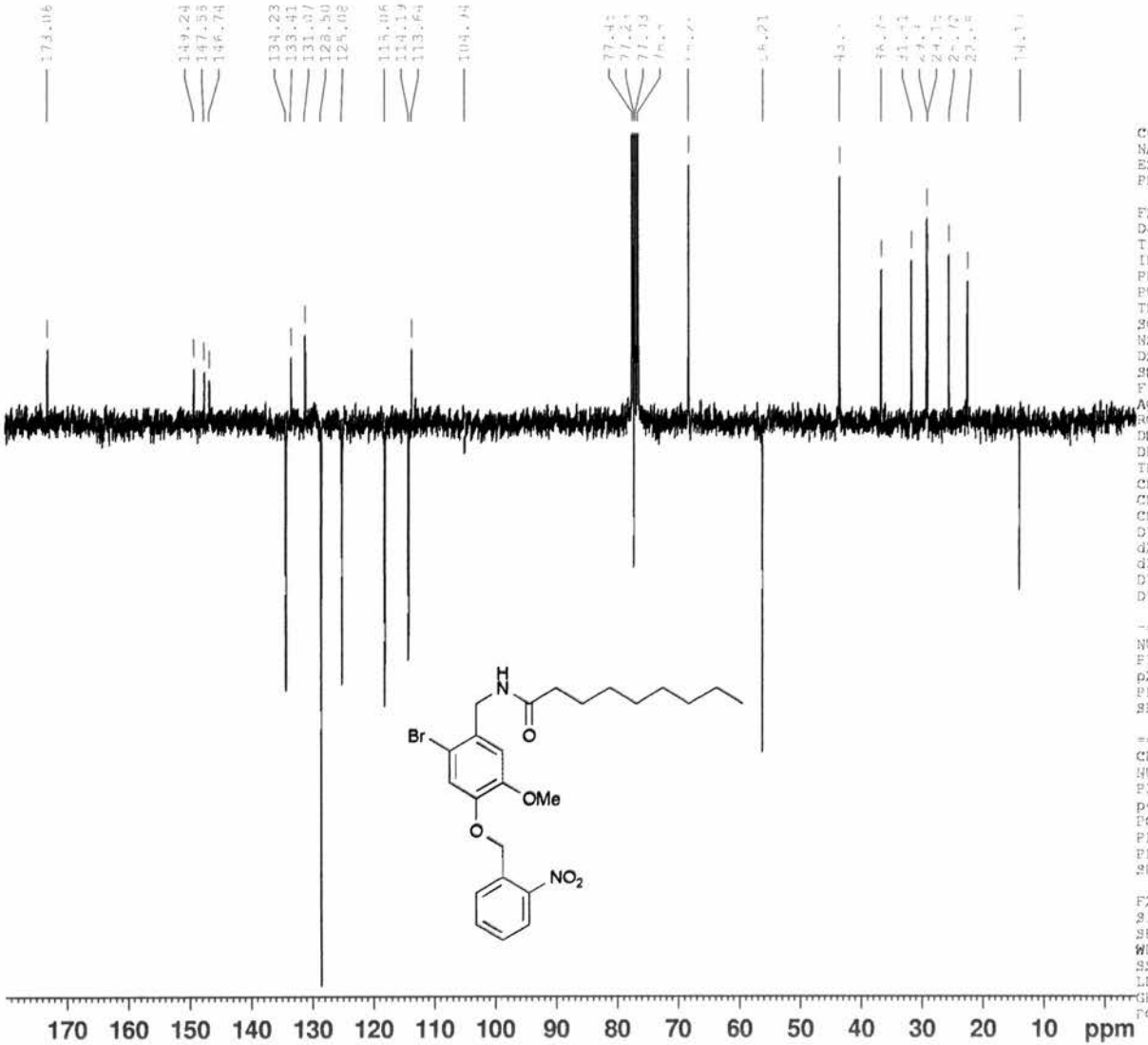


```
Current Data Parameters
NAME      09252005-17-michael
EXPNO                      10
PROCNO                      1

F2 - Acquisition Parameters
Date_              20050925
Time                  23.56
INSTRUM               av300
PROBHD   5 mm BBO BB-1H
PULPROG         pendantnew
TD                    65536
SOLVENT               CDCl3
NS                     2400
DS                        8
SWH               18115.941 Hz
FIDRES             0.276427 Hz
AQ                 1.8088436 sec
RG                   18390.4
DW                    27.600 usec
DE                     6.00 usec
TE                    294.8 K
CNST2            145.0000000
CNST3              1.0000000
CNST4              5.0000000
D1                 5.00000000 sec
d2                 0.00172414 sec
d3                 0.00431034 sec
D12                0.00002000 sec
D13                0.00000400 sec

======== CHANNEL f1 ========
NUC1                      13C
P1                      7.40 usec
p2                     14.80 usec
PL1                    -3.00 dB
SFO1              75.4764273 MHz

======== CHANNEL f2 ========
CPDPRG2              waltz16
NUC2                      1H
P3                      6.80 usec
p4                     13.60 usec
PCPD2                  80.00 usec
PL2                     0.00 dB
PL12                   22.00 dB
SFO2             300.1315007 MHz

F2 - Processing parameters
SI                       32768
SF                75.4677490 MHz
WDW                         EM
SSB                          0
LB                        2.00 Hz
GB                           0
PC                        1.40
```

4-Hydroxy-3-methoxy-*N*-nonanoylbenzylamine

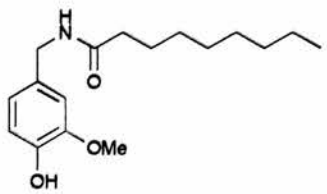

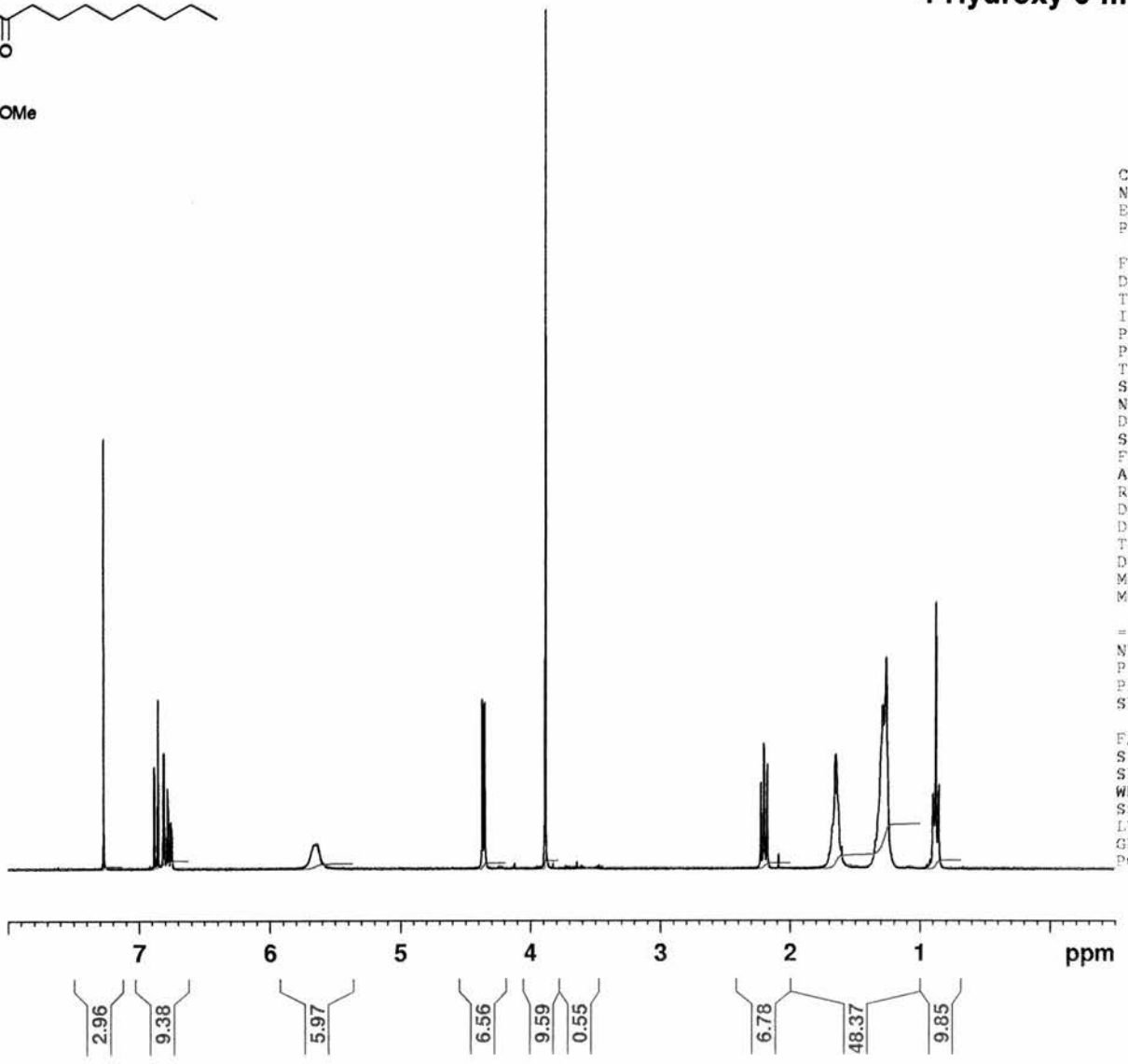


```
Current Data Parameters
NAME      01122006-5-michael
EXPNO                     10
PROCNO                     1

F2 - Acquisition Parameters
Date_              20060112
Time                  17.46
INSTRUM               av300
PROBHD   5 mm QNP  1H/1
PULPROG                zg30
TD                    32768
SOLVENT               CDCl3
NS                       16
DS                        2
SWH                4194.631 Hz
FIDRES             0.128010 Hz
AQ                 3.9059956 sec
RG                     645.1
DW                   119.200 usec
DE                     6.00 usec
TE                    294.4 K
D1                 1.00000000 sec
MCREST             0.00000000 sec
MCWRK              0.01500000 sec

======== CHANNEL f1 ========
NUC1                      1H
P1                      8.50 usec
PL1                     8.00 dB
SFO1           300.0618004 MHz

F2 - Processing parameters
SI                     32768
SF             300.0600000 MHz
WDW                       EM
SSB                        0
LB                      0.30 Hz
GB                         0
PC                      1.00
```

4-Hydroxy-3-methoxy-*N*-nonanoylbenzylamine

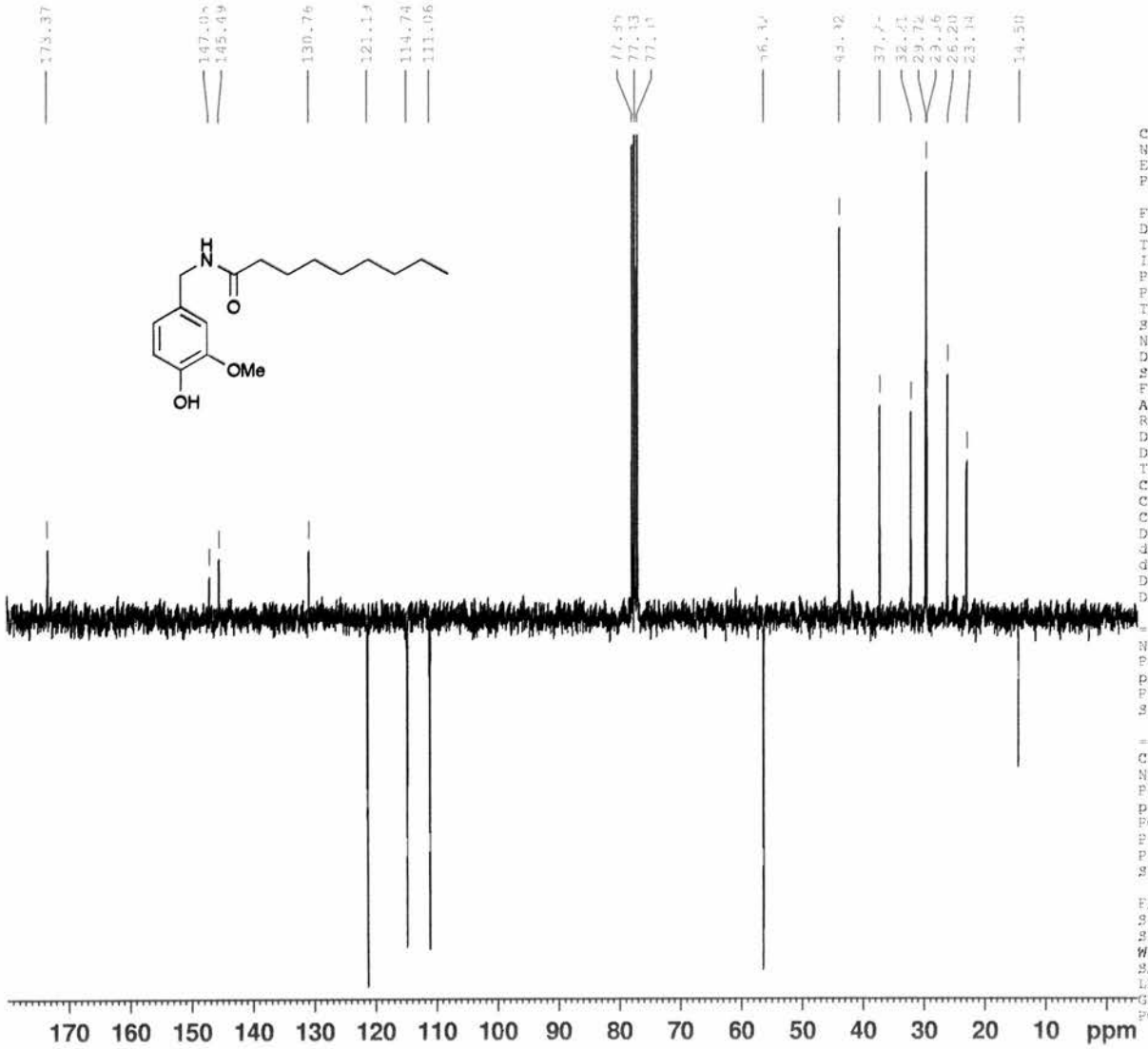


```
Current Data Parameters
NAME      06192005-26-michael
EXPNO                      11
PROCNO                      1

F2 - Acquisition Parameters
Date_              20050619
Time                  20.06
INSTRUM                av300
PROBHD   5 mm QNP  1H/1
PULPROG          pendantnew
TD                    65536
SOLVENT               CDCl3
NS                      800
DS                        8
SWH               18115.941 Hz
FIDRES             0.276427 Hz
AQ                 1.8088436 sec
RG                   18390.4
DW                    27.600 usec
DE                     6.00 usec
TE                    294.0 K
CNST2            145.0000000
CNST3              1.0000000
CNST4              5.0000000
D1                 1.50000000 sec
d2                 0.00172414 sec
d3                 0.00431034 sec
D12                0.00002000 sec
D13                0.00000400 sec

======== CHANNEL f1 ========
NUC1                      13C
P1                      7.50 usec
p2                     15.00 usec
PL1                     5.00 dB
SFO1              75.4587938 MHz

======== CHANNEL f2 ========
CPDPRG2              waltz16
NUC2                      1H
P3                      8.50 usec
p4                     17.00 usec
PCPD2                  80.00 usec
PL2                     8.00 dB
PL12                   27.47 dB
SFO2             300.0615003 MHz

F2 - Processing parameters
SI                     32768
SF                75.4501170 MHz
WDW                       EM
SSB                        0
LB                      2.00 Hz
GB                         0
PC                      1.40
```

3-Methoxy-4-(4,5-dimethoxy-2-nitrobenzyl)-*N*-nonanoylbenzylamine

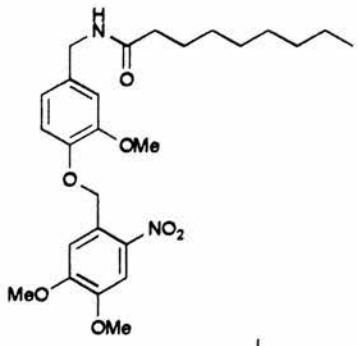

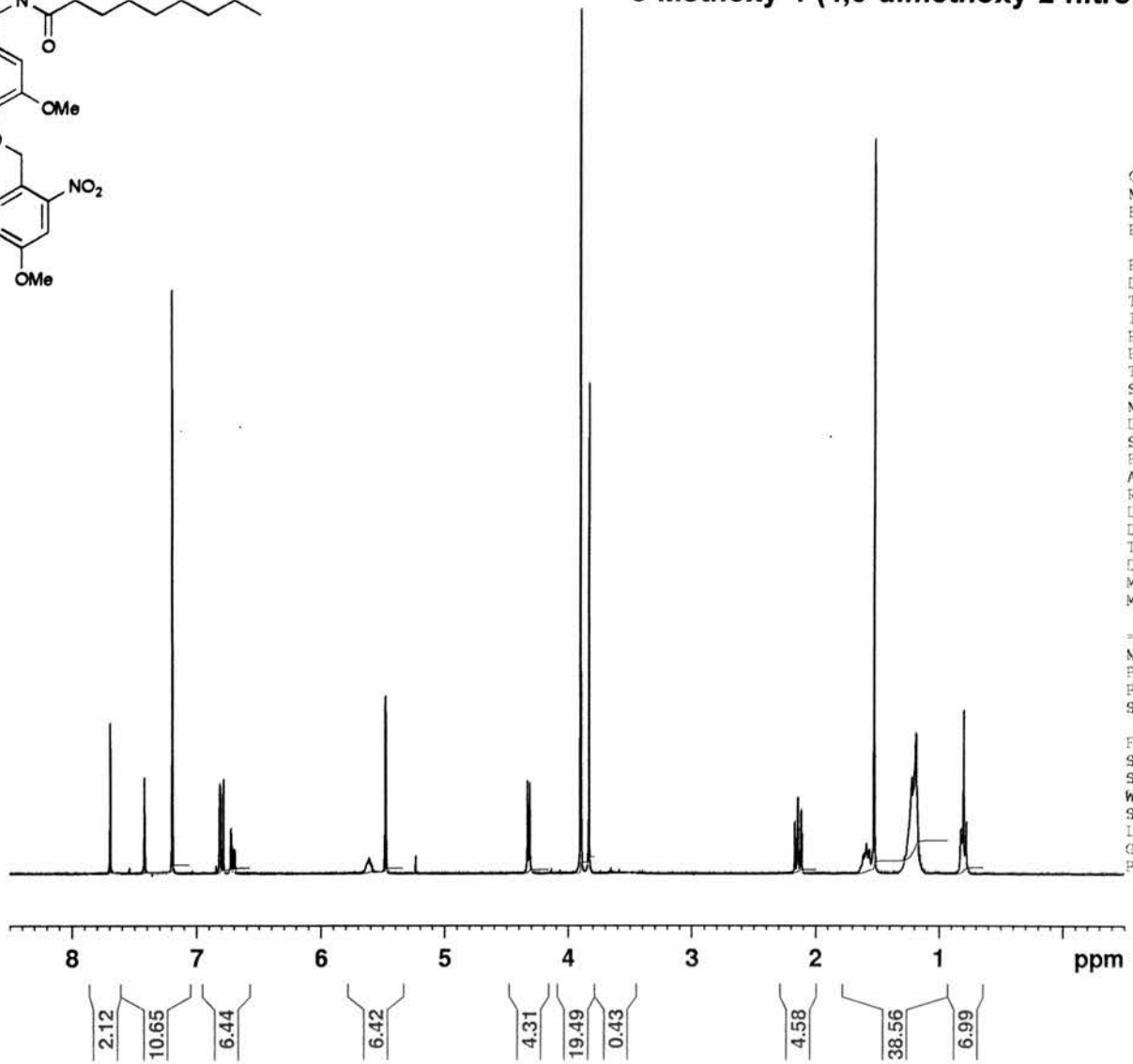


```
Current Data Parameters
NAME      06302005-5-michael
EXPNO                 10
PROCNO                 1

F2 - Acquisition Parameters
Date_           20050630
Time               19.42
INSTRUM            av300
PROBHD   5 mm QNP  1H/1
PULPROG             zg30
TD                 32768
SOLVENT            CDCl3
NS                    16
DS                     2
SWH             4194.631 Hz
FIDRES          0.128010 Hz
AQ             3.9059956 sec
RG                 724.1
DW               119.200 usec
DE                  6.00 usec
TE                 293.8 K
D1            1.00000000 sec
MCREST        0.00000000 sec
MCWRK         0.01500000 sec

======== CHANNEL f1 ========
NUC1                  1H
P1                  8.50 usec
PL1                 8.00 dB
SFO1         300.0618004 MHz

F2 - Processing parameters
SI                 32768
SF           300.0600220 MHz
WDW                   EM
SSB                    0
LB                  0.30 Hz
GB                     0
PC                  1.00
```

3-Methoxy-4-(4,5-dimethoxy-2-nitrobenzyl)-*N*-nonanoylbenzylamine

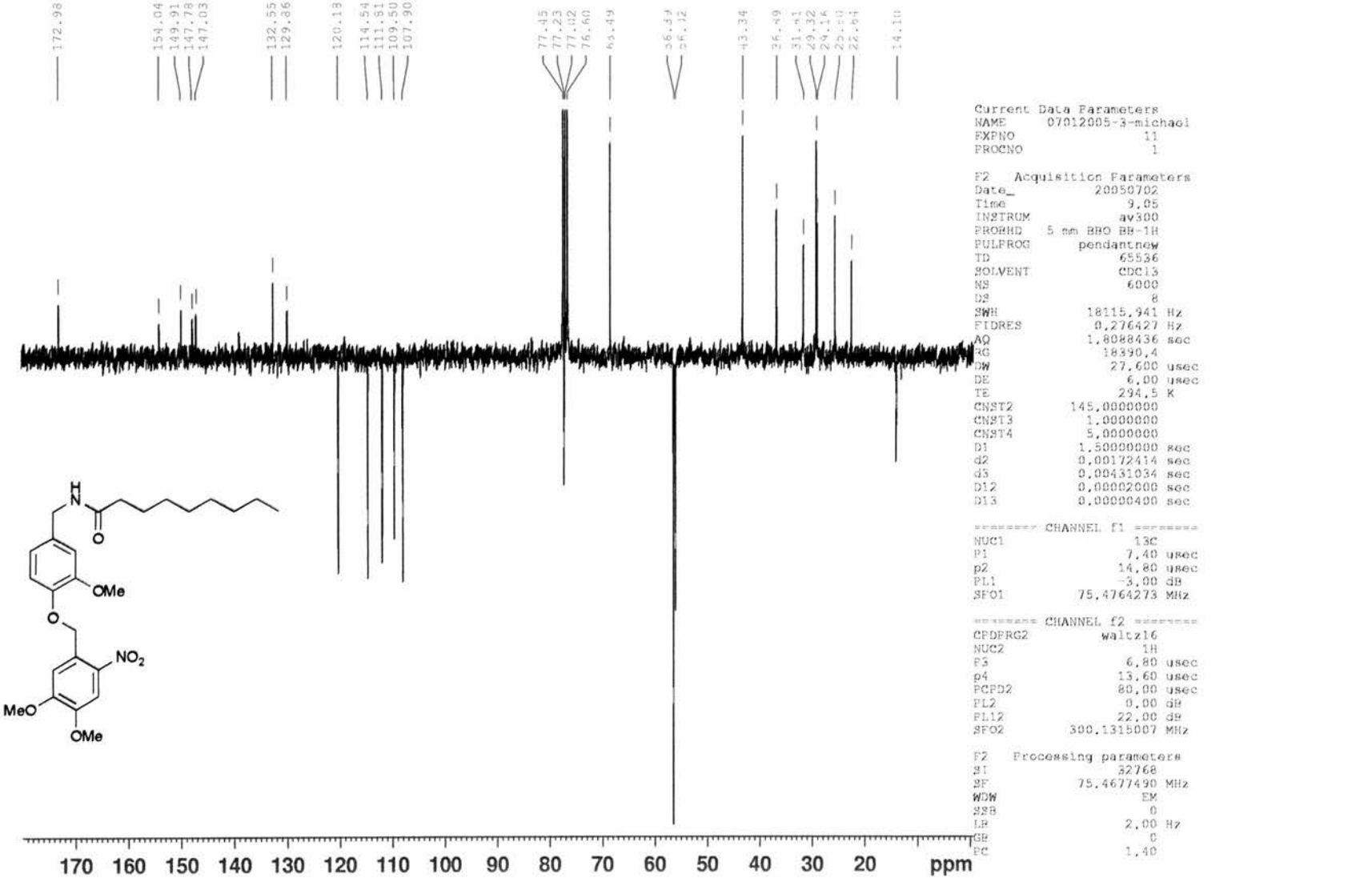

8 Reference

(1) W. A. Devane, F. A. Dysarz , M. R. Johnson, L. S. Melvin and A. C. Howlett, *Mol. Pharmacol.*, 1988, **34**, 605-613.

(2) L. A. Matsuda, S. J. Lolait, M. J. Brownstein, A. C. Young and T. I. Bonner, *Nature*, 1990, **346**, 561-564.

(3) S. Munro, K. L. Thomas and M. Abu Shaar, *Nature*, 1993, **365**, 61-65.

(4) W. A. Devane, L. Hanuš, A. Breuer, R. G. Pertwee, L. A. Steveson, F. Griffing, D. Gibson, A. Mandelbaum, A. Etinger and R. Mechoulam, *Science*, 1992, **258**, 1946-1949.

(5) T. Sugiura, S. Kondo, A. Sukagawa, S. Nakane, A. Shinoda, K. Itoh, A. Yamashita and K. Waku, *Biochem. Biophys. Res. Commun.*, 1995, **215**, 89-97.

(6) C. Montero, N. E. Campillo, P. Goya and J. A. Páez, *Eur. J. Med. Chem.*, 2005, **40**, 75–83.

(7) D. Shire, C. Carillon, M. Kaghad, B. Calandra, M. Rinaldi-Carmona, G. Le Fur, D. Caput and P. Ferrara, *J. Biol. Chem.*, 1995, **270**, 3726-3731.

(8) M. Herkenham, A. B. Lynn, B. R. De Costa and E. K. Richfield, *Brain Res.*, 1991, **547**, 267-274.

(9) A. J. Irving, A. A. Coutts, J. Harvey, M. G. Rae, K. Mackie, G. S. Bewick and R. G. Pertwee, *Neuroscience*, 2000, **98**, 253-262.

(10) L. Iversen and V. Chapman, *Curr. Opin. Pharmacol.*, 2002, **2**, 50-55.

(11) B. Lutz, *Prostaglandins, Leukotrienes Essent. Fatty Acids*, 2002, **66**, 123-142.

(12) R. G. Pertwee, *Pharmacol. Ther.*, 1997, **74**, 129-180.

(13) M. Herkenham, A. B. Lynn, M. R. Johnson, L. S. Melvin, B. R. De Costa and K. C. Rice, *J. Neurosci.*, 1991, **11**, 563-583.

(14) A. Zimmer, A. M. Zimmer, A. G. Hohmann, M. Kerkenham and T. I. Bonner, *Proc. Natl. Acad. Sci. U. S. A.*, 1999, **96**, 5780-5785.

(15) C. J. Heyser, R. E. Hampson and S. A. Deadwyler, *J. Pharmacol. Exp. Ther.*, 1993, **264**, 294-307.

(16) A. C. Howlett, *Prostaglandins Other Lipid Mediators*, 2002, **68-69**, 619-631.

(17) N. E. Buckley, S. Hansson, G. Harta and E. Mezey, *Neuroscience*, 1998, **82**, 1131-1149.

(18) S. Galiegue, S. Mary, J. Marchand, D. Dussossoy, D. Carriere, P. Carayon, M. Bouaboula, D. Shire, G. Le Fur and P. Casellas, *Eur. J. Biochem.*, 1995, **232**, 54-61.

(19) T. P. Malan Jr., M. M. Ibrahim, H. Deng, Q. Liu, H. P. Mata, T. Vanderah, F. Porreca and A. Makriyannis, *Pain*, 2001, **93**, 239-245.

(20) R. G. Pertwee and R. A. Ross, *Prostaglandins, Leukotrienes Essent. Fatty Acids*, 2002, **66**, 101-121.

(21) T. Bisogno, D. Melck, M. Y. U. Bobrov, N. M. Gretskaya, V. V. Bezuglov, L. De Petrocellis and V. Di Marzo, *Biochem. J.*, 2000, **351**, 817-824.

(22) S. M. Huang, T. Bisogno, M. Trevisani, A. Al-Hayani, L. De Petrocellis, F. Fezza, M. Tognetto, T. J. Petros, J. F. Krey, C. J. Chu, J. D. Miller, S. N. Davies, P. Geppetti, J. M. Walker and V. Di Marzo, *Proc. Natl. Acad. Sci. U. S. A.*, 2002, **99**, 8400-8405.

(23) A. C. Porter, J. M. Sauer, M. D. Knierman, G. W. Becker, M. J. Berna, J. Bao, G. G. Nomikos, P. Carter, F. P. Bymaster, A. B. Leese and C. C. Felder, *J. Pharmacol. Exp. Ther.*, 2002, **301**, 1020-1024.

(24) L. De Petrocellis, M. G. Casio and V. Di Marzo, *Br. J. Pharmacol.*, 2004, **141**, 765-774.

(25) O. Dasse, A. Mahadevan, L. Han, B. R. Martin, V. Di Marzo and R. K. Razdan, *Tetrahedron*, 2000, **56**, 9195-9202.

(26) R. Altundas, A. Mahadevan and R. K. Razdan, *Tetrahedron Lett.*, 2004, **45**, 5449-5451.

(27) I. V. Ivanov, S. G. Romanov, N. V. Groza, S. Nigam, H. Kuhn and G. I. Myagkova, *Bioorg. Med. Chem.*, 2002, **10**, 2335-2343.

(28) L. Qi, M. M. Meijler, S. Lee, C. Sun and K. D. Janda, *Org. Lett.*, 2004, **6**, 1673-1675.

(29) A. D. Khanolkar and A. Makriyannis, *Life Sci.*, 1999, **65**, 607-616.

(30) R. K. Razdan and A. Mahadevan, *Chem. Phys. Lipids*, 2002, **121**, 21-33.
(31) R. A. Ross, T. M. Gibson, H. C. Brockie, M. Leslie, G. Pashmi, S. J. Craib, V. Di Marzo and R. G. Pertwee, *Br. J. Pharmacol.*, 2001, **132**, 631-640.
(32) M. J. Caterina, M. A. Schumacher, M. Tominaga, T. A. Rosen, J. D. Levine and D. Julius, *Nature*, 1997, **389**, 816-824.
(33) S. E. Jordt and D. Julius, *Cell*, 2002, **108**, 421-430.
(34) A. Ferrer-Montiel, C. Garcý´a-Martý´Nez, C. Morenilla-Palao, N. Garcý´a-Sanz, A. Fernandez-Carvajal, G. Fernandez-Ballester and R. Planells-Cases, *Eur. J. Biochem.*, 2004, **271**, 1820-1826.
(35) A. Szalllasi and P.M. Blumberg, *Pharmacological Reviews*, 1999, **51**, 159-211.
(36) M. J. Caterina, A. Leffler, A. B. Malmberg, W. J. Martin, J. Trafton, K. R. Petersen-Zeitz, M. Koltzenburg, A. I. Basbaum and D. Julius, *Science*, 2000, **288**, 306-313.
(37) I. Nagy, P. Santha, G. Jancso and L. Urban, *Eur. J. Pharmacol.*, 2004, **500**, 351-369.
(38) E. K. Nelson, *J. Am. Chem. Soc.*, 1919, **41**, 1115-1121.
(39) E. Spath and S. F. Darling, *Ber. Dtsch. Chem. Ges.*, 1930, **63B**, 737-740.
(40) C. S. J. Walpole, R. Wriggleworth, S. Bevan, E. A. Campbell, A. Dray, I. F. James, M. N. Perkins, D. J. Reid and J. Winter, *J. Med. Chem.*, 1993, **36**, 2362-2372.
(41) C. S. J. Walpole, R. Wriggleworth, S. Bevan, E. A. Campbell, A. Dray, I. F. James, K. J. Masdin, M. N. Perkins and J. Winter, *J. Med. Chem.*, 1993, **36**, 2373-2380.
(42) C. S. J. Walpole, R. Wriggleworth, S. Bevan, E. A. Campbell, A. Dray, I. F. James, K. J. Masdin, M. N. Perkins and J. Winter, *J. Med. Chem.*, 1993, **36**, 2381-2389.
(43) R. Wriggleworth, C. S. J. Walpole, S. Bevan, E. A. Campbell, A. Dray, G. A. Hughes, I. James, K. J. Masdin and J. Winter, *J. Med. Chem.*, 1996, **39**, 4942-4951.
(44) M. J. Gunthorpe, H. K. Rami, J. C. Jerman, D. Smart, C. H. Gill, E. M. Soffin, S. Luis Hannan, S. C. Lappin, J. Egerton, G. D. Smith, A. Worby, L. Howett, D. Owen, S. Nasir, C. H. Davies, M. Thompson, P. A. Wyman, A. D. Randall and J. B. Davies, *Neuropharmacology*, 2004, **46**, 133-149.
(45) A. Szallasi and G. Appendino, *J. Med. Chem.*, 2004, **47**, 2717-2723.
(46) J. L. Carr, K. N. Wease, M. P. Van Ryssen, S. Paterson, B. Agate, K. A. Gallagher, T. A. Brown, R. H. Scott and S. J. Conway, *Bioorg. Med. Chem. Lett.*, 2006, **16**, 208–212.
(47) J. E. T. Corrie and D. R. Trentham, in *Bioorganic Photochemistry*, Ed. H. Morrison, John Wiley and Sons, New York, 1993, vol. 2, ch. 5, 243-305.
(48) J. H. Kaplan, B. Forbush and J. F. Hoffman, *Biochemistry*, 1978, **17**, 1929-1935.
(49) A. Patchornik, B. Amit and R. B. Woodward, *J. Am. Chem. Soc.*, 1970, **92**, 6333-6335.
(50) Y. V. Il'Ichev, M. A. Schworer and J. Wirz, *J. Am. Chem. Soc.*, 2004, **126**, 4581-4595.
(51) V. N. R. Pillai, *Synthesis*, 1980, 1-26.
(52) M. Gaplovsky, Y. V. Il'ichev, Y. Kamdzhilov, S. Kombarova, M. Mac, M. A. Schwörer and J. Wirz, *Photochem. Photobiol. Sci.*, 2005, **4**, 33-42.
(53) C. G. Bochet, *J. Chem. Soc., Perkin Trans. 1*, 2002, 125-142.
(54) J. C. Sheehan and G. D. Daves, *J. Org. Chem.*, 1964, **29**, 2006-2008.
(55) R. S. Givens, P. S. Athey, B. Matuszewski, L. W. Kueper Iii, J. Y. Xue and T. Fister, *J. Am. Chem. Soc.*, 1993, **115**, 6001-6012.
(56) K. Zhang, J. E. T. Corrie, V. R. N. Munasinghe and P. Wan, *J. Am. Chem. Soc.*, 1999, **121**, 5625-5632.
(57) C. Park and R. S. Givens, *J. Am. Chem. Soc.*, 1997, **119**, 2453-2463.
(58) A. Blanc and C. G. Bochet, *J. Org. Chem.*, 2002, **67**, 5567-5577.
(59) M. Ladlow, C. H. Legge, T. Neudeck, A. J. Pipe, T. Sheppard and L. L. Yang, *Chem. Commun.*, 2003, 2048-2049.
(60) D. L. Boger, H. Sato, A. E. Lerner, X. Guan and N. B. Gilula, *Bioorg. Med. Chem. Lett.*, 1999, **9**, 1151-1154.

(61) D. W. Pate, K. Järvinen, A. Urtti, P. Jarho, M. Fich, V. Mahadevan and T. Järvinen, *Life Sci.*, 1996, **58**, 1849-1860.
(62) E. X. Hu and J. M. Cassady, *Synth. Commun.*, 1995, **25**, 907-914.
(63) B. Faroux-Corley, L. Clary, C. Gadras, D. Hammache, J. Greiner, C. Santaella, A. Aubertin, P. Vierling and J. Fantini, *Carbohydr. Res.*, 2000, **327**, 223-260.
(64) R. J. Pearson, K. M. Evans, A. M. Z. Slawin, D. Philip and N. J. Westwood, *J. Org. Chem.*, 2005, **70**, 5055-5061.
(65) A. R. Katritzky, Y. J. Xu, A. V. Vakulenko, A. L. Wilcox and K. R. Bley, *J. Org. Chem.*, 2003, **68**, 9100-9104.
(66) G. Appendino, S. Harrison, L. De Petrocellis, N. Daddario, F. Bianchi, A. S. Moriello, M. Trevisani, F. Benvenuti, P. Geppetti and V. Di Marzo, *Br. J. Pharmacol.*, 2003, **139**, 1417-1424.
(67) K. P. M. Currie, J. F. Wooten and R. H. Scott, *J. Physiol.*, 1995, **482**, 291-307.
(68) B. V. Zemelman, N. Nesnas, G. A. Lee and G. Miesenböck, *Proc. Natl. Acad. Sci.*, 2003, **100**, 1352-1357.
(69) C. G. Bochet, *Tetrahedron Lett.*, 2000, **41**, 6341-6346.
(70) W. L. F. Armarego and C. L. L. Chai, in *Purification of Laboratory Chemicals*, Butterworth-Heinemann, Amsterdam, 5th Edn., 2003.
(71) P. G. Mattingly, *Synthesis*, 1990, 336-368.
(72) D. J. Miller, M. B. Surfraz, M. Akhtar, D. Gani and R. K. Allemann, *Org. Biomol. Chem.*, 2004, **2**, 671-688.
(73) W. L. F. Armarego, B. A. Milloy and W. Pendergast, *J. Chem. Soc., Perkin Trans. 1*, 1976, 2229-2237.
(74) A. Hopkins and A. Williams, *J. Chem. Soc., Perkin Trans. 2*, 1983, 891-896.
(75) G. Castaldi, A. Belli, F. Uggeri and C. Giordano, *J. Org. Chem.*, 1983, **48**, 357-368.
(76) E. Santaniello, M. G. Kienle and A. Manzocchi, *J. Chem. Soc., Perkin Trans. 1*, 1977, 1677-1683.